1.26 Heteroatomic p-Block (Main-Chain) Polymers

V Chandrasekhar, Indian Institute of Technology Kanpur, Kanpur, India
S Nagendran, Indian Institute of Technology Delhi, New Delhi, India

© 2013 Elsevier Ltd. All rights reserved.

1.26.1 Introduction

In this chapter, we examine four different types of inorganic polymeric systems containing elements of the p-block in their main chain and the small-molecule chemistry related to them. Among the various inorganic polymers known, polyphosphazenes and polysiloxanes have been the most well studied.[1–5] The latter also constitute the most important family of inorganic polymers from a commercial point of view. In addition to these two polymeric systems, in recent years, there have also been new synthetic methods that have allowed the assembly of polymers containing B–N and B–P repeat units. Although still nascent, these boron-containing polymer families are assuming importance particularly from the point

Copyright © 2013. Elsevier. All rights reserved.
Comprehensive Inorganic Chemistry II : From Elements to Applications, Elsevier, 2013. ProQuest Ebook Central, http://ebookcentral.proquest.com/lib/inflibnet-ebooks/detail.action?docID=1330977.
Created from inflibnet-ebooks on 2021-02-09 22:27:26.

of view of discovering new synthetic methods for preparing inorganic polymers. Unlike organic polymer synthesis, where general synthetic methods are available for the preparation of various types of polymers, development of inorganic polymer chemistry has suffered from the lack of such general preparative procedures. Recently, there appears to be some promise. For example, ring-opening polymerization (ROP) methodology seems to be well suited to a large number of inorganic rings containing P–N, P–N–E (E = S, S(O), C), and Si–O motifs.[1–5] Discovery of new polymerizable monomers such as the phosphoranimine, $Cl_3P{=}NSiMe_3$, also augurs well for this field. In addition, transition-metal-catalyzed dehydropolymerization of amine–borane and phosphane–borane compounds is a new and general strategy for preparing polymers containing B–N and B–P units.[5] This chapter aims at providing a summary of this field with an emphasis on some recent developments.

1.26.2 Polyphosphazenes

Polyphosphazenes, $[N{=}PR_2]_n$, are the largest family of inorganic polymers with over 800 members.[1–5] The structure and properties of polyphosphazenes are strongly dependent, apart from chain length, on the substituents that are present in phosphorus. Thus, depending on the substituent, polyphosphazenes can vary from being elastomers with low glass transition temperatures (T_g's) to polymers with high T_g's (Chart 1), from being extremely hydrophobic to hydrophilic, and from being hydrolytically stable to being readily susceptible to hydrolysis (Chart 2).[1,2]

While some members of this family have important biological applications, others are important from the point of view as new materials.[1–5]

Most poly(organophosphazene)s are prepared by a two-step procedure. First, the linear poly(dichloropolyphosphazene), $[NPCl_2]_n$, is prepared. This is followed by substitution reactions involving the P–Cl bonds of $[NPCl_2]_n$ affording $[NPR_2]_n$.[1–5] Polyphosphazenes, containing alkyl/aryl substituents on the phosphorus atoms, cannot be prepared by the methodology described above. This is because of chain scission reactions that occur during the reactions of $[NPCl_2]_n$ with Grignard reagents or organolithium reagents. On the other hand, such polymers can be prepared by a condensation polymerization strategy involving acyclic phosphoranimines.[6]

1.26.2.1 Poly(dichlorophosphazene): High-Temperature Synthesis

A rubbery material, dubbed as 'inorganic rubber,' with the composition of $[NPCl_2]_n$ was known to the American chemist Stokes by the end of the nineteenth century. This material was extremely sensitive to hydrolysis, was not soluble in organic

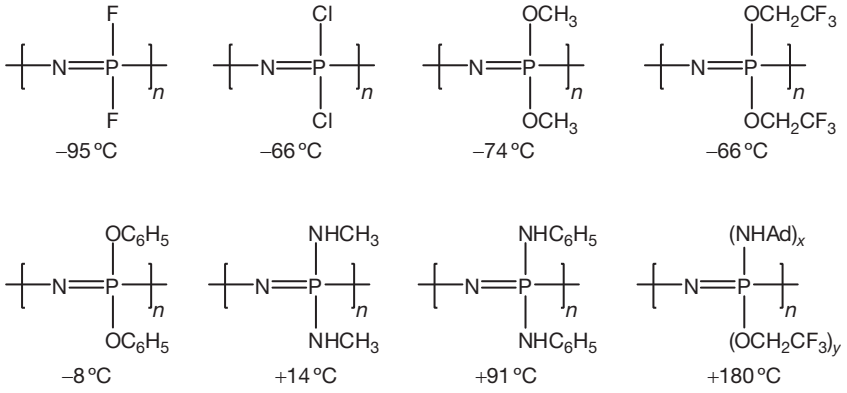

Chart 1 Representative examples of polyphosphazenes with varying T_g values.

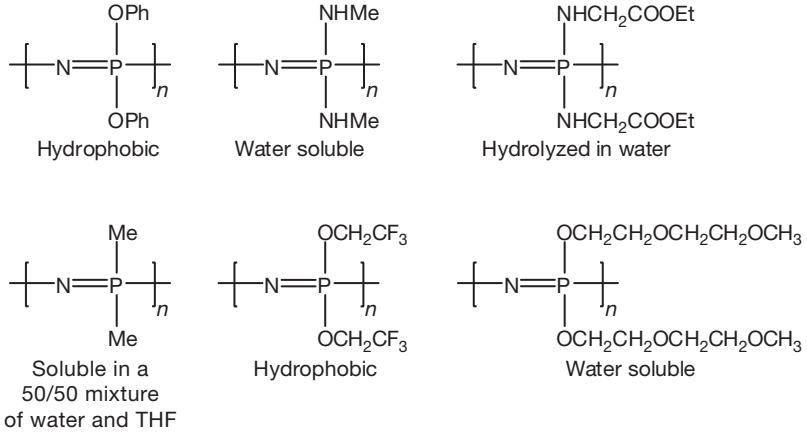

Chart 2 Representative examples of water-repelling, -soluble, and hydrolyzable polyphosphazenes.

Copyright © 2013. Elsevier. All rights reserved.

Comprehensive Inorganic Chemistry II : From Elements to Applications, Elsevier, 2013. ProQuest Ebook Central, http://ebookcentral.proquest.com/lib/inflibnet-ebooks/detail.action?docID=1330977.
Created from inflibnet-ebooks on 2021-02-09 22:27:26.

solvents (but would swell in them), and had 'rubbery' elastomeric properties. However, its intractability and extreme sensitivity to water detracted its possible utility for many years.[1–3] This field was opened by the discovery that hexachlorocyclotriphosphazene, $N_3P_3Cl_6$, can be subjected to a controlled ROP at 250 °C in high vacuum to afford a high-molecular-weight ($M_w \sim 10^6$), soluble polymer, $[NPCl_2]_n$ (Scheme 1).[1–3,7]

The polymer conversion is about 40% with a polydispersity index (PDI) >2.0; however, the problem of hydrolysis remained. Allcock hypothesized that the hydrolytic sensitivity of $[NPCl_2]_n$ was perhaps not due to an inherent backbone instability (of the P–N bonds) but probably due to the highly reactive nature of the P–Cl bonds. This reasoning advanced this subject considerably. Accordingly, macromolecular substitution of $[NPCl_2]_n$ with nucleophiles has become a viable strategy for the preparation of poly(organophosphazene)s $[NPR_2]_n$.[1–5,7]

1.26.2.2 Mechanism of ROP of $N_3P_3Cl_6$

The generally accepted mechanism of the ROP of $N_3P_3Cl_6$ is depicted in Scheme 2. The initiation step involves a heterolytic cleavage of the P–Cl bond to generate a phosphorus-centered cation. This is followed by a nucleophilic attack on this positive center by a nitrogen atom of another molecule leading to an opening of the ring.

The terminal phosphorus atom of the ring-opened fragment now bears the positive charge. Chain propagation is quite rapid (as experimentally evidenced by a quick increase in the viscosity of the melt). Chain termination can occur by a variety of reagents, which can quench the positive charge on the phosphorus center.

Evidence for the mechanism as outlined in Scheme 2 comes from various types of experiments. First, a noticeable increase in ionic conductivity of the $N_3P_3Cl_6$ melt is observed during the initial stages of polymerization. Second, the ROP is greatly facilitated by the addition of small amounts of water. Third, substrates such as $N_3P_3F_6$ have to be heated to very high temperatures (~350 °C) to effect polymerization because of the greater thermodynamic stability of the P–F bond.[1–3]

In spite of the above arguments, the ROP mechanism is still not considered completely understood. There have been several attempts to isolate the incipient cyclophosphazenium cation without success; however, recently a hexacation has been stabilized by the coordinative action of six pyridine bases (Chart 3).[8]

In addition, several Lewis acid adducts of $N_3P_3Cl_6$ have been isolated. Recently, one such adduct, $N_3P_3Cl_6{\cdot}AlBr_3$, has also been structurally characterized (Chart 4).[9]

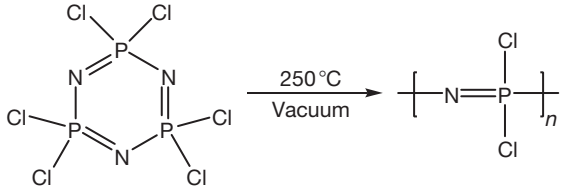

Scheme 1 Ring-opening polymerization (ROP) of $N_3P_3Cl_6$.

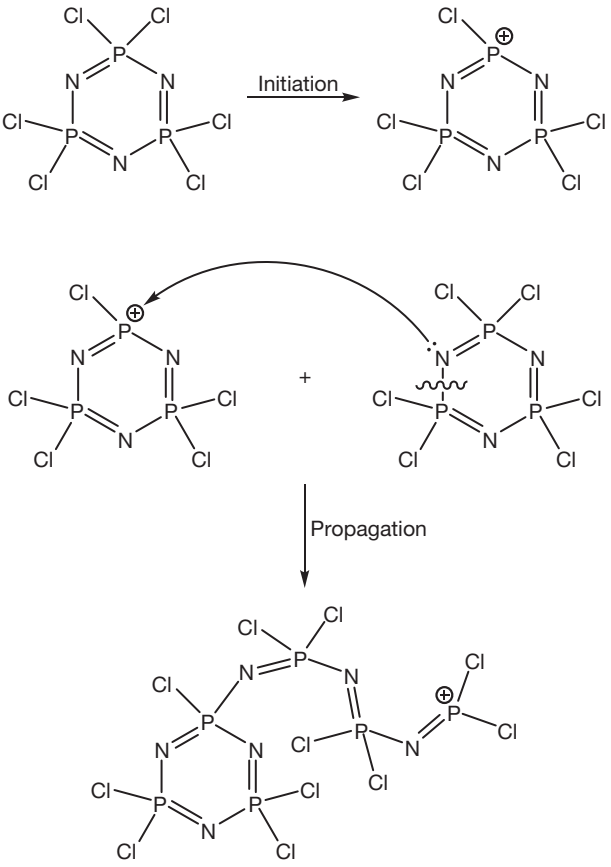

Scheme 2 Mechanism of the ROP of $N_3P_3Cl_6$.

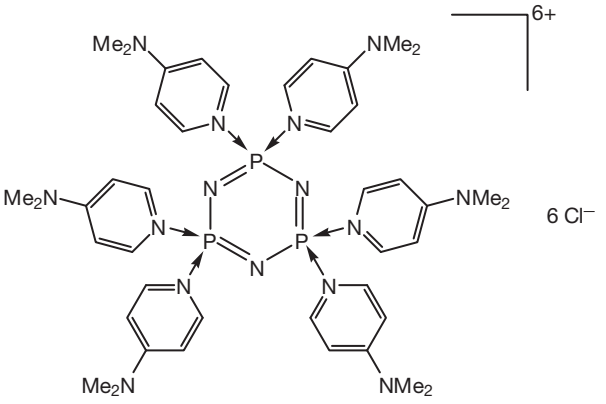

Chart 3 A cyclophosphazene hexacation stabilized by pyridine bases.

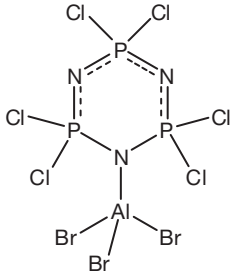

Chart 4 $N_3P_3Cl_6{\cdot}AlBr_3$ Lewis adduct.

Copyright © 2013. Elsevier. All rights reserved.

Comprehensive Inorganic Chemistry II : From Elements to Applications, Elsevier, 2013. ProQuest Ebook Central, http://ebookcentral.proquest.com/lib/inflibnet-ebooks/detail.action?docID=1330977.
Created from inflibnet-ebooks on 2021-02-09 22:27:26.

However, such adducts have been found to be unsuitable as monomers for ROP. Similarly, the reaction of $N_3P_3Cl_6$ with potent chloride-abstracting reagents such as $CHB_{11}R_5X_6^-$ (R = H, Me, X; X = Cl, Br) afforded *N*-adducts rather than the anticipated phosphazenium cations (Scheme 3).[10] Thus, it may be said that although there have been speculations on the involvement of the phosphazenium cations in the ROP of $N_3P_3Cl_6$, these have not been fully substantiated.

In a different development, recently, some of the Lewis-acid–Lewis-base adducts shown in Scheme 3 have been shown to be useful as initiators for an ambient-temperature ROP of $N_3P_3Cl_6$ (*vide infra*).[10,11]

In addition to the ROP of $N_3P_3Cl_6$, another high-temperature method for the preparation of $[NPCl_2]_n$ involves a condensation polymerization of the acyclic phosphazene $Cl_3P{=}N{-}P(O)Cl_2$ (Scheme 4).[12–14]

The polymerization of $Cl_3P{=}N{-}P(O)Cl_2$ proceeds through the elimination of $P(O)Cl_3$. This method affords $[NPCl_2]_n$ with an M_w of 200 000 which can be increased to 800 000, if the polymerization is carried out in molten trichlorobiphenyl.

1.26.2.3 Ambient-Temperature Synthesis of $[NPCl_2]_n$

A living cationic chain-growth polymerization of trichloro(*N*-trimethylsilyl)phosphoranimine, $Cl_3P{=}NSiMe_3$, was reported to afford linear poly(dichlorophosphazene), $[NPCl_2]_n$, at ambient temperature (Scheme 5).[15–18]

This reaction is initiated by the addition of a trace amount of PCl_5. Originally, the reaction was reported to occur in dichloromethane although later a bulk polymerization was also reported.[15] The molecular weights of $[NPCl_2]_n$ obtained by this method are quite high (M_n ~60 000), while the PDI, which is reflective of the molecular weight distribution, is quite low, ~1.1–1.3. The living nature of the polymerization has been ascertained by several methods including the preparation of block copolymers. For example, a diblock copolymer can be prepared by adding a different monomer, $Me_3SiN{=}PR_2Cl$, to the living polymer (Scheme 6).[19]

More recently, a block copolymer involving a segment of poly(ferrocenyl silane) and polyphosphazene has been prepared by using this method.[20] Dendritic, star-shaped polymers have also been assembled using the living poly(dichlorophosphazene) polymer.[1–3]

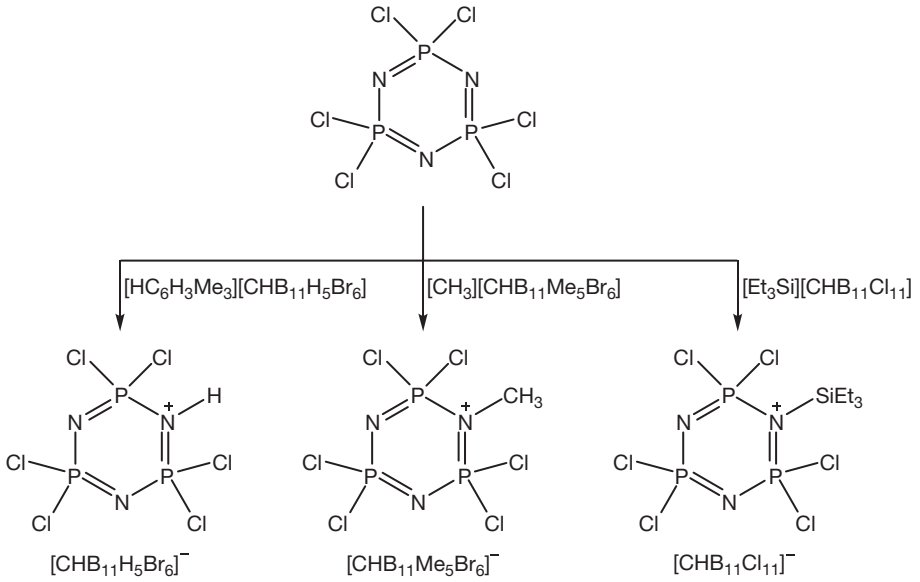

Scheme 3 Reaction of $N_3P_3Cl_6$ with $CHB_{11}R_5X_6^-$ (R = H, Me, X; X = Cl, Br).

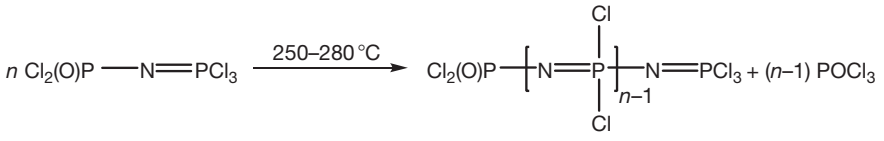

Scheme 4 Thermal polymerization of $Cl_3P{=}N{-}P(O)Cl_2$.

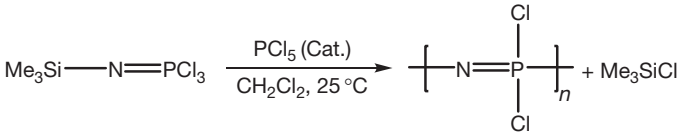

Scheme 5 Living cationic chain growth polymerization of $Cl_3P{=}NSiMe_3$.

Copyright © 2013. Elsevier. All rights reserved.

Comprehensive Inorganic Chemistry II : From Elements to Applications, Elsevier, 2013. ProQuest Ebook Central, http://ebookcentral.proquest.com/lib/inflibnet-ebooks/detail.action?docID=1330977.
Created from inflibnet-ebooks on 2021-02-09 22:27:26.

Several issues relating to this ambient-temperature polymerization are slowly getting resolved. First, the synthesis of the crucial monomer, $Cl_3P{=}NSiMe_3$, has been optimized recently.[21] There are several methods for its preparation (Scheme 7).

Method C, involving the preparation of $Cl_2PN(SiMe_3)_2$ followed by an oxidative chlorination, is a viable preparative procedure of $Cl_3P{=}NSiMe_3$. More recently, a more efficient method of synthesis of this crucial monomer has been discovered. This method involves the reaction of $[Cl_3P{=}N{-}PCl_3]^+[PCl_6]^-$ with one equivalent of 4-(dimethylaminopyridine) (DMAP) to afford $Cl_3P{=}N\text{-}SiMe_3$ along with $DMAP{\cdot}PCl_5$.[21]

The mechanism of polymerization of $Cl_3P{=}NSiMe_3$ has been probed. The initiation step consists of generating the key intermediate, $[Cl_3P{=}N{-}PCl_3]^+[PCl_6]^-$, which rapidly reacts in a chain-growth mechanism by the reaction with $Cl_3P{=}NSiMe_3$ affording the chain, $[Cl_3P{=}N(PCl_2{=}N)_nPCl_3]^+[PCl_6]^-$.[22] The chains are terminated by the addition of $Me_3SiN{=}P(OR)_3$ (Scheme 8).

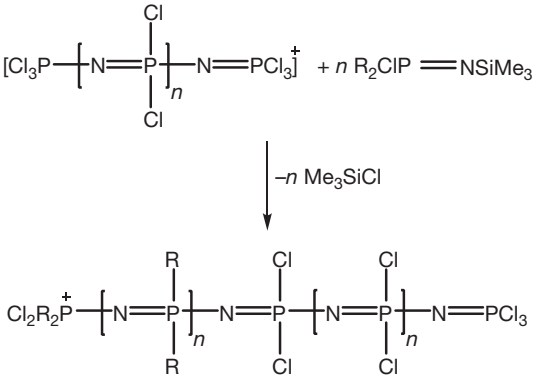

Scheme 6 Synthesis of a diblock copolymer by the reaction of $Me_3SiN{=}PR_2Cl$ with the living polymer obtained from the cationic polymerization of $Cl_3P{=}NSiMe_3$.

Notably, there is minimum chain transfer, leading to a linear living polymer. Recently, efforts to elucidate the mechanism of this polymerization revealed that the living cationic polymerization, while not strictly mono-directional, is faster at one end than the other. Further, it has been suggested that the counteranion $[PCl_6]^-$ can itself initiate oligomerization/polymerization. Presumably, these factors limit the PDIs in not approaching the theoretical value of 1.0 which would be anticipated for a strictly cationic living polymerization.[22]

1.26.2.4 Ambient-Temperature ROP of $N_3P_3Cl_6$

As mentioned above, the reaction of $N_3P_3Cl_6$ with silylium cations (containing weakly coordinating carborane anions) leads to *N*-coordinated adducts ($N{\rightarrow}Si$). Recently, such compounds have been tested for their efficacy as polymerization initiators. Thus, the reaction of $N_3P_3Cl_6$ (in a solution of 1,2-dichloroethane) with 10 mol.% of $[N_3P_3Cl_6{\cdot}SiEt_3]^+[HCB_{11}H_5Br_6]^-$ resulted in the ROP of the former at room temperature. It has been suggested that the *N*-silyl group readily undergoes an intramolecular R_3SiCl elimination generating an incipient $[N_3P_3Cl_5]^+$ cation which initiates the ROP of $N_3P_3Cl_6$.[10,11]

1.26.2.5 Summary

- Poly(dichlorophosphazene), $[NPCl_2]_n$, can be prepared by several routes.
- A high-temperature (~250 °C) ROP of $N_3P_3Cl_6$ (involving about 40% conversion) affords a high-molecular-weight polymer (M_w ~10^6) with a broad-molecular-weight distribution.
- High-temperature (200–250 °C) condensation polymerization of $Cl_3P{=}NP(O)Cl_2$ also affords $[NPCl_2]_n$ via the elimination of $POCl_3$. The polymer obtained has molecular weights ranging from 200 000 to 800 000 with a broad-molecular-weight distribution.

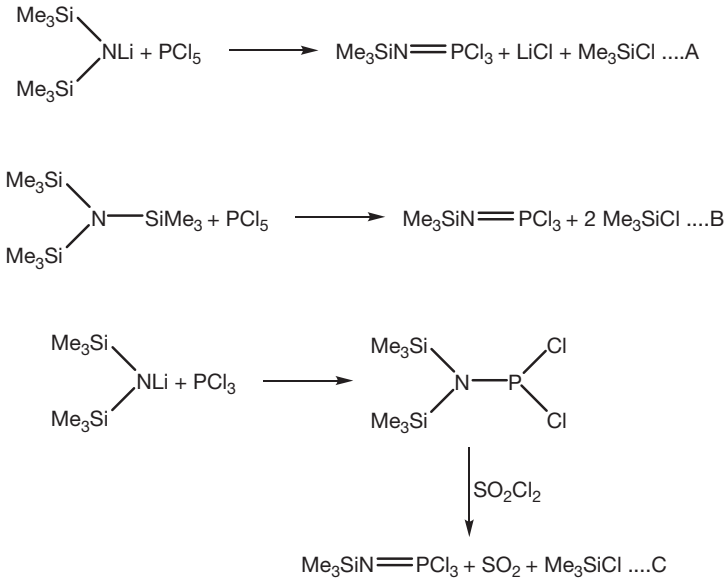

Scheme 7 Various methods for the synthesis of $Cl_3P{=}NSiMe_3$.

Copyright © 2013. Elsevier. All rights reserved.

Comprehensive Inorganic Chemistry II : From Elements to Applications, Elsevier, 2013. ProQuest Ebook Central, http://ebookcentral.proquest.com/lib/inflibnet-ebooks/detail.action?docID=1330977.
Created from inflibnet-ebooks on 2021-02-09 22:27:26.

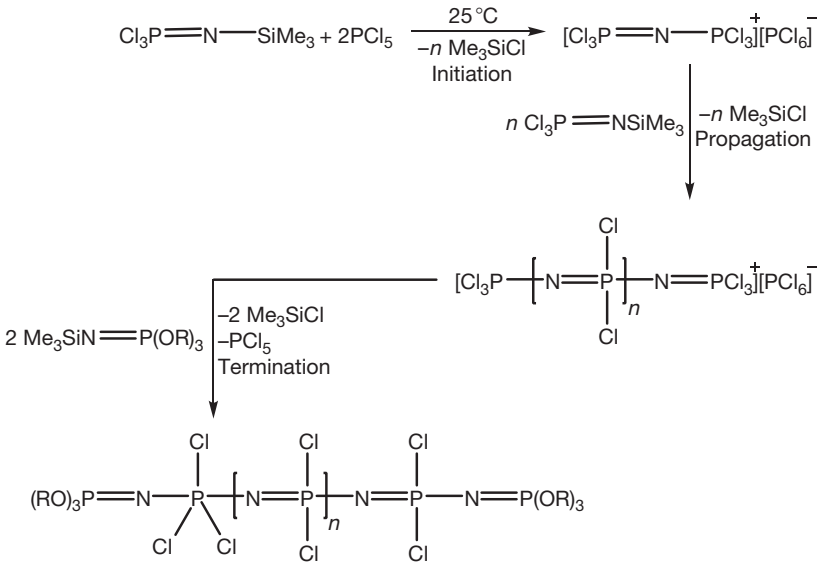

Scheme 8 Mechanism of ambient-temperature synthesis of $[NPCl_2]_n$.

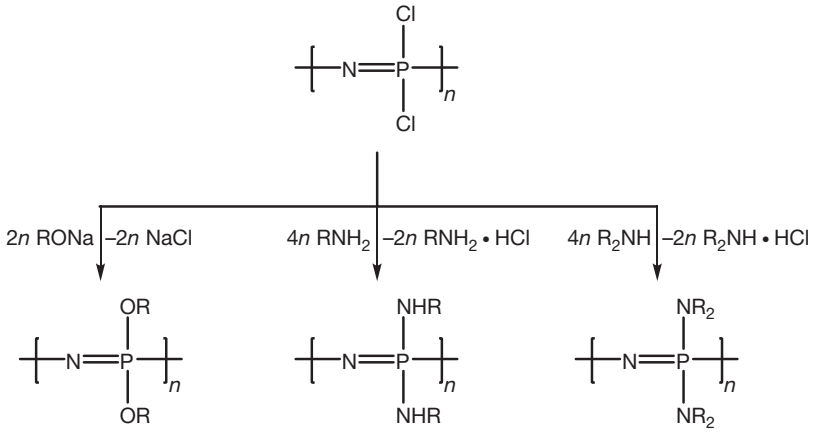

Scheme 9 Macromolecular substitution reactions of poly(dichlorophosphazene), $[NPCl_2]_n$.

- Ambient-temperature chain-growth cationic living polymerization of $Cl_3P{=}NSiMe_3$ affords $[NPCl_2]_n$ with a narrow PDI of 1.1–1.2.
- Ambient-temperature ROP of $N_3P_3Cl_6$ can be initiated by silyl-cyclophosphazene adducts, such as $[N_3P_3Cl_6{\cdot}SiEt_3]^+[HCB_{11}H_5Br_6]^-$. Polymers obtained by this method have an average molecular weight of 10^5 g mol^{-1} and a PDI of 1.8.

1.26.3 Poly(organophosphazene)s

1.26.3.1 Macromolecular Substitution of $[NPCl_2]_n$

As mentioned above, although high-molecular-weight poly(dichlorophosphazene), $[NPCl_2]_n$, can be prepared by various polymerization methods, this polymer is not useful for any practical applications because of its rapid hydrolysis. It has been found, however, that the hydrolytic sensitivity of $[NPCl_2]_n$ is 'not' due to an inherent instability of the inorganic P–N backbone, but rather due to the reactivity of the P–Cl bonds.[1–5] This suggests that macromolecular substitution of $[NPCl_2]_n$ by oxygen and nitrogen nucleophiles can result in hydrolytically stable polymers. However, at a first glance this is a formidable task. Even assuming an average value of 15 000 to be the degree of polymerization of $[NPCl_2]_n$ it would mean nearly 30 000 P–Cl substitutions for 'total' replacement of chlorine atoms in a given polymer chain. The fact that this can be done with a large number of nucleophiles is a testimony to the reactivity of the P–Cl bonds. The original disadvantage of $[NPCl_2]_n$ has thus been turned around as an advantage to introduce diversity in the polyphosphazene family.[1–5] This type of a general 'post-polymerization' modification is quite unique to polyphosphazenes. A typical macromolecular substitution pathway is summarized in **Scheme 9**.[1–7]

Macromolecular substitution of $[NPCl_2]_n$, remarkably successful as it is, still suffers from some drawbacks. One of its limitations is that the substitution reaction is not complete with sterically hindered nucleophiles. For example, the reaction of $[NPCl_2]_n$ with adamantyl amine, -alcohol, or -methanol

Copyright © 2013. Elsevier. All rights reserved.

Comprehensive Inorganic Chemistry II : From Elements to Applications, Elsevier, 2013. ProQuest Ebook Central, http://ebookcentral.proquest.com/lib/inflibnet-ebooks/detail.action?docID=1330977.
Created from inflibnet-ebooks on 2021-02-09 22:27:26.

does not go to completion, but only about 50% of chlorines are substituted.[23] A second and more important limitation is that polyphosphazenes containing alkyl/aryl substituents cannot be prepared by the macromolecular substitution strategy. Reactions of $[NPCl_2]_n$ with Grignard reagents, RMgX, or organolithium reagents, RLi, lead to chain-degradation reactions instead of substitution, owing presumably to the weakening of backbone P–N bonds as a result of nitrogen coordination to the metal ions of the organometallic reagents.[1,2,6,24,25] In view of these limitations, there have been constant efforts to prepare poly(organophosphazene)s by direct methods.

1.26.3.2 Thermal Polymerization of *N*-Silylphosphoranimines

N-Silylphosphoramines of the type $XRR'P{=}NSiMe_3$ ($R{=}R'$, $R{\neq}R'$, X = halogen/alkoxy) can be prepared by a multi-step procedure starting from silylaminophosphanes, $(SiMe_3)_2NPCl_2$ (Schemes 10 and 11).[6]

The reaction sequence includes the oxidation of $(SiMe_3)_2NPR_2$ with bromine, the final product of the reaction being a Me_3SiBr-eliminated phosphoranimine. The phosphoranimine $(Me_3Si)N{=}PR_2Br$ is unsuitable for thermal polymerization.[6] However, upon replacement of the bromine substituent by a trifluoroethoxy group the resultant phosphoranimine, $(CF_3CH_2O)R_2P{=}NSiMe_3$, undergoes smooth thermal polymerization to poly(dimethylphosphazene), $[NPMe_2]_n$ with the elimination of $Me_3SiOCH_2CF_3$. A number of poly(dialkyl-) and poly(alkyl/arylphosphazene)s have been prepared utilizing this condensation polymerization technique. Post-polymerization modification of poly(alkyl/arylphosphazene)s is possible and involves lithiation at the side chain followed by further reactions with suitable substrates (Scheme 12).[6]

The lithiated side chains can be used to initiate polymerization of monomers as diverse as hexamethyldisiloxane, styrene, and methyl methacrylate affording graft copolymers (Chart 5).[6]

The mechanism of the thermal polymerization of *N*-silylphosphoranimines has been suggested to proceed by a chain-growth process and is probably initiated by the heterolytic cleavage of the P–X bond. Until recently, evidence for such phosphoranimine cations was lacking. The reaction of the phosphoranimine $Br(CF_3CH_2O)_2P{=}NSiMe_3$ with various nitrogen bases such as 4-DMAP, 4,4′-bipyridine, or quinuclidine afforded the *N*-donor-stabilized phosphoranimine cations.[26,27] This halide abstraction is facilitated by silver triflate (Scheme 13).

Interestingly, the quinuclidine adduct of the dichlorophosphoranimine cation undergoes further reaction affording a piperidyl-substituted phosphoranimine (Scheme 14).[27]

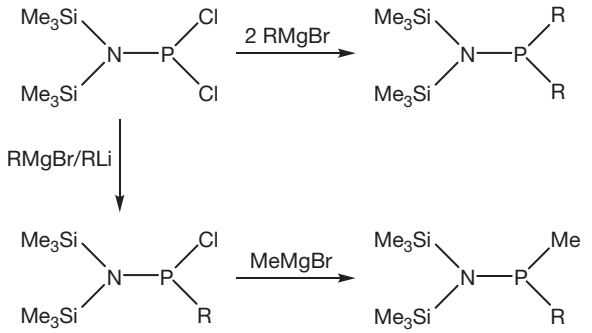

Scheme 10 General synthetic routes for the synthesis of $(SiMe_3)_2NPRR'$ ($R{=}R'$ or $R{\neq}R'$) from $(SiMe_3)_2NPCl_2$.

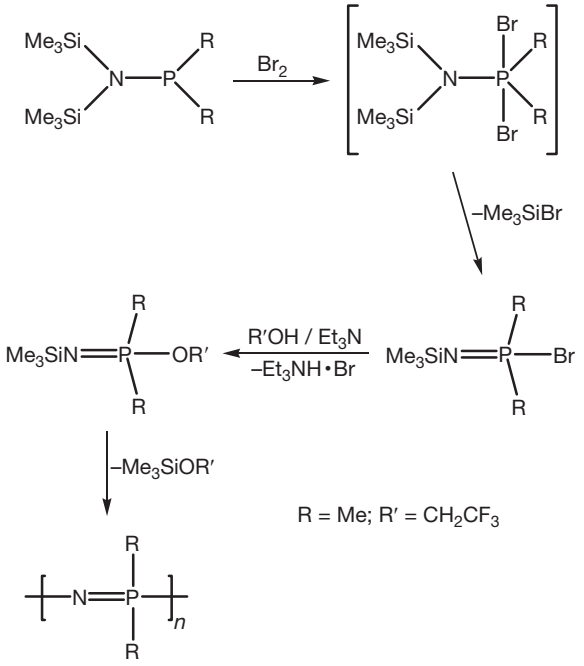

Scheme 11 Preparation of $[NPMe_2]_n$.

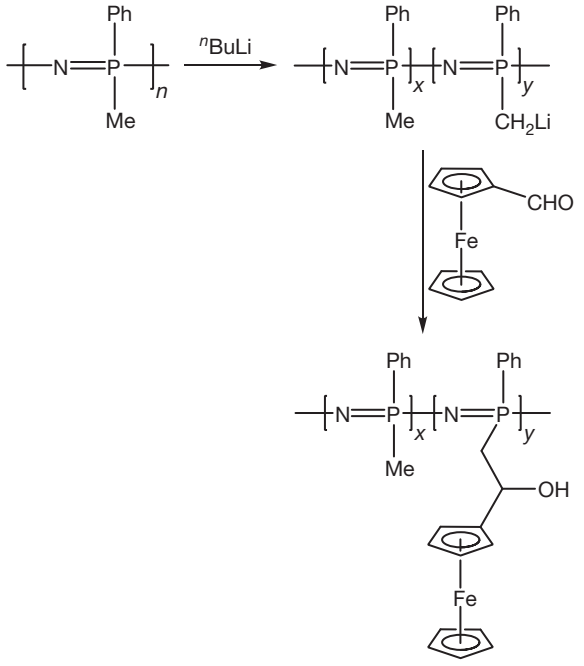

Scheme 12 Post-polymerization modification of poly(alkyl/arylphosphazene)s by the lithiation of side chains.

Copyright © 2013. Elsevier. All rights reserved.

Comprehensive Inorganic Chemistry II : From Elements to Applications, Elsevier, 2013. ProQuest Ebook Central, http://ebookcentral.proquest.com/lib/inflibnet-ebooks/detail.action?docID=1330977.
Created from inflibnet-ebooks on 2021-02-09 22:27:26.

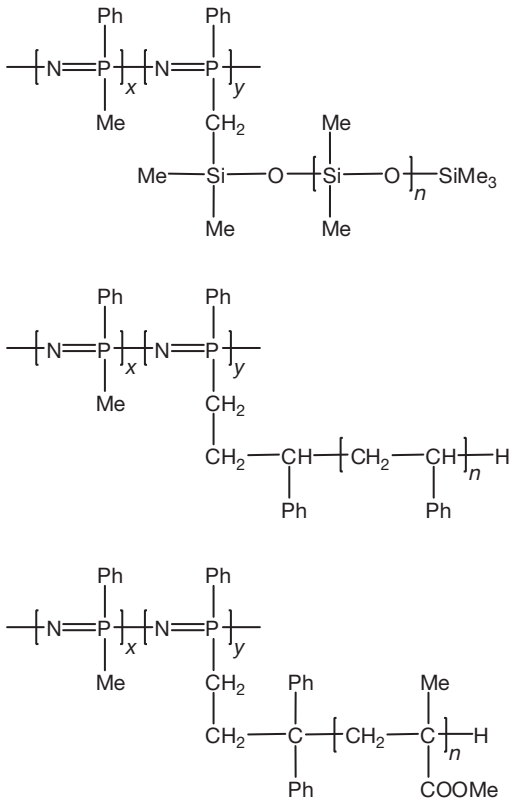

Chart 5 Graft copolymers on a poly(alkyl/arylphosphazene) backbone.

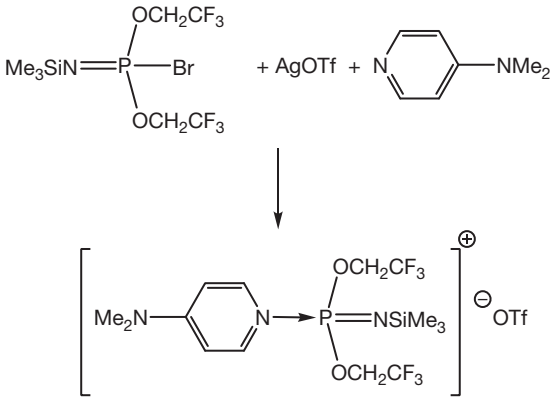

Scheme 13 Synthesis of a phosphoranimine cation stabilized by dimethylaminopyridine.

In a more recent development, several phosphane-stabilized phosphoranimine cations $[R_3P{\cdot}PR'{=}NSiMe_3]^+$ have been prepared by the direct reactions involving tertiary phosphanes and $BrMe_2P{=}NSiMe_3$ or $Br(CF_3CH_2O)_2P{=}NSiMe_3$.[28,29]

N-Silylphosphoranimines containing alkoxy substituents on phosphorus can be polymerized by an anionic polymerization methodology, initiated by $^nBu_4NF$ (Scheme 15).[30]

1.26.3.3 Ambient-Temperature Phosphite-Mediated Chain Growth Condensation Polymerization

In contrast to the high temperatures that are required to effect the elimination of $Me_3SiOCH_2CF_3$ from monomers such as $(Ph)(Me)(OCH_2CF_3)P{=}NSiMe_3$ giving rise to the polymer $[(Ph)(Me)P{=}N]_n$, recently a new ambient-temperature polymerization reaction has been described.[31] Accordingly, stoichiometric amounts of trimethylphosphite, $P(OMe)_3$, has been shown to effect the polymerization of *N*-silyl(halogeno) organophosphoranimines such as $BrRR'P{=}NSiMe_3$ in solvents such as chloroform affording $[RR'P{=}N]_n$ as reasonably high-molecular-weight polymers ($\sim 10^5$) (Scheme 16).[31]

Many different types of polymers were obtained by this methodology. These include polymers containing unsaturated side groups (Chart 6).[31]

Interestingly, the trichlorophosphoranimine, $Cl_3P{=}NSiMe_3$, could not be polymerized by using $P(OR)_3$. In addition, phosphite-initiated polymerization does not appear to be suitable for preparing block copolymers. However, random copolymers such as $\{(Ph)(Me)P{=}N\}_a\{(Ph)(^nBu)P{=}N\}_b$ could be prepared by using this method.[31]

1.26.3.4 Summary

1. Macromolecular substitution on poly(dichlorophosphazene), $[NPCl_2]_n$, by oxygen and nitrogen nucleophiles affords, in most cases, fully substituted poly(organophosphazene)s, $[NPR_2]_n$. However, reactions with sterically hindered nucleophiles result in partial substitution.
2. Poly(alkyl/arylphosphazene)s cannot be prepared by the reactions of Grignard/organolithium reagents with $[NPCl_2]_n$; instead, in these reactions chain scission products are formed. Poly(alkyl/aryl phosphazene)s, $[(R)(R')P{=}N]_n$, can be prepared by a thermal polymerization of *N*-silyl phosphoranimines or by a phosphite-catalyzed reaction at ambient temperature.

1.26.4 Structure and Properties of Polyphosphazenes

1.26.4.1 X-Ray Diffraction

X-ray diffraction studies on polyphosphazenes have been surprisingly limited.[1–5] It is therefore difficult to draw general conclusions. Two different chain conformations have been suggested for polyphosphazenes, the *trans–trans*-planar and the *cis–trans*-planar (Chart 7).[1–5]

In the *trans–trans*-planar conformation, with respect to every P–N bond, the immediate 'chain' neighboring atoms N and P are *trans*. The overall chain is present in a planar arrangement. In the *cis–trans*-planar arrangement with respect to one of the P–N bonds, the chain neighbors N and P are in a *cis* disposition; the adjacent P–N bond has a *trans* arrangement of the chain neighboring atoms (Chart 7). Thus, in this conformation, the polymer chain has alternately a *cis* P–N followed by a *trans* P–N motif. X-ray diffraction data for $[NPCl_2]_n$, $[NPF_2]_n$, $[NP(CH_3)_2]_n$, and $[NP(^nPr)_2]_n$ strongly support the *cis–trans*-planar conformation for these polymers.[1,2] This conformation is also the most favored one from a steric point of view since the steric repulsion between the substituents on alternate phosphorus atoms is minimized. Table 1 summarizes the metric parameters of some of the polyphosphazenes.[1–3]

Copyright © 2013. Elsevier. All rights reserved.

Comprehensive Inorganic Chemistry II : From Elements to Applications, Elsevier, 2013. ProQuest Ebook Central, http://ebookcentral.proquest.com/lib/inflibnet-ebooks/detail.action?docID=1330977.
Created from inflibnet-ebooks on 2021-02-09 22:27:26.

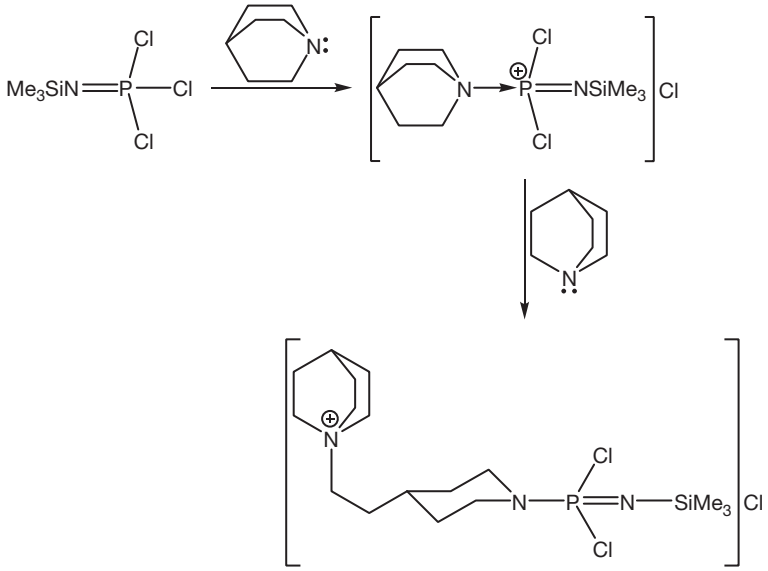

Scheme 14 Synthesis and reactivity of an unstable quinuclidine adduct of the dichlorophosphoranimine cation.

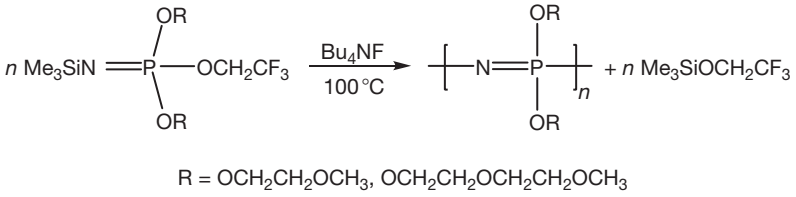

Scheme 15 Anionic polymerization of *N*-silylphosphoranimines.

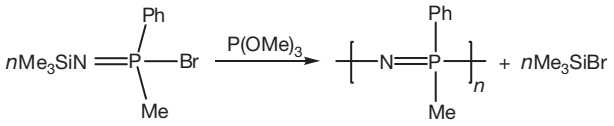

Scheme 16 Polymerization of *N*-silyl(halogeno) organophosphoranimines using $P(OMe)_3$

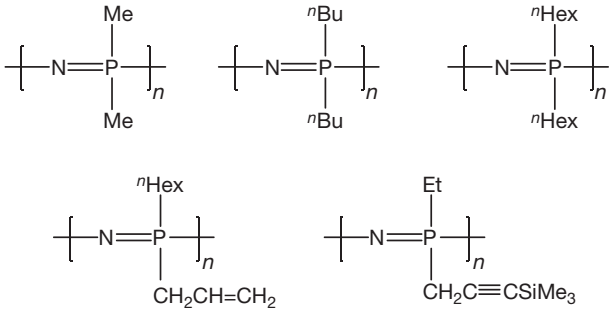

Chart 6 Various polymers prepared by the phosphite-mediated room-temperature polymerization of *N*-silyl(halogeno) organophosphoranimines.

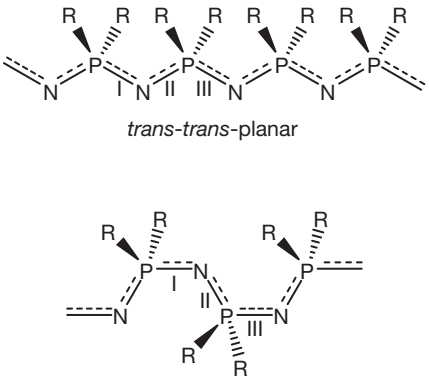

Chart 7 Chain conformations suggested for polyphosphazenes.

The x-ray data reveal that the P–N bond distances in poly (alkylphosphazene)s are longer (1.59–1.62 Å) compared to poly(halogenophosphazene)s. In $[NPF_2]_n$, the P–N bond distance is 1.52 Å. Two different measurements on $[NPCl_2]_n$ reveal slight variations in the metrical parameters; while one of these pegs the P–N distance at 1.52 Å, the other gives a short distance of 1.44 Å and a long distance of 1.67 Å. In spite of the limited data, it is clear that the P–N distances in the polymers are not very different from those found in the ring systems

Copyright © 2013. Elsevier. All rights reserved.

Comprehensive Inorganic Chemistry II : From Elements to Applications, Elsevier, 2013. ProQuest Ebook Central, http://ebookcentral.proquest.com/lib/inflibnet-ebooks/detail.action?docID=1330977.
Created from inflibnet-ebooks on 2021-02-09 22:27:26.

Table 1 Chain conformation, bond lengths, and bond angles for some polyphosphazenes

Polymer	*Polymer conformation*	*P=N bond distance (Å)*	*P–X bond distance (Å)*	*N–P–N bond angle (°)*	*P–N–P bond angle (°)*
$[NPCl_2]_n$	*Cis–trans*-planar	1.52	1.96	118	141.5
$[NPCl_2]_n$	*Cis–trans*-planar	1.44, 1.67	1.97, 2.04	115	131
$[NPF_2]_n$	*Cis–trans*-planar	1.52	1.47	119	136
$[NP(CH_3)_2]_n$	*Cis–trans*-planar	1.59, 1.56	1.80	112.5	135.9
$[NP(^nPr)_2]_n$	*Cis–trans*-planar	1.59	1.80	114.2	132.6

Table 2 Glass-transition temperatures of some representative polyphosphazenes

Polymer	T_g *(°C)*
$[NPF_2]_n$	−95
$[NPCl_2]_n$	−66
$[NP(OCH_2CH_2\ OCH_2CH_2OCH_3)_2]_n$	−84
$[NP(OCH_3)_2]_n$	−74
$[NP(OCH_2CF_3)_2]_n$	−66
$[NP(OC_6H_5)_2]_n$	−8
$[NP(CH_3)_2]_n$	−46
$[NP(Ph)(CH_3)]_n$	+37
$[NP(NHMe)_2]_n$	+14
$[NP(NHPh)_2]_n$	+91
$[NP(NHAd)(OCH_2CF_3)]_n$	+180

(cf. $N_3P_3Cl_6$, 1.58 Å; $N_3P_3F_6$, 1.57 Å; $N_4P_4Me_8$, 1.59 Å). One important feature of the structural data is that while the N–P–N bond angles are close to 120° (between 114° and 119°), similar to what is generally found in cyclophosphazenes, the angles at nitrogen (P–N–P) are considerably widened (132–141°), presumably to accommodate the more favorable *cis–trans*-planar configuration. It will be desirable to obtain more data on polyphosphazenes that will throw light on the influence of the substituents on the polymer conformation and metrical parameters.

1.26.4.2 ^{31}P Nuclear Magnetic Resonance

^{31}P nuclear magnetic resonance (NMR) is an important tool for the structural characterization of polyphosphazenes. In general, the ^{31}P NMR chemical shifts of polyphosphazenes are 20–30 ppm upfield shifted with respect to the corresponding ring systems (cf. $N_3P_3Cl_6$, +19.3 ppm; $[NPCl_2]_n$, −20.0 ppm; $N_3P_3(OPh)_6$, +8.3 ppm; $[NP(OPh)_2]_n$, −19.7 ppm; $N_3P_3(NHMe)_6$, +23.0 ppm; $[NP(NHMe)_2]_n$, +3.9 ppm).[1–7]

1.26.4.3 Skeletal Flexibility and Glass-Transition Temperatures

Polyphosphazenes can be considered as remarkably flexible polymers and in general have low T_g's.[1–7] T_g data for some representative polyphosphazenes are summarized in Table 2.[1–7]

The degree of torsional flexibility observed in polyphosphazenes is presumably due to two factors. First, in comparison to the average C–C bond distance of about 1.54 Å (in organic polymers with a C–C backbone) the average P–N distance is higher (1.59 Å). This enhanced distance allows greater torsional freedom. Second, unlike in organic polymers, where every atom of the backbone has a substituent, in polyphosphazenes only alternate atoms in the backbone, namely, the phosphorus atoms, bear the substituents. Thus, more free volume is available for the polymer for its chain to exhibit skeletal mobility. Finally, the wider bond angles at nitrogen in polyphosphazenes also appear to favor greater torsional freedom.

Although, inherently, for reasons explained above, the P–N backbone in polyphosphazenes is expected to possess considerable skeletal flexibility (as reflected in low T_g's), the substituents on phosphorus also play an important role in modulating this effect. Thus, the presence of small-sized substituents and those that are likely to have poor intermolecular interactions leads to low T_g's (cf. $[NPF_2]_n$, −95 °C; $[NPCl_2]_n$, −66 °C; $[NP(OCH_3)_2]_n$, −74 °C; $[NP(OCH_2CF_3)_2]_n$, −66 °C). Also, substituents that themselves possess flexibility tend to decrease the T_g (cf. $[NP(OCH_2CH_2OCH_2CH_2OCH_3)_2]_n$, −84 °C). Increase in the rigidity of substituents enhances the T_g (cf. $[NP(OC_6H_5)_2]_n$, −8 °C; $[NP(Ph)(CH_3)]_n$, +37 °C).[1–3] Finally, substituents that can be involved in intermolecular interactions lead to enhanced T_g's (cf. $[NP(NHMe)_2]_n$, +14 °C; $[NP(NHPh)_2]_n$, +91 °C; $[NP(NHAd)(OCH_2CF_3)]_n$, +180 °C).[1–3]

1.26.4.4 Applications

Polyphosphazenes have not acquired large-scale commercial applications. However, because of their unique structural features several niche applications are possible. In recent years, there has been considerable focus on the biomedical applications of polyphosphazenes.[1–5]

The unique structural features of polyphosphazenes allow properties such as flame retardancy and low-temperature flexibility. Highly flexible poly(trifluoroethoxyphosphazene), $[NP(OCH_2CF_3)_2]_n$ (T_g, −66 °C), and a mixed-substituent variant, $[NP(OCH_2CF_3)(OCH_2(CF_2)_3CF_2H)]_n$ (T_g, −70°), are viewed as unusual elastomers because coupled with their low T_g's they are extremely resistant to hydrocarbon fluids. Thus, O-rings and gaskets made from these materials are of potential interest in the petroleum industry. The hydrophobicity of $[NP(OCH_2CF_3)_2]_n$ (comparable to Teflon) and its bioinert nature make this polymer an attractive target for being used in fabrication of artificial body organs such as cardiovascular parts. Recently, superhydrophobic nanofibers of $[NP(OCH_2CF_3)_2]_n$ have been assembled and their applications are being explored.[32,33]

The nitrogen atoms of the backbone of polyphosphazenes are sufficiently basic; this property has not been sufficiently utilized. In one example, the polymer $[NP(NHMe)_2]_n$ has been shown to bind to $PtCl_2$, presumably in a *cis* coordination mode

Copyright © 2013. Elsevier. All rights reserved.

Comprehensive Inorganic Chemistry II : From Elements to Applications, Elsevier, 2013. ProQuest Ebook Central, http://ebookcentral.proquest.com/lib/inflibnet-ebooks/detail.action?docID=1330977.
Created from inflibnet-ebooks on 2021-02-09 22:27:26.

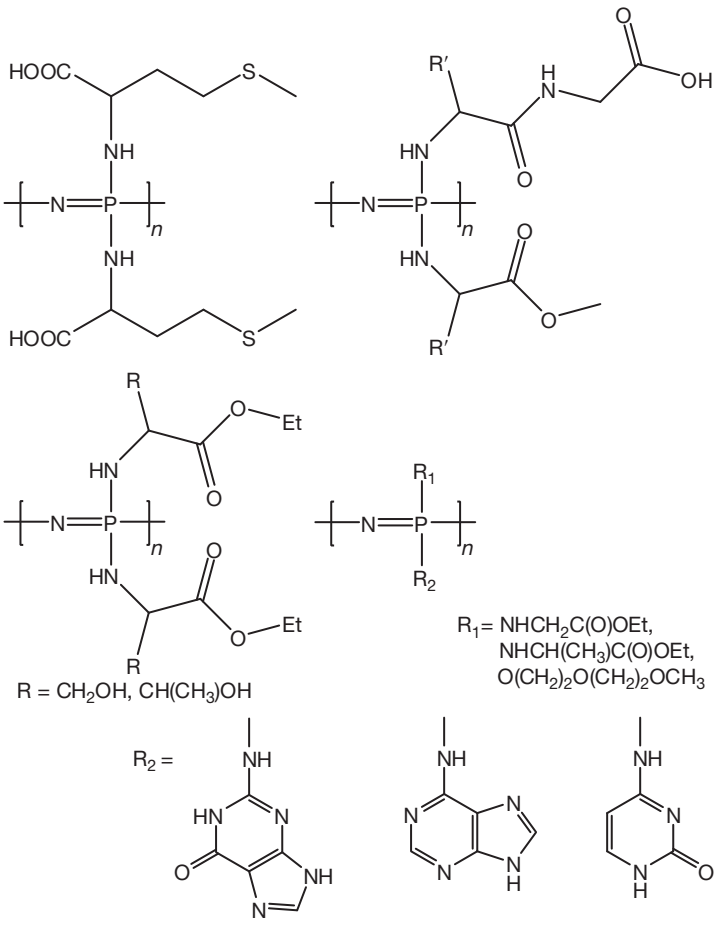

Chart 8 Polyphosphazenes containing biologically relevant side groups.

involving two skeletal nitrogen atoms.[34] In another example, poly(methylphenylpolyphosphazene), $[NP(Me)Ph]_n$, has been shown to stabilize gold nanoparticles as a result of their interaction with the basic nitrogen centers of the polymer backbone.[35]

Unlike conventional polymers, polyphosphazenes can be modified to suit specific applications by varying the nature of the substituents on phosphorus. Examples of this approach are illustrated by two potential applications.

1.26.4.5 Biomedical Applications

Polyphosphazenes containing biologically relevant side groups can be readily prepared by the macromolecular substitution strategy discussed above.[36–43] Thus, polyphosphazenes containing residues of amino acids, sugars, purines, and pyrimidines have been synthesized (**Chart 8**).[41]

Among these polymers, those containing amino acid ester side groups such as $[NP(NHCH_2COOEt)_2]_n$ and $[NP(NHCH(R)COOEt)_2]_n$ degrade in biological media affording biocompatible products such as ammonia, phosphate, amino acid, and ethanol.[42,43] Such polymers and their modified analogs could be used as advanced biological materials for sutures or drug-delivery systems. In order to improve their mechanical stability, increase of their T_g's by appropriate substituents has been attempted. Recognizing that biocompatible substituents would render such polymers useful, polyphosphazenes containing vitamin E, vitamin L, and vitamin B_6 along with amino acid ester side groups have been prepared. It has been reported that some members of this family show good promise as candidates for biotissue engineering (**Chart 9**).[36]

Similarly, polyphosphazene-(nano-hydroxy apatite) composite microspheres have been found to be good scaffolds for bone tissue engineering.[44]

1.26.4.6 Other Advanced Material Applications

Appropriately substituted polyphosphazenes have potential applications as several advanced materials such as polymer electrolytes and new photonic materials and these aspects have also been explored. The polymer $[NP(OCH_2CH_2OCH_2CH_2OCH_3)_2]_n$ (MEEP) containing etheroxy side units is an amorphous polymer ($T_g = -84\,^{\circ}C$).[45] This polymer and many related polymers of this type have been shown as excellent lithium-ion conductors (10^{-5}–10^{-4} S cm^{-1}).[46–49] Recently, layer-by-layer (LbL) assembled films of MEEP and poly(acrylic acid) (PAA) have been shown to possess very high ionic (proton) conductivity of 7×10^{-4} S cm^{-1} under fully humidified conditions at a pH of 3.5 which offers scope for the utility of such hybrid materials in devices such as fuel cells.[50]

Copyright © 2013. Elsevier. All rights reserved.

Comprehensive Inorganic Chemistry II : From Elements to Applications, Elsevier, 2013. ProQuest Ebook Central, http://ebookcentral.proquest.com/lib/inflibnet-ebooks/detail.action?docID=1330977.
Created from inflibnet-ebooks on 2021-02-09 22:27:26.

1.26.4.7 Organic Polymers Containing Cyclophosphazene Pendant Groups

In contrast to polyphosphazenes which contain an inorganic P–N backbone and organic side chains, a different type of polymer family can be envisaged where an organic (C–C backbone) polymer contains inorganic cyclophosphazene groups as pendant side chains. Cyclophosphazenes containing vinyl groups are precursors to such hybrid polymeric systems.[51–70] Several types of monomers have been prepared for this purpose (**Chart 10**).

Detailed polymerization studies on these systems revealed that many of the fluoro-cyclophosphazene monomers such as $N_3P_3F_5[C(Me)=CH_2]$ cannot be homopolymerized.[64] Two factors seem to mitigate against the homopolymerization process. First, the cyclophosphazene ring is σ-electron withdrawing. This results in a reduction of electron density in the vinyl moiety and makes it difficult to be polymerized (by free radical initiators). On the other hand, placing an electron-releasing group directly on the olefin[65,66] makes it sterically bulky which also prevents homopolymerization. Although homopolymerization was unsuccessful, such monomers could be readily copolymerized with a variety of organic monomers such as styrene and methylmethacrylate (MMA) to afford random copolymers[64–66] (**Chart 11**) with M_w of ~100 000 and with PDIs

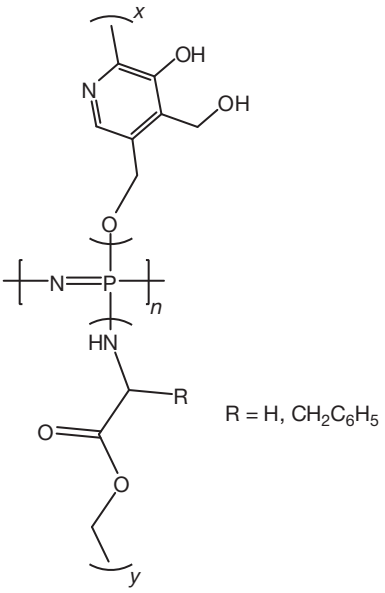

Chart 9 Examples of polyphosphazenes that are of potential interest in biotissue engineering.

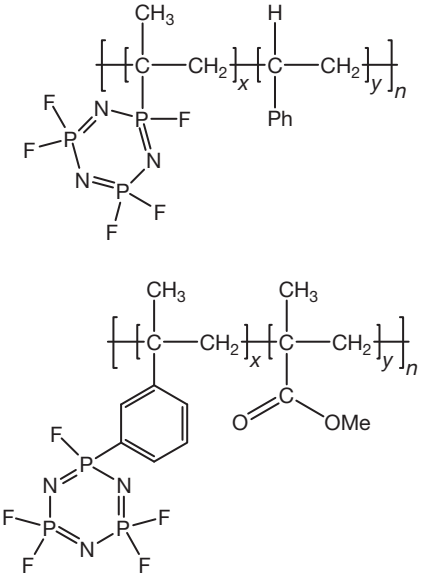

Chart 11 Copolymers obtained by the polymerization of $N_3P_3F_5[C(Me)=CH_2]$ and organic monomers such as styrene and MMA.

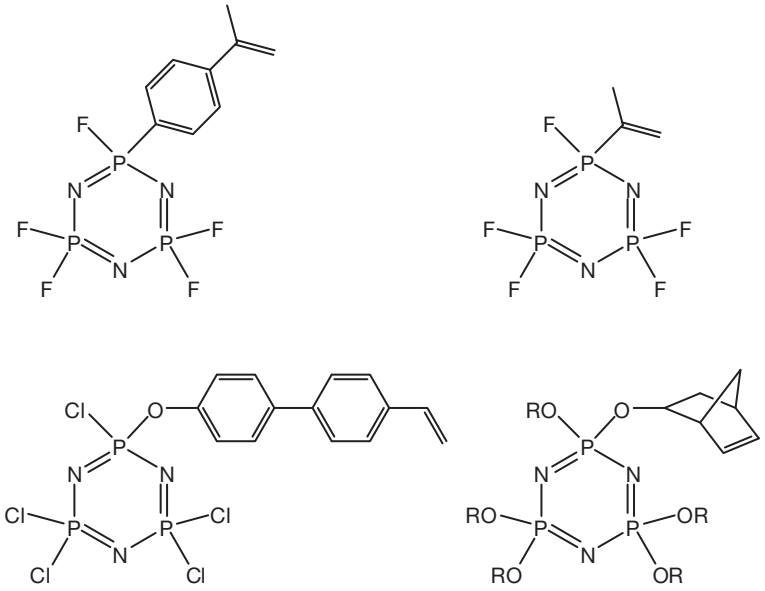

Chart 10 Cyclophosphazenes containing vinyl groups.

Copyright © 2013. Elsevier. All rights reserved.

Comprehensive Inorganic Chemistry II : From Elements to Applications, Elsevier, 2013. ProQuest Ebook Central, http://ebookcentral.proquest.com/lib/inflibnet-ebooks/detail.action?docID=1330977.
Created from inflibnet-ebooks on 2021-02-09 22:27:26.

ranging from 1.1 to 1.7. The extent of cyclophosphazene incorporation in these copolymers varies; for example, a maximum incorporation of 38% is found with $N_3P_3F_5[C(Me)=CH_2]$ in its styrene copolymer.[63] Interestingly, all of these polymers have flame-retardant properties and are in fact self-extinguishing.

The presence of a spacer group between the cyclophosphazene ring and the polymerizable vinyl group considerably enhances the opportunity for homopolymerization. Thus, $N_3P_3X_5(O\text{-}p\text{-}C_6H_4\text{-}p\text{-}C_6H_4\text{-}p\text{-}CH=CH_2)$ (X=F, Cl) could be readily homopolymerized to afford thermally stable polymers.[61,68,69] $N_3P_3Cl_5(O\text{-}p\text{-}C_6H_4\text{-}p\text{-}C_6H_4\text{-}p\text{-}CH=CH_2)$ can also be copolymerized along with styrene and methyl methacrylate to give copolymers which are flame resistant and have good thermal stability[70] (**Scheme 17**).

Utilizing the approaches known in cyclophosphazenes, carbophosphazene pendant polymers have also been prepared and characterized (**Scheme 18**).[71]

Some of the applications of cyclophosphazene pendant polymers include their utility as polymer-solid electrolytes[72–74] and polymeric ligands.[75–79]

1.26.5 Heterocyclophosphazenes

Heterocyclophosphazenes are compounds that contain one or more heteroatoms such as C, S, B, Al, or even transition metals in the P–N skeleton.[1] Some heterocyclophosphazenes, particularly those containing C and S, have been shown to be precursors for the corresponding linear polymers.[1] In this section, some of these heterocyclophosphazenes are discussed.

1.26.5.1 Cyclocarbophosphazenes

Cyclocarbophosphazenes are inorganic heterocyclic rings that contain P, N, and C in a closed ring system.[79–85] Representative examples of this family of compounds are shown in **Chart 12**.

The pentachlorocyclocarbophosphazene, $N_3P_2CCl_5$, can be prepared by several methods, although the reaction of cyanamide with $[Cl_3P=N=PCl_3]^+[Cl]^-$ appears to be a good route for preparing this compound (**Scheme 19**).[86,87]

Recently, the reaction of $[Cl_3P=N\text{–}PCl_2=N=PCl_3][Cl]$ with bis(trimethylsilyl)carbodiimide, $Me_3SiN=C=NSiMe_3$, has been reported to afford a 16-membered macrocycle along with the eight-membered $[NCCl(NPCl_2)_3]$ (**Scheme 20**).[88]

The molecular structure of the pentachlorocyclocarbophosphazene has been determined.[86,87] The six-membered ring is nearly planar. While only one type of C–N distance (~1.33 Å) is found, two P–N distances are observed; the one flanking the C–N bond is slightly longer (1.61 Å) in comparison to the other P–N distance (1.58 Å), the latter value being similar to what is observed in $N_3P_3Cl_6$. The reactions of pentachlorocarbophosphazene with various nucleophiles afford fully

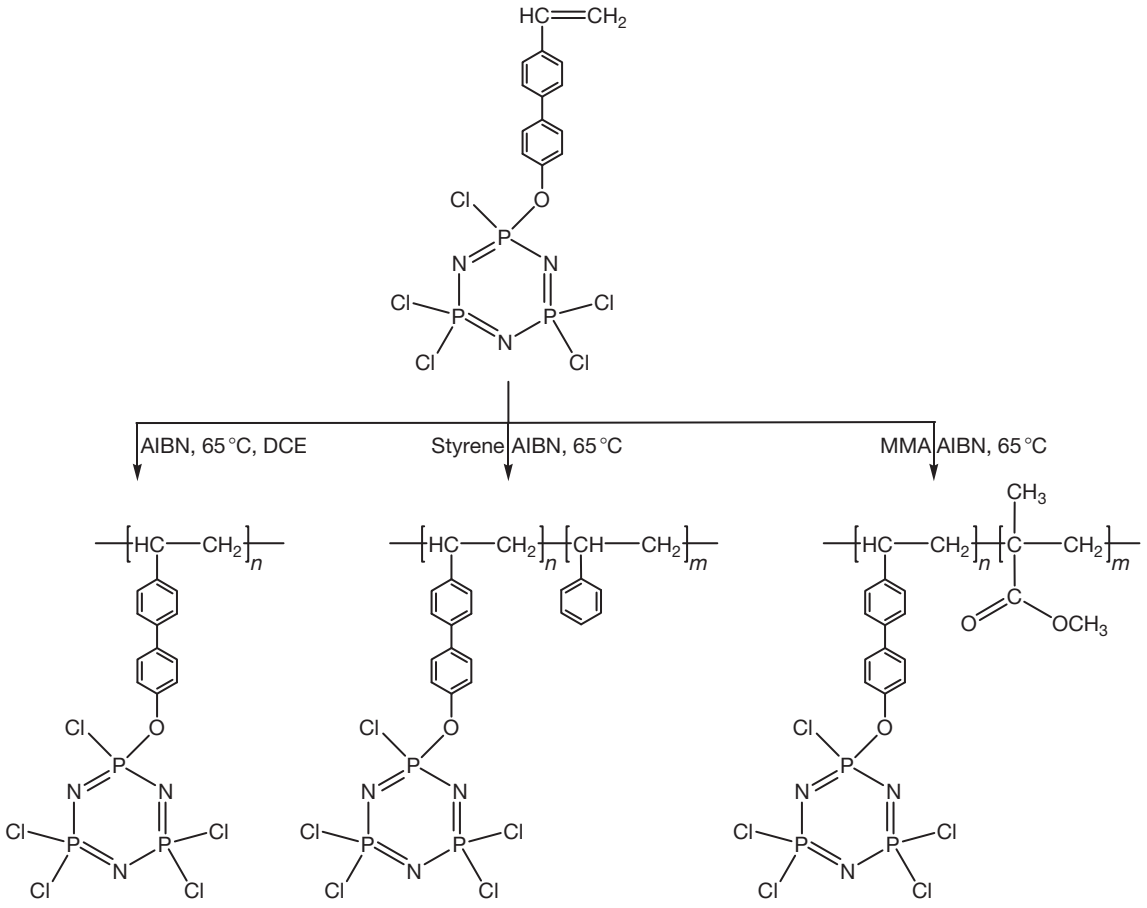

Scheme 17 Homo- and copolymerization of $N_3P_3Cl_5(O\text{-}p\text{-}C_6H_4\text{-}p\text{-}C_6H_4\text{-}p\text{-}CH=CH_2)$.

Copyright © 2013. Elsevier. All rights reserved.

Comprehensive Inorganic Chemistry II : From Elements to Applications, Elsevier, 2013. ProQuest Ebook Central, http://ebookcentral.proquest.com/lib/inflibnet-ebooks/detail.action?docID=1330977.
Created from inflibnet-ebooks on 2021-02-09 22:27:26.

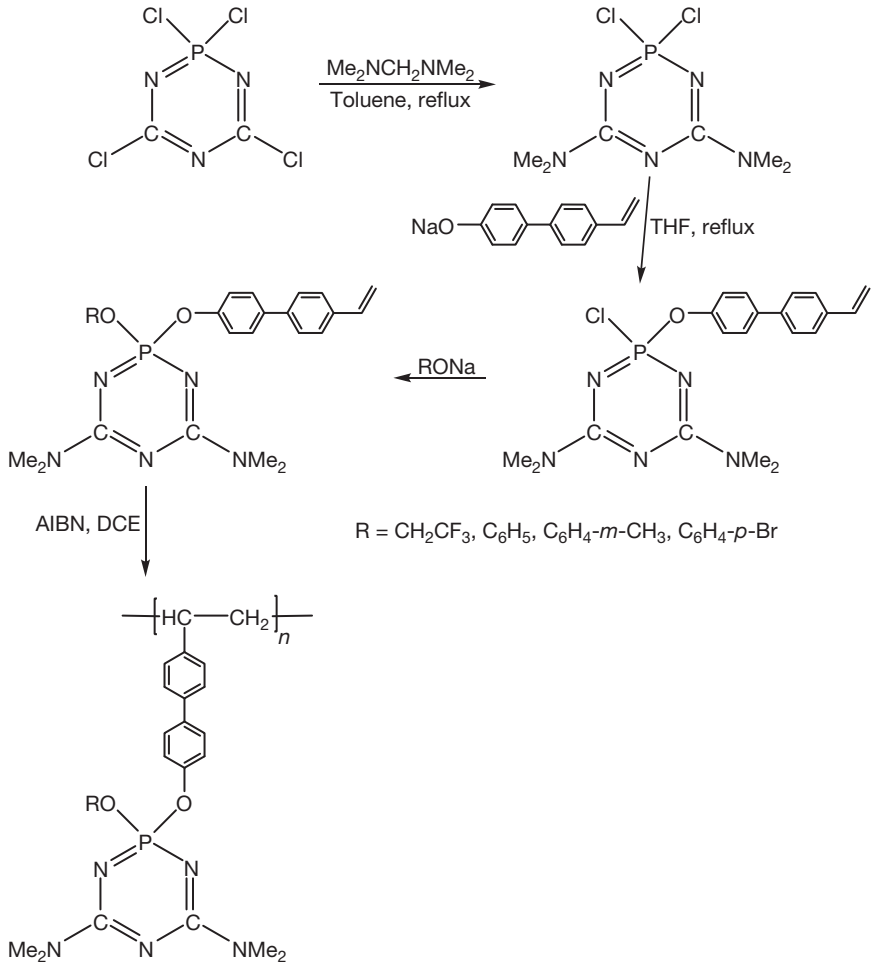

Scheme 18 Synthesis of polymers containing cyclocarbophosphazene pendant groups.

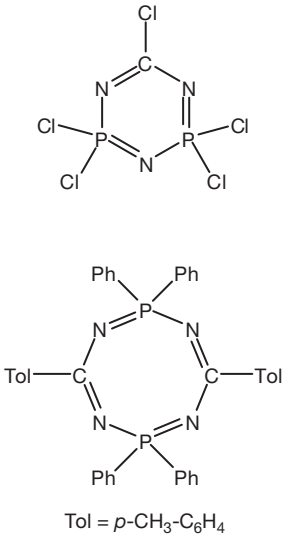

Chart 12 Representative examples of cyclocarbophosphazenes.

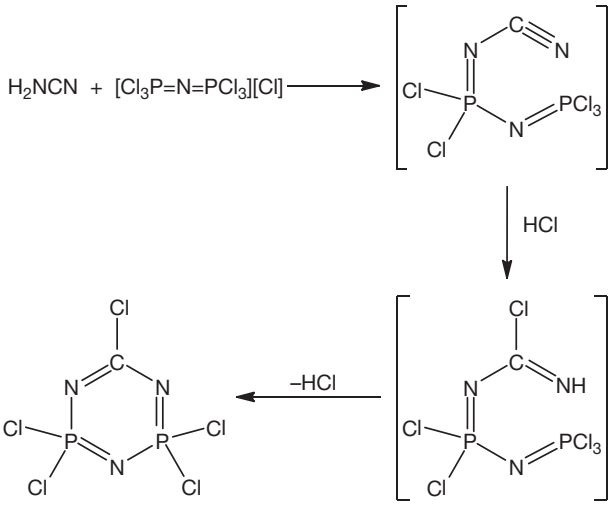

Scheme 19 Synthesis of $N_3P_2CCl_5$ starting from cyanamide.

Copyright © 2013. Elsevier. All rights reserved.

Comprehensive Inorganic Chemistry II : From Elements to Applications, Elsevier, 2013. ProQuest Ebook Central, http://ebookcentral.proquest.com/lib/inflibnet-ebooks/detail.action?docID=1330977.
Created from inflibnet-ebooks on 2021-02-09 22:27:26.

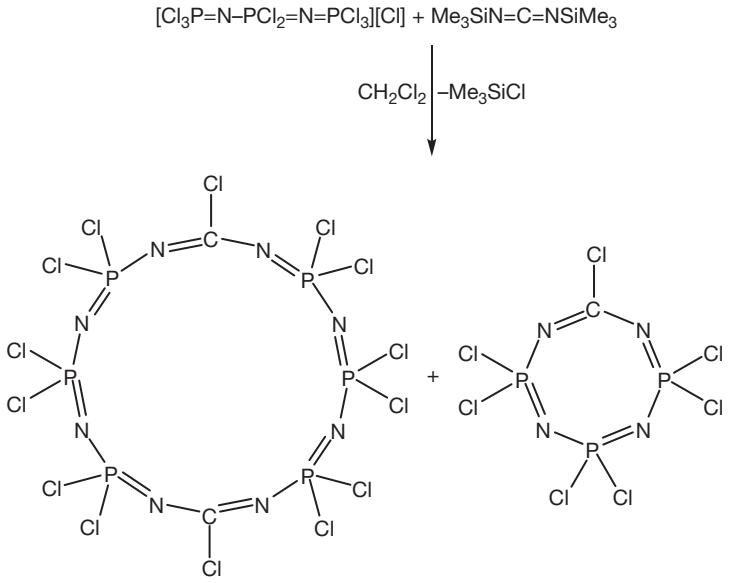

Scheme 20 Synthesis of 16- and 8-membered cyclocarbophosphazenes.

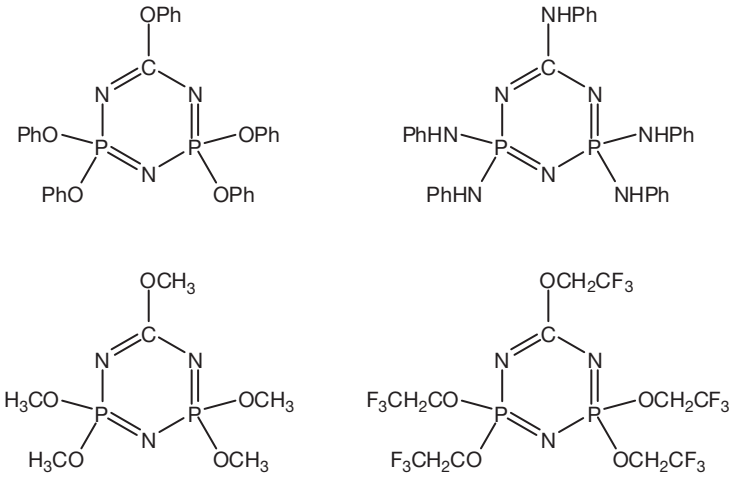

Chart 13 Substituted carbophosphazenes obtained by the reaction of $N_3P_2CCl_5$ with various nucleophiles.

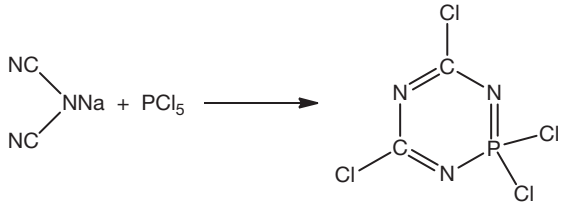

Scheme 21 Synthesis of $[(ClCN)_2(NPCl_2)]$.

substituted derivatives.[89,90] Some examples of such compounds are shown in Chart 13.

The tetrachlorodicarbophosphazene, $[(ClCN)_2(NPCl_2)]$, can be prepared in a reaction involving the sodium salt of dicyanamide with PCl_5 (Scheme 21).[91]

Investigation of the reactions of $[(ClCN)_2(NPCl_2)]$ revealed an interesting regiospecific substitution reaction with tertiary amines which is accompanied by a C–N bond cleavage. For example, the reaction of $[(ClCN)_2(NPCl_2)]$ with diazabicyclooctane (DABCO) occurs at the carbon centers as shown in Scheme 22.[83] On the other hand, the reaction of $[(ClCN)_2(NPCl_2)]$ with guanidine proceeds to afford regiospecific substitution at phosphorus (Scheme 23).[85]

1.26.5.2 Thio- and Thionylcyclophosphazenes

The two important six-membered rings of this family are the pentachlorothiocyclotriphosphazene, $[(ClSN)(NPCl_2)_2]$[92,93], and -thionylcyclotriphosphazene, $[(ClS(O)N)(NPCl_2)_2]$[94–96] (Chart 14).

The thiocyclotriphosphazene, $[(ClSN)(NPCl_2)_2]$, is prepared by the reaction of bis(trimethylsilyl)sulfurdiimide $S[N(SiMe_3)_2]$ with PCl_5 or $[Cl_3P{=}N{=}PCl_3]^+[Cl]^-$ (Scheme 24).[95]

Copyright © 2013. Elsevier. All rights reserved.

Comprehensive Inorganic Chemistry II : From Elements to Applications, Elsevier, 2013. ProQuest Ebook Central, http://ebookcentral.proquest.com/lib/inflibnet-ebooks/detail.action?docID=1330977.
Created from inflibnet-ebooks on 2021-02-09 22:27:26.

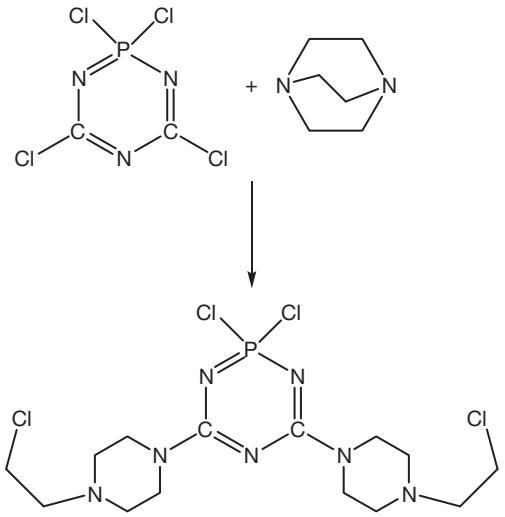

Scheme 22 Reaction of $[(ClCN)_2(NPCl_2)]$ with DABCO.

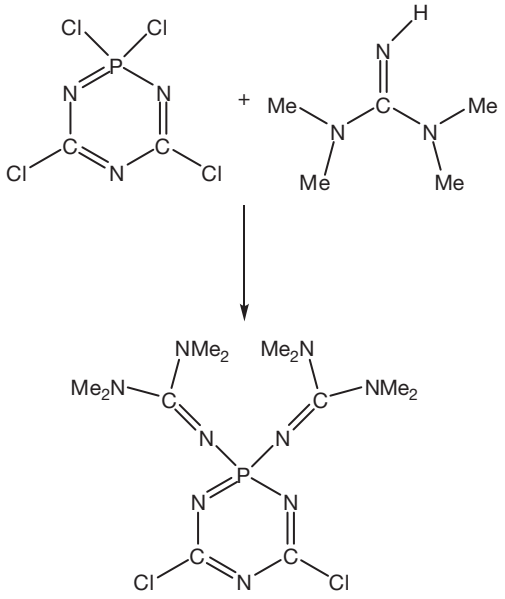

Scheme 23 Reaction of $[(ClCN)_2(NPCl_2)]$ with guanidine.

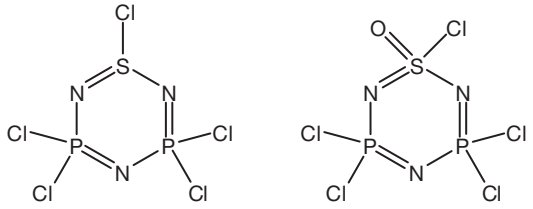

Chart 14 Pentachlorothiocyclotriphosphazene and pentachlorothionylcyclotriphosphazene.

On the other hand, the S(VI)-containing thionylphosphazene is prepared by a three-step process (Scheme 25).[99]

An interesting observation has been that the thermal treatment of $[\{NS(O)Cl\}\{NPCl_2)_2\}]$ leads to the formation of large 12- and 24-membered N–P–S(O) macrocyclic rings.[94,95]

1.26.5.3 Other Heterocyclophosphazenes

A boron-containing cyclophosphazene has been prepared by the reaction of $[Cl_3P{=}N{=}PCl_3]^+[Cl]^-$ with BCl_3 in the presence of methylammonium chloride (Scheme 26).[97]

The boron atom in the cyclic ring can be readily replaced by a variety of other main-group metals affording a large family of heterocyclophosphazenes (Scheme 27).[98–101]

Transition metal-containing cyclophosphazenes are few, but known. Some of these are synthesized as shown in Scheme 28, by a condensation of the Bezmann's salt $[Ph_2P(NH_2){=}N{=}P(NH_2)Ph_2][Cl]$ with metal precursors.[102–105]

1.26.6 Poly(heterophosphazene)s

The heterocyclophosphazenes, containing carbon and sulfur, namely, $[(NCCl)(NPCl_2)_2]$, $[(NSCl)(NPCl_2)_2]$, $[(NS(O)Cl)(NPCl_2)_2]$, and $[(NS(O)F)(NPCl_2)_2]$, can be polymerized by the ROP method (Scheme 29).[1] In comparison to the temperatures required for the ROP of $N_3P_3Cl_6$ (~250 °C) those involved for heterocyclophosphazenes are much lower, probably as a result of the ring strain introduced into the inorganic heterocyclic ring due to the introduction of the third heteroelement. The most prominent influence is seen in the ROP of $[(NSCl)(NPCl_2)_2]$ and $[(NCCl)(NPCl_2)_2]$ where the temperatures of polymerization are as low as 80 and 120 °C, respectively.[92,93] Even for the thionylphosphazene, $[(NS(O)Cl)(NPCl_2)_2]$, the temperature of polymerization is reduced to 160 °C.[106,107]

Ambient-temperature ROP has been achieved for $[(NS(O)Cl)(NPCl_2)_2]$ using Lewis acids in general, and $GaCl_3$ in particular, as the initiators.[108] The ROP of thiophosphazenes and thionylphosphazenes also has been speculated to be initiated by an incipient S–Cl bond cleavage. This has some support since the reaction of $[(NSCl)(NPCl_2)_2]$ with $SbCl_5$ leads to a planar six-membered sulfur-centered cation (Scheme 30).[109]

However, attempts to isolate such a cation with $[(NS(O)Cl)(NPCl_2)_2]$ by reaction with $AlCl_3$ [in the solvent 1,2-dichloroethane] leads to an unusual product, $[NS(O)(CHCHCl_2)(NPCl_2)_2]$.[110] This product is believed to have formed as a result of the reaction of $[NS(O)(NPCl_2)_2]^+$ with $CH_2{=}CHCl$, the latter being generated by a dehydrochlorination reaction from the solvent dichloroethane (Scheme 31). The ROP of $[(NS(O)Cl)(NPCl_2)_2]$ (at high or ambient temperature) is accompanied by the formation of cyclic products also.[94,95]

Poly(heterophosphazene)s show some similarities *vis-a-vis* polyphosphazenes. Thus, the ^{31}P NMR chemical shifts of the ring-opened polymers are upfield shifted with regard to the cyclic rings (Table 3). The molecular weights are quite high ($>10^5$); however, the PDIs are >2. All the chloro derivatives are extremely sensitive to moisture similar to the behavior of $[NPCl_2]_n$. Finally, these polymers also possess low T_g's, although the presence of the third heteroatom stiffens the chains somewhat (Table 3).[1] The polymers $[(NCCl)(NPCl_2)_2]_n$, $[(NSCl)(NPCl_2)_2]_n$, and $[(NS(O)Cl)(NPCl_2)_2]_n$ show single resonances in their ^{31}P NMR.[1] This is suggestive of a head-to-tail arrangement (Chart 15). An alternate head-to-head arrangement would have resulted in multiple ^{31}P resonances.

Copyright © 2013. Elsevier. All rights reserved.

Comprehensive Inorganic Chemistry II : From Elements to Applications, Elsevier, 2013. ProQuest Ebook Central, http://ebookcentral.proquest.com/lib/inflibnet-ebooks/detail.action?docID=1330977.
Created from inflibnet-ebooks on 2021-02-09 22:27:26.

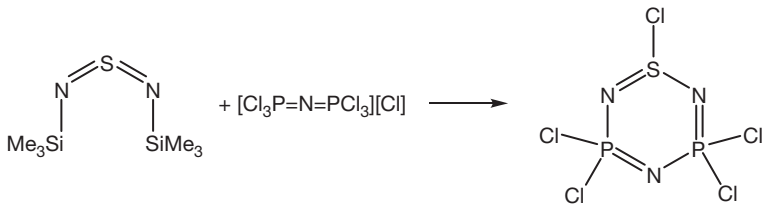

Scheme 24 Synthesis of thiocyclotriphosphazene.

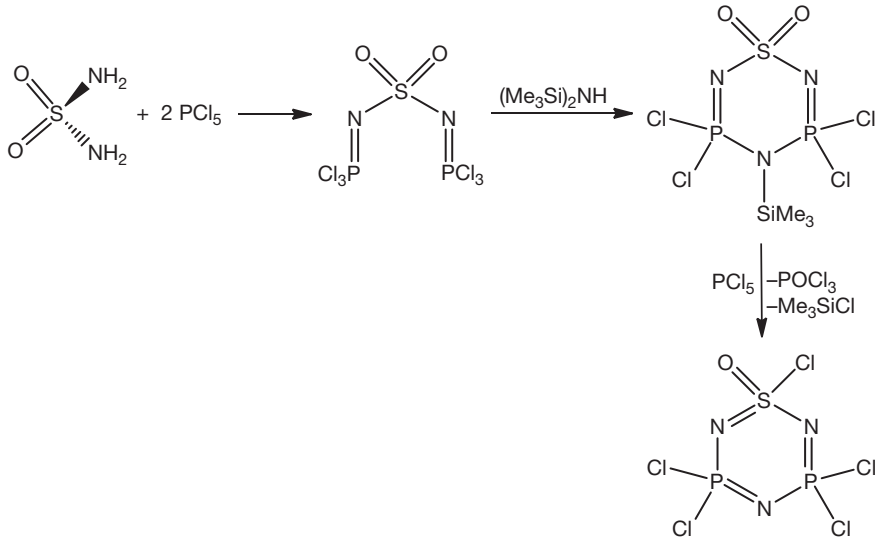

Scheme 25 Synthesis of thionylcyclotriphosphazene.

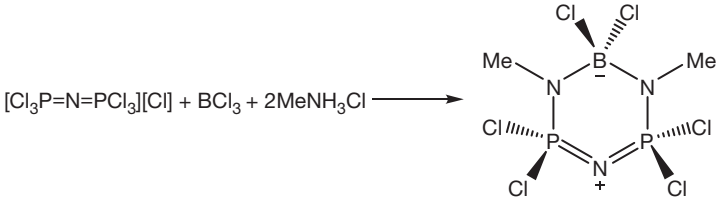

Scheme 26 Synthesis of a boron-containing cyclophosphazene.

An interesting feature of the poly(thiophosphazene)s and poly(thionylphosphazene)s is the regiospecificity of the nucleophilic substitution reaction involving the S–Cl or P–Cl bonds. Thus, in $[(NSCl)(NPCl_2)_2]_n$, S–Cl bonds are substituted first in the reaction with aryloxides[92,93] (Scheme 32). In contrast, in $[(NS(O)Cl)(NPCl_2)_2]_n$, the reaction with aryloxides proceeds with substitution of P–Cl bonds (Scheme 33).[107,111–114] On the other hand, the reaction with amines does not seem to involve any regiospecificity (Scheme 33).[107,111–114]

An interesting property of poly(aminothionylphosphazene)s is their excellent gas transport properties. Some interesting applications based on this property have been proposed.[94,95,113,115,116] Thus, the amino polymer $[(NS(O)NH^nBu)(NP(NH^nBu)_2]_n$ can be modified to incorporate phosphorescent Ru^{II}- (Chart 16) and Ir^{III}-based metal complexes. The phosphorescence of these complexes is quenched by dioxygen and therefore the intensity of phosphorescence can be related to the concentration of dioxygen and hence the air pressure. Sensing applications including flow visualization over aircraft in wind tunnels have been envisaged.[113,115,116] In another application, polyanionic derivatives of polythionyl phosphazenes have been prepared with a view to prepare polyelectrolytes.[117]

1.26.7 B–N Compounds and Polymers

Boron–nitrogen compounds have been of interest for a long time.[118–122] The isoelectronic relationship of the B–N unit with that of the C–C unit has intrigued chemists and spurred them to prepare B–N analogs of the well-known C–C compounds. In addition to the aforementioned isoelectronic relationship, the fact that the electronegativity of carbon (2.5) is a perfect mean of boron (2.0) and nitrogen (3.0) as well as the knowledge that the covalent radius of carbon (77 pm) is also a mean of the covalent radii of boron (88 pm) and nitrogen (70 pm) inspired the exploration of the chemistry of B–N compounds. While the chemistry of B–N compounds did not turn out to be similar to that of the C–C analogs, it became interesting in its own right.

Copyright © 2013. Elsevier. All rights reserved.

Comprehensive Inorganic Chemistry II : From Elements to Applications, Elsevier, 2013. ProQuest Ebook Central, http://ebookcentral.proquest.com/lib/inflibnet-ebooks/detail.action?docID=1330977.
Created from inflibnet-ebooks on 2021-02-09 22:27:26.

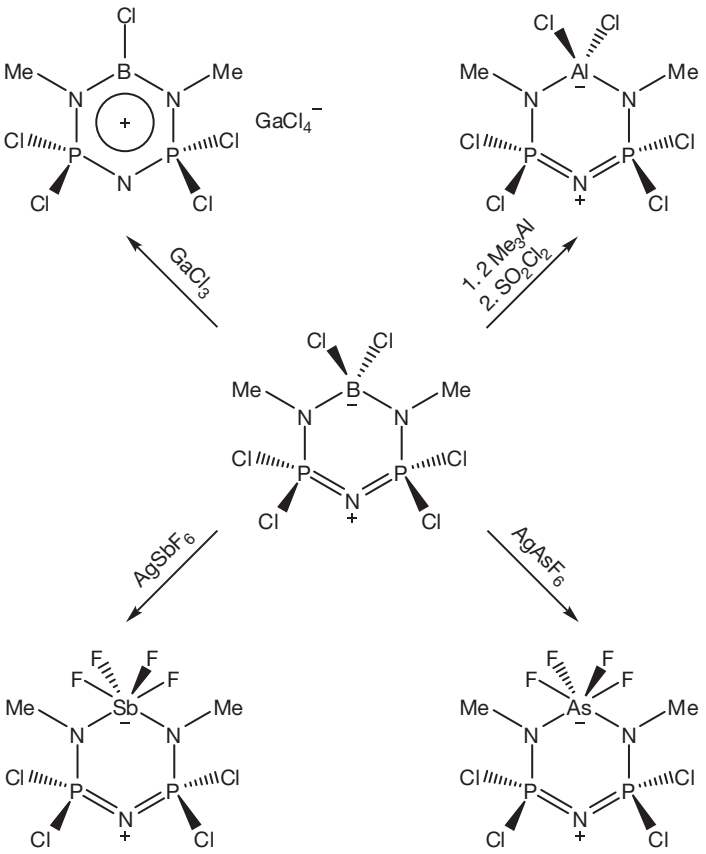

Scheme 27 Synthesis of main-group-metal-containing cyclophosphazenes from a boron-containing cyclophosphazene.

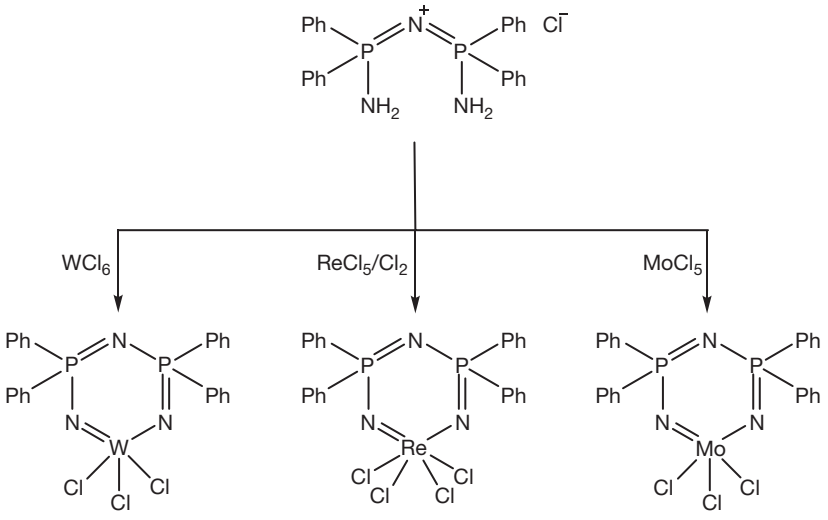

Scheme 28 Synthesis of transition-metal-containing cyclophosphazenes from the reaction of Bezmann's salt with appropriate metal halides.

Most of the unique features of the chemistry of this family arise from the electronegativity differences between boron and nitrogen and the consequent polarity of the $B^{\delta+}$–$N^{\delta-}$ bond.

One of the earliest reactions to be probed which results in the formation of B–N bonds is that of B_2H_6 with ammonia.[118,122] This reaction results in a predominantly unsymmetrical cleavage of diborane (Scheme 34).

On the other hand, the reaction of a sterically hindered amine such as trimethylamine proceeds to afford a symmetrical cleavage (Scheme 35).[123]

Although the simple ammonia–borane complex, $H_3N{\cdot}BH_3$, cannot be accessed in good yields in the direct reaction between ammonia and diborane, it can be prepared in a number of ways, some of which are shown in Scheme 36.[120]

Copyright © 2013. Elsevier. All rights reserved.

Comprehensive Inorganic Chemistry II : From Elements to Applications, Elsevier, 2013. ProQuest Ebook Central, http://ebookcentral.proquest.com/lib/inflibnet-ebooks/detail.action?docID=1330977.
Created from inflibnet-ebooks on 2021-02-09 22:27:26.

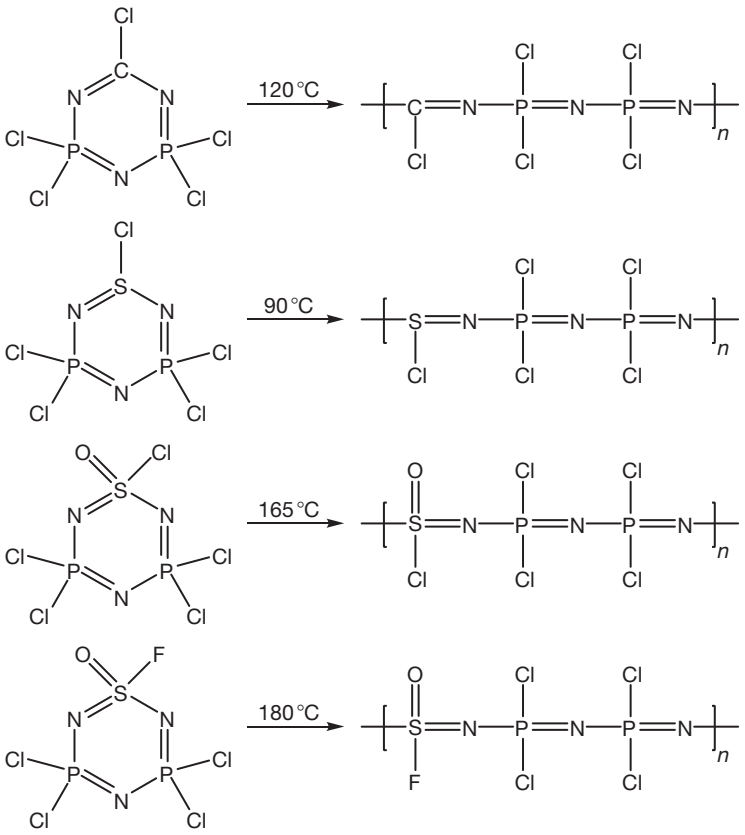

Scheme 29 Ring-opening polymerization of heterocyclophosphazenes containing carbon and sulfur.

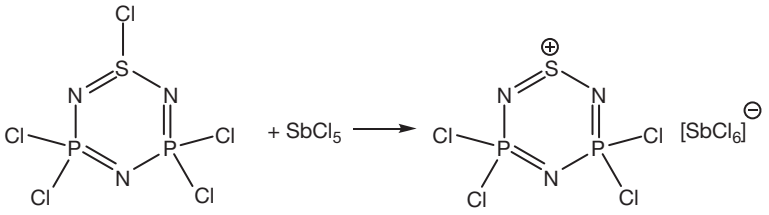

Scheme 30 Reaction of $[(NSCl)(NPCl_2)_2]$ with $SbCl_5$.

In recent years, there has been a resurgence in the chemistry of $H_3N{\cdot}BH_3$ as a result of its potential as a hydrogen storage material.[121,123–126] The molecular structure of ammonia–borane has been probed by a large variety of structural techniques, in gas phase, in an argon matrix, and in the condensed phase.[121] Depending on the technique and the state of the compound, the B–N bond length varies between 1.656 and 1.56 Å.[121] The B–N stretching frequency appears at 785 cm^{-1}.[121] In the condensed state, a strong intermolecular hydrogen bonding (dihydrogen bond, 2.02 Å) is observed which has been suggested to be the reason for the high melting point of $H_3N{\cdot}BH_3$ (112–114 °C).[121] It is interesting that the isoelectronic ethane has a melting point of −181.3 °C, indicating the importance of the polarity of B–N bond in the properties displayed by compounds containing this motif(s).

As mentioned earlier, ammonia–borane has been attracting a lot of interest in view of its potential as a hydrogen storage material.[121] The gravimetric storage density of ammonia–borane is quite high (~19.6 wt%). However, many problems, some very challenging, need to be sorted out before ammonia–borane can be contemplated as a hydrogen fuel. Chief among them is the issue of regenerating the spent fuel after its decomposition. Other problems include control of decomposition at reasonable temperatures, quick release of H_2, as well as avoiding side products such as ammonia or borazine which can be deleterious to the functioning of the fuel cell where hydrogen is to be used as a reactant. A number of strategies including decomposition of ammonia–borane in ionic liquids or its controlled solid-state decomposition in the presence of catalysts are being explored.[121] Although fundamental work on amine–borane has been going on for a long time, an extensive family of amine–borane analogs of alkanes has remained elusive.[127–130] Recently, a butane analog, $H_3NBH_2NH_2BH_3$, has been prepared by Shore et al.[127] The synthesis of this compound consists of preparation of aminodiborane, $NH_2B_2H_5$, followed by its reaction with ammonia

Copyright © 2013. Elsevier. All rights reserved.

Comprehensive Inorganic Chemistry II : From Elements to Applications, Elsevier, 2013. ProQuest Ebook Central, http://ebookcentral.proquest.com/lib/inflibnet-ebooks/detail.action?docID=1330977.
Created from inflibnet-ebooks on 2021-02-09 22:27:26.

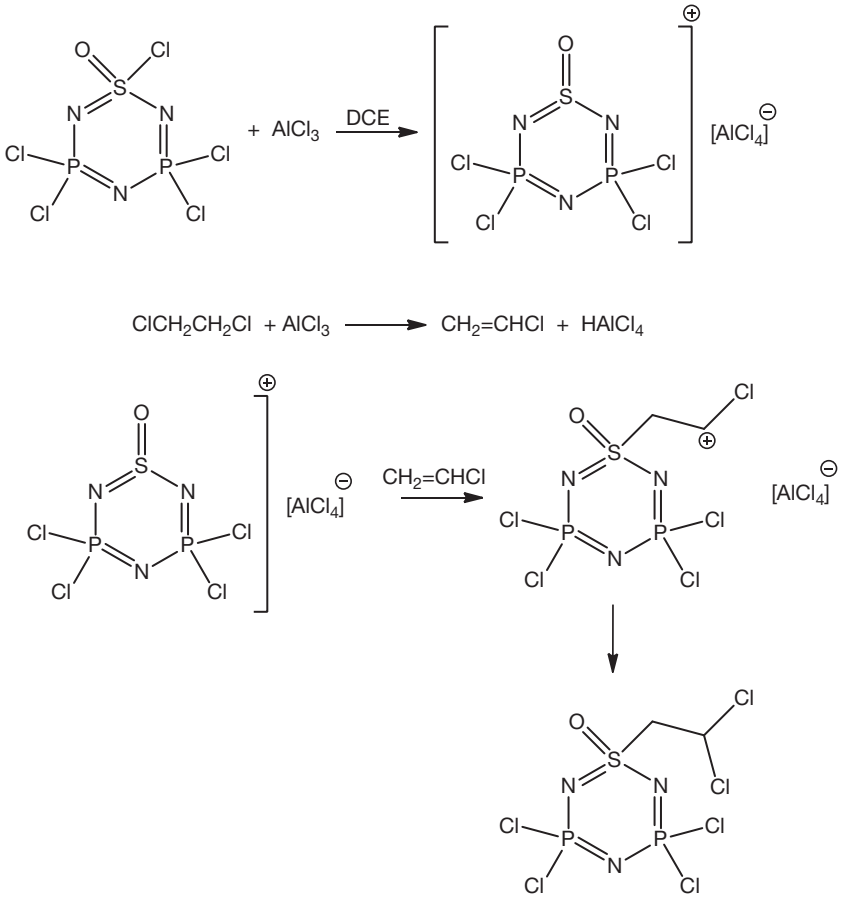

Scheme 31 Reaction of $[(NS(O)Cl)(NPCl_2)_2]$ with $AlCl_3$ in 1,2-dichloroethane(DCE).

Table 3 ^{31}P NMR chemical shifts and the T_g values of some heterophosphazenes and poly(heterophosphazene)s

	^{31}P (ppm)	T_g (°C)
$[(NCCl)(NPCl_2)_2]$	+36.5	–
$[(NCCl)(NPCl_2)_2]_n$	−3.7	−21
$[(NC(OPh))(NP(OPh)_2)_2]_n$	−10.4	+18
$[(NC(NHPh))(NP(NHPh)_2)_2]_n$	−9.1	+112
$[(NSCl)(NPCl_2)_2]$	+25.4	–
$[(NSCl)(NPCl_2)_2]_n$	−4.6	−40
$[(NS(O)Cl)(NPCl_2)_2]$	+26.1	–
$[(NS(O)Cl)(NPCl_2)_2]_n$	−10.0	−46
$[(NS(O)F)(NPCl_2)_2]_n$	−8.6	−56
$[(NS(O)Cl)(NP(OPh)_2)]_n$	−21.5	+10

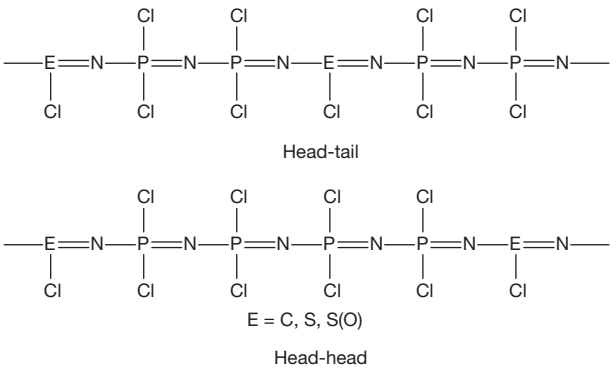

Chart 15 Head–tail and head–head isomers of $[(NECl)(NPCl_2)_2]_n$.

(Scheme 37). The formation of $NH_2B_2H_5$ is believed to be facilitated by a dihydrogen bond between the N–H of $BH_3{\cdot}NH_3$ and the B–H of $BH_3{\cdot}$THF (tetrahydrofuran). Subsequent hydrogen elimination affords $NH_2B_2H_5$. The dihydrogen bond formation, it is suggested, obviates the need for a catalyst for the dehydrogenation reaction.

The ^{11}B NMR spectrum of the amidodiborane shows a single chemical shift at −27.0 ppm. The molecular structure of this compound was determined by a single-crystal diffraction on its 18-crown-6-ether adduct, since $NH_2B_2H_5$ itself is a liquid at room temperature. The 18-crown-6-ether forms an adduct with $NH_2B_2H_5$ by means of weak hydrogen bonds. $NH_2B_2H_5$ is a four-membered ring containing a B–H–B bond. Reaction of $NH_2B_2H_5$ with ammonia breaks the B–H–B bridge to afford the *n*butane analog, $H_3NBH_2NH_2BH_3$. Unlike *n*butane, $H_3NBH_2NH_2BH_3$ is a crystalline solid at room temperature with a melting point of 62 °C. The molecular structure of $H_3NBH_2NH_2BH_3$ as its 18-crown-6-ether adduct reveals that it prefers the gauche conformation unlike the *anti*-conformation preferred by *n*butane (Chart 17).

Copyright © 2013. Elsevier. All rights reserved.

Comprehensive Inorganic Chemistry II : From Elements to Applications, Elsevier, 2013. ProQuest Ebook Central, http://ebookcentral.proquest.com/lib/inflibnet-ebooks/detail.action?docID=1330977.
Created from inflibnet-ebooks on 2021-02-09 22:27:26.

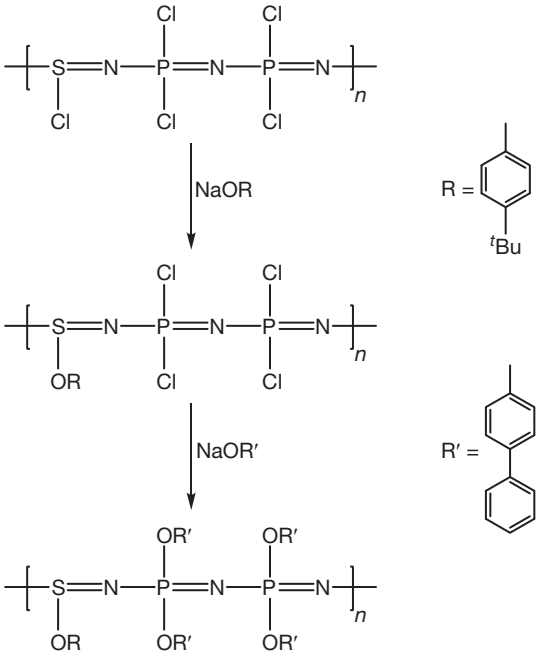

Scheme 32 Nucleophilic substitution reaction of $[(NSCl)(NPCl_2)_2]_n$ with sodium aryloxides.

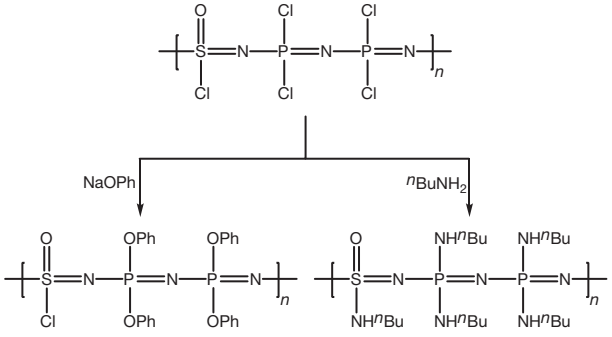

Scheme 33 Reaction of$[(NS(O)Cl)(NPCl_2)_2]_n$ with an aryloxide and a primary amine.

It has been suggested that weak dihydrogen bonds between N–H and B–H units are responsible for stabilizing the gauche form in $H_3NBH_2NH_2BH_3$.[127]

1.26.7.1 Cyclic B–N Compounds

The six-membered heterocyclic ring, borazine, $B_3N_3H_6$, is one of the oldest inorganic heterocyclic rings,[5,118,128] although the P–N ring systems, cyclophosphazenes, predate the B–N rings. Representative examples of B–N rings are shown in Chart 18.[5,129]

The six-membered borazine is traditionally synthesized by a thermal decomposition of the ammonia–borane

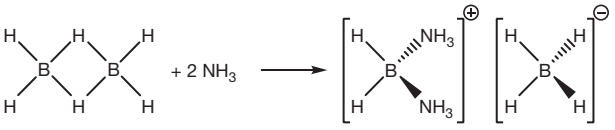

Scheme 34 Reaction of diborane with ammonia.

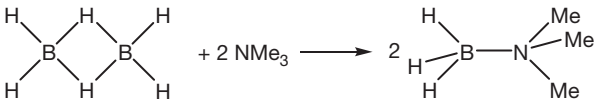

Scheme 35 Reaction of diborane with trimethyl amine.

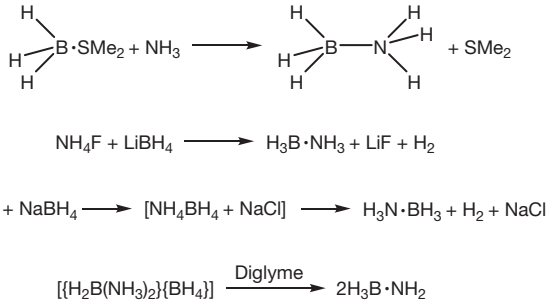

Scheme 36 Synthetic routes for the preparation of $H_3N{\cdot}BH_3$.

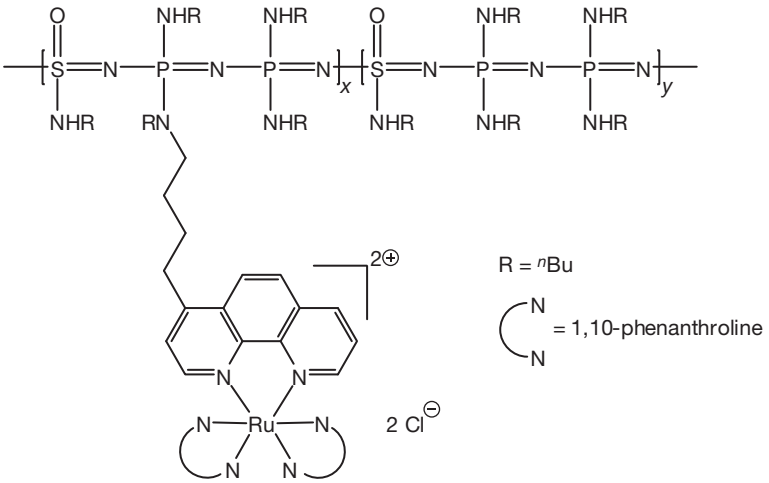

Chart 16 Modified $[(NS(O)NH^nBu)(NP(NH^nBu)_2]_n$ polymer containing a phosphorescent Ru^{II} complex as a pendant group.

Copyright © 2013. Elsevier. All rights reserved.

Comprehensive Inorganic Chemistry II : From Elements to Applications, Elsevier, 2013. ProQuest Ebook Central, http://ebookcentral.proquest.com/lib/inflibnet-ebooks/detail.action?docID=1330977.
Created from inflibnet-ebooks on 2021-02-09 22:27:26.

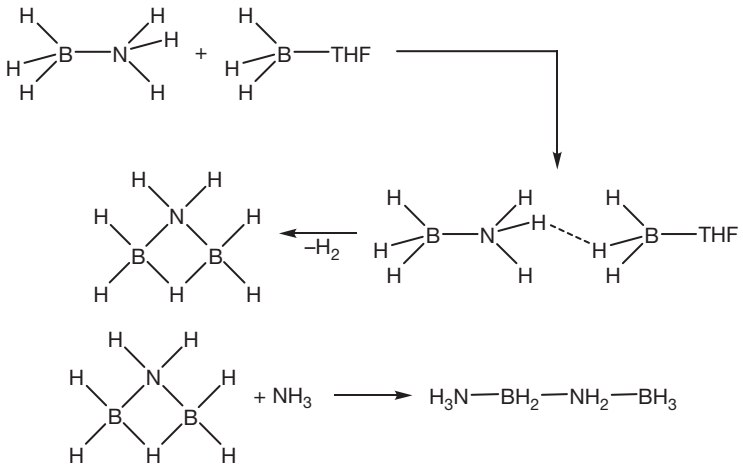

Scheme 37 Synthesis of amine–borane analog of butane, $H_3NBH_2NH_2BH_3$.

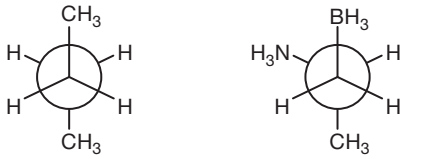

anti-conformation of $CH_3CH_2CH_2CH_3$ *gauche*-conformation of $BH_3NH_2BH_2NH_3$

Chart 17 Gauche conformation of $H_3NBH_2NH_2BH_3$ in comparison with the *anti* conformation of *n*butane.

compound.[130,131] Many other synthetic routes are now available for the preparation of this compound including the reaction of sodium borohydride with ammonium sulfate (Scheme 38).[131–135]

Alternatively, *B*-trichloroborazine can be reduced with $LiAlH_4$ to afford $B_3N_3H_6$ (Scheme 39).[5,118,132]

N-Silylated borazines are accessible by the reaction of trisilylamine with boron trichloride (Scheme 40).[133]

B-Alkylated products can also be prepared by the hydroboration reaction which is catalyzed by a Rh(I) catalyst (Scheme 41).[131]

Borazine, $B_3N_3H_6$, shows some remarkable similarities with benzene, in terms of its physical properties and for this reason has long been dubbed as the 'inorganic benzene.' Thus, $B_3N_3H_6$ is planar and possesses a D_{3h} symmetry similar to benzene. The B–N bond distances in borazine are equal (143.5 pm) and are shorter than B–N bond distances found in $H_3B{\cdot}NH_3$ (156.0 pm). Similar to benzene, borazine is a volatile liquid albeit with a lower boiling point (55 °C). Further, the liquid density and crystal density of benzene and borazine are quite comparable (liquid density (at boiling point): benzene, 0.81 g cm^{-3}, borazine, 0.81 g cm^{-3}; crystal density (at melting point): benzene, 1.01 g cm^{-3}; borazine, 1.00 g cm^{-3}).[5]

The question of borazine's aromaticity has been explored and the bond length equivalences have been rationalized by considering resonance structures such as those shown in Chart 19.[5]

Similar to benzene, borazine has 6π electrons, with these being formally contributed by the nitrogen atoms. A number of theoretical studies support a substantial extent of aromatic character. However, borazines do not show evidence for ring-current effects. Similarly, the nucleus-independent chemical shift (NICS), considered as a good method of estimating aromaticity of borazine, is −2.1 while for benzene it is −11.5. It appears, therefore, that the issue of the aromaticity of borazine has not yet been resolved.

Irrespective of the similarities of physical properties, the chemical behavior of borazine is dominated by the influence of the polar B–N bonds.[122] Thus, while Lewis bases add to boron, Lewis acids add to nitrogen. Addition across a B–N bond in borazine is quite facile unlike the situation in benzene as typified by the addition of HCl (Scheme 42).[118,122]

N-Alkylated products can be prepared by sequential reactions as shown in Scheme 43.[118]

Recently, a N-lithiated product has been isolated as its dimer (Scheme 44).[136]

η^1-Organometalic compounds can be prepared by a nucleophilic substitution at boron (Scheme 45).[137]

Interestingly, η^1-metal complexes can be formed by oxidative addition reactions also. Thus, the B–Br bond of $Br_3B_3N_3H_3$ adds oxidatively to palladium(0) or platinum(0) affording η^1-Pd(II) and -Pt(II) complexes, respectively (Scheme 46).[138]

In an obvious analogy with benzene–chromium tricarbonyl complex, the reaction of $B_3N_3Me_6$ with $Cr(CO)_6$ affords $B_3N_3Me_6{\cdot}Cr(CO)_3$ which is exceptionally stable similar to the benzene–chromium tricarbonyl complex and also possesses an η^6 coordination (Scheme 47).[118]

Thermal polymerization of borazine to polyborazylene occurs at fairly low temperatures (70–110 °C) by a dehydrogenation reaction. Polyborazylene seems to comprise of interconnected borazine rings and its formation is accompanied by a dehydrogenation reaction. Polyborazylenes appear to be excellent precursors for the ceramic, boron nitride.[1,5]

1.26.8 Transition-Metal-Catalyzed Dehydrogenation of Amine–Boranes: Formation of B–N Heterocyclic Rings

Thermal dehydrogenation of ammonia–borane and amine–boranes, though known for some time, has been receiving

Copyright © 2013. Elsevier. All rights reserved.

Comprehensive Inorganic Chemistry II : From Elements to Applications, Elsevier, 2013. ProQuest Ebook Central, http://ebookcentral.proquest.com/lib/inflibnet-ebooks/detail.action?docID=1330977.
Created from inflibnet-ebooks on 2021-02-09 22:27:26.

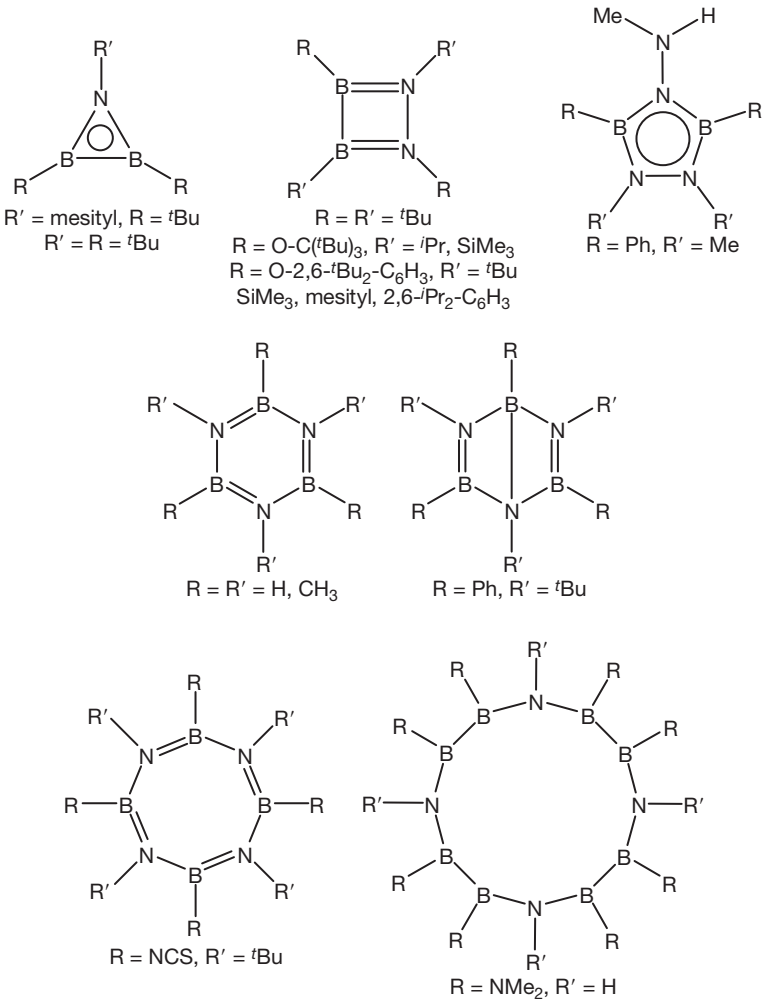

Chart 18 Representative examples of B–N ring systems.

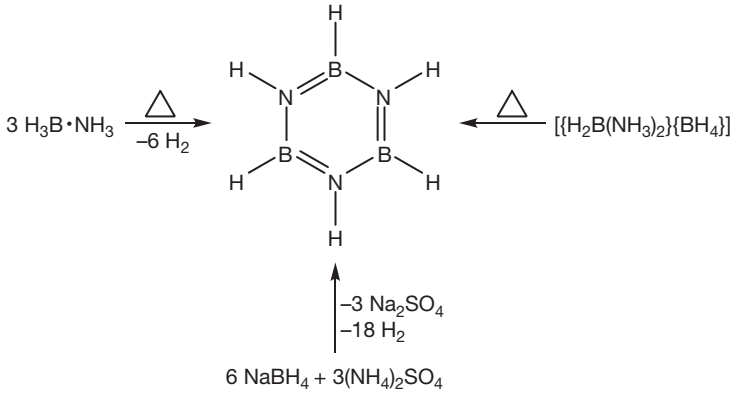

Scheme 38 Various synthetic routes for the preparation of borazine.

renewed attention in recent years.[120,121,139–142] Manners and coworkers reinvestigated the thermolysis of $Me_2NH{\cdot}BH_3$.[142–144] While it was known that the latter undergoes dehydrogenation in the melt at 130 °C to afford the amine–borane dimer $[Me_2N–BH_2]_2$ (Scheme 48), the intermediates involved and the manner of formation of $[Me_2N–BH_2]_2$ were unknown.

The key question was whether the dehydrogenation/coupling reaction is inter- or intramolecular. The latter would involve the possibility of $Me_2N{=}BH_2$ as the intermediate while the former would involve a linear $Me_2NH–BH_2–NMe_2–BH_3$ as a possible intermediate. Based on the observation that under hot tube conditions only minor amounts of

Copyright © 2013. Elsevier. All rights reserved.

Comprehensive Inorganic Chemistry II : From Elements to Applications, Elsevier, 2013. ProQuest Ebook Central, http://ebookcentral.proquest.com/lib/inflibnet-ebooks/detail.action?docID=1330977.
Created from inflibnet-ebooks on 2021-02-09 22:27:26.

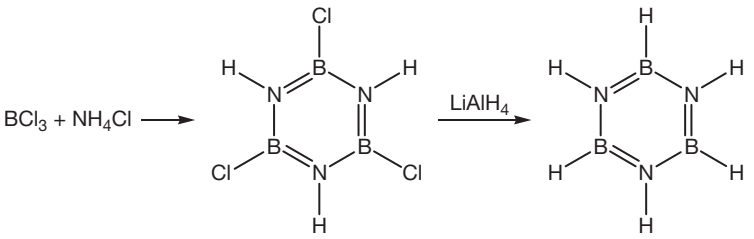

Scheme 39 Synthesis of borazine by the reduction of *B*-trichloroborazine.

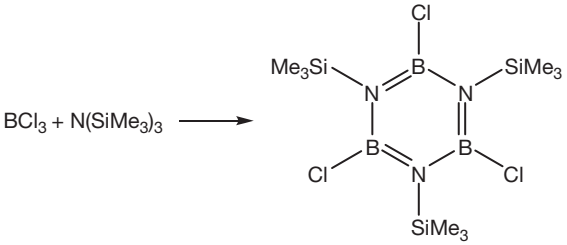

Scheme 40 Synthesis of *N*-silylated borazine.

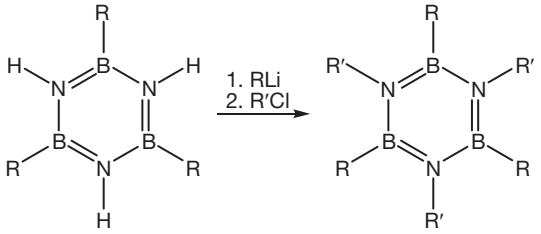

Scheme 43 Synthesis of N-alkylated borazines.

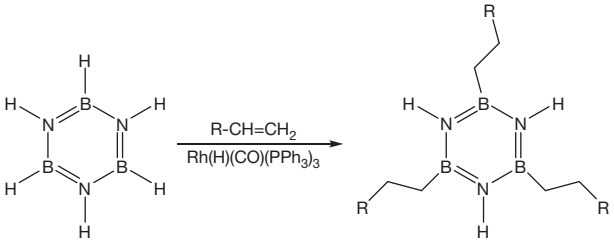

Scheme 41 Synthesis of B-alkylated borazines.

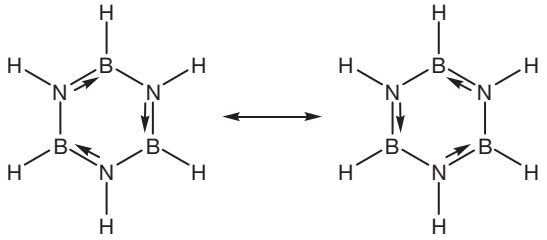

Chart 19 Resonance structures of borazine.

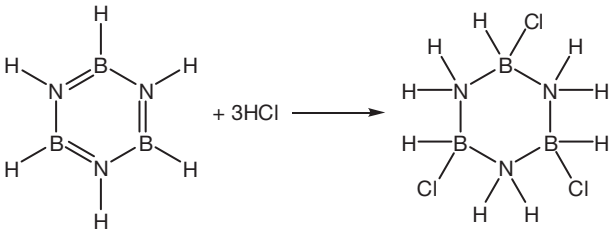

Scheme 42 Reaction of borazine with HCl.

$[Me_2N–BH_2]_2$ was formed, the authors suggested that the loss of hydrogen from $Me_2NH·BH_3$ in its melt reaction at 130 °C is an intermolecular process.[120,121]

The first example of a transition-metal-catalyzed dehydrogenation of amine–boranes involved the use of Rh(I) and Rh (III) complexes.[120,142–144] The reactions could be accomplished at relatively low temperatures (25–45 °C) with reasonable rates of conversion (Scheme 49).

An interesting case of the dehydrocoupling involved the dehydrogenation reaction of pyrrolidine–borane which afforded the cyclic four-membered B–N heterocyclic ring; in this case, two spirocyclic nitrogen centers are present. The unsymmetrical dimer $[(PhCH_2)(Me)N–BH_2]_2$ was isolated as a 1:1 mixture of *cis* and *trans* isomers.[144]

The four-membered B–N rings can be considered as dimers resulting from the dimerization of two ethylene analogs, $R_2N{=}BH_2$ (Scheme 50).

In keeping with the recent synthetic strategies involving kinetic stabilization of main-group compounds containing double/multiple bonds, the monomeric $^{i}Pr_2NH{=}BH_2$ could be isolated in the dehydrogenation reaction of $^{i}Pr_2NH·BH_2$ (Scheme 51).[144]

In the catalytic dehydrocoupling of primary amine–boranes, $RNH_2·BH_3$, and ammonia–borane $NH_3·BH_3$, cyclic borazines are formed in moderate to good yields (Scheme 52). The borazines are believed to form from the cyclohexane analogs, borazanes, $[RNHBH_2]_3$. At least in the case of dehydrogenation of $MeNH_2·BH_3$ and $PhNH_2·BH_3$ the intermediates $[MeNHBH_2]_3$ and $[PhNHBH_2]_3$ could be detected.[120,142]

In most of these reactions, formation of other dehydrocoupled products was inferred. Table 4 summarizes the ^{11}B NMR data for some representative products. Interestingly, the chemical shifts of the acyclic derivative, $^{i}Pr_2N{=}BH_2$, and the six-membered borazine rings appear downfield in comparison to the four-membered rings.[144]

The x-ray crystal structures of some representative dehydrocoupled products have been carried out. In the four-membered ring systems, the B–N bond distances are nearly similar and probably are closer to single bond distances. The bond angles at boron as well as nitrogen are quite acute and are close to 90°. On the other hand, the six-membered borazine rings are planar with shorter B–N bond distances; the bond angles at B and N

Copyright © 2013. Elsevier. All rights reserved.

Comprehensive Inorganic Chemistry II : From Elements to Applications, Elsevier, 2013. ProQuest Ebook Central, http://ebookcentral.proquest.com/lib/inflibnet-ebooks/detail.action?docID=1330977.
Created from inflibnet-ebooks on 2021-02-09 22:27:26.

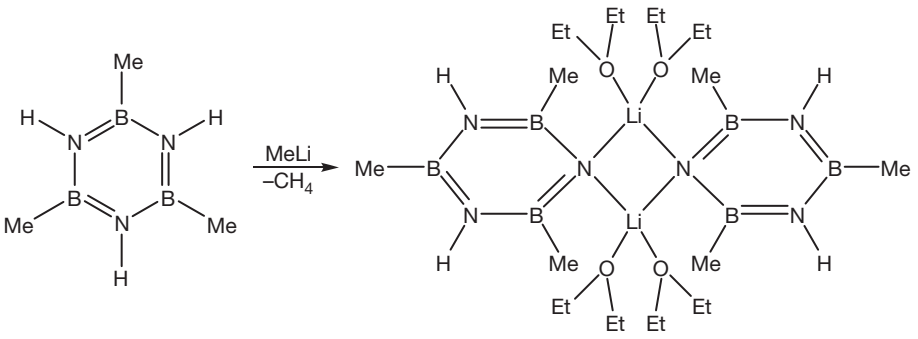

Scheme 44 Synthesis of a dimeric N-lithiated borazine derivative.

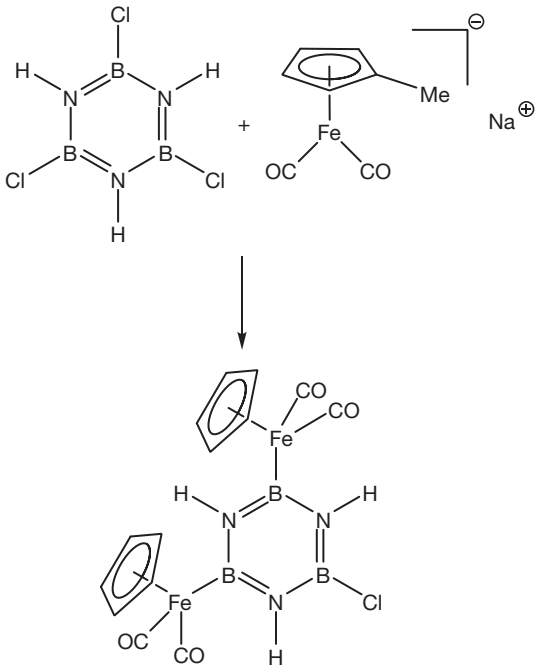

Scheme 45 Synthesis of a η^1-organometallic compound using $Cl_3B_3N_3H_3$.

are closer to the values anticipated at the sp^2 hybridized centers[120] (Table 5).

A number of Rh(I) and Rh(III)-based precatalysts have been used for the dehydrocoupling reactions.[120,142,144] Based on various experimental observations (that include (1) sigmoidal kinetics of product formation, (2) color change, (3) reaction arrest after nanofiltration of the reaction mixture, (4) reaction arrest after Hg(0) addition, and (5) transmission electron microscopy (TEM) characterization of 2-nm-sized Rh(0) particles after the reaction was completed), Manners and coworkers concluded that the dehydrocoupling was in fact being catalyzed by Rh(0) nanoparticles which were generated *in situ* in the reaction mixture. They were also able to show that free BH_3 forms a boride layer on such nanoparticles and deactivates them.[144–147] The postulation of active Rh(0) nanoparticles was contested. *In situ* catalyst characterization experiments by techniques such as extended x-ray absorption fine structure (EXAFS) seem to indicate the involvement of discrete Rh_4/Rh_6 clusters.[148,149]

In addition to the Rh-catalysts, a number of homogeneous catalytic systems seem to be equally effective in the dehydrocoupling of amine–boranes and ammonia–borane (Chart 20).[120,150–156]

The mechanism of the dehydrocoupling reaction of $Me_2NH{\cdot}BH_3$ seems to hinge on either the dimerization of $MeN{=}BH_2$ or the dehydrocoupling of $Me_2NHBH_2NMe_2BH_3$ (Scheme 53).[120,142,144]

An interesting tandem catalytic dehydrocoupling–hydrogenation reaction has been developed using amine–borane complexes.[157,158] For example, the dehydrogenation of $Me_2NH{\cdot}BH_3$ by an Rh-precatalyst liberates H_2; the latter has been utilized in hydrogenating a number of substrates.[158] A typical example is shown in Scheme 54.

In an interesting development, trialkyl group-14 triflates in combination with amine/pyridine bases have been shown to function as frustrated Lewis pairs (FLPs) and dehydrocouple amine–boranes (Scheme 55).[159]

1.26.9 Polyaminoboranes

Polymeric materials containing boron and nitrogen have been known for some time.[1,5] However, most reports deal with materials which are insoluble and whose structural identification does not confirm linear long chains containing alternate boron and nitrogen atoms in the backbone. Research on the dehydrocoupling of amine–boranes and ammonia–borane, as described in the previous section, suggested that appropriate catalysts would be able to effect a polymerization process. Goldberg and Heinekey and coworkers showed that the Ir(III) compound H_2IrPOCOP [POCOP$=\kappa^3$-1,3-$(OP^tBu_2)_2C_6H_3$] (Chart 21) was an extremely efficient catalyst for the dehydrocoupling of ammonia–borane, $H_3N{\cdot}BH_3$.[160,161] This reaction results in the elimination of one equivalent of H_2 very rapidly (14 min) and leads to the formation of an aminoborane which has been suggested to be a cyclic pentamer, $[NH_2BH_2]_5$.

Manners and coworkers utilized the catalyst, H_2IrPOCOP, to effect a dehydrocoupling of primary amine–borane adducts affording linear polymers.[162,163] Thus, the reaction of $MeNH_2{\cdot}BH_3$ with H_2IrPOCOP in THF for 20 min (0–20 °C) afforded $[MeNH{-}BH_2]_n$ (Scheme 56).

Copyright © 2013. Elsevier. All rights reserved.

Comprehensive Inorganic Chemistry II : From Elements to Applications, Elsevier, 2013. ProQuest Ebook Central, http://ebookcentral.proquest.com/lib/inflibnet-ebooks/detail.action?docID=1330977.
Created from inflibnet-ebooks on 2021-02-09 22:27:26.

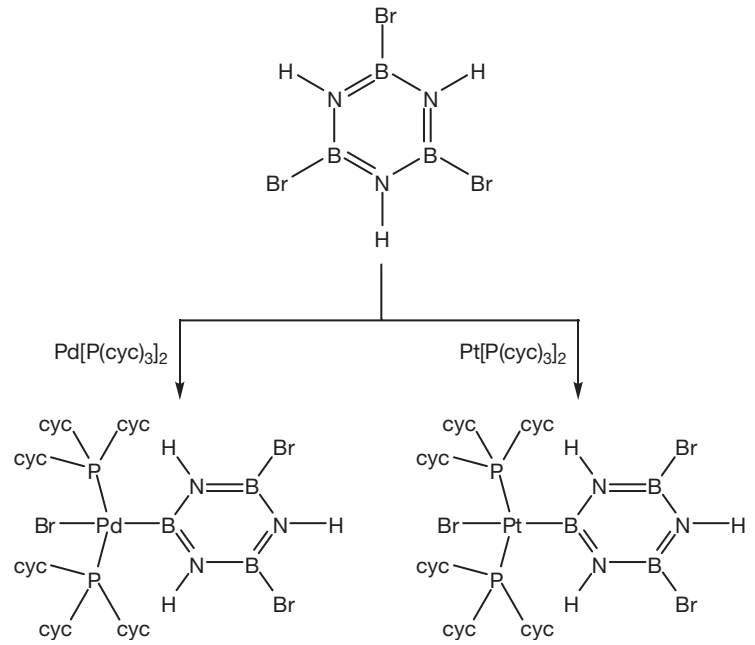

Scheme 46 Synthesis of η^1-organometallic compounds through the oxidative addition reactions of $Br_3B_3N_3H_3$.

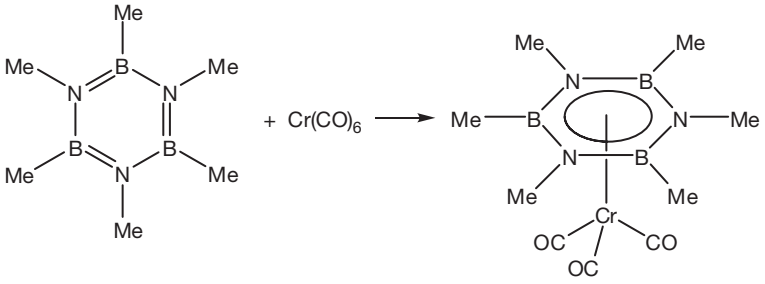

Scheme 47 An η^6-organometallic complex of $B_3N_3Me_6$.

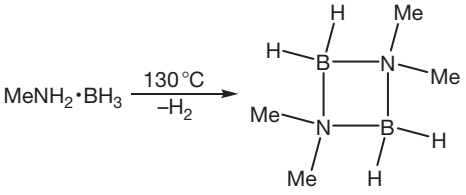

Scheme 48 Thermolysis of $Me_2NH{\cdot}BH_3$.

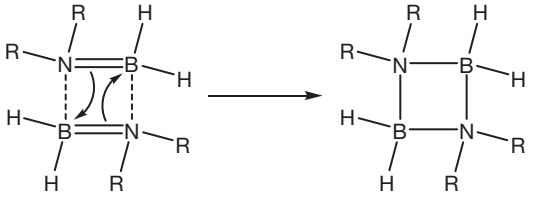

Scheme 50 Formation of the four-membered B–N rings from possible dimerization of $R_2N{=}BH_2$.

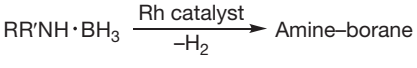

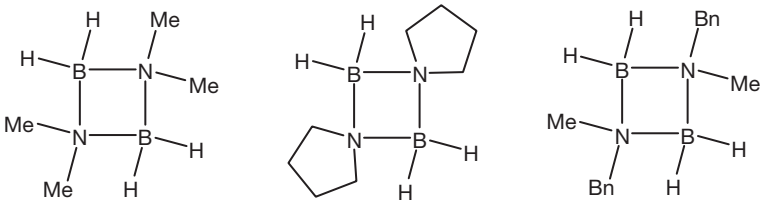

Scheme 49 Transition-metal-catalyzed dehydrogenation of amine–boranes.

Copyright © 2013. Elsevier. All rights reserved.

Comprehensive Inorganic Chemistry II : From Elements to Applications, Elsevier, 2013. ProQuest Ebook Central, http://ebookcentral.proquest.com/lib/inflibnet-ebooks/detail.action?docID=1330977.
Created from inflibnet-ebooks on 2021-02-09 22:27:26.

The $^{11}B\{^1H\}$ NMR of $[(Me)(H)N–BH_2]_n$ showed a broad peak at −6.5 ppm (cf. $^{11}B\{^1H\}$NMR of $[(Me)(H)N–BH_2]_3$ shows a singlet at −5.4 ppm). Interestingly, in the case of cyclophosphazenes and polyphosphazenes it has been shown that the ^{31}P chemical shifts of the polymers are always upfield shifted with respect to the corresponding six-membered rings. The infrared spectrum of $[(Me)(H)N–BH_2]_n$ revealed that the N–H, C–H, and B–H vibrations appear at 3256, 2985, and 2366 cm^{-1} respectively.[162,163]

Molecular weight measurements of the polyaminoborane proved slightly tricky. While a gel permeation chromatography (GPC) analysis of $[(Me)(H)N–BH_2]_n$ in THF containing 0.1 wt % of $^nBu_4NBr$ suggested a weight average molecular weight of 160 000 relative to polystyrene (PDI = 2.9), weight average molecular weight relative to poly(2-ethyl-2-azoline) was found to be 50 000. The hydrodynamic radius of $[(Me)(H)N–BH_2]_n$ as obtained by dynamic light scattering (DLS) is 3 nm. It appears that the molecular weights obtained relative to polystyrene are overestimated and the realistic weight average degree of polymerization of $[(Me)(H)N–BH_2]_n$ is about 600. Wide-angle x-ray scattering experiments suggest that $[(Me)(H)N–BH_2]_n$ is an amorphous polymer. Thermogravimetric analysis suggests a decomposition at 180 °C with a ceramic yield of 25% at 600 °C.[163]

Although polymerization of $NH_3·BH_3$ with H_2IrPOCOP did not yield a tractable material, a random copolymer could be obtained, when a mixture of $H_3N·BH_3$ and $MeNH_2·BH_3$ was treated with H_2IrPOCOP (Scheme 57).[163]

Table 6 summarizes some of the important features of the aforementioned polymers.[163]

The structure of $[(Me)(H)N–BH_2]_n$ was probed by solid-state ^{11}B NMR by performing multiple-quantum magic-angle spinning (MQMAS) experiments. It was revealed that $[MeNH–BH_2]_n$ was a linear material and possessed different ^{11}B environments [−5.8 (mid-chain BH_2 groups), −18.6 (end BH_3 groups)].

Although the full details of the mechanism of polymerization are still sketchy the following inferences could be made.[163] Experiments using varying amounts of catalyst loadings revealed that higher catalyst loadings lead to higher molecular weights. Thus a polymer with an M_w of 356 000 and a PDI of 3.1 was obtained using up to 6.6 mol% of catalyst. Experiments on the variation of M_n and M_w with respect to the conversion of the monomer to the polymer suggest the presence of high molecular weight polymers even at low conversions, an observation that seems to suggest a chain-growth polymerization. However, at higher conversions the molecular weight increases suggesting a nonconventional chain-growth process. It appears that a slow step involving an amino-borane monomer is first involved (Scheme 58).

The second, probably a fast chain-growth polymerization process, also involves the metal (Scheme 59).

While it is clear that a lot of work still needs to be done to delineate the precise mechanism of polymerization, recently there has been evidence in terms of trapping the first oligomerization event in the polymerization process.[164] Thus, the reaction of one equivalent of $H_3B·N(Me)H_2$ with $[Ir(PCy_3)_2(H)_2(\eta^2\text{-}H_3B·N(Me)(H)_2)][BArF_4]$ afforded a compound where $H_3B·N(Me)(H)BH_2·N(Me)(H)_2$ was bound to iridium (Scheme 60). This compound contains a four-membered BH–N(H)(Me)–BH_2–NH_2Me chain which is linked at its B-end to the Ir catalytic center through two bridging hydrogen atoms (Scheme 60). Presumably, compounds of this type are involved in the propagation of the polymerization.

Table 4 ^{11}B NMR data for some of the products obtained from the dehydrogenation of amine–boranes

Compound	*^{11}B NMR data (ppm)*
$^iPr_2N{=}BH_2$	34.7(t); (J_{BH} = 123 Hz)
$[Me_2N–BH_2]_2$	4.75(t); (J_{BH} = 110 Hz)
$[(1,4\text{-}C_4H_8)N–BH_2]_2$	2.56(t); (J_{BH} = 110 Hz)
$[PhCH_2(Me)N–BH_2]_2$	4.21(s, br) (mixture of *cis* and *trans*)
$[HBNH]_3$	30.2(d); (J_{BH} = 141 Hz)
$[HBNMe]_3$	33.2(d); (J_{BH} = 132 Hz)
$[HBNPh]_3$	32.8(s, br)

Table 5 Summary of the structural data acquired for some of the products obtained from the dehydrogenation of amine–boranes

Compound	*B–N ring*	*B–N bond distance*	*N–B–N bond angle*	*B–N–B bond angle*
$[H_2B·NMe_2]_2$	Four-membered	1.596(4) 1.595(4)	93.7(2)	86.3(2)
$[H_2B·N(1,4\text{-}C_4H_8)]_2$	Four-membered	1.584(4) 1.609(5)	92.9(3)	86.9(3)
$[HBNPh]_3$	Six-membered planar	1.429(2) 1.431(2)	119.0(2)	120.9(2)

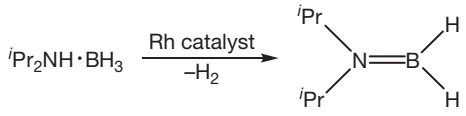

Scheme 51 Dehydrogenation reaction of $^iPr_2NH·BH_2$.

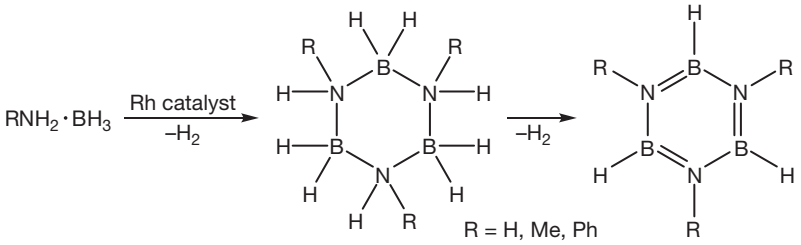

Scheme 52 Catalytic dehydrocoupling of primary amine–boranes, $RNH_2·BH_3$.

Copyright © 2013. Elsevier. All rights reserved.

Comprehensive Inorganic Chemistry II : From Elements to Applications, Elsevier, 2013. ProQuest Ebook Central, http://ebookcentral.proquest.com/lib/inflibnet-ebooks/detail.action?docID=1330977.
Created from inflibnet-ebooks on 2021-02-09 22:27:26.

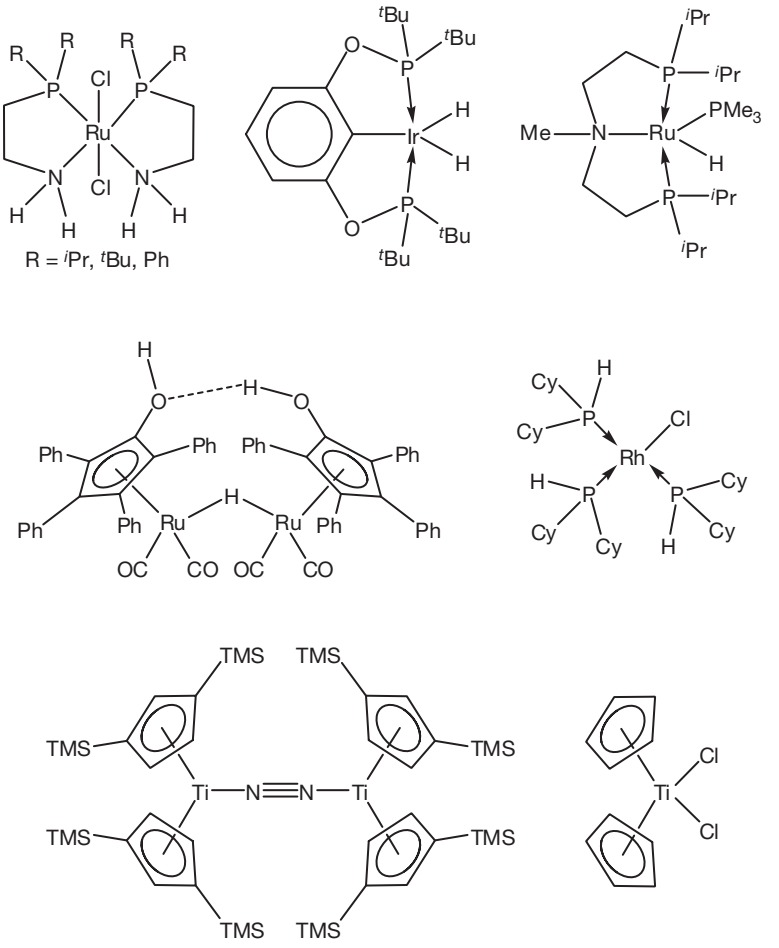

Chart 20 Homogeneous catalysts for the dehydrocoupling of amine–boranes and ammonia–borane.

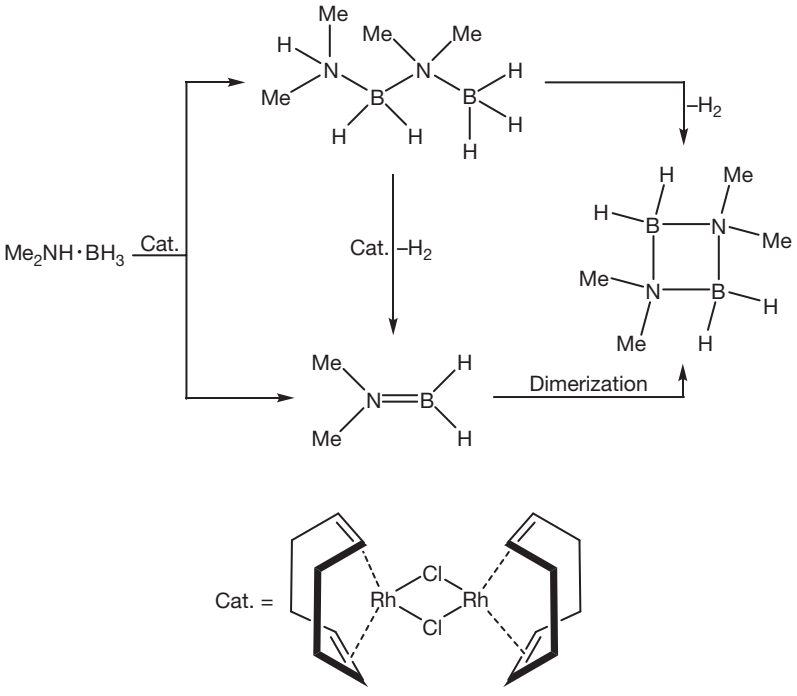

Scheme 53 Dehydrocoupling of an amine–borane using a homogeneous Rh catalyst.

Copyright © 2013. Elsevier. All rights reserved.

Comprehensive Inorganic Chemistry II : From Elements to Applications, Elsevier, 2013. ProQuest Ebook Central, http://ebookcentral.proquest.com/lib/inflibnet-ebooks/detail.action?docID=1330977.
Created from inflibnet-ebooks on 2021-02-09 22:27:26.

1.26.9.1 Other Catalysts

Apart from $H_2IrPOCOP$, many other catalysts have been found to be effective for the polymerization of $Me(H)_2N{\cdot}BH_3$.[165,166] A selected list of such catalysts is shown in Chart 22. Interestingly, apart from complexes containing pincer and chelating ligands, metal carbonyls have also been found to be effective. The latter need photoactivation before they can be used as catalysts.[165,166]

1.26.9.2 Limitations

In spite of the undeniable progress that has been achieved in terms of the preparation of linear polyaminoboranes, there is still no general method to access a large variety in this family. The most widely studied polymerization continues to be the dehydrocoupling of $Me(H)_2N{\cdot}BH_3$. Unless catalytic processes are discovered which can allow preparation of much larger members of this family, polyaminoboranes may not take off as new materials, particularly since $[Me(H)N{\cdot}BH_2]_n$ itself does not seem to possess any special properties. However, the utility of these polymers as precursors for B–N ceramics is an area that is fraught with interesting possibilities.

1.26.10 Dehydrocoupling of Phosphane–Borane Adducts

1.26.10.1 Acyclic and Cyclic Products

Early work on the thermal decomposition of phosphane–borane adducts was already indicative of the formation of cyclic and polymeric products, although the characterization of the products particularly the polymers was not unambiguous.[120] However, this early work did lay foundation for the more recent metal-catalyzed dehydrocoupling of phosphane–borane adducts.

It was reported in the late 1950s that thermolysis of neat $Ph_2(H)P{\cdot}BH_3$ at ~200 °C afforded the six-membered inorganic heterocyclic ring, $[Ph_2PBH_2]_3$ (Scheme 61).[167]

Recent reinvestigation of this reaction using Rh(I) precatalysts revealed that the dehydrogenation reaction can be accomplished at lower temperatures (Scheme 62).[168–170]

Thus, the thermolysis of $Ph_2(H)P{\cdot}BH_3$ in the presence of catalytic amounts of Rh(I) compounds afforded at 90 °C the linear compound $Ph_2(H)P{\cdot}BH_2{-}PPh_2(H){\cdot}BH_3$. This compound is characterized by the presence of two chemical shifts in its ^{31}P and ^{11}B NMR spectra: −3.3 (Ph_2PH), −17.7 (Ph_2P), −33.2 (BH_2), and −37.3 (BH_3). A single-crystal x-ray structure determination confirmed the linear structure. The P–B distances found in this compound are in the range of 1.90–2.00 Å and are comparable to such distances found in analogous

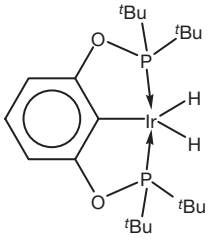

$H_2IrPOCOP$

Chart 21 Structure of the Ir(III) complex, $H_2IrPOCOP$.

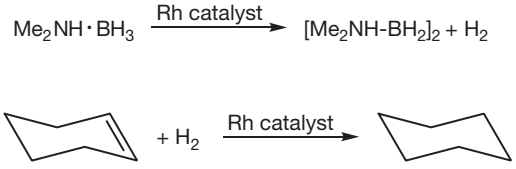

Scheme 54 A tandem catalytic dehydrocoupling–hydrogenation reaction using an amine–borane.

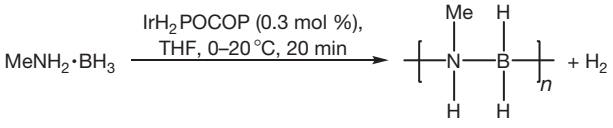

Scheme 56 Preparation of $[MeNH{-}BH_2]_n$ by the dehydrocoupling of $MeNH_2{\cdot}BH_3$ using $H_2IrPOCOP$.

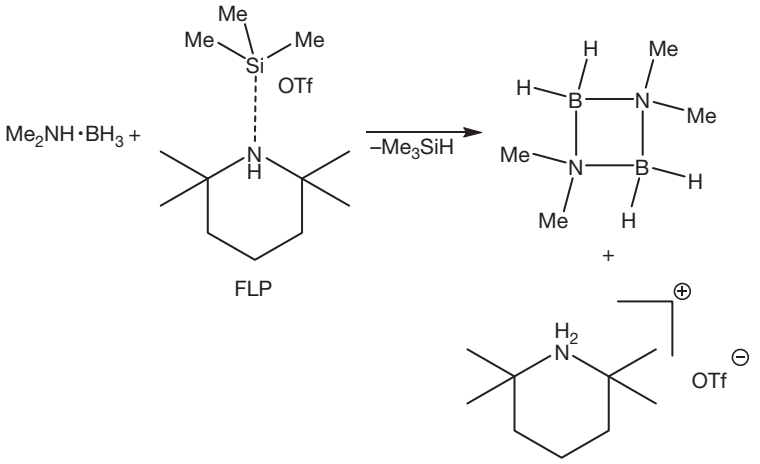

Scheme 55 Dehydrocoupling of an amine–borane by a frustrated Lewis base pair (FLP).

Copyright © 2013. Elsevier. All rights reserved.

Comprehensive Inorganic Chemistry II : From Elements to Applications, Elsevier, 2013. ProQuest Ebook Central, http://ebookcentral.proquest.com/lib/inflibnet-ebooks/detail.action?docID=1330977.
Created from inflibnet-ebooks on 2021-02-09 22:27:26.

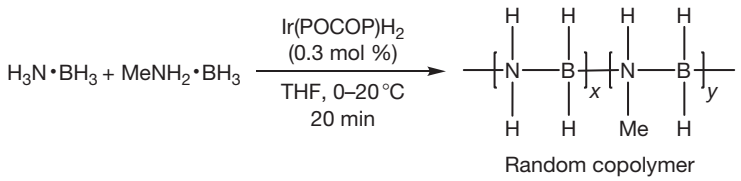

Scheme 57 Polymerization of $H_3N{\cdot}BH_3$ and $MeNH_2{\cdot}BH_3$ to obtain a random copolymer.

Table 6 Characterization data of $[(Me)(H)N–BH_2]_n$ and $[H_2N–BH_2]_x[(Me)(H)N–BH_2]_y$

Polymer	*^{11}B NMR data*	*M_w (PDI)*	*IR (cm^{-1})*
$[(Me)(H)N–BH_2]_n$	−6.5	160 000 (2.9)	3256 (ν NH) 2985 (ν CH) 2366 (ν NH)
$[H_2N–BH_2]_x[(Me)(H)N–BH_2]_y$ (random copolymer)[a]	−9.0 −11.0	156 000 (11.0)	

[a]Depending on *x* and *y* the weight average molecular weights obtained were different.

Scheme 58 First step in the plausible mechanism for the polymerization of $MeNH_2{\cdot}BH_3$.

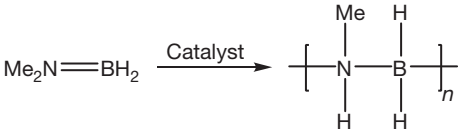

Scheme 59 Second step in the plausible mechanism for the polymerization of $MeNH_2{\cdot}BH_3$.

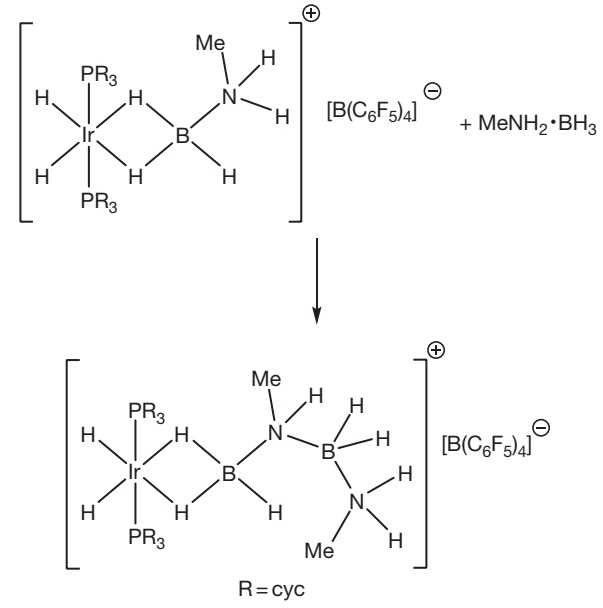

Scheme 60 Reaction of $H_3B{\cdot}N(Me)H_2$ with $[Ir(PCy_3)_2(H)_2(\eta^2\text{-}H_3B{\cdot}N(Me)(H_2))][BArF_4]$.

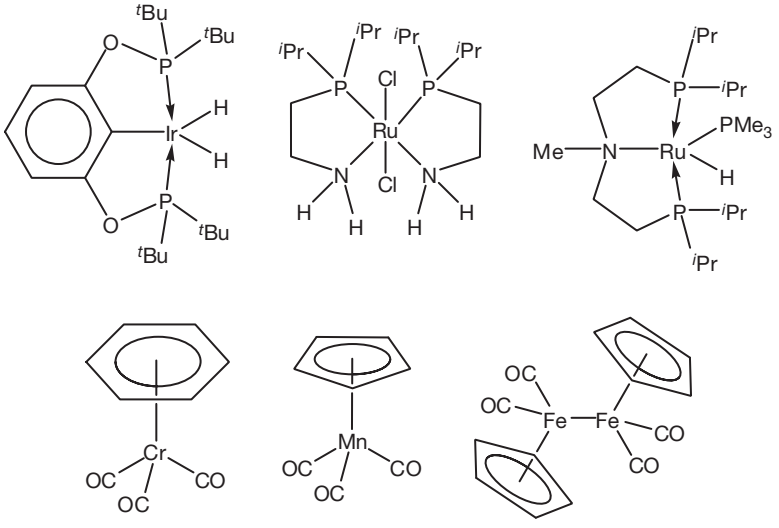

Chart 22 Examples of some catalysts that have been found effective for the polymerization of $Me(H)_2N{\cdot}BH_3$.

Copyright © 2013. Elsevier. All rights reserved.

Comprehensive Inorganic Chemistry II : From Elements to Applications, Elsevier, 2013. ProQuest Ebook Central, http://ebookcentral.proquest.com/lib/inflibnet-ebooks/detail.action?docID=1330977.
Created from inflibnet-ebooks on 2021-02-09 22:27:26.

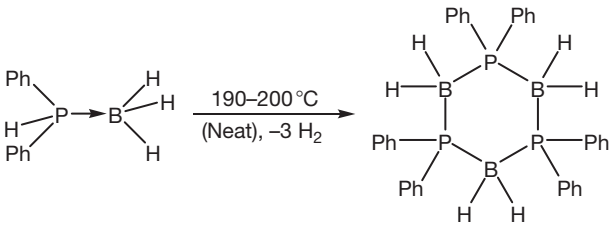

Scheme 61 Thermolysis of neat $Ph_2(H)P{\cdot}BH_3$.

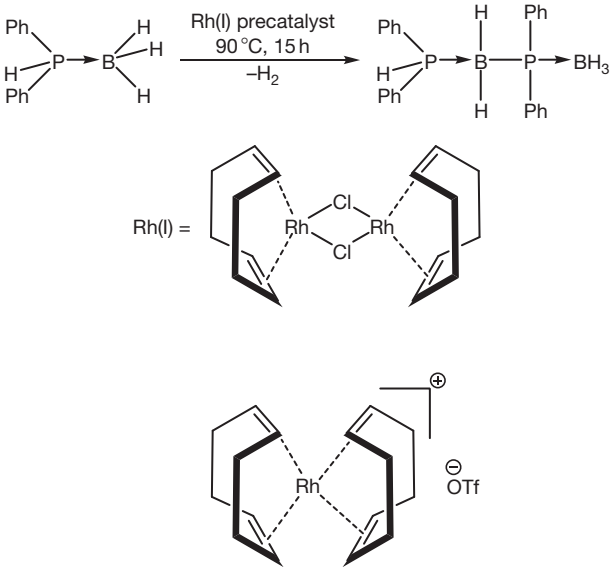

Scheme 62 Dehydrogenation reaction of $Ph_2(H)P{\cdot}BH_3$ using Rh(I) precatalysts.

compounds, $Ph_3P{\cdot}BH_3$ (1.917 Å), $(C_6H_{11})_2(H)P{\cdot}BH_3$ (1.919 Å), and $Ph(H)_2P{\cdot}BH_3$ (1.924 Å). The geometry at the boron and phosphorus centers is approximately tetrahedral (Table 7). Analogous linear products are also formed in the dehydrogenation reaction of $^tBu_2(H)P{\cdot}BH_3$ (Scheme 63),[170] although this reaction has been found to be far more sluggish. An interesting aspect of this reaction is the isolation of a chloro product in the presence of chlorine-containing rhodium complexes. The chloro-compound could not be separated from its chloro-free analog.

Cyclic products are obtained in the Rh-catalyzed dehydrogenation of $Ph_2(H)P{\cdot}BH_3$ if the reaction conditions are slightly altered by increasing the reaction temperature to 120 °C (Scheme 64).

The ^{31}P NMR spectra of the six- and eight-membered compounds reveal broad bands at −18.2 ppm while the corresponding ^{11}B NMR spectra reveal a peak at −33.8 ppm. The molecular structure of the eight-membered ring reveals a puckered boat–boat conformation. The average B–P–B bond angle is 120.4(2)°, while the average P–B–P bond angle is 114.2(3)°. The P–B bond distances range between 1.922(5) and 1.962(5) Å with an average value of 1.939 Å. In comparison, $[Me_2PBH_2]_4$ also revealed similar metrical parameters (P–B, 2.08 Å; B–P–B, 125(1)°; P–B–P, 104(2)°).

The molecular structure of the six-membered ring showed that it possessed a chair conformation with nearly similar metric parameters as that of the eight-membered rings (P–B, 1.948 Å; B–P–B, 114.3°; P–B–P, 112.6°) (Table 7).[170]

Although a number of metal catalysts were found to be effective for the dehydrogenation reactions of phosphane–borane adducts, best results seem to be obtained by the use of Rh(I) or Rh(III) precatalysts. Interestingly, in none of the experiments evidence of homohydrocoupling was found.[170]

Table 7 NMR and x-ray crystal structural data for acyclic and cyclic phosphinoboranes

Compound	*Chemical shift (ppm)*		*Bond distance (Å, average)*	*Bond angle (°, average)*	
	^{11}B	*^{31}P*	*P–B*	*P–B–P*	*B–P–B*
$(Ph_2)(H)P{\cdot}BH_2{-}P(Ph_2)(H){\cdot}BH_3$	−33.2 (BH_2) −37.3 (BH_3)	−3.3 (Ph_2PH) −17.7 (Ph_2P)	1.933	109.2	113.0
$^tBu_2PHBH{-}^tBu_2P{-}BH_3$	−37.2 to −40.8	39.3 ($^tBu_2PH$) 13.0 ($^tBu_2P$)	1.962	112.6	114.3
$[Ph_2P{-}BH_2]_3$ (chair conformation)	−32.9	−17.9	1.948	112.6	114.3
$[Ph_2P{-}BH_2]_4$ (boat–boat conformation)	−31.2	−19.1	1.939	114.1	120.5

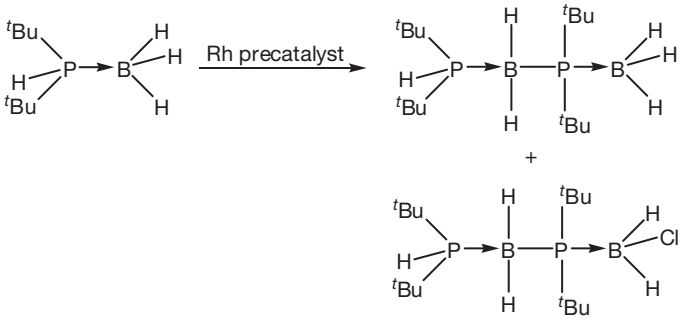

Scheme 63 Dehydrogenation reaction of $^tBu_2(H)P{\cdot}BH_3$ in the presence of the Rh precatalyst.

Copyright © 2013. Elsevier. All rights reserved.

Comprehensive Inorganic Chemistry II : From Elements to Applications, Elsevier, 2013. ProQuest Ebook Central, http://ebookcentral.proquest.com/lib/inflibnet-ebooks/detail.action?docID=1330977.
Created from inflibnet-ebooks on 2021-02-09 22:27:26.

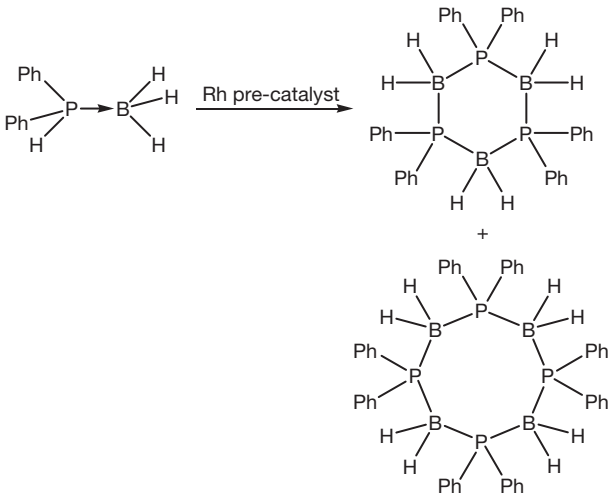

Scheme 64 Formation of cyclic products in the Rh-catalyzed dehydrogenation of $Ph_2(H)P{\cdot}BH_3$.

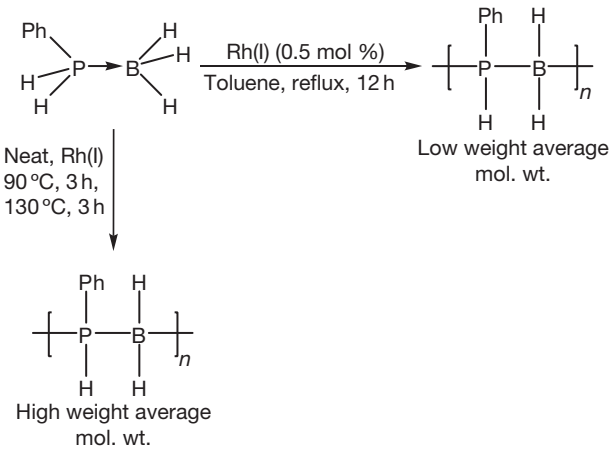

Scheme 66 Solution and bulk polymerization of $Ph(H)_2P{\cdot}BH_3$ using $[Rh(1,5\text{-}COD)_2][OTf]$.

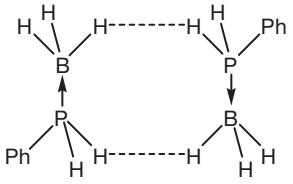

Chart 23 Dimeric structure of $Ph(H)_2P{\cdot}BH_3$.

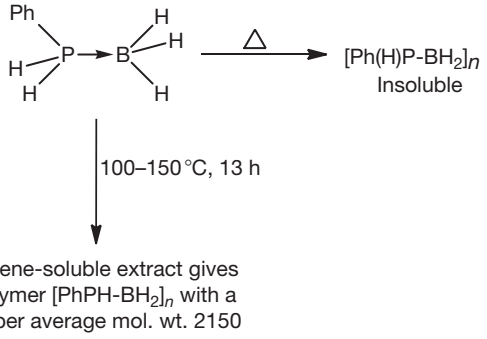

Scheme 65 Thermolysis of $Ph(H)_2P{\cdot}BH_3$: formation of soluble and insoluble polymers during shorter and prolonged heating.

Table 8 NMR, molecular weight, and thermal data of some polyphosphinoboranes

Polymer	*Chemical shift*		*Molecular weight*	T_g (°C)	*TGA* (°C)
	^{11}B	^{31}P			
$[(Ph)(H)P{-}BH_2]_n$	−34.7	−48.9	33300[a]	−9.0	160[a] 240[b,c]
$[(^i Bu)(H)P{-}BH_2]_n$	−36.0	−69.0	13100[a]	5.0	120[d] 150[b,e]
$[(p\text{-}^n BuC_6H_4)(H)P{-}BH_2]_n$	−35.7	−49.7	20800[f]	8.0	120[d] 160[b,g]
$[\{(p\text{-dodecyl})C_6H_4\}(H)P{-}BH_2]_n$	−37.5	−49.4	168000[h]	−1.0	[i]

[a]Weight average molecular weight from static light scattering.
[b]5% decomposition temperature.
[c]Char yield at 1000 °C = 75–80%.
[d]Onset of decomposition.
[e]Char yield at 1000 °C = 40–45%.
[f]Molecular weight from GPC using polystyrene as the standard ($M_w/M_n = 6$–7).
[g]Char yield at 1000 °C = 35–40%.
[h]Molecular weight from GPC using polystyrene as the standard ($M_w/M_n = 13.7$).
[i]Data not available.

1.26.11 Polyphosphinoboranes

The crystal structure of $Ph(H)_2P{\cdot}BH_3$ revealed that it exists as a dimer with dihydrogen bonds between the P–H and the B–H units (P–B, 1.924(4) Å, H——H, 2.47(6) Å) (Chart 23).[169]

The presence of the dihydrogen bonding suggests that, under suitable conditions, dehydrogenation reaction is likely to be facile with the concomitant formation of P–B bonds. Early Russian work had indicated that thermolysis of $(Ph)(H)_2P{\cdot}BH_3$ between 100 and 150 °C for 13 h affords a benzene-soluble polymer $[Ph(H)P{-}BH_2]_n$ with a number average molecular weight of 2150. Prolonged heating of $(Ph)(H)_2P{\cdot}BH_3$, however, leads to an insoluble material (Scheme 65).[171]

Rh(I) precatalysts have been found to be quite effective in the dehydrogenation–polymerization of $Ph(H)_2P{\cdot}BH_3$.[168–170,172,173] Thus, the reaction of the latter in the presence of $[Rh(1,5\text{-}COD)_2][OTf]$ (0.5 mol%) afforded a linear polymer $[Ph(H)P{-}BH_2]_n$ (^{31}P NMR: −48.9 ppm (cf. $Ph(H)_2P{\cdot}BH_3$: −47.0 ppm), ^{11}B NMR: −34.7 ppm; IR: ν(P–H), 2421 cm^{-1}; ν(B–H), 2381 cm^{-1}). Static light scattering measurements revealed that the M_w of this polymer was 5600. This reaction could be optimized and under neat polymerization conditions high-molecular-weight polymers (M_w 33300) could be obtained (Scheme 66).

Similarly, other poly(phosphinoborane)s $[^i Bu(H)P{-}BH_2]_n$, $[(p\text{-}^n Bu{-}C_6H_4)(H)P{-}BH_2]_n$, and $[((p\text{-dodecyl})C_6H_4)(H)P{-}BH_2]_n$ could also be prepared (Table 8). All of these polymers

Copyright © 2013. Elsevier. All rights reserved.

Comprehensive Inorganic Chemistry II : From Elements to Applications, Elsevier, 2013. ProQuest Ebook Central, http://ebookcentral.proquest.com/lib/inflibnet-ebooks/detail.action?docID=1330977.
Created from inflibnet-ebooks on 2021-02-09 22:27:26.

appear to be amorphous.[172] Reactions of these polymers with amines/phosphanes do not occur indicating the chemical stability of these systems.

1.26.12 Polysiloxanes

Polysiloxanes, containing alternately silicon and oxygen atoms in the backbone of a polymeric chain, $[R_2SiO_2]_n$, are the most important inorganic polymers from a commercial point of view.[1,3,5,174–178]. According to a recent analysis, the demand for various types of polysiloxanes, currently, is worth about 10–12 billion US dollars per annum.[179,180] It is forecast that this demand will increase to about 15 billion US dollars by 2015. Polysiloxanes and related systems have myriad applications in diverse areas: construction industry, automotive industry, transportation industry, electrical and electronic appliances, paintings and coatings as well as in biomedical applications.[179,180] In addition, this family of polymers also seems to have several emerging applications including in soft lithography.[181]

Polysiloxanes are isoelectronic with polyphosphazenes (Chart 24). These two polymer families also share other similar features such as the fact that only alternate atoms in the polymer backbone carry substituents. Further, in both these polymers one of the backbone atoms (nitrogen in the case of polyphosphazenes and oxygen in the case of polysiloxanes) possesses Lewis basicity owing to the presence of lone pair(s) of electrons.

1.26.12.1 Historical

Kipping laid the foundations of the organosilicon chemistry and has developed routes for the preparation of organosilicon compounds such as $RSiCl_3$, R_2SiCl_2, and R_3SiCl.[178] Typically, these compounds were prepared by the reactions of Grignard reagents with $SiCl_4$ (Scheme 67).

Kipping's efforts to prepare silanols yielded condensation products as a result of elimination of water (Scheme 68).

Diorganodichlorosilanes also underwent a similar reaction (Scheme 69). The condensation products of these reactions, $[R_2SiO]_n$, were called silicones because their chemical composition matched the corresponding organic ketones, $R_2C{=}O$, except for the presence of silicon (Scheme 69).

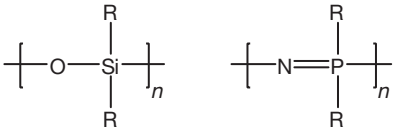

Chart 24 Isoelectronic relationship of polysiloxanes with polyphosphazenes.

$$RMgBr + SiCl_4 \longrightarrow RSiCl_3 + MgBrCl$$

Scheme 67 Synthesis of organosilicon compounds using Grignard reagents.

However, it was clear to Kipping that silicones were not structurally similar to organic ketones and possessed more complex structures. He was able to isolate some of these compounds in their pure form and was able to assign discrete cyclic ring structures such as $[Ph_2SiO]_3$ and $[Ph_2SiO]_4$.

Alfred Stock, another pioneer, developed the silicon hydride chemistry and probably was the first person to have obtained authentic samples of poly(dimethylsiloxane), $[Me_2SiO]_n$, by the hydrolysis of $(CH_3)_2SiH_2$.[178]

Although forgotten for some time, siloxane chemistry was revived by an industrial need for high-temperature-resistant insulation material. A polymer $[PhEtSiO]_n$, which could be cross-linked, and used continuously at 160 °C, was developed at Corning glass works.[178] The major breakthrough in this area came from Rochow's work at General Electric which revealed that a mixture of $MeSiCl_3$ and Me_2SiCl_2 could be hydrolyzed to give a polymer which could be cross-linked to give a high-temperature-resistant material. The commercial viability of these polymers became realized upon the development of the 'direct process' for the preparation of organochlorosilanes. The 'direct process', involving the reaction of methyl chloride with silicon in the presence of copper, afforded a mixture of methyl chlorosilanes which could be separated from each other as a result of differences in boiling points ($MeSiCl_3$, 57.3 °C; Me_2SiCl_2, 70.0 °C; Me_3SiCl, 57.3 °C; $SiCl_4$, 57.6 °C) between Me_2SiCl_2 and other chlorosilanes. The direct process was also developed, independently, by R. Müller in Germany. These initial and crucial breakthroughs led the foundation of the 'silicone' industry, a name that was retained because of the original nomenclature adopted by Kipping. A beautiful first-hand account of the history of the silicones is provided by Rochow in a small and readable book.[178] Currently, polysiloxanes are prepared by (1) ROP of cyclosiloxanes and (2) condensation polymerization involving condensation of hydrolysis products of organochlorosilanes.[1,3,5,174–177]

Cyclosiloxane chemistry is not as well developed as the cyclophosphazene chemistry, particularly since the rich nucleophilic chemistry available in chlorocyclophosphazenes is difficult to be implemented in the corresponding cyclosiloxane chemistry. Organosiloxanes can be prepared by a variety of ways, although hydrolysis of organochlorosilanes is an important method (Scheme 70).

Representative examples of cyclosiloxanes and a cage siloxane are illustrated in Chart 25.[1]

$$R_3SiCl + H_2O \longrightarrow R_3SiOH$$

$$2\ R_3SiOH \longrightarrow R_3Si{-}O{-}SiR_3 + H_2O$$

Scheme 68 Hydrolysis of triorganochlorosilanes and condensation of triorganosilanols.

$$R_2SiCl_2 + H_2O \longrightarrow R_2Si(OH)_2$$

$$nR_2Si(OH)_2 \longrightarrow (R_2SiO)_n + nH_2O$$

Scheme 69 Hydrolysis of diorganodichlorosilanes.

Copyright © 2013. Elsevier. All rights reserved.

Comprehensive Inorganic Chemistry II : From Elements to Applications, Elsevier, 2013. ProQuest Ebook Central, http://ebookcentral.proquest.com/lib/inflibnet-ebooks/detail.action?docID=1330977.
Created from inflibnet-ebooks on 2021-02-09 22:27:26.

In passing, it must be mentioned that the elusive, genuine silicone, possessing a formal Si=O bond, was recently isolated and structurally characterized by Driess and coworkers (Scheme 71). The isolation of this compound involved the reaction of a *N*-heterocyclic carbene (NHC)-stabilized silylene with nitrous oxide.[183] The resultant silanone has a Si–O bond distance of 1.541(2) Å which is shorter than normal Si–O bond distances found in other instances (cf. $[Me_2SiO]_3$, 1.61(4); $[Me_2SiO]_4$, 1.65; $[Ph_2SiO]_3$, 1.640(16); $[PhSiO]_4$,1.613(7) Å).

1.26.12.2 ROP of Cyclosiloxanes

Since there is virtually no ring strain in cyclosiloxanes, particularly in the puckered eight-membered rings, the driving force for their ROP cannot be enthalpy driven.[1,3,5,174] On the other hand, the polymers possess greater skeletal flexibility in comparison to cyclic analogs. It is therefore believed that entropy favors the ROP. Cyclosiloxanes can be converted into polymers by ROP by the use of cationic or anionic initiators. Protic acids (H_2SO_4, $HClO_4$, and CF_3SO_3H) or Lewis acids ($AlCl_3$ and $SnCl_4$) are effective in ROP of cyclosiloxanes. Depending on the exact conditions used, short-chain oligomers or high-molecular-weight polymers can be prepared. Short-chain oligomers, such as $Me_3Si(OSiMe_2)_nOSiMe_3$, are useful as silicone oils which have high-temperature stability as well as low-viscosity-temperature coefficients. The latter imply little or no change in the viscosity of the fluid with variation of temperature. It is because of this feature that a number of silicone oils can be used at extremely low temperatures such as −80 °C.

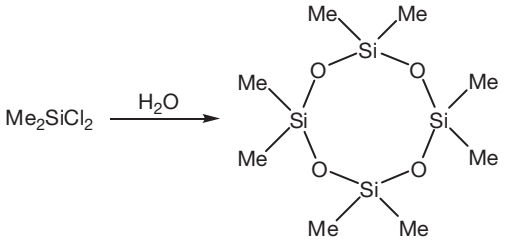

Scheme 70 Synthesis of an eight-membered cyclosiloxane.

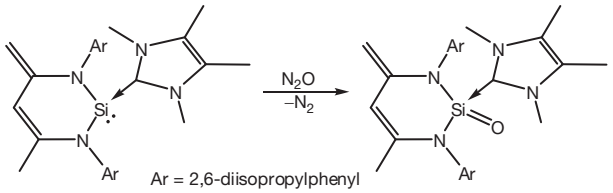

Scheme 71 Synthesis of the NHC-stabilized silanone complex.

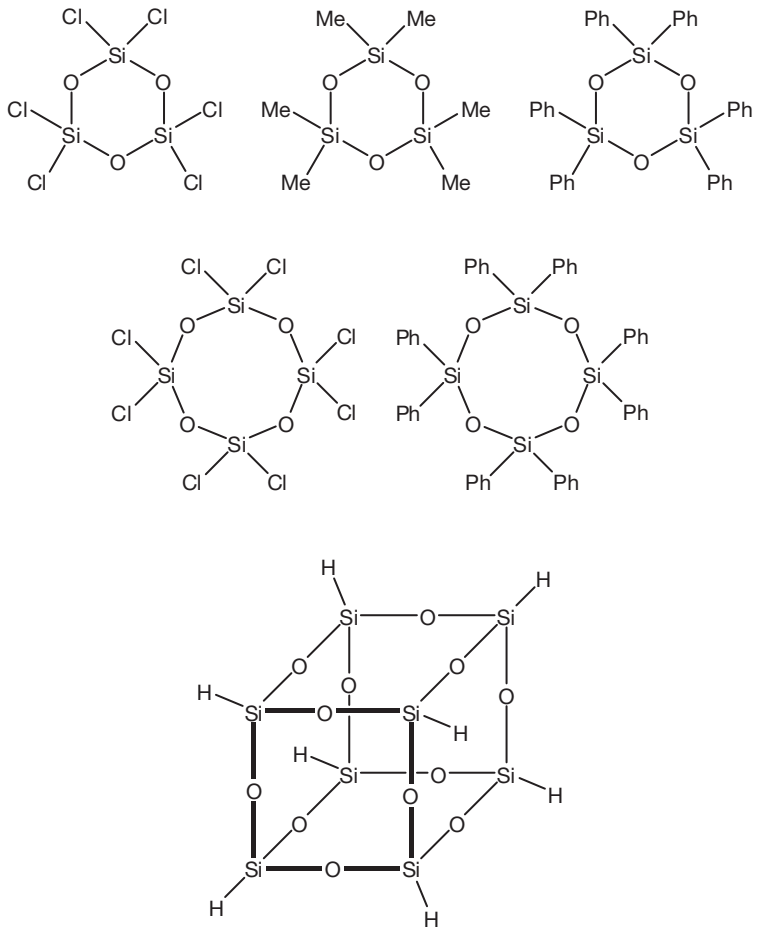

Chart 25 Representative examples of cyclosiloxanes and a cage siloxane.

Copyright © 2013. Elsevier. All rights reserved.

Comprehensive Inorganic Chemistry II : From Elements to Applications, Elsevier, 2013. ProQuest Ebook Central, http://ebookcentral.proquest.com/lib/inflibnet-ebooks/detail.action?docID=1330977.
Created from inflibnet-ebooks on 2021-02-09 22:27:26.

Anionic polymerization methods are more effective for the ROP of cyclosiloxanes. Several initiators including KOH are effective for this purpose. Very high molecular weights, up to 10^6, are realized by this method. In general, all the polymerization techniques use end capping by Me_3Si groups to afford stability to the polymer chains.

Condensation polymerization methods involve condensation of silanols which are compounds containing Si–OH groups. Such compounds are first obtained by the hydrolysis of organochlorosilanes which subsequently undergo condensation reactions (Scheme 72).

These hydrolysis/condensation reactions are extremely sensitive to the reaction conditions. Modulation of molecular weights as well as control in the formation of linear versus cyclic products can be effected by change of reaction conditions.

1.26.12.3 Cross-Linking

A number of applications of polysiloxanes depend crucially upon curing or cross-linking reactions.[1,3,174] This process converts these polymers into advanced elastomers which then find use in a variety of applications. Among the many cross-linking methodologies available, generating intermolecular $-CH_2-CH_2-$ linkages is an important one (Schemes 73 and 74).

The first method (Scheme 73) involves generation of a carbon-centered radical which allows intermolecular coupling reaction. The second method (Scheme 74) involves coupling a Si–H group with a $Si-CH_2=CH_2$ unit by the hydrosilylation reaction. It must be emphasized that several other types of cross-linking reactions are possible and find use depending on the need.[1]

1.26.12.4 Structure and Properties of Polysiloxanes

Polysiloxanes have distinct properties that have allowed them to carve out an important niche in the polymer industry. Briefly these are:

1. unusual skeletal flexibility that is retained over a wide temperature range,
2. high gas permeability, including oxygen,
3. good thermal and oxidative stability,
4. high hydrophobicity,
5. low surface tension,
6. low toxicity, and
7. biocompatibility.

Many of the above-mentioned properties result from the intrinsic structural features that characterize the polysiloxane backbone.[1,3,174,184] One of the important features of the polysiloxane structure is that only alternate atoms in the polymer backbone have substituents. This allows considerable torsional freedom about the Si–O bond which in turn imparts great skeletal flexibility to the polysiloxane chains. Second, in comparison to organic polymers, the bond distances about silicon are longer. For example, in poly(dimethylsiloxane), the Si–C distance is about 1.87–1.90 Å, while the Si–O distance is about 1.64 Å. In comparison, in organic polymers, the C–C bond distances are about 1.54 Å. Therefore, over all, there is much less steric strain in a polysiloxane chain. Third, the Si–O–Si bond angles in cyclosiloxanes, polysiloxanes, and even in silicate materials vary considerably and even angles close to 180° are found in some situations. Studies on polysiloxanes concur

Scheme 72 Synthesis poly(dimethylsiloxane) through condensation polymerization.

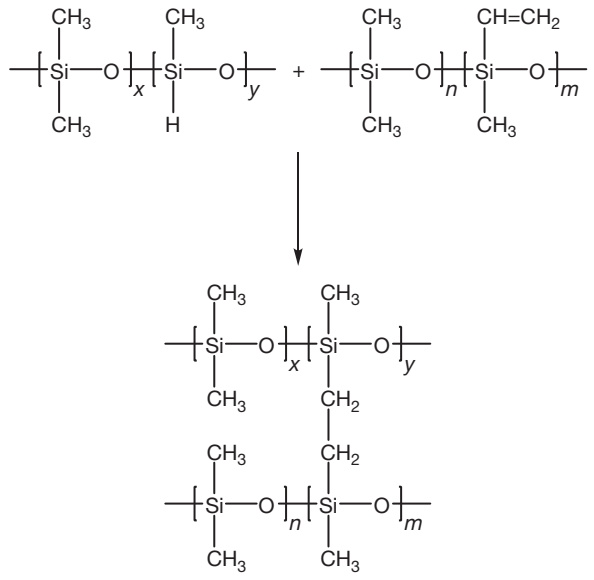

Scheme 74 Generation of intermolecular $-CH_2-CH_2-$ linkages through hydrosilylation reaction.

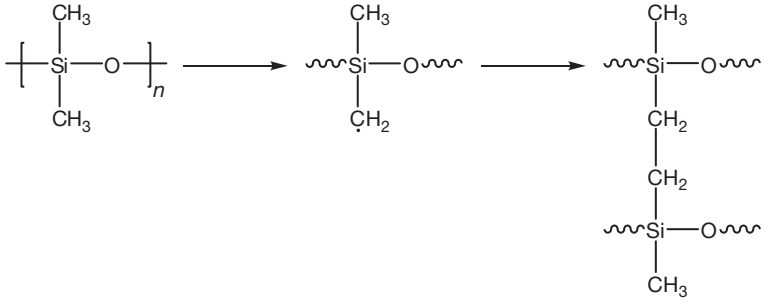

Scheme 73 Free-radical-mediated curing of polydimethylsiloxane through the formation of intermolecular $-CH_2-CH_2-$ linkages.

Copyright © 2013. Elsevier. All rights reserved.

Comprehensive Inorganic Chemistry II : From Elements to Applications, Elsevier, 2013. ProQuest Ebook Central, http://ebookcentral.proquest.com/lib/inflibnet-ebooks/detail.action?docID=1330977.
Created from inflibnet-ebooks on 2021-02-09 22:27:26.

with these arguments and reveal a nearly unrestricted rotation about the polymer backbone.[184] Experimentally, this is reflected in very low T_g's: $[Me_2SiO]_n$, −123 °C; $[MeHSiO]_n$, −138 °C; $[MePhSiO]_n$, −33 °C; $[Et_2SiO]_n$, −139 °C. In comparison, the data for other well-known elastomers are: natural rubber, −72 °C and $[NPCl_2]_n$, −66 °C. Thus, polysiloxanes possess the lowest T_g's for any polymeric system.

The water-repelling properties of polysiloxanes emerge as a result of the hydrophobic sheath of methyl groups which effectively shield the Si–O–Si backbone. As a result of the nonpolar, external sheath of methyl groups, intermolecular interactions among poly(dimethylsiloxane) chains are minimum.[184]

1.26.12.5 Summary

1. In general, commercially important polysiloxanes can be prepared by hydrolysis/condensation reactions of organochlorosilanes or by an ROP of cyclosiloxanes.
2. Polysiloxanes possess many unique properties among polymer families. These include low-temperature flexibility and high-temperature resistance. Many of these unique properties arise as a result of the structural features of this polymeric system which includes a highly flexible Si–O–Si bond. In addition, the longer Si–O and Si–C distances found in polysiloxanes, when compared to the C–C bond distances found in organic polymers, also increase the torsional freedom in these polymers.
3. In poly(dimethylsiloxane), the methyl groups provide a very effective organic sheath around the Si–O–Si polymeric chain, imparting highly hydrophobic properties to these polymers.
4. Many of the elastomer-related applications of polysiloxanes need cross-linking or curing of the parent polymer chains.

1.26.13 Conclusion

Assembling inorganic polymers remains a synthetic challenge. One of the major reasons for the success of the organic polymers is the rich functional group chemistry of organic compounds which allows preparation of a wide range of polymers whose properties can be modulated by changing the nature of the monomer(s). Unfortunately, among inorganic systems, such versatile functional group chemistry is still not available. As a result, every polymeric system needs specific synthetic methodologies. Consequently, large families of inorganic polymers are still not available. Interestingly, even with such a scenario, polysiloxanes and related members have been tremendously successful from a commercial point of view. Thus, if more types of inorganic polymers can be prepared, it is quite likely that some of them would find interesting practical applications. Among the polymers discussed in this chapter, polyphosphazenes and polysiloxanes can be prepared by an ROP of the corresponding rings, $N_3P_3Cl_6$ and $[Me_2SiO]_4$. Polysiloxanes can also be prepared by a hydrolysis/condensation of organochlorosilanes.

ROP has also been found to be successful in the case of some cycloheterophosphazenes. Among polyphosphazenes, macromolecular substitution on $[N{=}PCl_2]_n$ continues to be the predominant way for preparing new types of polymers. New synthetic methods for the preparation of $[N{=}PCl_2]_n$ involving cationic living polymerization of monomers such as $Cl_3P{=}NSiMe_3$ have become available which augurs well for this family. Condensation polymerization techniques involving phosphoranimines were earlier known for the preparation of poly(alkyl/arylphosphazene)s. New synthetic methods such as dehydrogenation/coupling offer a great deal of promise in the preparation of polymers containing B–N and B–P motifs. Clearly, many such new methods are required if more types of inorganic polymers are to be realized. For related chapters in this Comprehensive, we refer to **Chapters 1.02** and **1.07**.

Acknowledgments

VC is grateful to IIT Kanpur for support and facilities. He is also thankful to the Department of Science and Technology, New Delhi, India for the National J. C. Bose research fellowship. SN is thankful to IIT Delhi for support and facilities. SN is thankful to the Department of Science and Technology, New Delhi, India, for generous research support.

References

1. Chandrasekhar, V. *Inorganic and Organometallic Polymers*. Springer-Verlag: Heidelberg, Germany, 2005.
2. Allcock, H. R. *Chemistry and Applications of Polyphosphazenes*. Wiley-Interscience: New York, 2003.
3. Mark, J. E.; West, R.; Allcock, H. R. *Inorganic Polymers*. Oxford University Press: Toronto, 2005.
4. Gleria, M., De Jaeger, R., Eds.; In *Phosphazenes – A World-Wide Insight*; Nova Science: New York, 2004.
5. Chivers, T.; Manners, I. *Inorganic Rings and Polymers of the p-Block Elements*. RSC Publishing: Cambridge, 2009.
6. Neilson, R. H.; Wisian-Neilson, P. *Chem. Rev.* **1988**, *88*, 541.
7. Allcock, H. R. *Chem. Rev.* **1972**, *72*, 315.
8. Boomishankar, R.; Ledger, J.; Guilbaud, J.-B.; Campbell, N. L.; Bacsa, J.; Bonar-Law, R.; Khimyak, Y. Z.; Steiner, A. *Chem. Commun.* **2007**, 5152.
9. Tun, Z.-M.; Heston, A. J.; Panzner, M. J.; Medvetz, D. A.; Wright, B. D.; Savant, D.; Dudipala, V. R.; Banerjee, D.; Rinaldi, P. L.; Youngs, W. J.; Tessier, C. A. *Inorg. Chem.* **2011**, *50*, 8937.
10. Zhang, Y.; Tham, F. S.; Reed, C. A. *Inorg. Chem.* **2006**, *45*, 10446.
11. Zhang, Y.; Huynh, K.; Manners, I.; Reed, C. A. *Chem. Commun.* **2008**, *4*, 494.
12. Jaeger, R. D.; Gleria, M. *Prog. Polym. Sci.* **1998**, *23*, 179.
13. Jaeger, R. D.; Potin, P. In *Phosphazenes – A World-Wide Insight*; Gleria, M., De Jaeger, R., Eds.; Nova Science: New York, 2004; pp 25–48.
14. Halluin, G. D.; Jaeger, R. D.; Chambrette, J. P.; Potin, P. *Macromolecules* **1992**, *25*, 1254.
15. Blackstone, V.; Soto, A. P.; Manners, I. *Dalton Trans.* **2008**, *33*, 4363.
16. Honeyman, C. H.; Manners, I.; Morrissey, C. T.; Allcock, H. R. *J. Am. Chem. Soc.* **1995**, *117*, 7035.
17. Wang, B.; Rivard, E.; Manners, I. *Inorg. Chem.* **2002**, *41*, 1690.
18. Allcock, H. R.; Crane, C. A.; Morrissey, C. T.; Nelson, J. M.; Reeves, S. D.; Honeyman, C. H.; Manners, I. *Macromolecules* **1996**, *24*, 7740.
19. Nelson, J. M.; Primrose, A. P.; Hartle, T. J.; Allcock, H. R.; Manners, I. *Macromolecules* **1998**, *31*, 947.
20. Soto, A. P. P.; Manners, I. *Macromolecules* **2009**, *42*, 40.
21. Rivard, E.; Lough, A. J.; Manners, I. *Inorg. Chem.* **2004**, *43*, 2765.
22. Blackstone, V.; Lough, A. J.; Murray, M.; Manners, I. *J. Am. Chem. Soc.* **2009**, *131*, 3658.
23. Allcock, H. R.; Krause, W. E. *Macromolecules* **1997**, *30*, 5683.
24. Chandrasekhar, V.; Krishnan, V. *Adv. Inorg. Chem.* **2002**, *53*, 159.
25. Allcock, H. R.; Desorcie, J. L.; Riding, G. H. *Polyhedron* **1987**, 119.
26. Huynh, K.; Rivard, E.; Lough, A. J.; Manners, I. *Chem. Eur. J.* **2007**, *13*, 3431.

Copyright © 2013. Elsevier. All rights reserved.

Comprehensive Inorganic Chemistry II : From Elements to Applications, Elsevier, 2013. ProQuest Ebook Central, http://ebookcentral.proquest.com/lib/inflibnet-ebooks/detail.action?docID=1330977.
Created from inflibnet-ebooks on 2021-02-09 22:27:26.

27. Huynh, K.; Rivard, E.; Lough, A. J.; Manners, I. *Inorg. Chem.* **2007**, *46*, 9979.
28. Huynh, K.; Lough, A. J.; Manners, I. *J. Am. Chem. Soc.* **2006**, *128*, 14002.
29. Huynh, K.; Lough, A. J.; Forgeron, M. A. M.; Bendle, M.; Soto, A. P.; Wasylishen, R. E.; Manners, I. *J. Am. Chem. Soc.* **2009**, *131*, 7905.
30. Montague, R. A.; Matyjaszewski, K. *J. Am. Chem. Soc.* **1990**, *112*, 6721.
31. Taylor, T. J.; Soto, A. P.; Huynh, K.; Lough, A. J.; Swain, A. C.; Norman, N. C.; Russell, C. A.; Manners, I. *Macromolecules* **2010**, *43*, 7446.
32. Singh, A.; Steely, L.; Allcock, H. R. *Langmuir* **2005**, *21*, 11604.
33. Allcock, H. R.; Steely, L. B.; Kim, S. H.; Kim, J. H.; Kim, B.-K. *Langmuir* **2007**, *23*, 8103.
34. Allcock, H. R.; Allen, R. W.; O'Brien, J. P. *J. Am. Chem. Soc.* **1977**, *99*, 3984.
35. Walker, C. H.; St. John, J. V.; Wisian-Neilson, P. *J. Am. Chem. Soc.* **2001**, *123*, 3846.
36. Morozowich, N. L.; Weikel, A. L.; Nichol, J. L.; Chen, C.; Nair, L. S.; Laurencin, C. T.; Allcock, H. R. *Macromolecules* **2011**, *44*, 1355.
37. Weikel, A. L.; Owens, S. G.; Fushimi, T.; Allcock, H. R. *Macromolecules* **2010**, *43*, 5205.
38. Weikel, L.; Krogman, N. R.; Nguyen, N. Q.; Nair, L. S.; Laurencin, C. T.; Allcock, H. R. *Macromolecules* **2009**, *42*, 636.
39. Krogman, N. R.; Weikel, A. L.; Nguyen, N. Q.; Nair, L. S.; Laurencin, C. T.; Allcock, H. R. *Macromolecules* **2008**, *41*, 7824.
40. Krogman, N. R.; Steely, L.; Hindenlang, M. D.; Nair, L. S.; Laurencin, C. T.; Allcock, H. R. *Macromolecules* **2008**, *41*, 1126.
41. Krogman, N. R.; Hindenlang, M. D.; Nair, L. S.; Laurencin, C. T.; Allcock, H. R. *Macromolecules* **2008**, *41*, 8467.
42. Allcock, H. R.; Fuller, T. J.; Mack, D. P.; Matsumara, K.; Smeltz, K. M. *Macromolecules* **1977**, *10*, 824.
43. Allcock, H. R.; Fuller, T. J.; Matsumara, K. *Inorg. Chem.* **1982**, *21*, 515.
44. Nukavarapu, S. P.; Kumbar, S. G.; Brown, J. L.; Krogman, N. R.; Weikel, A. L.; Hindenlang, M. D.; Nair, L. S.; Allcock, H. R.; Laurencin, C. T. *Biomacromolecules* **2008**, *9*, 1818.
45. Blonsky, P. M.; Shriver, D. F.; Austin, P.; Allcock, H. R. *J. Am. Chem. Soc.* **1984**, *106*, 6854.
46. Allcock, H. R.; Sunderland, N. J.; Ravikiran, R.; Nelson, J. M. *Macromolecules* **1998**, *31*, 8026.
47. Chandrasekhar, V. *Adv. Polym. Sci.* **1998**, *135*, 139.
48. Selvaraj, I.; Chaklanobis, S.; Chandrasekhar, V. *Polym. Int.* **1998**, *46*, 111.
49. Chaklanobis, S.; Chandrasekhar, V. *J. Electrochem. Soc.* **1995**, *142*, 3434.
50. Argun, A.; Ashcraft, J. N.; Herring, M. K.; Lee, D. K. Y.; Allcock, H. R.; Hammond, P. T. *Chem. Mater.* **2010**, *22*, 226.
51. Dupont, J. G.; Allen, C. W. *Inorg. Chem.* **1978**, *17*, 3093.
52. Allen, C. W.; Bright, R. P. *Inorg. Chem.* **1983**, *22*, 1291.
53. Shaw, J. C.; Allen, C. W. *Inorg. Chem.* **1986**, *25*, 4632.
54. Chandrasekhar, V.; Thomas, K. R. J. *Struct. Bond* **1993**, *81*, 41.
55. Bosscher, G.; Meetsma, A.; Van de Grampel, J. C. *Inorg. Chem.* **1996**, *35*, 6646.
56. Van de Grampel, J. C.; Alberda van Ekenstein, G. O. R.; Baas, J.; Buwalda, P. L.; Jekel, A. P.; Oosting, G. E. *Phosphorus Sulfur Silicon* **1992**, *64*, 91.
57. Bosscher, C.; Meetsma, A.; Van de Grampel, J. C. *Dalton Trans.* **1997**, 1667.
58. Ramachandran, K.; Allen, C. W. *Inorg. Chem.* **1983**, *22*, 1445.
59. Allen, C. W.; Ramachandran, K.; Brown, D. E. *Inorg. Synth.* **1987**, *25*, 74.
60. Brown, D. E.; Allen, C. W. *Inorg. Chem.* **1987**, *26*, 934.
61. Inoue, K.; Takagi, M.; Nakano, M.; Nakamura, H.; Tanigaki, T. *Makromol. Chem. Rapid Commun.* **1988**, *9*, 345.
62. Van de Grampel, J. C. *Hybrid Inorganic–Organic Phosphazene Polymers*. In *Phosphazenes – A World-Wide Insight*; Gleria, M., De Jaeger, R., Eds.; Nova Science: New York, 2004; p 143.
63. Allcock, H. R.; Laredo, W. R.; Kellam, E. C.; Morford, R. V. *Macromolecules* **2001**, *34*, 787.
64. DuPont, J. G.; Allen, C. W. *Macromolecules* **1979**, *12*, 169.
65. Allen, C. W.; Bright, R. P. *Macromolecules* **1986**, *19*, 571.
66. Allen, C. W.; Shaw, J. C.; Brown, D. E. *Macromolecules* **1988**, *21*, 2653.
67. Brown, D. E.; Ramachandran, K.; Carter, K.; Allen, C. W. *Macromolecules* **2001**, *34*, 2870.
68. Inoue, K.; Nakano, M.; Takagi, M.; Tanigaki, T. *Macromolecules* **1989**, *22*, 1530.
69. Inoue, K.; Nakamura, H.; Ariyoshi, S.; Takagi, M.; Tanigaki, T. *Macromolecules* **1989**, *22*, 4466.
70. Selvaraj, I.; Chandrasekhar, V. *Polymer* **1997**, *38*, 3617.
71. Chandrasekhar, V.; Athimoolam, A.; Dastagiri Reddy, N.; Nagendran, S.; Steiner, A.; Zacchini, S.; Butcher, R. *Inorg. Chem.* **2003**, *42*, 51.
72. Inoue, K.; Nishikawa, Y.; Tanigaki, T. *Macromolecules* **1991**, *24*, 3464.
73. Inoue, K.; Kinoshita, K.; Nakahara, H.; Tanigaki, T. *Macromolecules* **1990**, *23*, 1227.
74. Allcock, H. R.; Welna, D. T.; Stone, D. A. *Macromolecules* **2005**, *38*, 10406.
75. Chandrasekhar, V.; Nagendran, S. *Chem. Soc. Rev.* **2001**, *30*, 193.
76. Chandrasekhar, V.; Athimoolam, A. P.; Vivekanandan, K.; Nagendran, S. *Tetrahedron Lett.* **1999**, *40*, 1185.
77. Chandrasekhar, V.; Athimoolam, A. P.; Srivatsan, S. G.; Sundaram, P. S.; Varma, S.; Steiner, A.; Zacchini, S.; Butcher, R. *Inorg. Chem.* **2002**, *41*, 5162.
78. Chandrasekhar, V.; Deria, P.; Krishnan, V.; Athimoolam, A. P.; Singh, S.; Madhavaiah, C.; Srivatsan, S. G.; Varma, S. *Bioorg. Med. Chem. Lett.* **2004**, *14*, 1559.
79. Chandrasekhar, V.; Athimoolam, A. P. *Org. Lett.* **2002**, *4*, 2113.
80. Elias, A. J.; Jain, M.; Reddy, N. D. *Phosphorus Sulfur Silicon* **1998**, *140*, 203.
81. Vij, A.; Elias, A. J.; Kirchmeier, R. L.; Shreeve, J. M. *Inorg. Chem.* **1997**, *36*, 2730.
82. Ramakrishna, T. V. V.; Elias, A. J. *Phosphorus Sulfur Silicon* **2002**, *177*, 2513.
83. Reddy, N. D.; Elias, A. J.; Vij, A. *J. Chem. Soc. Dalton Trans.* **1999**, 1515.
84. Chandrasekhar, V.; Senapati, T.; Dey, A.; Hossain, S.; Gopal, K. *Cryst. Growth Design* **2011**, *11*, 1512.
85. Chandrasekhar, V.; Krishnan, V.; Azhakar, R.; Senapati, T.; Dey, A.; Suriyanarayanan, R. *Inorg. Chem.* **2011**, *50*, 2568.
86. Manners, I.; Allcock, H. R. *J. Am. Chem. Soc.* **1989**, *111*, 5478.
87. Allcock, H. R.; Coley, S. M.; Manners, I.; Visscher, K. B.; Parvez, M.; Nuyken, O.; Renner, G. *Inorg. Chem.* **1993**, *32*, 5088.
88. Rivard, E.; Lough, A. J.; Manners, I. *Inorg. Chem.* **2004**, *43*, 2765.
89. Allcock, H. R.; Coley, S. M.; Manners, I.; Renner, G. *Macromolecules* **1991**, *24*, 2024.
90. Allcock, H. R.; Coley, S. M.; Morrissey, C. T. *Macromolecules* **1994**, *27*, 2904.
91. Becke-Goehring, M.; Jung, D. *Z. Anorg. Chem.* **1970**, *372*, 233.
92. Dodge, J. A.; Manners, I.; Allcock, H. R.; Renner, G.; Nuyken, O. *J. Am. Chem. Soc.* **1990**, *112*, 1268.
93. Allcock, H. R.; Dodge, J. A.; Manners, I. *Macromolecules* **1993**, *26*, 11.
94. Gates, D. P.; Manners, I. *Dalton Trans.* **1997**, 2525.
95. Manners, I. *Angew. Chem. Int. Ed.* **1996**, *35*, 1602.
96. Suzuki, D.; Akagi, H.; Matsumura, K. *Synth. Commun.* **1983**, 369.
97. Gates, D. P.; Ziembinski, R.; Manners, I.; Rheingold, A. L.; Haggerty, B. S. *Angew. Chem. Int. Ed. Engl.* **1994**, *33*, 2277.
98. Gates, D. P.; Liable-Sands, L. M.; Yap, G. P. A.; Rheingold, A. L.; Manners, I. *J. Am. Chem. Soc.* **1997**, *119*, 1125.
99. Gates, D. P.; McWilliams, A. R.; Ziembinski, R.; Liable-Sands, L. M.; Guzei, I. A.; Yap, G. P. A.; Rheingold, A. L.; Manners, I. *Chem. Eur. J.* **1998**, *4*, 1489.
100. McWilliams, A. R.; Rivard, E.; Lough, A. J.; Manners, I. *Chem. Commun.* **2002**, *10*, 1102.
101. Rivard, E.; Ragogna, P. J.; McWilliams, A. R.; Lough, A. J.; Manners, I. *Inorg. Chem.* **2005**, *44*, 6789.
102. Witt, M.; Roesky, H. W. *Chem. Rev.* **1994**, *94*, 1163.
103. Roesky, H. W.; Katti, K. V.; Seseke, U.; Witt, M.; Egert, E.; Herbst, R.; Sheldrick, G. M. *Angew. Chem. Int. Ed.* **1986**, *25*, 477.
104. Roesky, H. W.; Katti, K. V.; Seseke, U.; Schmidt, H. G.; Egert, E.; Herbst, R.; Sheldrick, G. M. *Dalton Trans.* **1987**, 847.
105. Katti, K. V.; Roesky, H. W.; Mietzel, M. *Inorg. Chem.* **1987**, *26*, 4032.
106. Liang, M.; Manners, I. *J. Am. Chem. Soc.* **1991**, *113*, 4044.
107. Ni, Y.; Stammer, A.; Liang, M.; Massey, J.; Vancso, G. J.; Manners, I. *Macromolecules* **1992**, *25*, 119.
108. Nobius, N.; McWilliams, A. R.; Nuyken, O.; Manners, I. *Macromolecules* **2000**, *33*, 7707.
109. Roesky, H. W. *Angew. Chem. Int. Ed.* **1972**, *11*, 642.
110. McWilliams, A. R.; Gates, D. P.; Edwards, M.; Liable-Sands, L. M.; Guzei, I.; Rheingold, A. L.; Manners, I. *J. Am. Chem. Soc.* **2000**, *122*, 8848.
111. Manners, I. *Coord. Chem. Rev.* **1994**, *137*, 109.
112. McWilliams, A. R.; Manners, I. In *Phosphazenes – A World-Wide Insight*; Gleria, M., De Jaeger, R., Eds.; Nova Science: New York, 2004; pp 191–208.
113. McWilliams, A. R.; Dorn, H.; Manners, I. *Top. Curr. Chem.* **2002**, *220*, 141.
114. Ni, Y.; Park, P.; Liang, M.; Massey, J.; Waddling, C.; Manners, I. *Macromolecules* **1996**, *29*, 3401.
115. Wang, Z.; McWilliams, A. R.; Evans, C. E. B.; Lu, X.; Chung, S.; Winnik, M. A. *Adv. Funct. Mater.* **2002**, *12*, 415.
116. Huynh, L.; Wang, Z.; Yang, J.; Stoeva, V.; Lough, A.; Manners, I.; Winnik, M. A. *Chem. Mater.* **2005**, *17*, 4765.
117. Wang, Z.; Manners, I. *Macromolecules* **2005**, *38*, 5047.
118. Greenwood, N.; Earnshaw, A. *Chemistry of the Elements*, 2nd ed.; Butterworth-Heinemann: Oxford, UK, 1997.
119. Paine, R. T.; Narula, C. K. *Chem. Rev.* **1990**, *90*, 73.
120. Staubitz, A.; Robertson, A. P. M.; Sloan, M. E.; Manners, I. *Chem. Rev.* **2010**, *110*, 4023.

Copyright © 2013. Elsevier. All rights reserved.

Comprehensive Inorganic Chemistry II : From Elements to Applications, Elsevier, 2013. ProQuest Ebook Central, http://ebookcentral.proquest.com/lib/inflibnet-ebooks/detail.action?docID=1330977.
Created from inflibnet-ebooks on 2021-02-09 22:27:26.

121. Staubitz, A.; Robertson, A. P. M.; Manners, I. *Chem. Rev.* **2010**, *110*, 4079.
122. Housecroft, C. E.; Sharpe, A. G. *Inorganic Chemistry*, 3rd ed.; Pearson Education: Harlow, Essex, 2008.
123. Karkamkar, A.; Aardahl, C.; Autrey, T. *Mater. Matters* **2007**, *2*, 6.
124. Peng, B.; Chen, J. *Energy Environ. Sci.* **2008**, *1*, 479.
125. Stephens, F. H.; Pons, V.; Baker, R. T. *Dalton Trans.* **2007**, 2613.
126. Marder, T. B. *Angew. Chem. Int. Ed.* **2007**, *46*, 8116.
127. Chen, X.; Zhao, J. C.; Shore, S. G. *J. Am. Chem. Soc.* **2010**, *132*, 10658.
128. Woollins, J. D. *Non-metal Rings, Cages and Clusters*. Wiley: Chichester, 1988.
129. Bramham, G.; Charmant, J. P. H.; Cook, A. J. R.; Norman, W. C.; Russell, C. A.; Saithong, S. *Chem. Commun.* **2007**, 4605.
130. Wideman, T.; Sneddon, L. G. *Inorg. Chem.* **1996**, *34*, 1002.
131. Fazen, J.; Sneddon, L. G. *Organometallics* **1994**, *13*, 2867.
132. Maringgele, W. In Haiduc, I., Sowerby, D. B., Eds.; The Chemistry of Inorganic Homo- and Hetero-Cycles; Academic Press: London, 1987; Vol. 1, Chapter 2, pp 17–101.
133. Anand, B.; Noth, H.; Schwenk- Kircher, H.; Troll, A. *Eur. J. Inorg. Chem.* **2008**, 3186.
134. Wakamiya, A.; Ide, T.; Yamaguchi, S. *J. Am. Chem. Soc.* **2005**, *127*, 14859.
135. Sham, H. T.; Kwok, C.-C.; Che, C.-M.; Zhu, N. *Chem. Commun.* **2005**, 3547.
136. Noth, H.; Rojas-Lima, S.; Troll, A. *Eur. J. Inorg. Chem.* **2005**, 1895.
137. Braunschweig, H.; Kollann, C.; Müller, M. *Eur. J. Inorg. Chem.* **1998**, 291.
138. Braunschweig, H.; Green, H.; Radacki, K.; Uttinger, K. *Dalton Trans.* **2008**, 3531.
139. Niedenzu, K.; Dawson, J. W. *Boron–Nitrogen Compound*. Springer-Verlag: New York, 1965.
140. Burg, A. B.; Randolph, C. L. *J. Am. Chem. Soc.* **1949**, *71*, 3451.
141. Ryschkewitsch, G. E.; Wiggins, J. W. *Inorg. Chem.* **1970**, *9*, 314.
142. Clark, T. J.; Lee, K.; Manners, I. *Chem. Eur. J.* **2006**, *12*, 8634.
143. Jaska, C.; Temple, K.; Lough, A. J.; Manners, I. *Chem. Commun.* **2001**, 962.
144. Jaska, C.; Temple, K.; Lough, A. J.; Manners, I. *J. Am. Chem. Soc.* **2003**, *125*, 9424.
145. Jaska, C.; Clark, T. J.; Clendenning, B. S.; Grozea, D.; Turak, A.; Lu, Z.-H.; Manners, I. *J. Am. Chem. Soc.* **2005**, *127*, 5116.
146. Jaska, C.; Manners, I. *J. Am. Chem. Soc.* **2004**, *126*, 1334.
147. Jaska, C.; Manners, I. *J. Am. Chem. Soc.* **2004**, *126*, 9776.
148. Fulton, J. L.; Linehan, J. C.; Autrey, T.; Balasubramanian, M.; Chen, Y.; Szymczak, N. K. *J. Am. Chem. Soc.* **2007**, *129*, 11936.
149. Rousseau, R.; Schenter, G. K.; Fulton, J. L.; Linehan, J. C.; Engelhard, M. H.; Autrey, T. *J. Am. Chem. Soc.* **2009**, *131*, 10516.
150. Friedrich, A.; Drees, M.; Schneider, S. *Chem. Eur. J.* **2009**, *15*, 10339.
151. Sloan, M. E.; Clark, T. J.; Manners, I. *Inorg. Chem.* **2009**, *48*, 2429.
152. Pun, D.; Lobkovsky, E.; Chirik, P. J. *Chem. Commun.* **2007**, 3297.
153. Clark, T. J.; Russell, C. A.; Manners, I. *J. Am. Chem. Soc.* **2006**, *128*, 9582.
154. Conley, B. L.; Williams, T. J. *Chem. Commun.* **2010**, *46*, 4815.
155. Sloan, M. E.; Staubitz, A.; Clark, T. J.; Russell, C. A.; Lloyd-Jones, G. C.; Manners, I. *J. Am. Chem. Soc.* **2010**, *132*, 3831.
156. Blaquiere, N.; Diallo-Garcia, S.; Gorelsky, S. I.; Black, D. A.; Fagnou, K. *J. Am. Chem. Soc.* **2008**, *130*, 14034.
157. Jaska, C. A.; Manners, I. *J. Am. Chem. Soc.* **2004**, *126*, 2698.
158. Sloan, M. E.; Staubitz, A.; Lee, K.; Manners, I. *Eur. J. Org. Chem.* **2011**, 672.
159. Whittell, G. R.; Balmond, E. I.; Robertson, A. P. M.; Patra, S. K.; Haddow, M. F.; Manners, I. *Eur. J. Inorg. Chem.* **2010**, 3967.
160. Denney, M. C.; Pons, V.; Hebden, T. J.; Heinekey, D. M.; Goldberg, K. I. *J. Am. Chem. Soc.* **2006**, *128*, 12048.
161. Dietrich, B. L.; Goldberg, K. I.; Heinekey, D. M.; Autrey, T.; Linehan, J. C. *Inorg. Chem.* **2008**, *47*, 8583.
162. Staubitz, A.; Soto, A. P.; Manners, I. *Angew. Chem. Int. Ed.* **2008**, *47*, 6212.
163. Staubitz, A.; Sloan, M. E.; Robertson, A. P. M.; Friedrich, A.; Schneider, S.; Gates, P. J.; Manners, I. *J. Am. Chem. Soc.* **2010**, *132*, 13332.
164. Johnson, H. C.; Robertson, A. P. M.; Chaplin, A. B.; Sewell, L. J.; Thompson, A. L.; Haddow, M. F.; Manners, I.; Weller, A. S. *J. Am. Chem. Soc.* **2011**, *133*, 11076.
165. Vance, J. R.; Robertson, P. M.; Lee, K.; Manners, I. *Chem. Eur. J.* **2011**, *17*, 4099.
166. Kakizawa, T.; Kawano, Y.; Nageneyama, K.; Shimoi, M. *Chem. Lett.* **2011**, *40*, 171.
167. Gee, W.; Holden, J. B.; Shaw, R. A.; Smith, B. C. *J. Chem. Soc.* **1965**, 3171.
168. Dorn, H.; Singh, R. A.; Massey, J. A.; Lough, A. J.; Manners, I. *Angew. Chem. Int. Ed.* **1999**, *88*, 3321.
169. Dorn, H.; Singh, R. A.; Massey, J. A.; Nelson, J. M.; Jaska, C. A.; Lough, A. J.; Manners, I. *J. Am. Chem. Soc.* **2000**, *122*, 6669.
170. Dorn, H.; Vejzovic, E.; Lough, A. J.; Manners, I. *Inorg. Chem.* **2001**, *40*, 4327.
171. Korshak, V. V.; Zamyatina, V. A.; Solomatina, A. I. *Izv. Akad. Nauk SSSR Ser. Khim.* **1964**, *8*, 1541.
172. Dorn, H.; Rodezno, J. M.; Brunnhöfer, B.; Rivard, E.; Massey, J.; Manners, I. *Macromolecules* **2003**, *36*, 291.
173. Jaska, C. A.; Temple, K.; Lough, A. J.; Manners, I. *Chem. Commun.* **2001**, 962.
174. Clarson, S. J., Semlyen, J. A., Eds.; In *Siloxane Polymers*; Prentice Hill: Englewood Cliffs, NJ, 1993.
175. Jones, R. G., Ando, W., Chojnowski, J., Eds.; In *Silicon-Containing Polymers*; Kluwer Academic: Dordrecht, Netherlands, 2000.
176. Noll, W. *Chemistry and Technology of Silicones*. Academic Press: New York, 1968.
177. Lebrunn, J. J.; Porte, H. *Polysiloxanes (593–609)*. In *Comprehensive Polymer Science*; Eastmond, G. C., Ledwith, A., Russo, S., Sigwalt, P., Eds.; Pergamon: Oxford, 1993; Vol. 4.
178. Rochow, E. G. *Silicon and Silicones*. Springer-Verlag: Heidelberg, 1987.
179. Acmite Market Intelligence, Market Report: World Silicon Market, Ratingen, Germany, 2009.
180. Global Industry Analysts, Inc., USA (www.Strategy.com/Silicon_Market_Report.asp) Silicone – A Global Strategic Business Report, July 2011.
181. McDonald, J. C.; Whitesides, G. M. *Acc. Chem. Res.* **2002**, *35*, 491.
182. Seyferth, D. *Organometallics* **2001**, *20*, 4978.
183. Xiong, Y.; Yao, S.; Driess, M. *J. Am. Chem. Soc.* **2009**, *131*, 7562.
184. Mark, J. E. *Acc. Chem. Res.* **2004**, *37*, 946.

Copyright © 2013. Elsevier. All rights reserved.

Comprehensive Inorganic Chemistry II : From Elements to Applications, Elsevier, 2013. ProQuest Ebook Central, http://ebookcentral.proquest.com/lib/inflibnet-ebooks/detail.action?docID=1330977.
Created from inflibnet-ebooks on 2021-02-09 22:27:26.

1.27 Boron-Containing Polymers

A Doshi, Rutgers University-Newark, Newark, NJ, USA
F Jäkle, Rutgers University-Newark, Newark, NJ, USA

© 2013 Elsevier Ltd. All rights reserved.

Nomenclature

ADMET	Acyclic diene metathesis polymerization
AIE	Aggregation-induced emission
ATRP	Atom-transfer radical polymerization
9-BBN	9-Borabicyclononane
bipy	2,2′-Bipyridine
BNCT	Boron neutron capture therapy
BODIPY	4,4-Difluoro-4-bora-3a,4a-diaza-*s*-indacene
cod	Cyclooctadiene
Cp*	Pentamethylcyclopentadienyl
COF	Covalent organic framework
CTA	Chain-transfer agent
DLS	Dynamic light scattering
dppp	Bis(diphenylphosphinopropane)
FRET	Förster resonance energy transfer
Ind	Indenyl
ITO	Indium tin oxide
LCST	Lower critical solution temperature
Mes	2,4,6-Trimethylphenyl
Mes*	2,4,6-Tri-*tert*-butylphenyl
nbd	Norbornadiene
NMP	Nitroxide-mediated polymerization
PCL	Polycaprolactone
PDMA	Poly(N,N-dimethylacrylamide)
PEDOT	Poly(ethylenedioxythiophene)
PEG	Poly(ethylene glycol)
PEO	Poly(ethylene oxide)
Pin	Pinacolato
PNIPAM	Poly(N-isopropylacrylamide)
POSS	Polyhedral oligomeric silsesquioxane
PS	Polystyrene
PSS	Poly(styrene sulfonate)
PVA	Poly(vinyl alcohol)
RAFT	Reversible addition-fragmentation chain transfer
ROMP	Ring-opening metathesis polymerization
SEM	Scanning electron microscopy
SWNT	Single-walled carbon nanotubes
TEM	Transmission electron microscopy
TFSI	Bis(trifluoromethylsulfonyl)imide, triflimide
Tip	2,4,6-Tri-*iso*-propylphenyl

Copyright © 2013. Elsevier. All rights reserved.

Comprehensive Inorganic Chemistry II : From Elements to Applications, Elsevier, 2013. ProQuest Ebook Central, http://ebookcentral.proquest.com/lib/inflibnet-ebooks/detail.action?docID=1330977.
Created from inflibnet-ebooks on 2021-02-09 22:27:26.

1.27.1 Introduction and Scope

Since the first reports of oligomeric and polymeric boron-containing compounds, the polymer chemistry of boron has gained tremendous ground. Boron-containing polymers now find applications in a variety of fields, including their use as polymeric precursors for high-performance ceramic materials, flame retardants, components of lithium ion batteries, supramolecular nanomaterials, polymer-supported reagents and catalysts for organic transformations, in drug delivery, as optoelectronic materials, sensors for anions and toxic small molecules, etc.[1–3] These developments have been driven by several fundamental and unique characteristics of boron and its compounds.[1] The ability to delocalize π-electrons and to form Lewis acid–base complexes is of great importance for catalytic, sensory, and electronic applications and results from the presence of an empty p_B-orbital in tricoordinate boranes. For medical applications in boron neutron capture therapy (BNCT) (see Chapter 3.30) and for nuclear detectors and shielding, the exceptionally large cross section of the ^{10}B isotope is critical. Finally, many applications in high-performance materials rely on the ability of boranes to react with oxygen at high temperature to form B_2O_3 char or with ammonia to yield boron-nitride and boron-carbonitride ceramic materials.[1]

This chapter provides an overview of the most significant recent developments in the area of boron-containing polymers. We describe the synthesis, characterization, and application of new polymeric materials that feature boron as an integral component with a clear effect on the chemical or physical properties. The chapter is organized such that different classes of polymers are discussed separately according to the type of boron-containing functional group incorporated. We start with organoborane polymers, in which borane or borate groups are linked through boron–carbon bonds or are embedded into the organic polymer backbone itself. In the following section, research on boron polymers comprising boron heterocyles, such as borazanes, pyrazaboles, boron quinolates, boron diketonates, and 4,4-difluoro-4-bora-3a,4a-diaza-*s*-indacene (BODIPY) moieties, will be discussed, followed by an overview of boronic acid and boronic ester-functionalized polymers and related materials. The final section is dedicated to the synthesis and applications of polymers that feature carboranes and other boron cluster species. For each of the specific classes of polymers discussed, interesting properties and applications will be highlighted.

Polymers that consist of B–N and B–P linkages in the main chain are not included; they are discussed in a separate chapter (see Chapter 1.26). Also not covered in detail are solid-state materials such as coordination polymers (see Chapter 1.29), covalent organic frameworks (COFs), and boron-containing ceramic materials.

1.27.2 Organoborane Polymers

1.27.2.1 General Considerations and Synthetic Aspects

This section discusses primarily polymeric materials, in which all the boron substituents are carbon based, and introduces some of their most important applications. Heteroatom-substituted materials are covered separately in Sections 1.27.3 and 1.27.4, according to the particular functional group that is attached to boron. Tricoordinate organoborane polymers have been investigated extensively for a variety of different purposes. A major thrust has been to explore organoborane-functionalized polymers as versatile intermediates to functional (boron-free) organic polymers.[4–7] Methods for the preparation of suitable borane polymer intermediates include (co)polymerization of boron-functionalized olefinic monomers and the use of borane chain transfer agents (CTAs) – typically in Ziegler–Natta or free radical polymerizations,[4,8–16] polymer functionalization by hydroboration[17,18] or transition metal-catalyzed C—H activation,[19–25] and the polyhomologation of alkylboranes.[26,27] Earlier studies also involved ring-opening metathesis polymerization (ROMP) procedures.[28–30] Some representative procedures are outlined in Figure 1.

The resulting borane-functionalized polymers were typically converted *in situ* to organic functional groups, for example, by oxidative treatment with $NaOH/H_2O_2$, which provided access to OH-functionalized copolymers. Moreover, the facile reaction of aliphatic organoboranes with dioxygen to form peroxides was exploited for the grafting of other (organic) monomers with the goal of generating more complex polymer architectures.[4,31]

In recent years, however, it has become apparent that organoborane polymers are interesting in their own right, especially when desirable properties can be derived from the presence of electron-deficient borane moieties. The high Lewis acidity of organoboranes is, for example, important for applications in Lewis acid catalysis[32–34] and in the detection of Lewis basic species, most notably in the field of anion recognition. (see Chapter 1.34).[35–37] Moreover, the incorporation of electron-deficient borane moieties into extended organic π-systems often leads to effective p_B–π* orbital overlap with the empty p-orbital on boron, which in turn results in desirable electronic effects and interesting photophysical characteristics.[3,38–42] Thus, incorporation of these functional groups into polymeric materials can lead to remarkable and unique properties.

Polymer modification reactions have thus far proved to be most versatile for attachment of more complex functional organoborane moieties to polyolefins. Early work relied mostly on organolithium and organomercury intermediates, but issues with selectivity, low conversion, and unintended cross-linking severely limited the utility and prevented wider implementation. A more recently introduced method that addresses these shortcomings is the borylation of silated polystyrenes by Jäkle and coworkers (Figure 2).[43,44] Their approach was to 'mask' polystyrene with trimethylsilyl groups (**1**) that can then be replaced quantitatively with boron tribromide to give the reactive polymer poly(4-dibromoborylstyrene) (**2**). Other advantages of this strategy include that (a) silylated styrene can be polymerized with excellent molecular weight control using atom transfer radical polymerization (ATRP) and (b) the flexibility to replace the bromines in **2** with a broad range of different functional groups (R) allows for facile fine-tuning of the properties and leads to a family of styrene polymers (**3**) with diverse potential applications in catalysis and materials science.[43–52] The technique was also successfully extended to other polymer architectures; random, block, and telechelic polymers were all readily obtained using similar protocols.[46,48,53]

Copyright © 2013. Elsevier. All rights reserved.

Comprehensive Inorganic Chemistry II : From Elements to Applications, Elsevier, 2013. ProQuest Ebook Central, http://ebookcentral.proquest.com/lib/inflibnet-ebooks/detail.action?docID=1330977.
Created from inflibnet-ebooks on 2021-02-09 22:27:26.

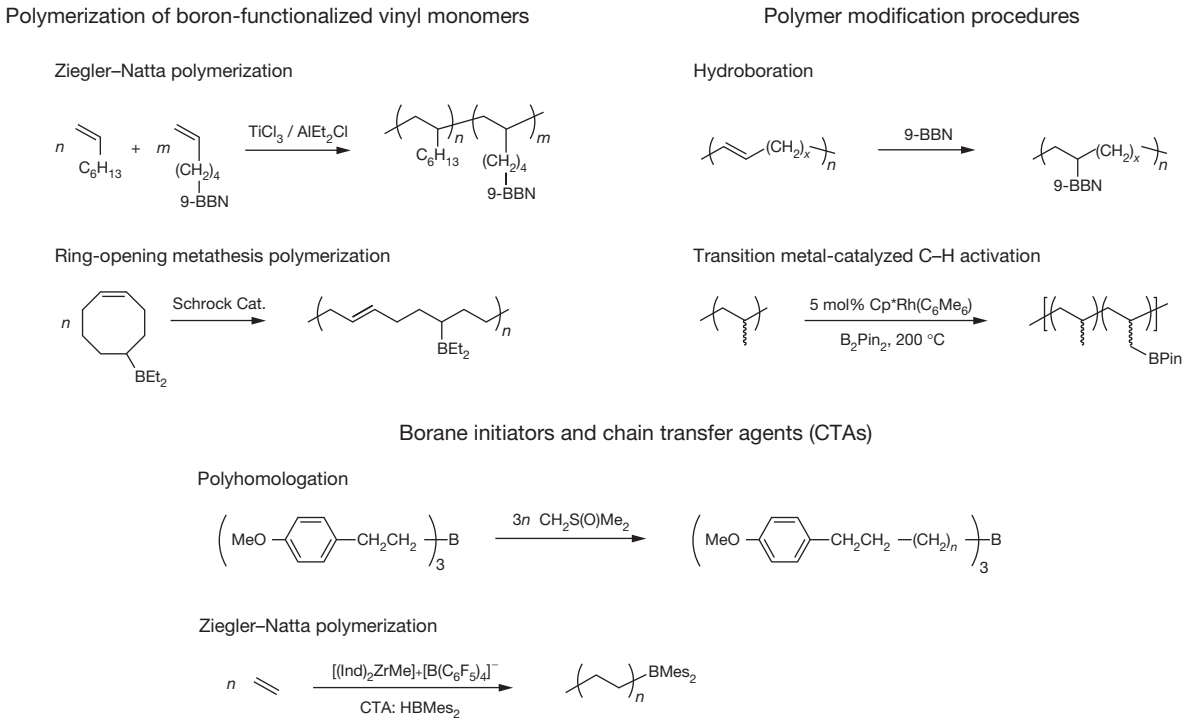

Figure 1 Examples of borylated polymers used as intermediates to functional organic polymers.

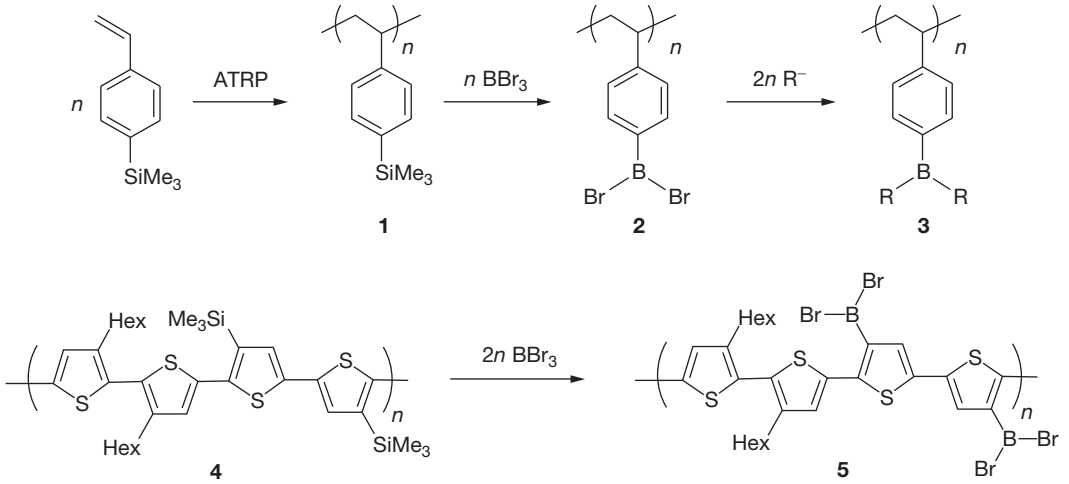

Figure 2 Synthesis of borylated polymers via silicon–boron exchange with BBr_3.

The silicon–boron exchange was exploited also to install functional organoborane moieties on polythiophenes and related conjugated polymers (**5**, Figure 2).[54–56] Other conjugated polymers with pendant borane moieties were prepared by the direct polymerization of boron-functionalized monomers, for example, utilizing Pd-catalyzed Sonogashira–Hagihara or Ni-catalyzed Yamamoto coupling.[57,58]

A broad range of methods for boron incorporation into the main chain of conjugated organic polymers has been developed as well. These include hydroboration (and related haloboration and phenylboration) polymerization protocols, organometallic polycondensation, transition metal-catalyzed C—C coupling processes, ring-opening polymerization (ROP), and the spontaneous polycondensation of arylboranes, $Ar(BH_2)_2$ and $Ar(BHBr)_2$. The different methods are summarized in Figure 3. As discussed already for polyolefins, post-polymerization modification is possible when reactive B–H and B–X (X = Cl, Br) functionalities are present and can be exploited for further tuning of the polymer properties.[59–62]

1.27.2.2 Optical, Electronic, and Sensory Materials

1.27.2.2.1 Main chain-type conjugated organoborane polymers

Hydroboration polymerization is one of the most frequently used methods for the synthesis of main chain-type conjugated organoborane polymers. A bifunctional borane (comprising a

Copyright © 2013. Elsevier. All rights reserved.

Comprehensive Inorganic Chemistry II : From Elements to Applications, Elsevier, 2013. ProQuest Ebook Central, http://ebookcentral.proquest.com/lib/inflibnet-ebooks/detail.action?docID=1330977.
Created from inflibnet-ebooks on 2021-02-09 22:27:26.

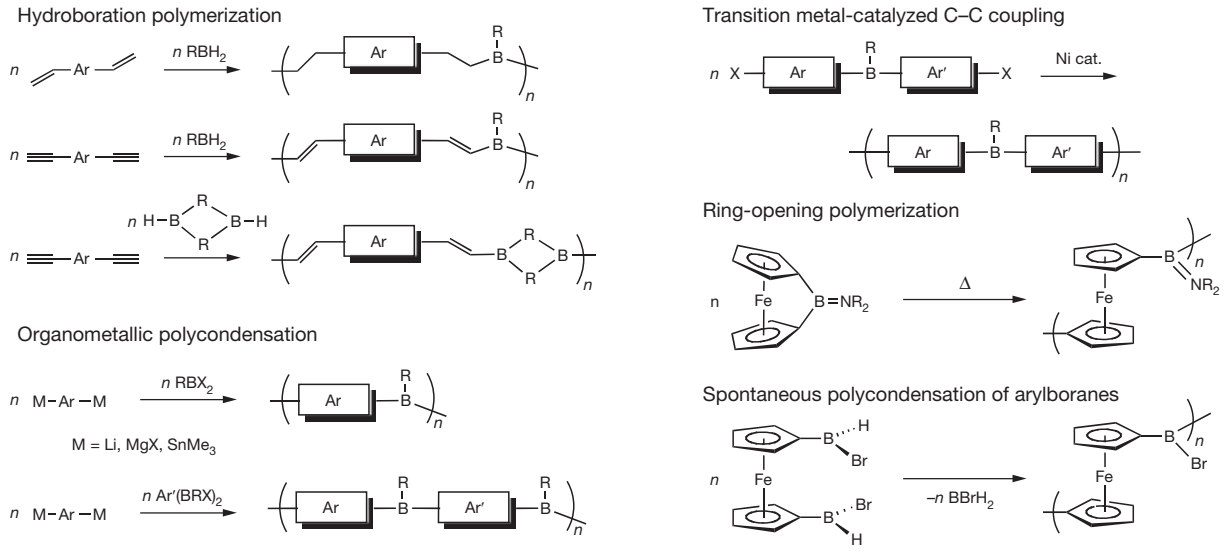

Figure 3 Methods for the synthesis of main chain-type organoborane polymers (Ar, Ar' = arylene).

BH_2 or two linked B–H moieties) adds across two multiple bonds that are linked by an organic or organometallic framework. Benefits include the high chemo- and regioselectivity, generally mild reaction conditions, and the absence of small molecule by-products, which facilitates isolation of the polymeric products. Polymers **6** and **7** are representative examples of a wide range of different conjugated materials that Chujo and coworkers prepared by hydroboration polymerization.[63–67] An important breakthrough in this chemistry was the discovery that sterically demanding boranes such as mesitylborane or tripylborane (mesityl = 2,4,6-trimethylphenyl, tripyl = 2,4,6-tri-*iso*-propylphenyl) not only result in selective formation of vinylborane species without detectable amounts of alkylboranes, but also lead to materials that exhibit much improved stability toward air and moisture. Chujo reported molecular weights of up to $M_n = 10\,500$ Da for **6a** (Ar = Mes), which corresponds to an average of 41 repeating units. The molecular weights did, however, vary considerably with the particular dialkyne and borane employed. Closely related polymers were obtained by haloboration or phenylboration polymerization, which lead to B–X or B–Ph addition across the carbon–carbon triple bonds of dialkyne precursors.[68,69]

Variation of the dialkyne building block in **6** resulted in different luminescent properties. Polymers with a phenylene or fluorenylene linker (**6a**, **6b**) were strongly blue luminescent, whereas the more electron-rich dialkoxybenzene moiety in **6c** led to green luminescence.[63] In terms of photostability, the best results were obtained with alkoxy (**6c**) or CF_3 (**6d**) groups attached to the phenylene linker, likely as a result of steric protection of the vinyl functionalities.[70] Wagner and Jia independently pursued the hydroboration of dialkynes with the bifunctional cyclic building block 9,10-diboraanthracene to give conjugated polymers such as **7**.[71,72] A possible advantage is that the tricoordinate boron is embedded into a planar conjugated π-system. The polymers displayed yellow-green luminescence comparable to that of polymer **6c**.

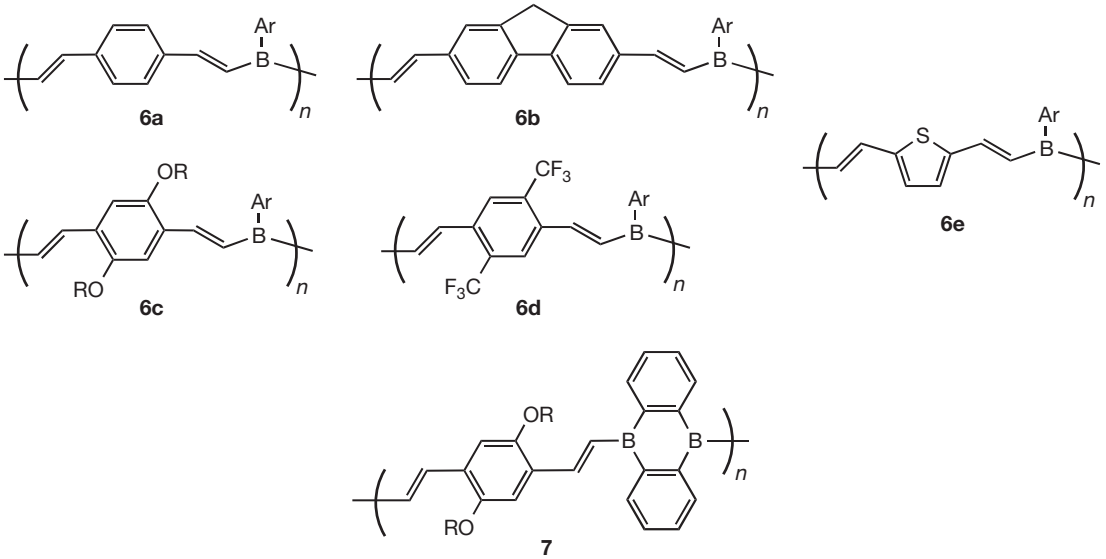

Copyright © 2013. Elsevier. All rights reserved.

Comprehensive Inorganic Chemistry II : From Elements to Applications, Elsevier, 2013. ProQuest Ebook Central, http://ebookcentral.proquest.com/lib/inflibnet-ebooks/detail.action?docID=1330977.
Created from inflibnet-ebooks on 2021-02-09 22:27:26.

Chujo and coworkers found that the presence of electron-deficient borane moieties in the conjugated polymer structure of **6a** and **6b** (Ar = Tip) leads to *n*-type electrical conductivity after doping with triethylamine.[73,74] Moreover, nonlinear optical measurements on **6a** and **6b** (Ar = Mes) revealed unusually large third-order susceptibilities.[42] More recently, Pignataro and coworkers explored the use of **6a** (Ar = Tip) as an electron-acceptor material in photovoltaic devices (**Figure 4**).[75] Blends of **6a** (PDB) with poly(3-hexylthiophene) (P3HT) were prepared, and morphological studies based on atomic force microscopy indicated effective microphase separation. The device characteristics were among the best reported thus far for all-polymer photovoltaic devices. Finally, the Lewis acidity of the boron sites in **6a** (Ar = Mes, Tip) was exploited for fluoride anion detection. Even small amounts of fluoride led to effective quenching of the blue luminescence of the polymers.[76] Other halides had no effect on the absorption and emission properties, demonstrating the high selectivity for fluoride.

The hydroboration methods described above are not applicable to the synthesis of conjugated organboranes, in which individual borane moieties are linked together by alkynyl or aryl groups. The latter are expected to display higher thermal stability, because retro-hydroboration does not present a pathway for degradation. Organometallic condensation methods are typically employed to attach aryl and alkynyl groups to boron. Polymers **8** and **9** were prepared by reaction of bifunctional Grignard and organolithium reagents with arylboronic esters ($ArB(OMe)_2$; Ar = Mes, Tip).[77,78] However the molecular weights were significantly lower than those of polymers **6**, possibly because of the high reactivity of the organometallic reagents and the fact that they had to be used *in situ*. Readily isolable and mild organotin reagents present a valuable alternative for the formation of aryleneborane polymers.[79–81] Jäkle and coworkers demonstrated that tin–boron-exchange reactions between aryltin species and arylbromoboranes lead to selective formation of poly(thiopheneborane)s (**10**) and the poly(fluoreneborane) (**11a**). Polymer **11a** in turn served as a precursor to a range of poly(fluoreneborane)s by nucleophilic replacement of the Br substituents.[80] Molecular weights of up to $M_n = 10\,400$ Da were reached (**11b**) and, as expected for post-polymerization modification processes, the calculated number of repeating units was similar for polymers with different pendant groups attached to boron. The formation of polymers of similar molecular weight is important when comparing the electronic structure and optical properties of conjugated materials.

Variation of the pendant boron substituents allowed for tuning of the optical properties and electronic structure. For instance, polymers **10** displayed blue luminescence with Ar = Ph, green luminescence with $Ar = C_6F_5$, and red luminescence with $Ar = Ph_2N—Th_2$ (Th_2 = bithiophenediyl).[79,82] The conjugated polymer **12** contains both electron-deficient arylborane and electron-rich arylamine moieties in the main chain.[81] As a result of this ambipolar character, redox processes corresponding to both reduction of the borane and oxidation of the amine moieties were observed by cyclic voltammetry, and solvatochromic effects were evident from the emission spectra. Polymer **13** was designed by Jia and coworkers to be highly electron deficient, comprising a fluorinated C_6F_4 linker.[72] As a result, mixing of **13** with P3HT led to luminescence quenching, indicative of energy transfer from the electron-rich P3HT to the electron-deficient polymer **13**. This observation suggests potential use as an electron-acceptor material in photovoltaic devices.

Polymers **10** were also studied as fluorescent sensor materials for pyridine, while **11b** was used in the detection of fluoride and cyanide anions.[79,80] In both cases signal amplification effects were observed, that is, the fluorescence was effectively quenched in the presence of only small amounts of the nucleophile (**Figure 5**). Effective anion recognition was also reported by Bonifacio and Scherf for polymer **14**.[83]

Ferrocene-containing organoborane polymers are of interest as redox-active materials. Very different synthetic methods had to be developed. In early studies, Manners, Braunschweig, and coworkers pursued the ROP of boron-bridged ferrocenophanes. Thermal ring opening occurred at elevated temperatures to give polymers **15**.[84,85] However, the soluble fraction of the polymers proved to consist of relatively low-molecular-weight material. Manners and coworkers also incorporated ferrocenylborane units into the main chain of a poly(ferrocenylenesilane).[86] More recently, Wagner and coworkers obtained higher-molecular-weight poly(ferrocenylborane)s via spontaneous condensation of *in situ* generated ferrocenylboranes 1,1′-fc$(BXH)_2$ (X = H, Br; see **Figure 3**).[61,62,87] Initially, polymers with reactive

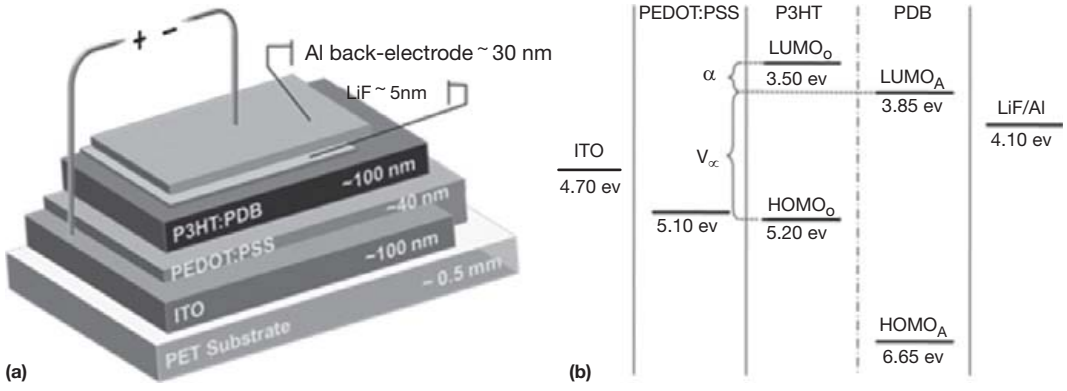

Figure 4 (a) Device architecture and (b) energy-level diagram of a photovoltaic device with a blend of P3HT and polymer **6a** (PDB) as the active layer. Reproduced from Cataldo, S.; Fabiano, S.; Ferrante, F.; Previti, F.; Patane, S.; Pignataro, B. *Macromol. Rap. Commun.* **2010**, *31*, 1281–1286, with permission. Copyright 2010 Wiley-VCH Verlag GmbH & Co. KGaA.

Copyright © 2013. Elsevier. All rights reserved.

Comprehensive Inorganic Chemistry II : From Elements to Applications, Elsevier, 2013. ProQuest Ebook Central, http://ebookcentral.proquest.com/lib/inflibnet-ebooks/detail.action?docID=1330977.
Created from inflibnet-ebooks on 2021-02-09 22:27:26.

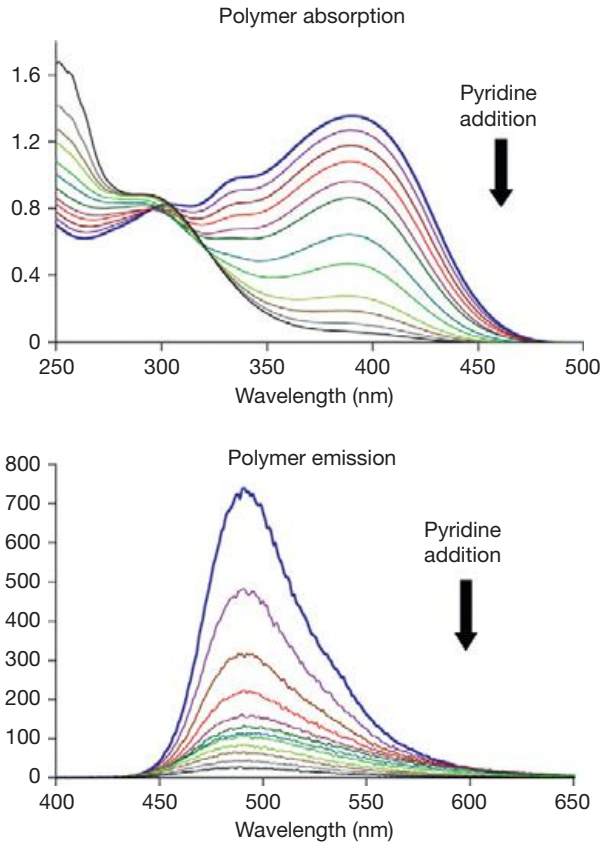

Figure 5 Absorption and fluorescence spectra (λ_{exc} = 390 nm) for the titration of **10** (Ar = ^{t}BuPh) with pyridine in CH_2Cl_2. Adapted from Sundararaman, A.; Victor, M.; Varughese, R.; Jäkle, F. *J. Am. Chem. Soc.* **2005**, *127*, 13748–13749, with permission. Copyright 2005 American Chemical Society.

B–Br and B–H functional groups were prepared, which were then further modified by nucleophilic replacement of Br for bulky mesityl groups (**16**) or by hydroboration of alkynes (**17**). An interesting observation was that the highly Lewis acidic organoborane moieties in **16** very effectively promote electronic

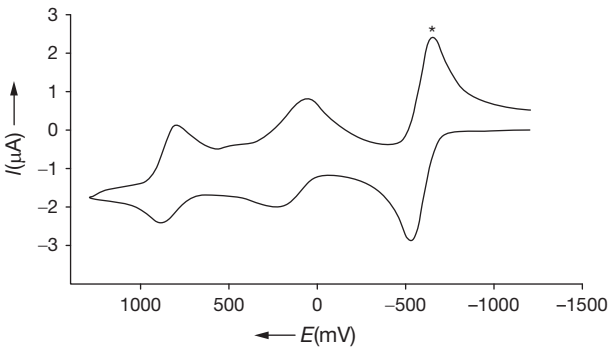

Figure 6 Cyclic voltammogram of polymer **16** (0.1 M $Bu_4N[B(C_6F_5)_4]$ in CH_2Cl_2; starred wave: Cp^*_2Fe reference). Reproduced from Heilmann, J. B.; Scheibitz, M.; Qin, Y.; Sundararaman, A.; Jäkle, F.; Kretz, T.; Bolte, M.; Lerner, H.-W.; Holthausen, M. C.; Wagner, M. *Angew. Chem. Int. Ed.* **2006**, *45*, 920–925, with permission. Copyright 2006 Wiley-VCH Verlag GmbH & Co. KGaA.

communication between the iron centers along the polymer chain as evidenced by two redox waves that are separated by an unusually large redox splitting in the cyclic voltammogram (Figure 6).[87]

Jäkle and coworkers explored boratabenzene-derived metallocene analogs as versatile new building blocks for metallopolymers.[88] First, bisborinatoiron(II) complexes of the type Fe$(C_5H_5B—R)_2$ (R = C≡CH, C≡CSiMe$_3$) were synthesized. Polymerization of Fe$(C_5H_5B—C≡CH)_2$ with 2,5-bis(dodecyloxy)-1,4-diiodobenzene by Sonogashira–Hagihara coupling yielded the film-forming polymer **18**, whereas 'click-type' polymerization with 1,4-bis(4-azidobutoxy)benzene gave the corresponding metallopolymer **19**. Both polymers proved to be redox-active due to the presence of the Fe complexes according to cyclic voltammetry measurements. Extension of conjugation in **18** was anticipated to occur through interaction of iron-centered d-orbitals and orbitals on the borabenzene π-system, including the boron p-orbitals; however, a pronouced red shift of the absorption relative to the molecular building blocks was not observed.

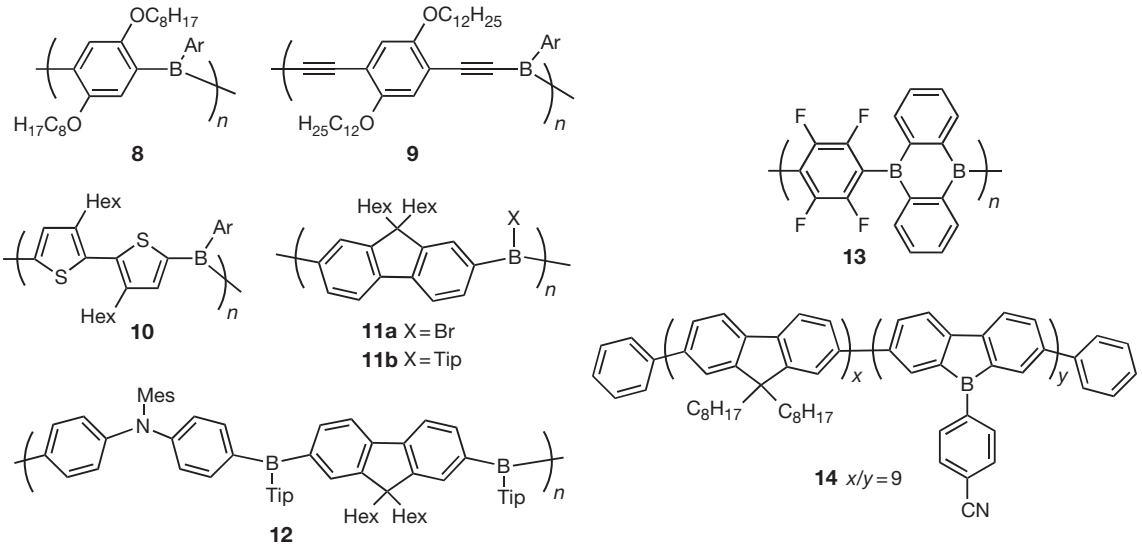

Copyright © 2013. Elsevier. All rights reserved.

Comprehensive Inorganic Chemistry II : From Elements to Applications, Elsevier, 2013. ProQuest Ebook Central, http://ebookcentral.proquest.com/lib/inflibnet-ebooks/detail.action?docID=1330977.
Created from inflibnet-ebooks on 2021-02-09 22:27:26.

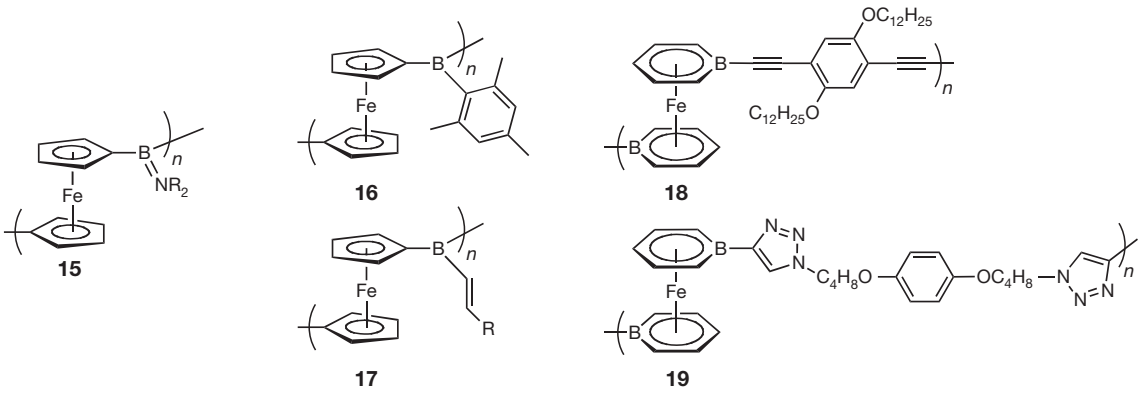

1.27.2.2.2 Side chain-functionalized organoborane polymers

As discussed above, conjugated, tricoordinate organoboranes frequently display interesting photoluminescence properties as a result of effective overlap of the conjugated π-system with the empty p-orbital on boron.[89] An alternative to incorporating conjugated borane moieties into the polymer main chain is the attachment as pendant groups to polyolefins and other nonconjugated or conjugated polymer scaffolds. For instance, polymer **20** was prepared by Shirota from the respective borane-functionalized vinyl monomer by standard free-radical polymerization.[90] The polymer displayed a bipolar character, as it contains both an arylamine donor and an arylborane acceptor in each repeating unit, which facilitate hole and electron transport, respectively. Use of **20** as an emitter in a multilayer organic light-emitting device (OLED) resulted in green electroluminescence with spectral features similar to the photoluminescence of a thin film (**Figure 7**), but the luminance and efficiency were modest in comparison to small molecule devices.[90] In related work, Ziegler–Natta polymerization was used by Do and Lee and coworkers to prepare a luminescent polyethylene derivative (**21**).[91] Since the phenylene moiety only allows for modest extension of conjugation, the emission maximum for this polymer was in the ultraviolet (UV) at 382 nm, with only a slight tailing into the visible region; a thin film showed an additional, comparatively weaker, lower energy feature at 420–500 nm, which was attributed to aggregate formation. Systems that contain electron-donor and electron-acceptor groups separated by a conjugated linker also commonly display interesting nonlinear optical properties.[92]

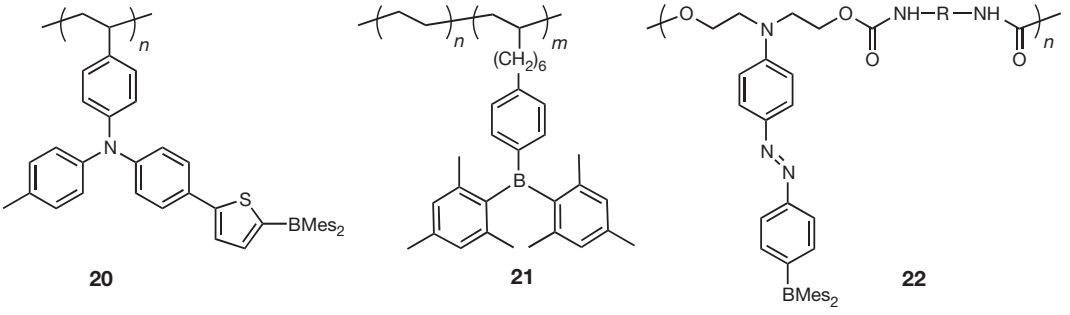

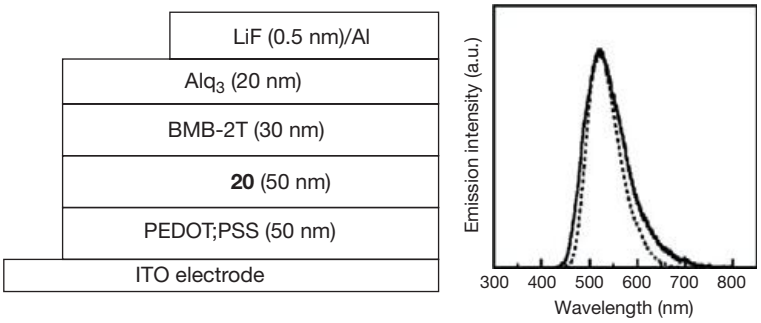

Figure 7 An organic light-emitting device (OLED) structure with polymer **20** as the emitting layer (BMB-2T = bis(dimesitylboryl-2,2′-bithiophene)) and comparison of electroluminescence (solid line) and photoluminescence spectra (dotted line) of a thin film of **20**. Adapted from Mutaguchi, D.; Okumoto, K.; Ohsedo, Y.; Moriwaki, K.; Shirota, Y. *Org. Electron.* **2003**, *4*, 49–59, with permission. Copyright 2003 Elsevier B. V.

Copyright © 2013. Elsevier. All rights reserved.

Comprehensive Inorganic Chemistry II : From Elements to Applications, Elsevier, 2013. ProQuest Ebook Central, http://ebookcentral.proquest.com/lib/inflibnet-ebooks/detail.action?docID=1330977.
Created from inflibnet-ebooks on 2021-02-09 22:27:26.

Lequan studied the polyurethane **22** in this respect and found a desirable second harmonic response.[93,94]

The synthesis of high-molecular-weight luminescent polystyrenes by post-polymerization modification of poly(4-dibromoboryl styrene) (**2**) was reported by Jäkle and coworkers. In polymers **23**–**26**, the conjugated organic π-system overlaps very efficiently with the empty p-orbital on boron.[50,52] Moreover, the high modularity of the polymer modification approach allows for facile variation of the optical properties. For instance, bithiopheneborane-functionalized polymers **23** with $R^1 = H$, C_6H_{13} proved to be strongly emissive in the blue region with a maximum at $\lambda_{em,\ max} = 463$ nm, while the respective amino-functionalized derivative ($R^1 = NPh_2$) emits in the green at $\lambda_{em,\ max} = 537$ nm. In a recent study, the bulkier Tip groups were employed in combination with fluorene and carbazole derivatives (**24**, **25**), resulting in strongly blue-emissive materials ($\lambda_{em,\ max}$ in the range from 390 to 420 nm) with further improved stability to air and moisture.[52] Related redox-active ferrocene derivatives (**26**) were also examined with a focus on the effect of switching between Fe(II) and Fe(III) redox states on the electronic structure.[51]

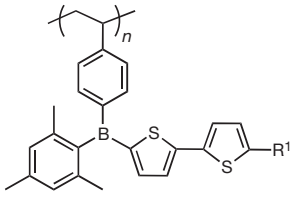

23

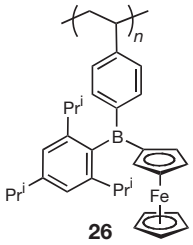

26

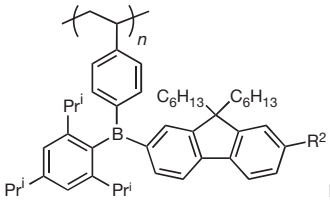

24

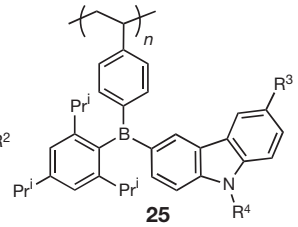

25

Exposure of polymers **23** to anions triggered a distinct change of the optical properties.[50] For example, fluoride or cyanide binding switched the emission color of **23** ($R^1 = NPh_2$) from green to blue. The borane polymers were selective for fluoride and cyanide over various other anions (e.g., Cl^-, Br^-, NO_3^-). Intriguingly, amplified quenching effects were observed in the case of fluoride binding to **23** ($R^1 = n$-hexyl), allowing for highly efficient detection in the low micromolar concentration range. The amplification effect, which is more commonly encountered for conjugated polymers (see **Section 1.27.2.2.1**),[95] was tentatively attributed to through-space energy migration to weakly emissive low-energy states. A smaller amplification effect was observed for polymer **21**, possibly due to the bulkier structure of the dimesitylborane moiety, which does not allow for effective alignment of chromophores in adjacent polymer repeat units.[91]

A major advantage of attaching conjugated organoborane moieties to polyolefins is that molecular weight control can be achieved by means of controlled/living polymerization techniques and that high-molecular-weight materials with good processibility are quite readily obtained. However, the conjugated segments are relatively small and for the most part the chromophores act independently. An alternative approach is to connect electron-deficient borane moieties to conjugated polymers in such a way that the conjugation path of the organic π-conjugated polymer is maintained; yet the electronic structure and optical properties are influenced by cross-conjugation with the empty p-orbitals of the pendant organoborane moieties.[96] Several classes of this type of polymers have been introduced.

Yamaguchi and coworkers reported the synthesis of poly(*p*-phenyleneethynylene)s (**27**) by Sonogashira–Hagihara coupling of a bis(borane)-functionalized diethynylbenzene building block with different diiodoarene species.[97,57] 2,6-Dimethyl-4-*n*-hexylphenyl groups were chosen as substituents on boron to provide both steric protection of the boron–carbon bonds and good solubility of the polymeric materials in organic solvents. The absorption and emission colors could be tuned by variation of the aromatic co-monomer, and exceptionally high quantum yields were achieved. The strongly emissive character was attributed to steric shielding of the conjugated polymer chain by the bulky diarylborane moieties and the effective extension of π-conjugation.

Lambert and coworkers examined two different polycarbazole derivatives (**28**, **29**), one of which had the carbazole moieties linked through the 2,7-positions and the other through the 3,6-positions.[58] The polymers were obtained by Ni-catalyzed polycondensation of borane-functionalized dichlorocarbazole derivatives. Very different optical properties were observed for the two isomers. For the 2,7-linked polymer **28**, the absorption and emission properties were dominated by the organic π-conjugated backbone, whereas a low-energy carbazole-to-borane charge transfer band appeared in the spectra of the 3,6-linked polymer **29**. The ambipolar nature of the polymers is advantageous for optoelectronic device applications, and the 3,6-linked polymer was further studied in a single-layer OLED. At an applied voltage of 8.5 V, blue electroluminescence ($\lambda = 463$ nm) similar to the photoluminescence of the polymer film was observed.

Using a polymer modification approach, Jäkle and coworkers prepared polythiophene **30** and related copolymers.[54–56] As illustrated in **Figure 2**, they first prepared silyl-substituted polymers, which were reacted with BBr_3, followed by treatment with mesityl copper for steric stabilization. Analysis by experimental methods and theoretical calculations revealed that the lowest-energy absorption is due to a π–π* transition, whereas a more intense higher-energy transition originates from charge transfer to a cross-conjugated state localized on the borane moieties. The borane-functionalized polymers proved to be surprisingly weakly emissive. This was exploited in the detection of fluoride and cyanide anions, where borate formation led to a strong turn-on of fluorescence.[98]

Bazan and coworkers explored the binding of fluoride to the conjugated organoborane polymer **31** in an effort at generating a chemically fixed p–n heterojunction for polymer electronics (**Figure 8**).[99] The polymer was obtained by hydroboration of alkynyl side chains with $(HBMes_2)_2$. A solution of polymer **31** and poly(ethylene oxide) (PEO) was spin-coated onto polystyrene-sulfonate (PSS)-modified

Copyright © 2013. Elsevier. All rights reserved.

Comprehensive Inorganic Chemistry II : From Elements to Applications, Elsevier, 2013. ProQuest Ebook Central, http://ebookcentral.proquest.com/lib/inflibnet-ebooks/detail.action?docID=1330977.
Created from inflibnet-ebooks on 2021-02-09 22:27:26.

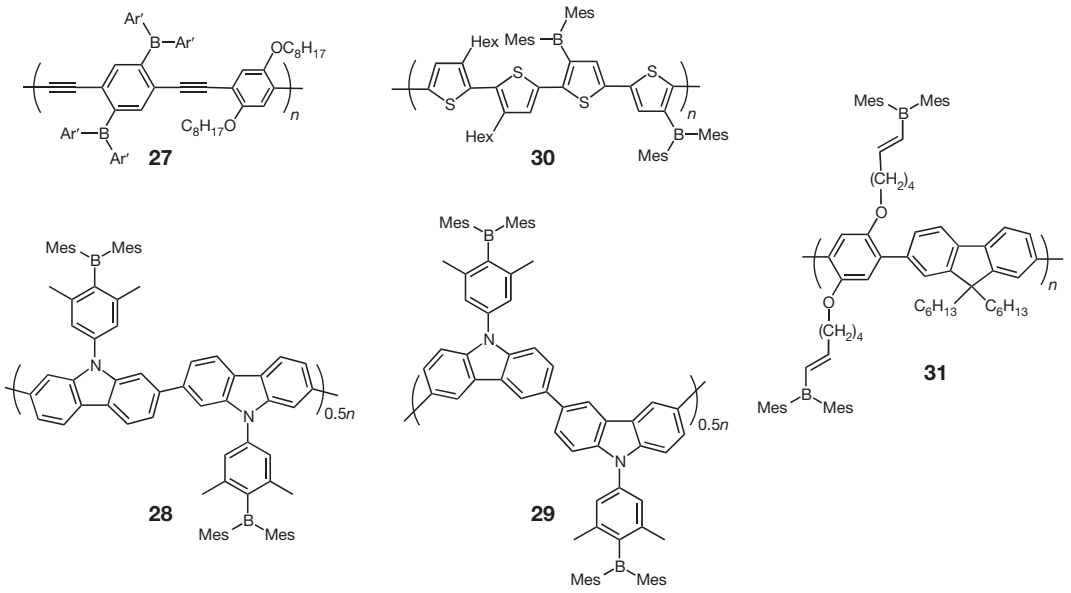

Figure 8 Formation of a chemically fixed p–n heterojunction by fluoride complexation to polymer **31** (PFP-BMes). Reprinted from Hoven, C. V.; Wang, H. P.; Elbing, M.; Garner, L.; Winkelhaus, D.; Bazan, G. C. *Nat. Mater.* **2010**, *9*, 249–252, with permission. Copyright 2010 MacMillan Publishers Ltd.

Copyright © 2013. Elsevier. All rights reserved.

poly (ethylenedioxythiophene) (PEDOT), followed by a layer of an ammonium fluoride-functionalized conjugated polymer. Vacuum deposition of an Al cathode completed the device fabrication. Application of a bias led to charge injection and migration of the fluoride ions to the neutral borane polymer layer. After this initial step, which resulted in fluoride complexation to boron, electrochemically induced light-emitting behavior was observed.

In a complementary approach, organoborane complexation to organic polymers that feature Lewis basic sites has also been explored for electronic and sensory applications. For instance, doping of polyaniline with BF_3 led to strongly enhanced conductivity, whereas a blue emissive material was isolated when the polyaniline was first deprotonated, followed by addition of boron halides.[100,101] More recently, Wang and coworkers demonstrated that exposure of benzobisthiadiazole-based polymers to BF_3 shifts the absorption and emission maxima from the visible region into the near-infrared.[102] Bazan and coworkers investigated the effect of $B(C_6F_5)_3$ on benzothiadiazole- and thiadiazolylpyridine-type conjugated

Comprehensive Inorganic Chemistry II : From Elements to Applications, Elsevier, 2013. ProQuest Ebook Central, http://ebookcentral.proquest.com/lib/inflibnet-ebooks/detail.action?docID=1330977.
Created from inflibnet-ebooks on 2021-02-09 22:27:26.

polymers (**32**), which resulted in partial complexation.[103,104] B$(C_6F_5)_3$ binding to the pyridine groups in **32b** proved to be more effective than to the thiadiazole nitrogens. This process led to significantly red-shifted absorption features, consistent with very small bandgaps. In different research, Matsumi and coworkers utilized BEt_3-complexed poly(vinylcarbazole) for fluorescent anion detection based on the release of the organoborane moiety from the (luminescent) polymeric material upon exposure to fluoride anions.[105]

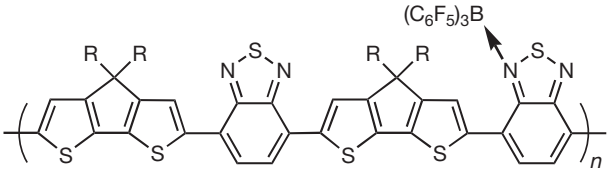

32a

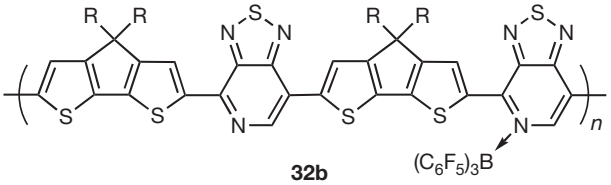

32b

1.27.2.3 Polymeric Reagents and Catalysts

With an increased demand for sustainable chemistry pathways, polymer-supported reagents and catalysts are experiencing renewed interest. A representative recent example of the use of polymer-supported borane reagents is shown in **Figure 9**, where Ganesan used a two-step procedure to load a Merrifield resin with 9-borabicyclononane (9-BBN).[106] Initially, a 1,5-cyclooctadiene-functionalized resin was prepared, which was then further reacted with BH_3·THF. The resulting organoborane resin (**33**) was used in the hydroboration of a wide range of olefinic substrates. Regioselectivities were similar to those of molecular 9-BBN, but the recyclability of the supported reagent is attractive. Supports that are functionalized with sterically hindered bis(tri-*iso*-propylphenyl)boryl moieties (**34**) were prepared by Smith and coworkers from a bromo-functionalized PS resin or by treatment of Merrifield's resin with sodium naphthalenide and subsequent reaction with Tip_2BF.[107] The triarylborane resins were converted to the respective hydroborate resins by treatment with *t*-BuLi or KH and then used in the stereoselective reduction of ketones.

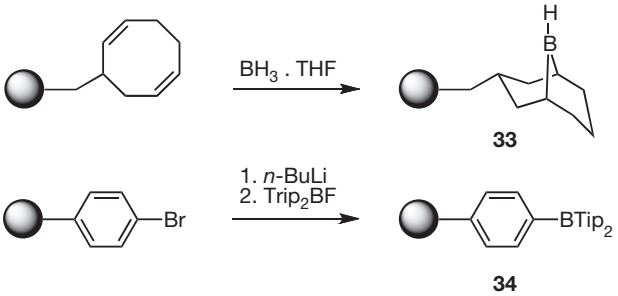

Figure 9 Synthesis of organoborane-functionalized polymer resins.

Polymers that are functionalized with fluorinated arylborane moieties have been a target of much interest, because of the exceptional properties of $B(C_6F_5)_3$ and related compounds as Lewis acid catalysts and activators in olefin polymerization (see also **Chapters 1.24** and **1.35**). The $(C_6F_5)_2$B-modified polystyrene derivative **35** was prepared from **2** (**Figure 2**) by treatment with $(C_6F_5Cu)_4$.[43,44] The polymer was soluble in common organic solvents, all borane sites were accessible for binding of Lewis basic substrates based on ^{11}B NMR studies, and the Lewis acidity of the individual sites was only slightly lower than that of $B(C_6F_5)_3$.[43,44] A carbosilane dendrimer that is decorated with fluorinated arylborane moieties (**36**) was reported by Piers and successfully utilized in the hydrosilation of acetophenone.[108] A related hyperbranched carbosilane system was prepared by Rieger via hydroboration of vinyl terminal groups with $[HB(C_6F_5)_2]_2$.[109] Propylene polymerization experiments using zirconocene catalysts in combination with this hyperbranched borane polymer as the activator showed higher activities than those achieved with $B(C_6F_5)_3$, despite the relatively lower Lewis acidity of boron in $RB(C_6F_5)_2$ (R = alkyl).

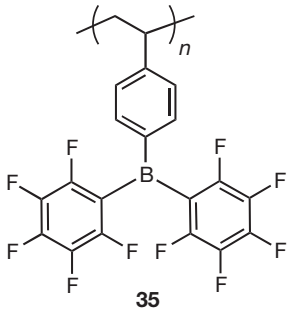

35

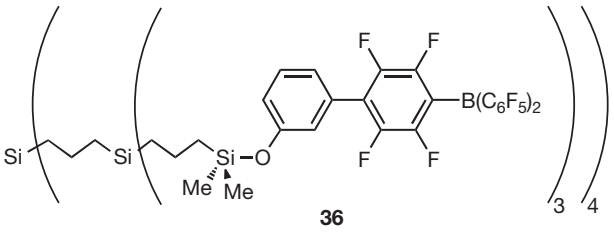

36

1.27.2.4 Supramolecular Polymers via Lewis Acid–Base Interactions

Given the presence of multiple Lewis acidic sites in the arylborane polymers described above, these materials are also promising as building blocks of supramolecular polymers that are assembled by reversible Lewis acid–base complexation. Supramolecular polymeric materials[110] continue to be a topic of much current interest, but the work carried out thus far has relied almost exclusively on hydrogen bonding[111,112] and transition metal–ligand coordination.[113–120] Wagner and coworkers examined the assembly of ferrocene-containing polymers from bifunctional organoboranes and bifunctional pyridines or pyrazine (**37**, **Figure 10**).[121–126] Stable polymeric adducts formed in the solid state at room temperature as

Copyright © 2013. Elsevier. All rights reserved.

Comprehensive Inorganic Chemistry II : From Elements to Applications, Elsevier, 2013. ProQuest Ebook Central, http://ebookcentral.proquest.com/lib/inflibnet-ebooks/detail.action?docID=1330977.
Created from inflibnet-ebooks on 2021-02-09 22:27:26.

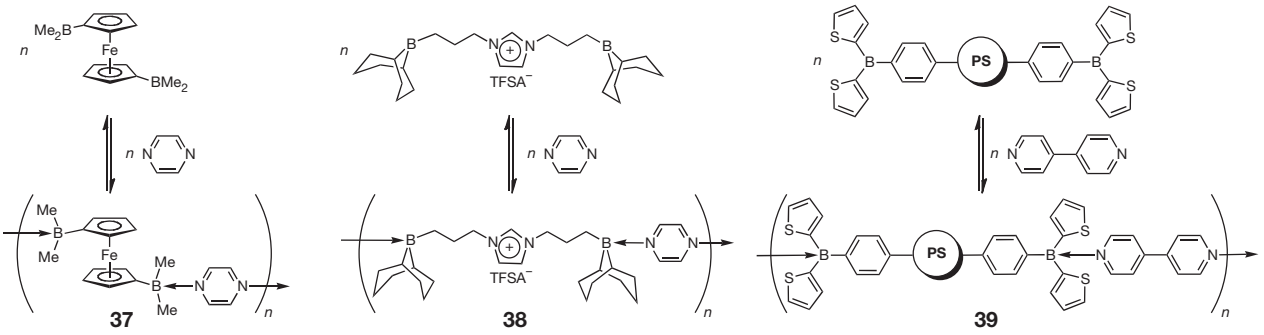

Figure 10 Supramolecular polymers via Lewis acid–base complex formation (PS = polystyrene).

confirmed by infrared (IR) and X-ray diffraction analyses; at elevated temperature, in solution, the polymer chains broke up with reformation of the molecular building blocks. Related work with boronate-functionalized building blocks was reported by Severin.[127] Moreover, Matsumi and coworkers prepared diborylated ionic liquids and studied their supramolecular assembly in the presence of pyrazine (**38**), 4,4′-bipyridine, and 1,4-diazabicyclo[2.2.2]octane (DABCO).[128] The products were examined as polymer electrolytes for lithium-ion battery applications (see **Section 1.27.4.4**).

The concept of Lewis acid–base assembly can be extended to end-group (telechelic) and side chain borane-functionalized polymers. The Jäkle group isolated well-defined polymeric Lewis acid–base complexes upon treatment of **35** and related polymers with pyridine or phosphane derivatives.[49,129] By contrast, a temperature-dependent equilibrium between coordinated and uncoordinated sites was established when **35** was exposed to weaker donors such as tetrahydrofuran (THF).[129] In another example, the assembly of a di-telechelic borane-functionalized polystyrene with 4,4′-bipyridine as a bifunctional donor gave the supramolecular polymer **39** (**Figure 10**).[53] With polymeric donor systems, the reversible assembly of even more complex polymer architectures such as *block*- and *graft*-copolymers might be envisioned.

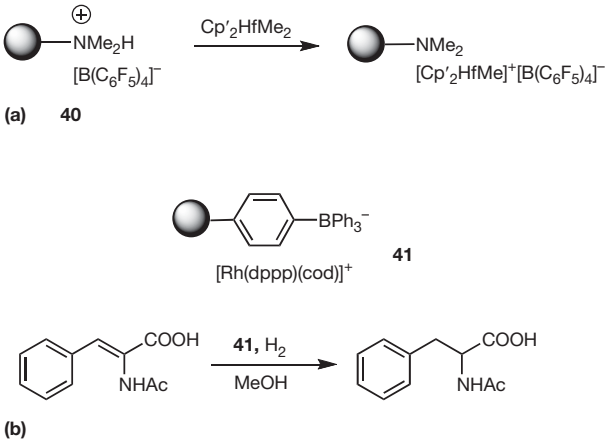

Figure 11 (a) Fréchet's immobilization of Ziegler–Natta catalysts (Adapted from Roscoe, S. B.; Fréchet, J. M. J.; Walzer, J. F.; Dias, A. J. *Science* **1998**, *280*, 270–273, with permission.). (b) Organoborate-functionalized PS particles as support for Rh hydrogenation catalysts. (Adapted from Sablong, R.; van der Vlugt, J. I.; Thomann, R.; Mecking, S.; Vogt, D. *Adv. Synth. Catal.* **2005**, *347*, 633–636, with permission.)

1.27.2.5 Borate-Functionalized Polymers

The organoborane polymers discussed so far contain Lewis acidic tricoordinate boron centers, and their applications rely on formation of neutral Lewis acid–base complexes. The functionalization of polymers with ionic organoborate moieties has been motivated primarily by the prospect for applications as 'weakly coordinating' anions[130] that stabilize catalytically active cationic transition metal complexes (see also **Chapter 1.22**). Two conceptually different approaches have been pursued. Early efforts focused on ammonium-functionalized polymeric supports with organoborates as the counterions. In this case, electrostatic forces served to anchor the organoborate and ultimately the catalytically active transition metal cations. For example, Fréchet and coworkers reacted lightly cross-linked chloromethylated polystyrene beads with dimethylamine, followed by treatment with $[PhNMe_2H][B(C_6F_5)_4]$.[131–133] The functionalized micron-sized beads (**40**, **Figure 11**) were then loaded with a Ziegler–Natta-type catalyst such as bis (tetramethylcyclopentadienyl) dimethylhafnium, Cp'_2HfMe_2. They found that copolymerization of ethylene and 1-hexene with this catalyst results in well-defined spherical polyolefin particles in the size range of 0.3–1 mm.

Mecking and coworkers used a similar approach to immobilize a catalytically active rhodium complex onto a soluble quaternary ammonium borate polyelectrolyte by electrostatic interactions between the ammonium groups and a multiply sulfonated phosphane ligand.[134] The rhodium complex was then loaded by partially replacing the weakly coordinating borate anions with the multiply charged phosphane ligands. The electrostatically supported metal complex was applied in the hydroformylation of 1-hexene and recovered almost quantitatively by ultracentrifugation.

An alternative is to covalently link the borate moieties to organic polymers by direct polymerization of borate-functionalized monomers or post-polymerization modification of suitable precursor polymers. The synthesis of borate polymers derived from styryl monomers (e.g., $[CH_2{=}CH{-}Ar{-}B(C_6F_5)_3]^-$; Ar = aromatic spacer unit) by standard free-radical polymerization and their use in olefin polymerization was first claimed in the patent literature.[135–138] More

Copyright © 2013. Elsevier. All rights reserved.

Comprehensive Inorganic Chemistry II : From Elements to Applications, Elsevier, 2013. ProQuest Ebook Central, http://ebookcentral.proquest.com/lib/inflibnet-ebooks/detail.action?docID=1330977.
Created from inflibnet-ebooks on 2021-02-09 22:27:26.

recently, Mecking and Vogt and coworkers prepared polymer particles by emulsion polymerization of styrene in the presence of sodium triphenylstyrylborate as a co-monomer, divinylbenzene (DVB) as a cross-linker, a *p*-vinylbenzyl terminated poly (ethylene oxide) macromonomer, and a water-soluble free-radical initiator.[139] The formation of submicron particles was promoted by the borate co-monomer, which acted as a surfactant to stabilize the colloidal lattices in the emulsion polymerization. A rhodium catalyst, $[Rh(dppp)(cod)]BF_4$ (dppp, bis(diphenylphosphinopropane); cod, cyclooctadiene), was loaded through ion exchange, and the immobilized catalyst (**41**, **Figure 11**) was successfully applied in the hydrogenation of α-acetamidocinnamic acid.

Uozumi and coworkers used a polymer modification method to prepare perfluorophenylborate-functionalized resins.[140] Ion exchange with trityl cations resulted in polymer-supported borate activators that were tested in combination with *rac*-Et[Ind]$_2$ZrCl$_2$ in the Ziegler–Natta polymerization of ethylene and propylene. Mager developed related soluble dendrimers that were decorated with $RB(C_6F_5)_3^-$ (R = alkyl linker) moieties.[141] They replaced trimethylsilane groups on the periphery of a carbosilane dendrimer with $-B(C_6F_5)_3$ moieties by stepwise reaction with BCl_3 and then C_6F_5Li. After conversion to dimethylanilinium borate moieties, the dendrimers were tested as cocatalysts for zirconocene-mediated olefin polymerization. Styrene block copolymers that are functionalized with weakly coordinating perfluoroarylborate moieties were prepared by Jäkle and coworkers (**Figure 12**). The amphiphilic block copolymer **42** self-assembles into reverse micelles in toluene, which is a good solvent for polystyrene but a poor solvent for the ionic block.[142] Transmission electron microscopy (TEM) analysis after loading with the cationic complex [Rh(cod)dppb)]$^+$ confirmed that the borate moieties are confined to the core of the micelles (**Figure 12**).

It is worth mentioning that borates with heteroarene substituents have also been studied for catalysis applications. While the borate moieties in the polymers discussed above are generally weakly coordinating, tris(pyrazolyl)borate (Tp) functionalities result in strong binding to metal complexes. Carbosilane dendrimers of this type were decorated with Rh(nbd)$^+$ (nbd = norbornadiene) and Ir(cod)$^+$ (cod = cyclooctadiene) moieties by Casado, Ciriano, and coworkers.[143] Polystyrene copolymers with Tp functional groups were prepared by Jäkle[48] and complexed with redox-active [CpRu]$^+$ moieties (**43**).

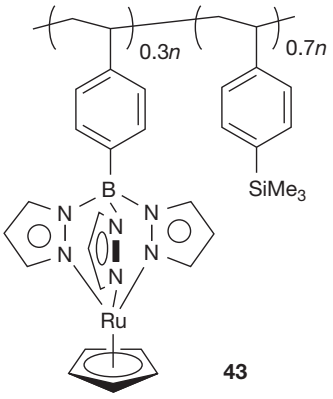

43

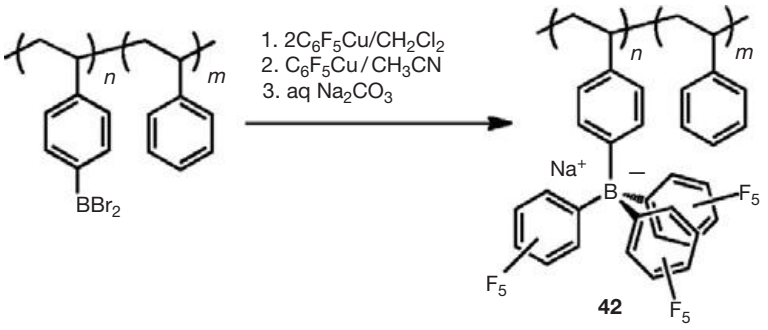

42

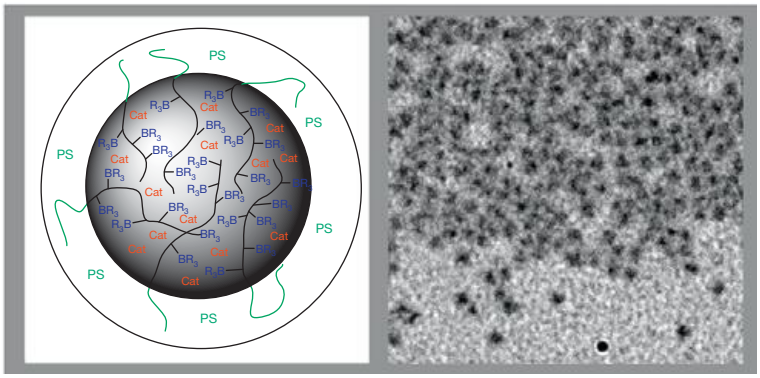

Figure 12 Synthesis of block copolymer **42** and illustration of reverse micelles loaded with [Rh(cod)dppb]$^+$ (Cat). Adapted from Cui, C. Z.; Bonder, E. M.; Jäkle, F. *J. Am. Chem. Soc.* **2010**, *132*, 1810–1812, with permission. Copyright 2010 American Chemical Society.

Copyright © 2013. Elsevier. All rights reserved.

Comprehensive Inorganic Chemistry II : From Elements to Applications, Elsevier, 2013. ProQuest Ebook Central, http://ebookcentral.proquest.com/lib/inflibnet-ebooks/detail.action?docID=1330977.
Created from inflibnet-ebooks on 2021-02-09 22:27:26.

1.27.3 Polymers Containing Conjugated Boron Heterocycles

In Section 1.27.2.2, we have discussed polymers that display interesting optical and electronic properties as a result of overlap of the empty p-orbital of tricoordinate boranes with conjugated organic π-systems. Typically, these compounds require steric stabilization by bulky organic substituents, such as 2,4,6-trimethylphenyl (Mes), 2,4,6-tri-*iso*-propylphenyl (Tip), or 2,4,6-tri-*tert*-butylphenyl (Mes*) groups.[89] Another approach to boron-containing optical and electronic materials that has proven very successful is to incorporate the boron atom into heterocyclic structures (Figure 13).[144–147] Chelation with organic ligands that contain two binding sites, most frequently N/N, N/O, and O/O, leads to cyclization and tetracoordination of the boron atom. Examples include boracycles that are derived from dipyrromethene, 8-hydroxyquinolate (q), diketonate, and 2,2′-bipyridine (bipy) chelate ligands. In other instances, formal dimerization of amino- or iminoboranes results in a heterocyclic structure. This is the case, for example, for cyclodiborazanes $(R^1HC{=}N\text{-}BHR^2)_2$ and pyrazaboles $(R_2B(\mu\text{-}pz))_2$ (pz = pyrazolyl).[148,149] As a result of coordinative saturation of boron and incorporation into a cyclic structure, the polymers generally display good stability to air and moisture. If conjugated chelate ligands are utilized, interesting optical properties, such as strong luminescence in the UV, visible (vis), or even near infrared (NIR) region, can be realized. The optical properties typically depend on the nature of the organic chromophore, but attachment to the borane moiety can have a significant impact on the position of the highest occupied molecular orbital (HOMO) and lowest unoccupied molecular orbital (LUMO) energy levels. Cyclization also leads to a more rigid structure, which tends to favor radiative over nonradiative decay and hence often results in excellent fluorescence quantum yields. In some cases, phosphorescence has also been observed, and even dual-emissive compounds that emit simultaneously from singlet and triplet excited states have been reported.[150] In the following, we will discuss in more detail selected examples of polymeric materials that contain these organoboron heterocycles as pendant groups or directly embedded in the polymer main chain.

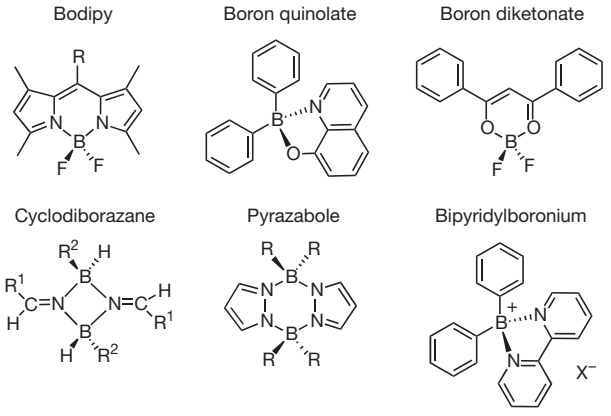

Figure 13 Structures of boron heterocycles commonly used in polymeric materials.

1.27.3.1 Cyclodiborazane-Functionalized Polymers

Addition of an organoborane species RBH_2 to a nitrile leads to cyclodiborazane species, in which B–N donor–acceptor interactions result in formal dimerization of the iminoboranes. Chujo and coworkers utilized this method to prepare a large variety of polymers (**44**) that contain cyclodiborazane rings embedded in the polymer main chain.[148] An alternative procedure that involves Sonogashira–Hagihara coupling of bromoaryl-functionalized cyclodiborazane monomers with dialkynes resulted in slightly higher-molecular-weight products.[151] The borane substituents R (R = ^{t}Bu, Mes, Tip) were chosen to be relatively bulky in order to sterically stabilize the products.[64] The borane $IpcBH_2$ (Ipc = isopinocampheyl) was also employed to generate chiral polymers.[152] Interesting optical and electronic properties were realized by variation of the bridging group that connects the nitrile functionalities. Phenylene, fluorene, anthracene, oligothiophene, disilane, dithiafulvene, and even transition metal complexes were incorporated.[64,148,153–158] Some degree of color tuning was achieved by extension of the π-conjugation of the linker or by choosing an electron-rich aromatic bridging group that favors a donor–acceptor structure in the resulting polymer chain.[154,156]

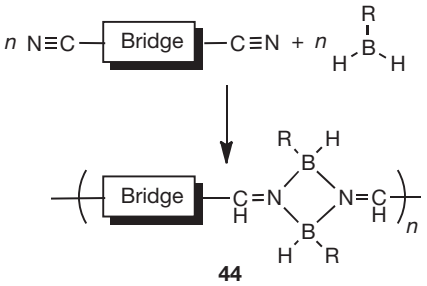

44

1.27.3.2 Pyrazabole-Functionalized Polymers

Six-membered boron–nitrogen heterocycles based on the pyrazabole framework are known for their exceptionally high stability. Moreover, they can be easily derivatized with various functional groups on boron or the pyrazole moieties.[149,159] Early work by Wagner and coworkers took advantage of pyrazabole moieties as building blocks for shape-persistent macrocycles.[126] Chujo and coworkers synthesized polymers that contain pyrazaboles in the main chain using metal-catalyzed coupling reactions. Sonogashira–Hagihara coupling of diiodopyrazabole and dialkynylarylene monomers, or coupling of diethynylpyrazabole and dibromoarylenes, gave polymers **45** (Ar = phenylene, dialkoxyphenylene, fluorenylene, and anthracenediyl) with remarkably high molecular weights of up to 34 000 Da.[160,161] A significant red shift of the UV–vis absorption compared to the monomer was not observed, indicating that no significant extension of conjugation via the pyrazabole moiety occurred. The polymers showed intense blue to violet fluorescence with emission maxima in the range $\lambda_{em,\ max} = 383\text{–}470$ nm ($\Phi_F = 0.43\text{–}0.67$). Electron-withdrawing groups on the bridging arylene moiety (Ar) shifted the fluorescence to shorter wavelengths. Interestingly, polymer **45** (Ar = 1,4-phenylene) was also found to act as a

Copyright © 2013. Elsevier. All rights reserved.

Comprehensive Inorganic Chemistry II : From Elements to Applications, Elsevier, 2013. ProQuest Ebook Central, http://ebookcentral.proquest.com/lib/inflibnet-ebooks/detail.action?docID=1330977.
Created from inflibnet-ebooks on 2021-02-09 22:27:26.

scintillator, that is, the material proved to be emissive upon exposure to a neutron flux.[162]

Related transition-metal-containing pyrazabole polymers were synthesized by coupling of late transition metal complexes with a dialkynyl-functionalized pyrazabole. Metal-to-ligand charge transfer (MLCT) absorption bands could be observed for Ni- and Pt-containing polymers (**46**), but not for the polymer with M = Pd. The latter showed only structured high-energy bands that were assigned to the pyrazabole moiety.[163]

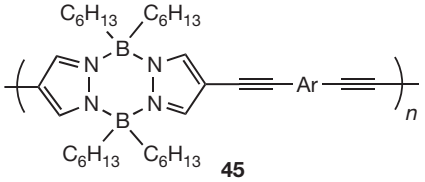

45

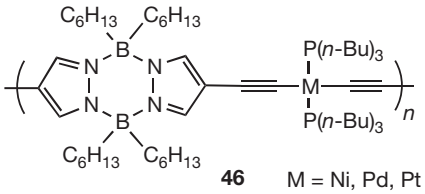

46 M = Ni, Pd, Pt

1.27.3.3 BODIPY-Functionalized Polymers

BODIPY dyes are notable for their uniquely small Stokes shifts, narrow absorption bands, sharp emissions, high fluorescence quantum yields, and excellent chemical and photostability.[146,164,165] The combination of these desirable attributes makes BODIPY fluorophores attractive as tools in a variety of applications, for example, in biochemical labeling, light-emitting devices, supramolecular fluorescent gels, light harvesting systems, and as sensitizers in solar cells.

First efforts at incorporating BODIPY dyes into conjugated polymers were reported by Li and coworkers in 2008.[166] They used Sonogashira coupling of 2,6-diiodo-functionalized BODIPY to prepare conjugated polymers **47** and **48**. The molecular weights of $M_n = 1700–6000$ Da, however, were modest. BODIPY-centered π–π* transitions gave rise to absorptions in the range of 570–640 nm and corresponding emissions in the red region (615–664 nm) with quantum yields of up to 25%. Liu and coworkers introduced solubilizing groups at the phenyl moiety in the *meso*-position and also explored long-chain alkyl-substituted arylene (Ar) bridges for polymers **47**. The enhanced solubility in organic solvents resulted in significantly higher molecular weights in the range of $M_n =$ 15 000–25 000 Da. The polymers displayed strong red emissions (640–680 nm), similar to the results reported by Li and coworkers.[167,168]

Suzuki coupling presents an alternative synthetic route that allowed for the preparation of copolymers, in which aromatic building blocks alternate with BODIPY moieties (**49**, Ar = phenylene, fluorenylene).[169,170] While the emission maxima were generally at shorter wavelengths in comparison to the alkynyl-bridged polymers **47** and **48**, significantly higher quantum yields of up to 85% were realized. Other methods for BODIPY incorporation in the main chain of conjugated polymers include the Ni-catalyzed Yamamoto-coupling polymerization, which yields BODIPY homopolymers (**50**), and the electro-polymerization of thiophene-substituted BODIPY derivatives.[170,171]

A fundamentally different approach to BODIPY functionalization was taken by Chujo and coworkers. They linked the BODIPY dyes to π-conjugated phenylene–ethynylene segments via Sonogashira coupling of iodophenyl substituents on boron, which formally results in organoborane polymers (**51**) with pendant dipyrromethene moieties.[172] The resulting polymers showed multiple absorptions. Bands at ca. 519 nm correspond to excitation of the BODIPY moiety, while higher-energy absorptions in the range of 348–372 nm were attributed to excitation of the conjugated linker. The observation of single emissions at 532 nm with quantum yields Φ_F ranging from 70% to 85% indicated very effective energy transfer from the conjugated organic linker to the BODIPY chromophores. Gel permeation chromatography (GPC) and scanning electron microscopy (SEM) analyses revealed the presence of larger aggregates, which were thought to result from self-assembly of the rod–coil-type structure, where the rigid π-conjugated polymer main chain represents the rod and the decyl group the coil, respectively. Yet another possibility is to link the BODIPY moieties via the *meso*-substituents. This approach was taken by Burgess and coworkers, who copolymerized diiodophenyl-substituted

Pyrollyl linkage

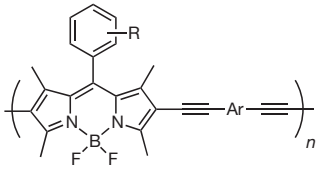

47

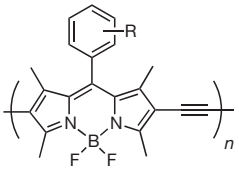

48

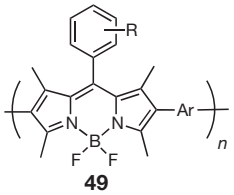

49

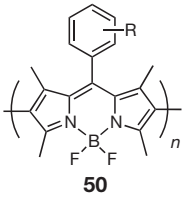

50

Boron linkage

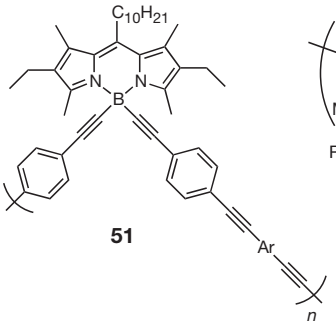

51

Meso linkage

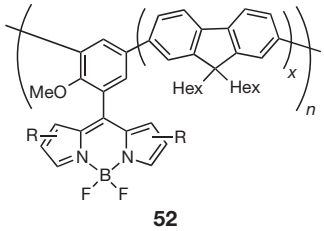

52

Copyright © 2013. Elsevier. All rights reserved.

Comprehensive Inorganic Chemistry II : From Elements to Applications, Elsevier, 2013. ProQuest Ebook Central, http://ebookcentral.proquest.com/lib/inflibnet-ebooks/detail.action?docID=1330977.
Created from inflibnet-ebooks on 2021-02-09 22:27:26.

BODIPY derivatives with 2,7-diiodofluorene and 2,7-bis(boronic acid)fluorene.[173] Similar to **51**, polymers **52** showed exceptionally strong emission as a result of efficient energy transfer (86–98% efficiency) from high-energy states localized on the strongly absorbing oligofluorene linker to the BODIPY acceptors.

Applications of conjugated BODIPY polymers are envisioned in electronic devices and in the biomedical field. Thayumanavan explored BODIPY polymers as semiconductor materials for organic electronics. They prepared donor–acceptor-type copolymers **47** with Ar = quinoxalene, benzothiodiazole, as well as naphthalene and perylene tetracarboxylic dimide acceptor moieties.[174] *n*-Type semiconducting behavior was confirmed for the rylene dye copolymers. Fréchet, Ma, Liu, and coworkers utilized polymers **47** (Ar = 3-docecylthiophene) and **48** as donors in bulk-heterojunction (BHJ) photovoltaic devices with [6,6]-phenyl C_{61} butyric acid methyl ester (PCBM) as the acceptor. A respectable power conversion efficiency of 2% was realized. Recent efforts by Sauvé were aimed at utilizing aza-BODIPY dye-functionalized polymers as acceptors in all-polymer photovoltaics.[175]

For biomedical applications it is desirable to shift the absorptions and emissions further into the near-IR region. Liu obtained near-IR emissive materials similar to **47** by introducing one or two styryl groups at the 3,5-positions of the BODIPY moiety (λ_{em} = 715, 760 nm).[176] Red shifts in the absorption and emission spectra were also accomplished by ring fusion[177] or use of aza-BODIPY dyes.[175,178] Another important requirement for biomedical applications is to achieve site-selective accumulation. Burgess and coworkers fabricated the highly emissive oligofluorene copolymers **52** into nanoparticles of ca. 40 nm diameter and studied their uptake into rat liver cells.[173] While molecularly dispersed polymer chains were not delivered into the cells, successful uptake of the nanoparticles could be confirmed by confocal imaging.

BODIPY moieties were also introduced as side groups in polyolefins. Acrylate polymers that are functionalized with BODIPY were studied extensively for applications as luminescent materials and for lasing applications.[179–181] Another attractive goal has been the development of thermo-responsive luminescent materials for sensory applications. Copolymerization of BODIPY-functionalized monomers with suitable thermo-responsive monomers proved to be a viable approach. For instance, Chujo and coworkers prepared BODIPY copolymers with dimethylaminoethyl methacrylate (DMAEMA) (**53**) via reversible addition–fragmentation chain transfer polymerization (RAFT) copolymerization, whereas Liras and coworkers resorted to ATRP to prepare copolymers with 2-(2-methoxyethoxy)ethyl methacrylate (**54**).[182,183] In both cases, a strong increase in fluorescence intensity was observed when an aqueous solution of the polymer was heated above the lower critical solution temperature (LCST). This allows for reversible fluorescence switching as illustrated for an aqueous solution of polymer **53** in Figure 14. Post-polymerization modification of *N*-isopropylacrylamide/chloromethylstyrene copolymers with pyridine-functionalized BODIPY dyes also led to luminescent materials with temperature-dependent emission properties.[184,185]

Controlled radical polymerization methods allow for the preparation of nanostructured luminescent materials. Chujo and coworkers used RAFT polymerization to prepare BODIPY-functionalized random and block copolymers (**55**).[186] Self-assembly in THF solution led to fluorescent nanoparticles with quantum yields of >70%. The self-assembly process was attributed to favorable π–π stacking interactions. Luminescent polymer/silica hybrid materials, on the other hand, were obtained by random copolymerization of a BODIPY-functionalized methacrylate monomer with hydroxyethyl methacrylate (HEMA), followed by sol–gel reaction with methyl trimethoxysilane.[187] Chujo and coworkers also attached BODIPY as a terminal group to poly(*N*-isopropylacrylamide) (PNIPAM).[188] RAFT polymerization of *N*-isopropylacrylamide (NIPAM) with a BODIPY-functionalized CTA gave the end-functionalized polymer **56** (Figure 15). The controlled character of the polymerization was confirmed by a relatively narrow molecular weight distribution of the product (PDI = 1.28) and a linear increase of molecular weight with conversion. Treatment with $HAuCl_4$ resulted in stable BODIPY-modified gold nanoparticles (AuNPs) with an average size of ~10 nm in water solution.[188] In this case, heating of the nanoparticles above the LCST led to efficient luminescence quenching, which was attributed to dye–dye quenching and Förster resonance energy transfer (FRET) as a result of shrinking of the polymer shell toward the Au nanoparticle core, which acts as a quencher.

1.27.3.4 Boron Hydroxyquinolate- and Aminoquinolate-Functionalized Polymers

Another family of luminescent boron-containing heterocycles that has been extensively studied are the boron quinolates. Boron 8-hydroxyquinolate compounds may be viewed as analogs of aluminum 8-hydroxyquinolate (Alq_3; q = 8-hydroxyquinolate),[189] which is among the most widely utilized electron-transport materials in OLEDs.[189–191] The boron species, studied extensively by Wang and others,[192–194] have been reported to be comparatively more stable. Similar to the

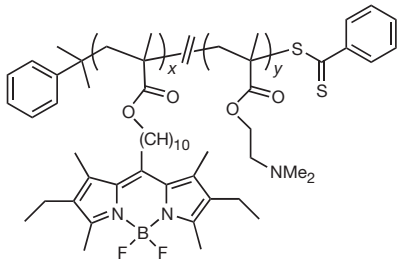

53

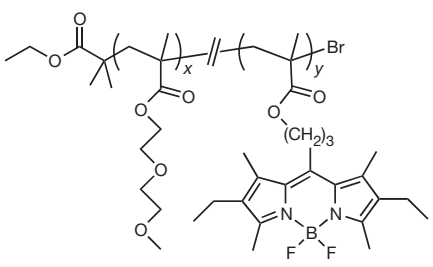

54

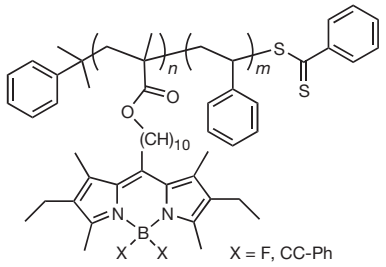

55

Copyright © 2013. Elsevier. All rights reserved.

Comprehensive Inorganic Chemistry II : From Elements to Applications, Elsevier, 2013. ProQuest Ebook Central, http://ebookcentral.proquest.com/lib/inflibnet-ebooks/detail.action?docID=1330977.
Created from inflibnet-ebooks on 2021-02-09 22:27:26.

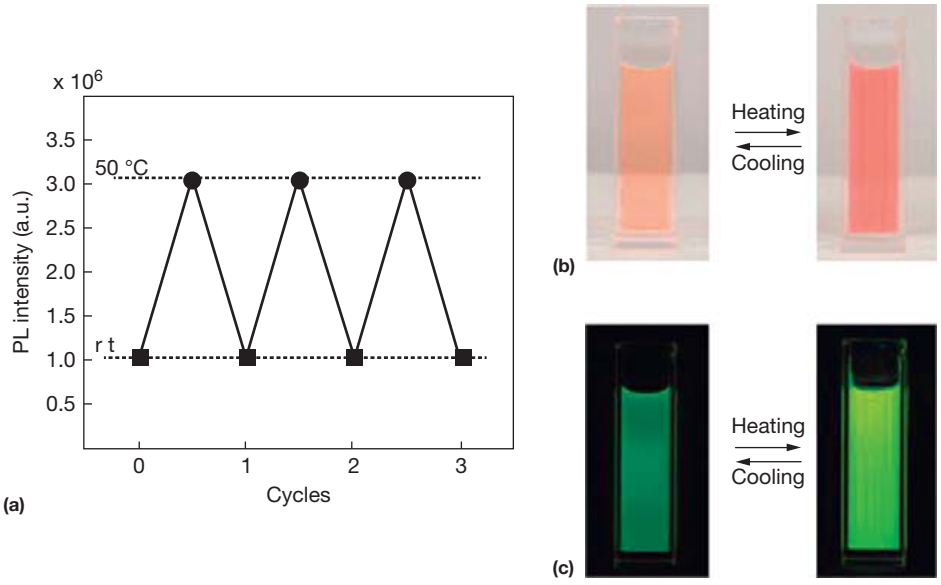

Figure 14 (a) Thermal switching of photoluminescence intensity of **53** in water (1.0 wt.%, λ_{exc} = 521 nm). (b) Photographs at RT and 50 °C. (c) Photographs under UV irradiation at RT and 50 °C. Reproduced from Nagai, A.; Kokado, K.; Miyake, J.; Chujo, Y. *J. Polym. Sci. A Polym. Chem.* **2010**, *48*, 627–634, with permission. Copyright 2010 Wiley-VCH Verlag GmbH & Co. KGaA.

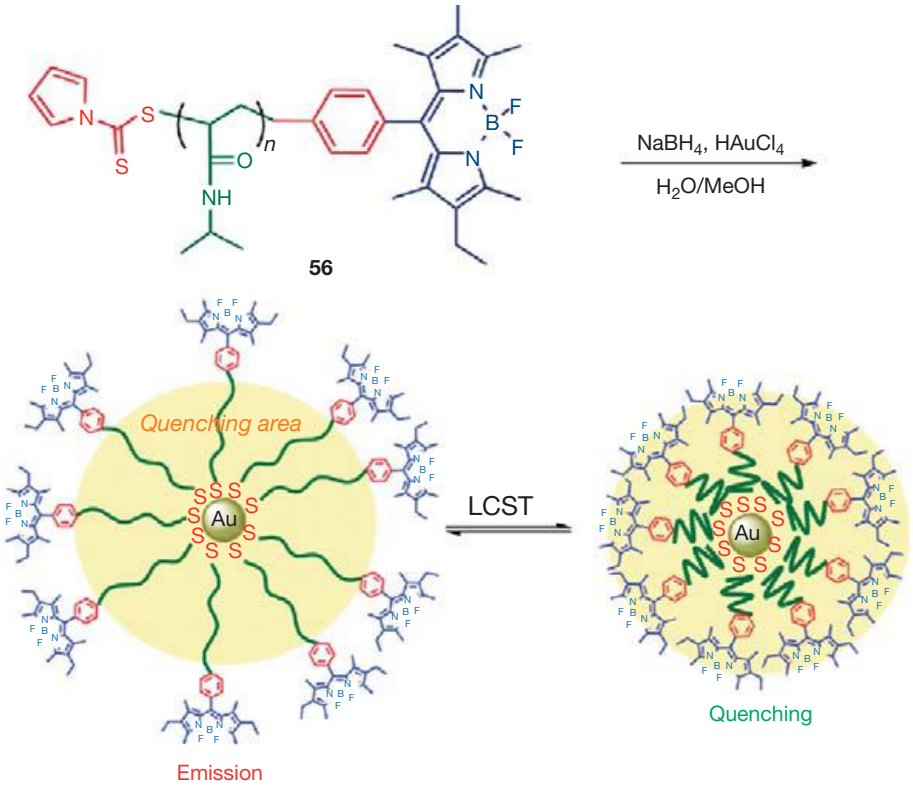

Figure 15 Schematic illustration of the proposed mechanism for the photoluminescence switching of Au nanoparticles functionalized with **56**. Reproduced from Nagai, A.; Yoshii, R.; Otsuka, T.; Kokado, K.; Chujo, Y. *Langmuir* **2010**, *26*, 15644–15649, with permission. Copyright 2010 American Chemical Society.

respective aluminum complexes,[195–197] their emission properties can be easily fine-tuned by varying the ligand-substitution pattern. Not unlike the BODIPY systems, polymers that are comprised of boron 8-hydroxyquinolate moieties are attractive because of the facile synthetic access, tunable emission, and high stability. For conjugated polymers that bear the 8-hydroxyquinolate moieties in the main chain, efficient energy transfer from higher-energy states localized on the polymer backbone to the boron 8-hydroxyquinolate chelate complexes has been observed.[198,199]

Copyright © 2013. Elsevier. All rights reserved.

Comprehensive Inorganic Chemistry II : From Elements to Applications, Elsevier, 2013. ProQuest Ebook Central, http://ebookcentral.proquest.com/lib/inflibnet-ebooks/detail.action?docID=1330977.
Created from inflibnet-ebooks on 2021-02-09 22:27:26.

Jäkle and coworkers reported the first examples of polymers that are functionalized with boron 8-hydroxyquinolate complexes.[45,47] Polymers **57** were prepared by post-polymerization modification of BBr_2-functionalized polystyrene (see **2**, Section 1.27.2.1) with different 8-hydroxyquinoline derivatives. High-molecular-weight materials with close to quantitative chromophore functionalization were obtained. Upon photoexcitation, the polymer that contained the parent 8-hydroxyquinolate moiety (X = H) emitted green light with quantum yields in the range of ca. 20–30%.[45] The emission of the polymers was fine-tuned over almost the entire visible spectrum by varying the substituent X at the 5-position of the ligand from electron-donating to electron-withdrawing character (Figure 16).[47] A complementary approach was chosen by Weck and coworkers who prepared boron hydroxyquinolate copolymers from 8-hydroxyquinoline-functionalized organic polymers.[200] The emission spectra were similar in solution and thin films, consistent with the notion that the chromophores act independently, even in the thin film state. The latter is desirable for applications as emissive layers in OLED devices. Jäkle and coworkers more recently reported the direct polymerization of luminescent 8-hydroxyquinolate-based organoboron monomers by the RAFT[201] polymerization method.[202] Use of a PEO–macro-CTA led to luminescent amphiphilic block copolymers (**58**). In water the polymers formed stable luminescent micellar solutions, which is important for potential applications as nano-sized fluorophores in biological environments.

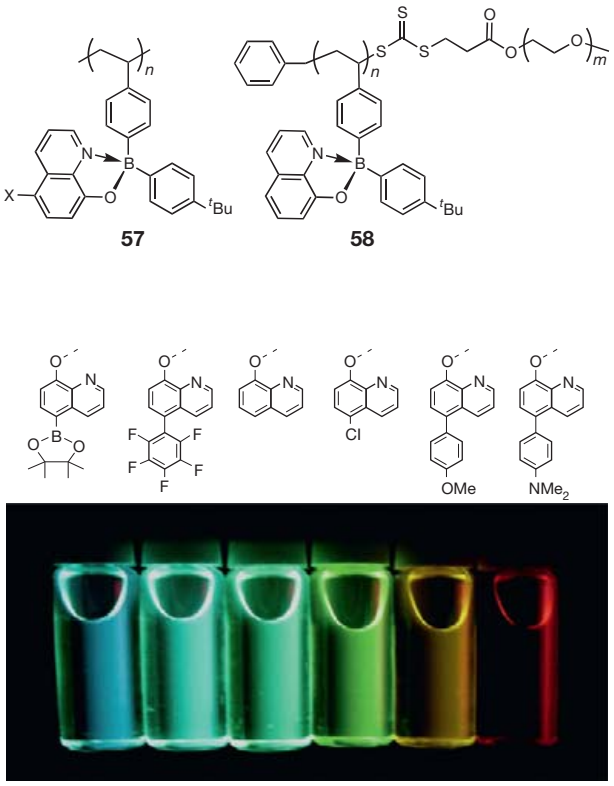

Figure 16 Tuning of the emission of polymers **57** by variation of the substituent X. Adapted from Qin, Y.; Kiburu, I.; Shah, S.; Jäkle, F. *Macromolecules* **2006**, *39*, 9041–9048, with permission. Copyright 2006 American Chemical Society.

The incorporation of organoboron quinolate moieties into the backbone of conjugated polymers was accomplished by Sonogashira–Hagihara coupling of diiodo-functionalized boron quinolate monomers. Chujo's group reported a wide range of fluorescent polymers of this type and selected examples are displayed (**59**).[199,203–206] The emission color of the polymers was tuned by modification of the ligand with methyl groups at different positions or by changing the substituent at the 8-position of the quinoline from hydroxy to thiol, selenol, as well as amino groups.[203,204] Polymer modification reactions can also be utilized and this approach was taken by Jäkle and coworkers.[80] For instance, treatment of the poly(fluorenylene bromoborane) **11a** (see Section 1.27.2.2.1) with 8-methoxyquinoline resulted in the formation of polymer **60**. The reaction occurred under mild conditions with MeBr as the only by-product. The molecular weights were determined by the average number of repeating units of the precursor polymer **11a** (ca. 16–18 units).

The polymers described above feature the quinolate ligand as a pendant group, with the borons linked by covalent B–C bonds in the main chain. An alternative design is to incorporate the chelate ligand itself into the polymer chain. This approach was taken by Chujo and coworkers, when they prepared polymers **61** and **62** by treatment of 8-hydroxyquinole-type conjugated polymers with BPh_3.[198,206] The fluorescence quantum yield for the orange-emissive **61** is only 0.29%, but that of **62** was measured to be 16%. It is important to point out that, as a result of facile energy transfer from higher energy states of the strongly absorbing conjugated organic polymer backbone to lower-energy charge transfer states localized on the quinolate chromophore, these polymers are highly emissive, even when the quantum yields are relatively low. Furthermore, the electron mobilities of polymer **62** and of a derivative with fluorinated phenyl groups on boron were determined from the space-charge-limited current (SCLC) in an electron-only device structure of ITO/Ca/polymer/LiF/Al. The mobilities of 3.9 and 2.0×10^5 $cm^2\,V^{-1}\,s^{-1}$, respectively, were close to that determined for a reference device with Alq_3.[206]

Yet another possibility is to link individual borane moieties in the polymer chain via chelate formation. In this respect, the Jäkle group introduced a mild method in which a bifunctional bis(bromoborane) monomer was reacted with a bis(8-methoxyquinoline) species.[207] Polycondensation via boron-induced ether cleavage led to the luminescent polymer **63**. Chujo and coworkers prepared structurally related, optically active organoboron aminoquinolate coordination polymers (**64**) via Sonogashira–Hagihara coupling.[208,209] They incorporated L-alanine-based chiral side chains in an effort at stabilizing the polymer structure via a combination of π-stacking and hydrogen-bonding interactions. The circular dichroism (CD) response proved to be solvent and concentration dependent, which is indicative of changes in the supramolecular polymer structure.

1.27.3.5 Boron Diketonate-Functionalized Polymers

Boron diketonates present another family of versatile boron chelate dyes that has attracted attention as a light-emitting material. Desirable characteristics include large molar

Copyright © 2013. Elsevier. All rights reserved.

Comprehensive Inorganic Chemistry II : From Elements to Applications, Elsevier, 2013. ProQuest Ebook Central, http://ebookcentral.proquest.com/lib/inflibnet-ebooks/detail.action?docID=1330977.
Created from inflibnet-ebooks on 2021-02-09 22:27:26.

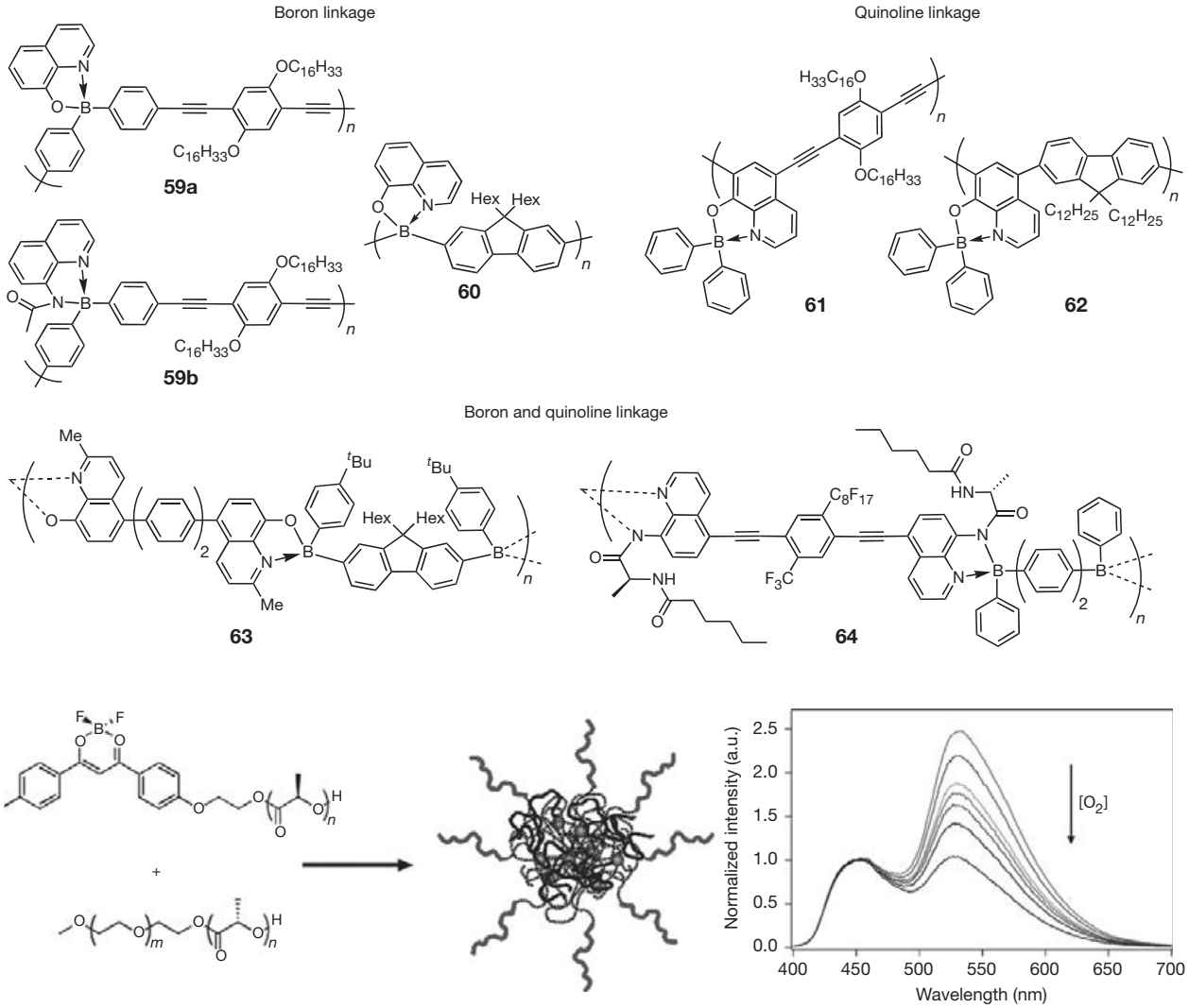

Figure 17 Schematic illustration of the formation of stereocomplexed poly(lactic acid)–poly(ethylene glycol) with dual emissive boron dyes and quenching of phosphorescence in the presence of oxygen. Adapted from Kersey, F. R.; Zhang, G. Q.; Palmer, G. M.; Dewhirst, M. W.; Fraser, C. L. *ACS Nano* **2010**, *4*, 4989–4996, with permission. Copyright 2010 American Chemical Society.

absorption coefficients, high fluorescence quantum yields, the observation of dual emissive behavior, two-photon absorption, and of mechanochromic luminescence.[210–213] Fraser and coworkers prepared hydroxyl-functionalized difluoroboron dibenzoylmethane (Φ_F ca. 95%), which was employed as an initiator in the ROP of caprolactone and DL-lactide to give the respective boron diketonate end-functionalized polymers **65** and **66**.[150,210,214,215] The polylactide **65** exhibited high fluorescence quantum yields and simultaneous phosphorescent emission, even at room temperature. The polymer emission was reported to depend on the temperature, the polarity and rigidity of the medium, and also the molecular weight of the polymer, which in turn directly correlates with the chromophore concentration.[214,216,217] Generally, fluorescence was the favored pathway at room temperature, but phosphorescence could be promoted by introducing a heavy atom (e.g., X = I in **65**).[218]

For biomedical imaging applications, nanoparticles of these materials were prepared by injecting a dimethylformamide

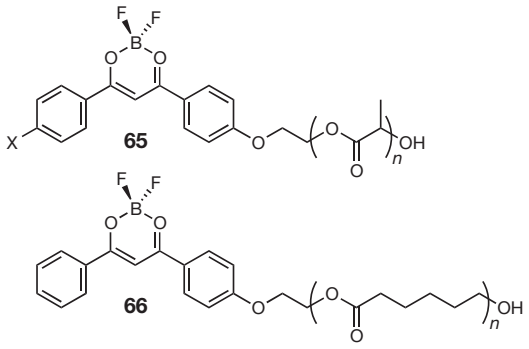

(DMF) solution of the polymer into water.[219,220] An alternative method is to form stereocomplexes of **65** with poly(lactic acid)-*block*-poly(ethylene oxide), which also self-assemble into nanostructured, dual-emissive materials (Figure 17).[221] A particularly promising application of these materials is in

Copyright © 2013. Elsevier. All rights reserved.

Comprehensive Inorganic Chemistry II : From Elements to Applications, Elsevier, 2013. ProQuest Ebook Central, http://ebookcentral.proquest.com/lib/inflibnet-ebooks/detail.action?docID=1330977.
Created from inflibnet-ebooks on 2021-02-09 22:27:26.

tumor hypoxia imaging. The presence of oxygen led to quenching of the lower-energy phosphorescence but not the fluorescence, effectively resulting in a ratiometric oxygen sensor (Figure 17).[218,222]

Chujo and coworkers reported the incorporation of β-diketonate moieties into the backbone of conjugated polymers by chelation of a 1,3-diketone-functionalized poly(*p*-phenylene–ethynylene) derivative with arylboron compounds.[223] The desired organoboron chelate-functionalized polymers **67** were obtained by the reaction of a Boc-protected precursor polymer ($M_n = 5100$) with Ph_3B or $(C_6F_5)_2BF{\cdot}OEt_2$, respectively. The molecular weights of the boron polymers measured by GPC were consistent with that of the precursor polymer.

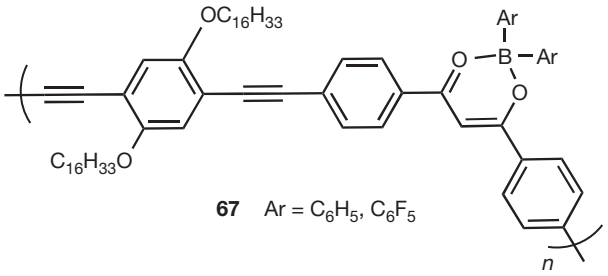

67 Ar = C_6H_5, C_6F_5

1.27.3.6 Bipyridylboronium-Functionalized Polymers

We have so far focused on anionic chelate ligands that result in formation of neutral luminescent organoboron heterocycles. By contrast, reaction of organoboron halides with neutral bidentate ligands such as 2,2′-bipyridine results in cationic boronium species.[224] Heterocycles of this type have been reported to display high stability and attracted considerable interest, for example, as components of new ionic liquids and as multistep redox-active materials.[225,226] Jäkle and coworkers explored their incorporation into polymeric materials.[227] Polyelectrolytes such as **68** were obtained by treatment of bromoboryl-functionalized polystyrene with an excess of 2,2′-bipypridine. The solubility characteristics of the resulting ionic polymers strongly depended on the counterion ($X^- = Br^-$, PF_6^-); with $X^- = Br^-$ the polymers dissolved even in MeOH or water. Related amphiphilic diblock copolymers based on bipyridylboronium-functionalized polystyrene and unfunctionalized polystyrene as a second block were also prepared. In MeOH as a good solvent for the boronium moieties but a poor solvent for polystyrene, self-assembly resulted in highly regular spherical micelles.[228] These polymers present a potential alternative to ammonium-based cationic polymers in areas such as membrane technologies and antimicrobial surface functionalization. The boronium-type polymer **69** contains multiple redox-active sites (ferrocene and bipyridylboronium) and could prove interesting for battery applications.[229]

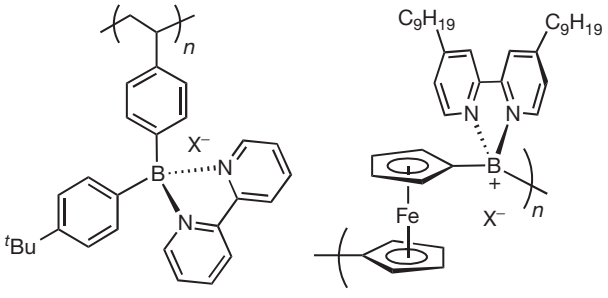

68 **69**

1.27.4 Polymers Containing Boronic Acid, Boronic Ester, and Boroxine Groups

Another important class of boron-containing polymers are those containing boronic acid functionalities.[230] In anhydrous organic solvents, boronic acids typically establish an equilibrium with their anhydrides, the boroxines (Figure 18). Boronic acid groups also reversibly bind to substrates containing a 1,2- or 1,3-diol moiety, which is the principle behind their widespread use in the sensing of saccharides, glycoproteins, RNA, and other biologically relevant entities. Moreover, boronic acid-functionalized polymers are promising as stimuli-responsive materials based on the fact that boronic ester formation can be controlled by changes in pH or temperature. Other applications of boronic acid polymers include self-healing materials, flame retardants, holographic materials, separating agents, therapeutic agents, and self-regulated drug-delivery systems.[6] Biomedical applications of boronic acid polymers have recently been reviewed by Sumerlin and coworkers.[231] Similarly, the use of boronic acids as building blocks to nanostructures, microporous COFs, and supramolecular polymeric materials has been reviewed by Severin and Mastalerz.[232,233] Hence, only selected recent examples will be introduced here.

1.27.4.1 Responsive Materials Based on Block Copolymers

Much research has been done over the years with 4-vinylphenylboronic acid and 3-acrylamidophenylboronic acid and closely related monomers, which are readily polymerized by

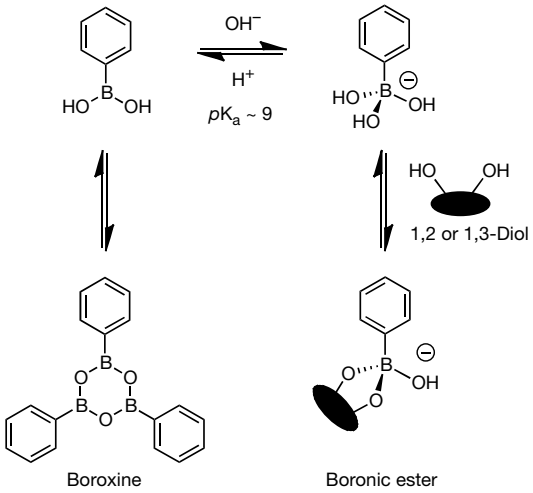

Figure 18 Schematic illustration of boronic ester and boroxine formation.

Copyright © 2013. Elsevier. All rights reserved.

Comprehensive Inorganic Chemistry II : From Elements to Applications, Elsevier, 2013. ProQuest Ebook Central, http://ebookcentral.proquest.com/lib/inflibnet-ebooks/detail.action?docID=1330977.
Created from inflibnet-ebooks on 2021-02-09 22:27:26.

standard free-radical polymerization.[6] To introduce boronic acid functionalities into more complex polymer architectures, with good control over the position of the functional groups, is a challenge that has been tackled more recently. Significant advances have been achieved using controlled radical polymerization methods such as the ATRP technique, nitroxide-mediated polymerization (NMP), and RAFT.[234–237] In 2005, Jäkle and coworkers reported a post-polymerization modification approach for the synthesis of the boronic acid-functionalized styrene block copolymer PSBA-*b*-PS (**70**).[46] Initially, a silylated block copolymer was prepared by ATRP (see **Section 1.27.2.1**). Reaction with BBr_3 led to replacement of the silyl groups for BBr_2 moieties, which were subsequently hydrolyzed to boronic acid groups. Dynamic light scattering and TEM studies revealed the formation of highly regular spherical micelles in basic aqueous solution (**Figure 19**).[238] In the presence of an organic co-solvent, other morphologies, including vesicles and bundles of rod-like assemblies, formed at neutral pH.

Jäkle and coworkers also demonstrated the controlled polymerization of 4-pinacolatoborylstyrene by ATRP, and the resulting boron-containing polymer was used as a macro-initiator in the chain extension with styrene to prepare poly(4-pinacolatoborylstyrene)-*b*-polystyrene.[46] More recently, van Hest and coworkers synthesized the block copolymer PEG-*b*-PSBA (**71**) by ATRP of 4-pinacolatoborylstyrene with a poly(ethylene glycol) (PEG) macroinitiator, followed by deprotection of the boronic ester groups.[239] This diblock copolymer is responsive to both changes in pH and the presence of sugar molecules. The polymer was used to assemble a nanoreactor, whose walls consist of a mixture of PEG-*b*-PS and PEG-*b*-PSBA. van Hest also developed related block copolymers with amino groups in ortho-position to the boronic acid moieties (**72**). The latter are capable of binding to the Lewis acidic boron sites.[240] These so-called Wulff-type receptors facilitate sugar binding in water at neutral pH.

Sumerlin and coworkers reported boronic acid-functionalized acryl amide block copolymers as efficient sugar sensors, as well as pH and temperature responsive materials. For instance, they synthesized a block copolymer by direct polymerization of 4-pinacolatoborylstyrene monomer with *N*,*N*-dimethylacrylamide using the RAFT technique.[241] The pinacol protecting groups were removed by passing the polymer through a column that contained immobilized boronic

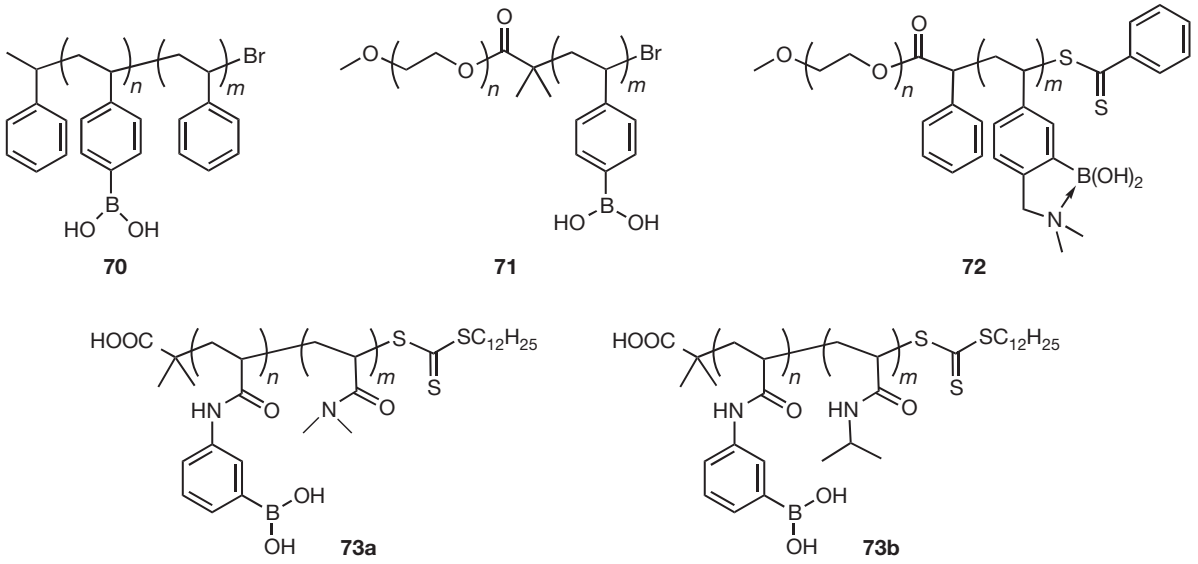

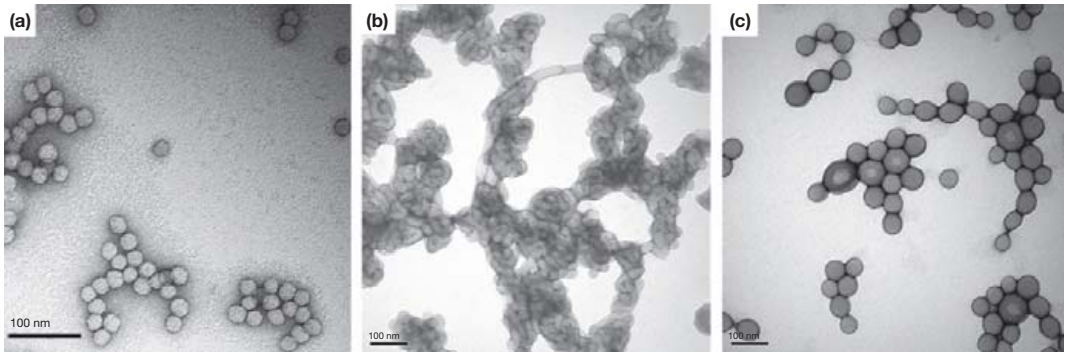

Figure 19 Boronic acid-functionalized nanostructures of block copolymer **70** in (a) 0.1 M NaOH aqueous solution; (b) THF water at pH 7. Adapted from Cui, C. Z.; Bonder, E. M.; Qin, Y.; Jäkle, F. *J. Polym. Sci. A Polym. Chem.* **2010**, *48*, 2438–2445, with permission. Copyright 2010 Wiley-VCH Verlag GmbH & Co. KGaA.

Copyright © 2013. Elsevier. All rights reserved.

Comprehensive Inorganic Chemistry II : From Elements to Applications, Elsevier, 2013. ProQuest Ebook Central, http://ebookcentral.proquest.com/lib/inflibnet-ebooks/detail.action?docID=1330977.
Created from inflibnet-ebooks on 2021-02-09 22:27:26.

acid moieties. More recently, they discovered that boronic acid-functionalized acrylamide monomers can be directly polymerized using RAFT methodologies, which avoids the need for additional post-polymerization functionalization steps.[242] The block copolymer PAPBA-*b*-PDMA (**73a**, PDMA = poly(*N*, *N*-dimethylacrylamide)) proved to be sugar responsive. At a pH lower than the pK_a of the boronic acid moieties (p$K_a \sim 9$), the polymer formed micellar aggregates. Dissociation of the micelles could be triggered by addition of glucose. A boronic acid block copolymer with NIPAM as the co-monomer, PAPBA-*b*-PNIPAM (**73b**), proved to be thermo-responsive, in addition to the pH- and sugar-responsive behavior of the boronic acid polymer block, resulting in a triply-responsive material.[243] According to dynamic light scattering (DLS) studies, at high pH or upon glucose addition, the block copolymer was molecularly dissolved. However, when heated above the LCST of the PNIPAM block, micellization occurred and the PNIPAM block was incorporated into the core of the micelles.

1.27.4.2 Boronic Acid-Functionalized Conjugated Polymers

Conjugated polymers that are functionalized with boronic acid or boronic ester groups are promising as sensory materials that function based on electrochemical or optical detection mechanisms. For instance, Fabre and coworkers reported the synthesis of boronic acid and boronate ester-functionalized polypyrrole (**74**) and its use as a conductimetric fluoride sensor.[244,245] Freund and coworkers prepared boronic acid-functionalized polyaniline (**75**, poly(aniline boronic acid) (PABA)) and showed that the polymer was highly efficient as a saccharide sensor.[246–248] Recently, they also demonstrated the formation of conducting PABA nanoparticles, with an average size of 12–15 nm, without the use of any surfactants.[249,250] These nanoparticles proved to be resistant to degradation at extreme electrochemical potentials and hence may find applications as coatings or may be used for fabrication of nanoscale devices. He and coworkers developed a novel PABA/DNA/SWNT composite for the detection of dopamine in the diagnosis of Parkinson's disease.[251,252] The detection of dopamine is based on conductivity changes upon formation of complex (**76**). Single-stranded DNA (ss-DNA) and single-walled carbon nanotubes (SWNTs) served as templates for *in situ* formation of self-doped PABA. He and coworkers also discovered that ss-DNA and SWNTs facilitate the polymerization of aniline boronic acid, leading to higher rates. The quality and the stability of the polymer greatly increased, and the electrical performance of the SWNTs improved due to the presence of a thin film of PABA on the ss-DNA and SWNT.[253,254]

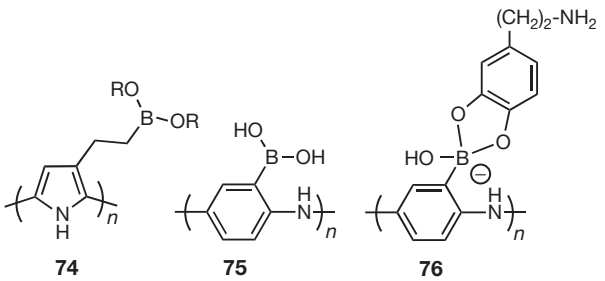

74 **75** **76**

1.27.4.3 Supramolecular Polymers via Reversible Covalent B–O Bond Formation

In the field of supramolecular materials, the reversibility of covalent B–O bond formation is attractive. Two distinct processes have been explored, that is, the reaction of boronic acids with diols and the condensation of three boronic acid moieties to form six-membered boroxine ring systems (see **Figure 18**).[232] These methods have been extensively utilized for the preparation of porous COFs.[255–259] Given that these 3D materials are typically insoluble or disassemble upon dissolution, they are not further discussed in this chapter. However, when the concept of reversible covalent B–O bond formation is applied to one-dimensional chains or star-shaped molecules, interesting supramolecular polymeric materials can be obtained that are highly soluble in organic solvents, while retaining their polymeric structure.[260–262] Lavigne and coworkers studied the self-assembly of the conjugated boronate ester polymer **77** by condensation of 9,9-dihexylfluorene-2,7-diboronic acid and 1,2,4,5-tetrahydroxybenzene.[261] Compound **77** was obtained in high yield by the azeotropic removal of water in THF with molecular weights of up to $M_w \sim 25\,000$ Da and a PDI of 2.4. The absorption and emission spectra showed clear evidence of extension of conjugation with increasing polymer chain length. Trogler's group reported the polymerization of 3′,6′-bis(pinacolatoboron)fluoran with pentaerythritol.[263] The molecular weight of **78** was determined by GPC to be $\sim 10\,000$ Da with a PDI of 1.5. Exposure of this non-luminescent polymer to hydrogen peroxide vapors (concentrations >3.8 ppm) resulted in polymer degradation with concomitant turn-on of fluorescence due to the release of fluorescein.

Lee and coworkers introduced conjugated polymeric materials based on borasiloxane cages.[264,265] In contrast to the previous examples, polymers **79** were prepared by electrochemical polymerization of pre-formed borasiloxane cage compounds that were functionalized with thiophene groups. These polymers were comparatively much more robust and showed no tendency of disassembly even in the presence of water. They were utilized for the colorimetric detection of amine vapors, based on the reversible coordination of amines to the Lewis acidic boron sites.

Condensation of boronic acids to boroxine rings results in star-like architectures. The Jäkle and Sumerlin groups independently synthesized and characterized polystyrenes with boronic acid terminal groups by controlled free-radical polymerization.[53,266] Jäkle's group used chemical dehydration to assemble the boroxine core, whereas Sumerlin opted for a Lewis base-facilitated trimerization[267] route. This concept was taken one step further by Iovine and coworkers who prepared polycaprolactone (PCL) tri-arm star polymers with functional pyridyl or porphyrine (**80**) moieties attached at the nonboronated terminus of the polymer chain.[268] Boroxine polymers have also found applications in the development of flame retardants, and ion-selective transport membranes.[267]

Copyright © 2013. Elsevier. All rights reserved.

Comprehensive Inorganic Chemistry II : From Elements to Applications, Elsevier, 2013. ProQuest Ebook Central, http://ebookcentral.proquest.com/lib/inflibnet-ebooks/detail.action?docID=1330977.
Created from inflibnet-ebooks on 2021-02-09 22:27:26.

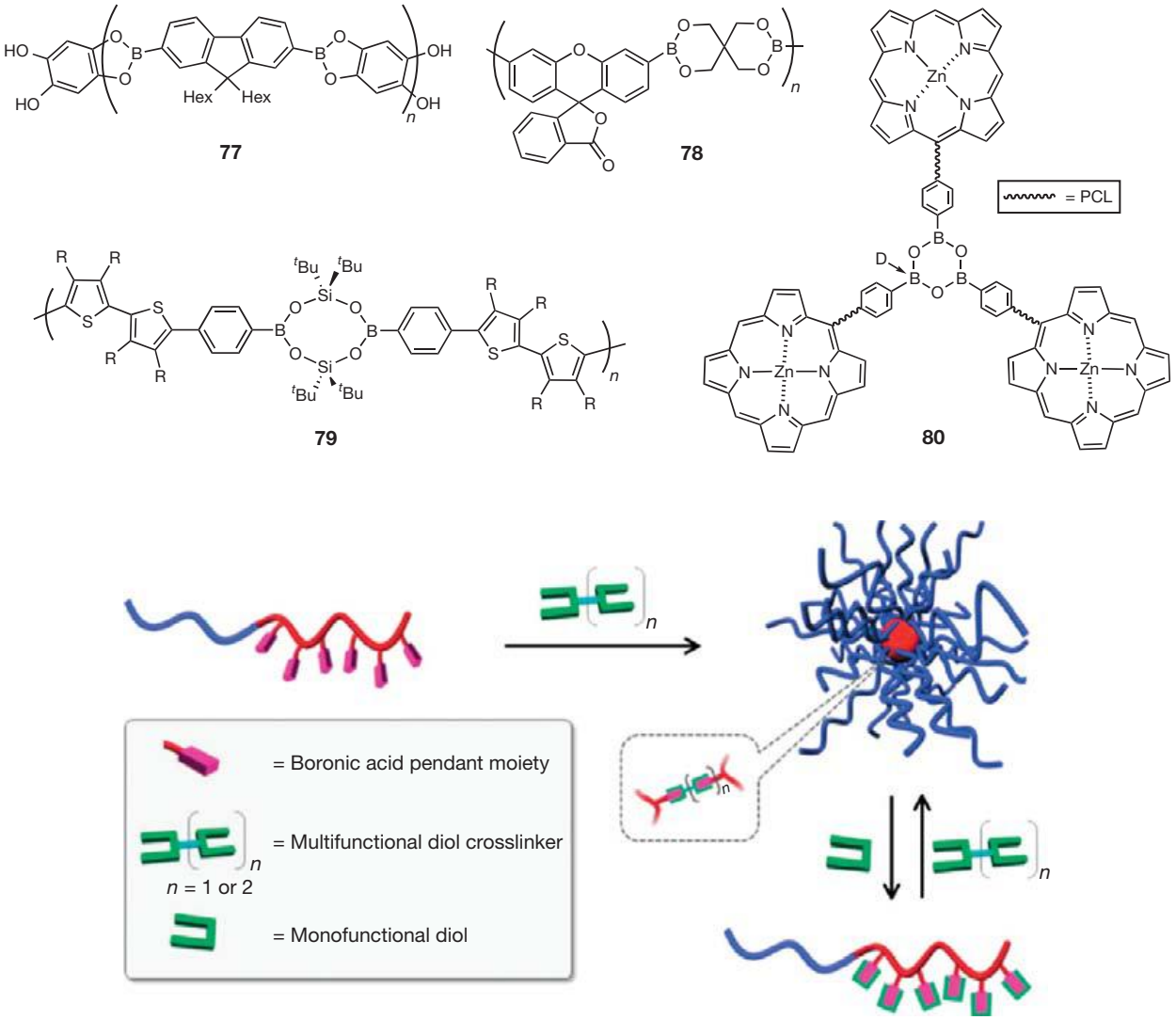

Figure 20 Reversible formation of star polymers from PDMA-*b*-PAPBA (**73a**) and multifunctional diol cross-linkers. Reproduced from Bapat, A. P.; Roy, D.; Ray, J. G.; Savin, D. A.; Sumerlin, B. S. *J. Am. Chem. Soc.* **2011**, *133*, 19832–19838, with permission. Copyright 2011 American Chemical Society.

In an interesting twist to this topic, Sumerlin and coworkers recently reported the reversible formation of microgel-type star polymers from PDMA-*b*-PAPBA (**73a**).[269] In the presence of multifunctional diols, such as diglycerol or sorbitol, the PAPBA block reacted with the diol moieties, which effectively led to the formation of core-cross-linked micelles as illustrated in Figure 20. The cross-linking process was reversed by addition of a monofunctional diol such as pinacol.

1.27.4.4 Borate and Organoboronate Polymer Electrolytes

Polymeric materials derived from borates, boronates, and boroxines serve important roles as solid electrolytes in lithium-ion batteries, electrochromic devices, and other devices that require large ionic conductivities.[270–274] Typically, the active components are prepared by treatment of the boron-containing polymer with a lithium salt such as lithium perchlorate, lithium triflate, or lithium triflimide (TFSI). Covalent bond formation, on the other hand, is achieved by reaction with organolithium species such as *n*-butyllithium, phenyllithium, pentafluorophenyllithium, or naphthyllithium.[275–277] This process results in anionic borate species that only weakly coordinate to the lithium counterions. The weakly coordinating nature of the borate anions precludes strong ion pairing, a prerequisite for high ionic conductivity. To achieve large lithium transference numbers, polyether-type polymers are typically employed.

A commonly used method for formation of the boron-containing polymers is to react hydroxy-terminated poly(ethylene glycol) or poly(vinyl alcohol) (PVA) with a borane source such as B_2O_3 or BH_3·THF, which results in star- or comb-shaped polymers (e.g., **81a** and **81b**) that contain Lewis acidic boric ester sites.[272,277–280] Linear organoboronate polymers (e.g., **81c**) were obtained by condensation of poly(ethylene glycol) with $MesBH_2$ or $[MesBH_3]Li$.[275,276,281] Boroxine-functionalized polymers

Copyright © 2013. Elsevier. All rights reserved.

Comprehensive Inorganic Chemistry II : From Elements to Applications, Elsevier, 2013. ProQuest Ebook Central, http://ebookcentral.proquest.com/lib/inflibnet-ebooks/detail.action?docID=1330977.
Created from inflibnet-ebooks on 2021-02-09 22:27:26.

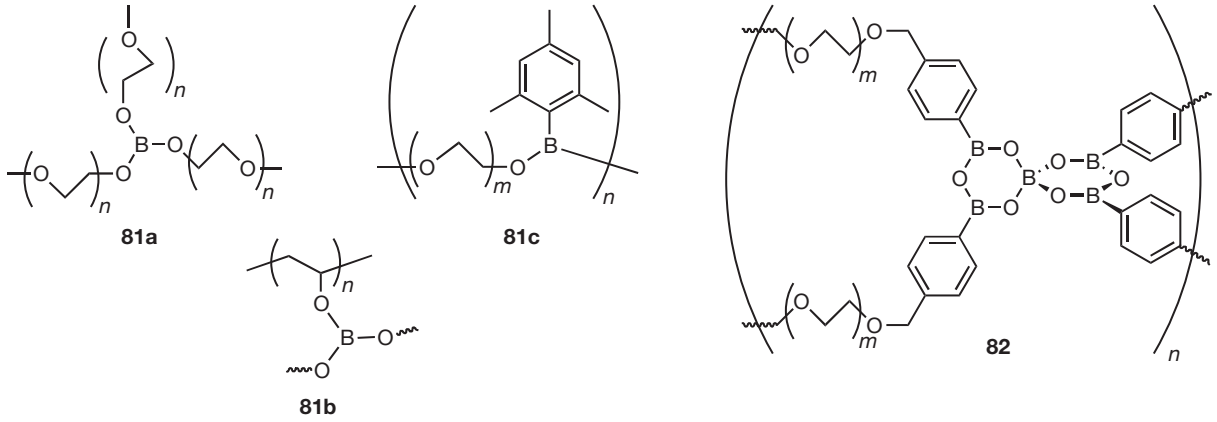

were also prepared,[282] and tetraarylpentaborate systems (**82**)[283] formed upon condensation of arylboronic acid-functionalized polymers in the presence of LiOMe.[267]

Watanabe and coworkers introduced polymer gel electrolytes, which were generated by copolymerization of boronate ester-functionalized acrylates with polyfunctional vinyl cross-linkers.[273,284] A comparatively simpler approach was more recently reported by Ohno and coworkers, who examined the condensation of cellulose and boric acid in ionic liquids to prepare gel materials with enhanced ionic conduction.[285]

1.27.5 Polymers Containing Boron Clusters

Borane, carborane, and metallaborane cages are useful synthetic building blocks in the fields of organometallic chemistry, materials science, and in medicinal chemistry.[286–288] Borane clusters have been extensively studied as precursors for advanced ceramics and ceramic-composite materials. The development of polymer-based ceramic precursors is desirable due to the favorable processability, as well as film- and fiber-forming properties. The formation of nanostructured and mesoporous materials is also possible.[289,290] Carborane-containing macromolecules have attracted much attention due to their interesting electronic structure, exceptionally large boron content, and high thermal stability.[288] They have potential applications as high-temperature and luminescent materials. In addition, due to the large neutron capture cross section of ^{10}B atoms and generally low toxicity, carborane- and metallaborane-functionalized dendrimers and polymers are promising for BNCT in the treatment of cancer (see **Chapter 3.30**) and as components of neutron shields.

1.27.5.1 Preceramic Polymers

Research by Sneddon and coworkers focused on Ziegler–Natta[291,292] and metathesis polymerization methods[293–295] of vinyl-functionalized borane cages to obtain high boron content polymers that can in turn be pyrolyzed to form boron carbide/carbon networks.[292] Decaborane-modified norbornene (**83**) and cyclooctene (**84**) were successfully polymerized by ROMP, yielding polymers with molecular weights of up to 32 000 Da.[289,294,295] Blends of poly(norbornenyldecaborane)

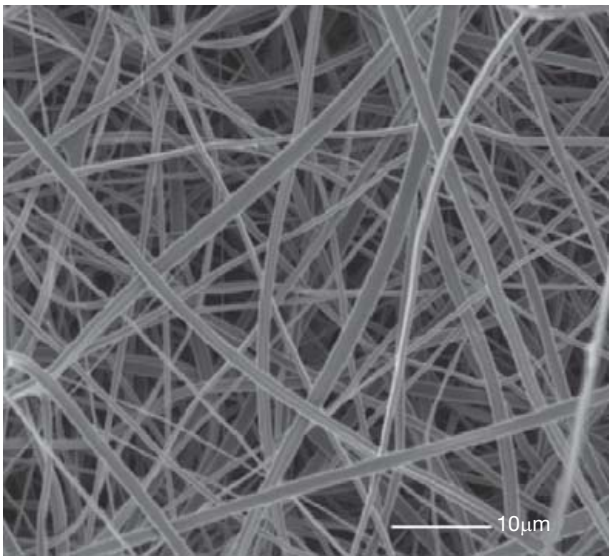

Figure 21 SEM image of boron–carbide/silicon–carbide ceramic fiber mats obtained from a 2.55:1 blend of **85**:poly(methylcarbosilane) by pyrolysis at 1300 °C. Reproduced from Guron, M. M.; Wei, X.; Welna, D.; Krogman, N.; Kim, M. J.; Allcock, H.; Sneddon, L. G. *Chem. Mater.* **2009**, *21*, 1708–1715, with permission. Copyright 2009 American Chemical Society.

(**85**) with commercially available silicon carbide preceramic polymers, such as poly(methylcarbosilane) or allylhydridopolycarbosilane, proved to be excellent processable precursors to boron–carbide/silicon–carbide ceramic composite materials and fibers (**Figure 21**).[296]

Malenfant, Wan, and coworkers used ROMP for the synthesis of polynorbornene-*block*-poly(norbornenyldecaborane) copolymers by sequential polymerization of norbornene and the functional monomer **83**.[297] GPC confirmed the formation of high-molecular-weight block copolymers in the range of 50–100 kDa with PDIs of <1.2. Variation of the solvents and conditions used for polymer deposition resulted in different self-assembled morphologies. The transformation into nano-ordered boron carbonitride ceramics was achieved by pyrolysis in ammonia.

Shore and coworkers reported the synthesis of homo- and copolymers from vinyl monomers **86** and **87**.[298] Standard

Copyright © 2013. Elsevier. All rights reserved.

Comprehensive Inorganic Chemistry II : From Elements to Applications, Elsevier, 2013. ProQuest Ebook Central, http://ebookcentral.proquest.com/lib/inflibnet-ebooks/detail.action?docID=1330977.
Created from inflibnet-ebooks on 2021-02-09 22:27:26.

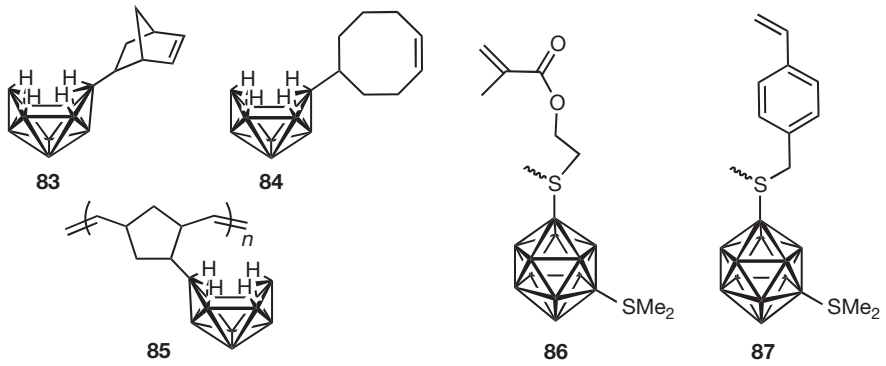

free-radical polymerizations were conducted in toluene, 2-methyltetrahydrofuran, or in bulk using azo-bis(isobutyronitrile) (AIBN) as the initiator. Moderate- to high-molecular-weight polymers were obtained. The glass transition temperatures increased with increasing B_{12} cage content. The thermal properties were studied by thermogravimetric analysis (TGA), but the ceramic products were not further investigated.

1.27.5.2 Thermally Robust Materials and Neutron Shielding Materials

Similar to all-boron cages, one of the potential applications of carborane-derived polymers is in the production of boron carbide ceramic fibers and matrices. However, the comparatively much higher stability renders carboranes interesting also as building blocks for numerous other applications. The high stability can be exploited, for example, for the formation of more thermally robust engineering plastics. A broad range of organic copolymers that contain carborane building blocks in the main chain have been reported.[1,299]

In recent work, Keller and coworkers explored poly(meta-carborane-disiloxane-diacetylene)s, which are attractive because the polymers maintain elastomeric properties while gaining thermal and oxidative stability from the carborane building block.[300,301] The diacetylene component is prone to cross-linking and hence further enhances the thermal stability. The prototype polymer (**88**) contains a 1:2:1 ratio of carborane to siloxane to diacetylene, but the properties can be optimized by variation of the relative amounts of these components.[302] A related siloxyl–diacetylene–ferrocenylene–carboranyl polymer gave a ferromagnetic ceramic material upon heating

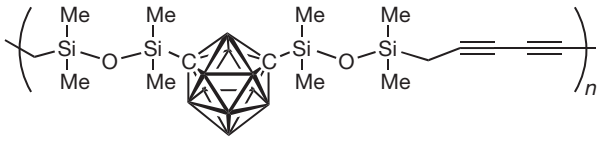

88

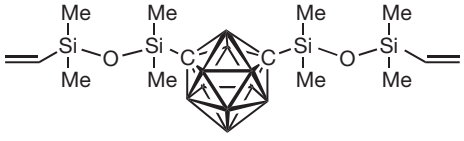

89

to 1000 °C.[303] Hydrosilation chemistries were utilized to form siloxane networks from the meta-carborane building block **89** and branched siloxane or polyhedral oligomeric silsesquioxanes (POSSs).[304,305] Alternative syntheses were explored by Zhang and coworkers.[306]

Several new approaches to polyolefin functionalization with carborane cages have been developed. Using Ziegler–Natta polymerization, Lee and coworkers prepared carborane-functionalized polyethylene,[307] whereas Hosmane and coworkers used click reactions to attach carborane moieties to polystyrene.[308] Sneddon and coworkers took advantage of ruthenium-catalyzed acyclic diene metathesis polymerization (ADMET) of dialkenyl-substituted ortho- and meta-carboranes to prepare main chain organo-carborane polymers.[293] The metathesis reaction of **90** gave cyclic product as well as polymers with molecular weights in the range from $M_n = 4700$ to 11 000 Da.

As already discussed for borane cage-functionalized polymers, ROMP is a powerful tool for controlled polymerization of functional monomers and the generation of polymers with more complex architectures such as block copolymers. Coughlin and coworkers reported the synthesis of an oxonorbornene-functionalized *o*-carborane monomer (**91**) and its ROMP to give low-polydispersity and high-molecular-weight carborane-based homo-, random-, and block copolymers.[309,310] A copolymer of **91** with cyclooctene was also prepared and hydrogenated to give a 'polyethylene-like' material with pendant carborane moieties. This polymer was envisioned to act as a neutron shielding material for space applications. The aliphatic hydrocarbon segments are thought to thermalize neutrons through inelastic collision, while the ^{10}B atoms have a high cross section for neutron capture.[310] The formation of amphiphilic block copolymers was achieved via sequential monomer addition.[309]

1.27.5.3 Nanosized Materials for BNCT Applications

Controlled radical polymerization presents an alternative to ROMP when architectural control is important. In an effort at developing nanosized structures with high ^{10}B content for BNCT, Adronov and coworkers subjected the carborane-containing monomers **92** and **93** to ATRP and NMP, respectively.[311,312] A dendron-functionalized styrene monomer led to dendronized polymers as illustrated in **Figure 22**.[312] Water-soluble materials with very high boron content and molecular weights in excess of 70 kDa were obtained.

Copyright © 2013. Elsevier. All rights reserved.

Comprehensive Inorganic Chemistry II : From Elements to Applications, Elsevier, 2013. ProQuest Ebook Central, http://ebookcentral.proquest.com/lib/inflibnet-ebooks/detail.action?docID=1330977.
Created from inflibnet-ebooks on 2021-02-09 22:27:26.

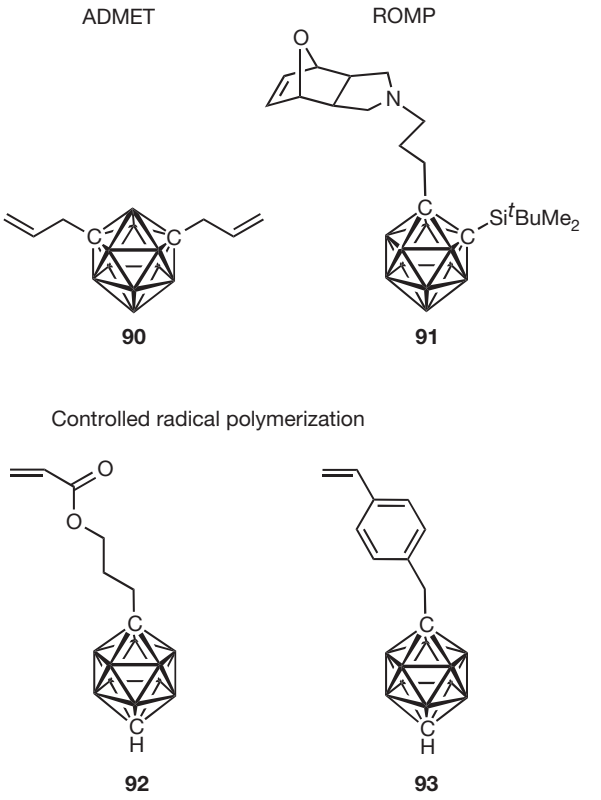

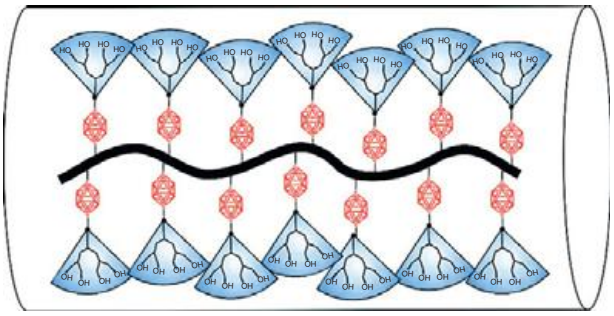

Figure 22 Schematic illustration of dendronized carborane polymers. Reproduced from Benhabbour, S. R.; Parrott, M. C.; Gratton, S. E. A.; Adronov, A. *Macromolecules* **2007**, *40*, 5678–5688, with permission. Copyright 2007 American Chemical Society.

Nagasaki and coworkers took a different approach for the synthesis of nanostructured polymers with high boron loading. They used 1,2-bis(4-vinylbenzyl)-*closo*-carborane as a bifunctional cross-linker for the core-cross-linking of poly(ethylene glycol)-*block*-poly(lactide) (PEG-*b*-PLA) micelles.[313] The PEG-*b*-PLA polymer contained an acetal group at the PEG end and a polymerizable methacryloyl (MA) group at the PLA end (acetal-PEG-*b*-PLA-MA). The cross-linking ensured minimal leakage of carborane from the micelles, suggesting superior properties as a nanocarrier for boron cages.

Dendrimers that are functionalized with carborane or metallaborane clusters in the periphery have also received tremendous recent interest. Carbosilanes,[314] aliphatic polyester,[315–317] and poly(alkylaryl ether)s[318–320] have all been utilized and functionalized with boron cage compounds.[288,321] A particularly interesting aspect is that decapitation of neutral *closo*-carboranes with base leads to ionic structures that in many cases are soluble in aqueous media, a requirement for *in vivo* biomedical applications.[314,318,322] Many of these dendritic molecules are luminescent both before and after decapitation. Related metallacarborane-functionalized dendrimers were also investigated.[319,320]

1.27.5.4 Conjugated and Luminescent Materials

Early studies by Grimes, Michl, Hawthorne, Wade, and others on conjugated oligomers and macrocycles that feature carborane cage compounds have set the stage for more recent exploration of larger conjugated structures.[323–326] Recent efforts by Hosmane and coworkers focused on the luminescent properties of dendritic structures with an oligophenylene core (e.g., **94**).[327–329] The premise of this research was that the presence of sterically demanding carboranes or metallaborane in the periphery of the dendrimers prevents π–π stacking interactions between the organic luminophores, resulting in enhanced emission intensities.

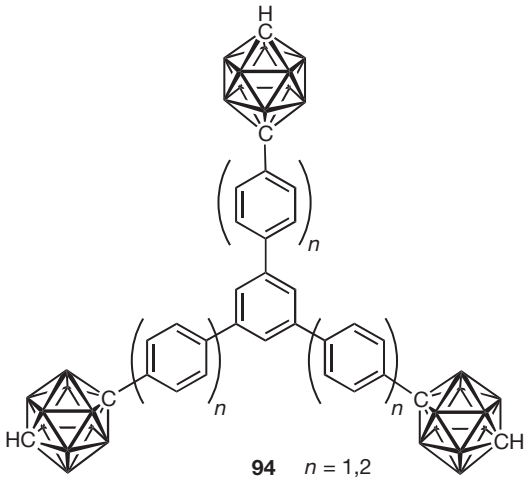

A versatile method for the attachment of carboranes and metallaboranes as pendant groups to conjugated polymers is the electropolymerization of pyrrole- and thiophene-substituted derivatives (e.g., **95** and **96**). Repeated potential cycling leads to deposition of conductive thin films as illustrated in Figure 23.[330–334] The polymer films obtained from **95a** displayed enhanced thermal and electrochemical stability in comparison to polypyrrole itself, which was attributed to the hydrophobicity and electron-withdrawing character of the carborane cages.[331] Among several polythiophene materials with different cluster structures, those derived from ortho-carboranes (**95b**) displayed higher conductivities than the respective meta- and para-carboranes.[334] Similarly, monomer **96** was used to prepare polythiophenes with in-chain cobaltabisdicarbollides.[335] Conducting probe AFM measurements indicated that the products behave like heavily doped semiconductors. Mean conductivities of up to 1.4×10^{-4} S cm^{-1} were measured.

Chemical polymerization methods have also been explored, and a recent example is the functionalization of

Copyright © 2013. Elsevier. All rights reserved.

Comprehensive Inorganic Chemistry II : From Elements to Applications, Elsevier, 2013. ProQuest Ebook Central, http://ebookcentral.proquest.com/lib/inflibnet-ebooks/detail.action?docID=1330977.
Created from inflibnet-ebooks on 2021-02-09 22:27:26.

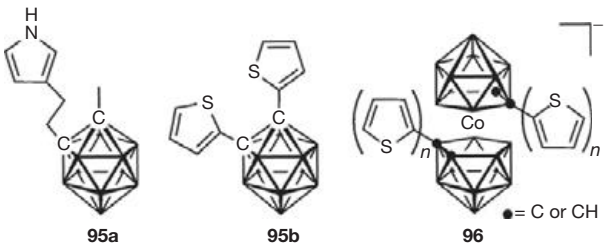

95a 95b 96

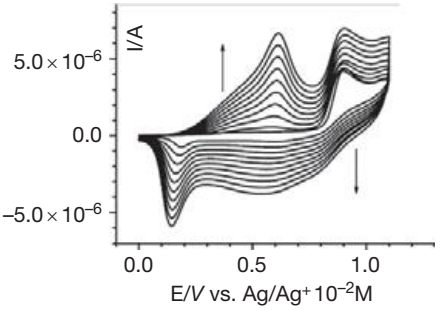

Figure 23 Successive cyclic voltammograms for the electropolymerization of **95b** (2×10^{-1} M $Bu_4N[PF_6]$, 0.1 Vs^{-1}). Reproduced from Barriere, F.; Fabre, B.; Hao, E. H.; LeJeune, Z. M.; Hwang, E.; Garno, J. C.; Nesterov, E. E.; Vicente, M. G. H. *Macromolecules* **2009**, *42*, 2981–2987, with permission. Copyright 2009 American Chemical Society.

polyfluorenes with carborane moieties by Coughlin and Carter and coworkers.[336] They used microwave-accelerated, Ni-catalyzed Yamamoto coupling of a carboranyl-functionalized 2,7-dibromofluorene to prepare the strongly luminescent polymer **97**. The molecular weight of the homopolymer of $M_n = 7300$ Da was much lower than what is typically achieved in polyfluorene synthesis, possibly due to the steric constraints of the bulky carborane moieties. To attain higher-molecular-weight materials that are more easily processable, copolymers with 9,9-dihexylfluorene were prepared. Differential scanning calorimetery (DSC) studies indicated an increase in the glass transition temperature with carborane content. Potential applications in neutron detection devices were suggested.

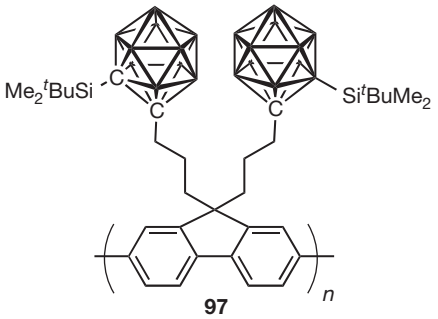

97

98

The incorporation of carboranes into the main chain of conjugated materials has been motivated mainly by an anticipation that the 3D aromaticity of *closo*-carboranes would result in unusual electronic properties. Carter and Coughlin and coworkers prepared fluorenyl-substituted para-carborane derivatives and subjected them to Yamamoto coupling.[337] Polymerization resulted in a high-molecular-weight copolymer (**98**, $M_n = 50\,000$ Da) comprised of bis(fluorene) and para-carborane moieties. The polymer was strongly blue luminescent with an emission maximum at 400 nm that is red-shifted compared to a bifluorene model system, signifying the electronic effect of the carborane moieties.

Aggregation-induced emission (AIE), a phenomenon in which polymers that are nonluminescent in solution become highly emissive due to aggregation upon film formation, was observed when ortho-carborane building blocks were used. For instance, an ortho-carborane–fluorene copolymer with otherwise similar structure to that of **98** displayed dual emission with maxima at 415 and at 565 nm, giving the solution an orange appearance under UV irradiation.[338] The band at 415 nm was assigned to emission from the conjugated organic linker and the band at 565 nm to energy transfer from the bis(fluorene) segments to the carborane cages. By contrast, single green emission at 525 nm was observed in the thin film state, which was attributed to an AIE phenomenon. The different emission pathways are illustrated in **Figure 24**. Another interesting observation was that exposure of the ortho-carborane polymer to different solvent vapors led to variations in the emission color. This behavior was exploited for the fluorescent detection of amines.[339]

Chujo and coworkers used Sonogashira–Hagihara coupling to prepare alternating copolymers consisting of ortho- or meta-carborane in combination with ethynylene–arylene–ethynylene segments (e.g., **99**, Ar = phenylene, carbazolyl).[340–342] High-molecular-weight polymers were obtained with meta-carborane,

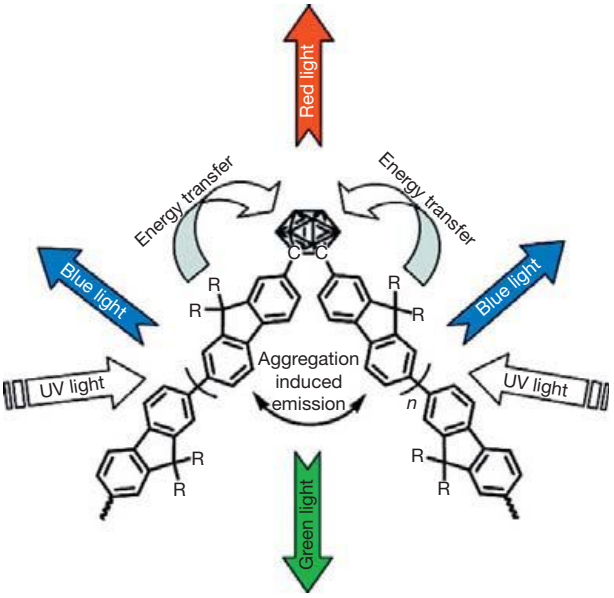

Figure 24 Proposed emission pathways in conjugated polymers with ortho-carborane building blocks. Reproduced from Peterson, J. J.; Davis, A. R.; Werre, M.; Coughlin, E. B.; Carter, K. R. *ACS Appl. Mater. Interf.* **2011**, *3*, 1796–1799, with permission. Copyright 2011 American Chemical Society.

Copyright © 2013. Elsevier. All rights reserved.

Comprehensive Inorganic Chemistry II : From Elements to Applications, Elsevier, 2013. ProQuest Ebook Central, http://ebookcentral.proquest.com/lib/inflibnet-ebooks/detail.action?docID=1330977.
Created from inflibnet-ebooks on 2021-02-09 22:27:26.

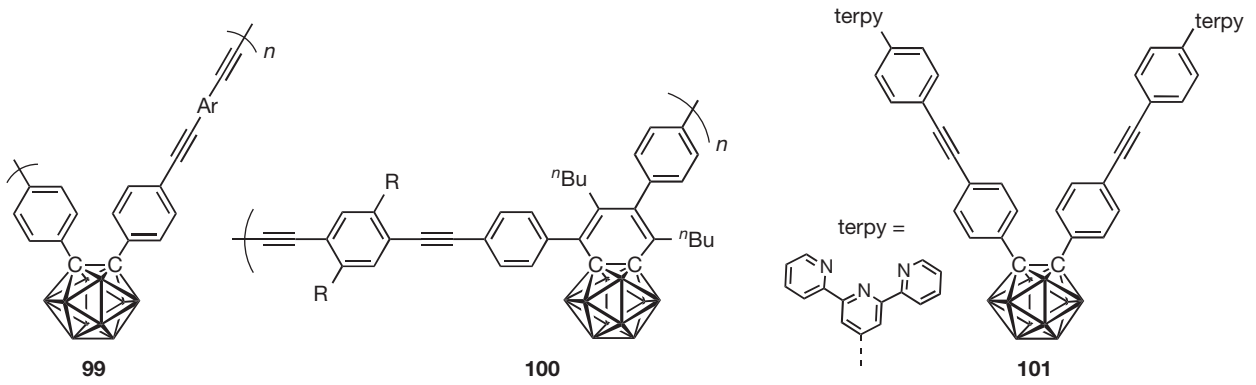

and they exhibited strong blue fluorescence in solution ($\Phi_F = 0.11–0.26$). With ortho-carborane, the molecular weights were comparatively lower, possibly due to steric effects. More importantly, the blue emission of the conjugated organic chromophore in **99** was almost completely quenched. The fluorescence quenching in the solution state was attributed to energy transfer from the electron-rich ethynylene–arylene–ethynylene to lower energy states localized on the ortho-carborane moieties upon photoexcitation. Support for this conclusion comes from the observation that electron-deficient phenylene linkers with fluorinated alkyl groups as substituents exhibit unquenched blue luminescence. When the polymers with electron-donating Ar linkers were dispersed in a mixture of THF and water (1:99), nanoparticles formed that displayed strong orange emission. A similar emission was also observed for thin films and attributed to AIE effects.

In contrast to the ortho-carborane polymers discussed above, the benzocarborane polymers **100** (R = alkoxy, fluoroalkyl), in which a carborane moiety is fused to an organic conjugated π-system, display strong emission in solution (Φ_F ca. 40–50%).[343] A distinct change in the emission with solvent polarity (solvatochromic effect) suggested a pronounced charge transfer character. Presumably, the carborane moiety acts as an acceptor and the arylene–ethynylene bridges as the donor, resulting in an alternating $(D–A)_n$ structure. These results suggest that the benzocarborane moiety could prove to be useful as a new type of acceptor building block for π-conjugated materials.

The ortho-carborane–phenylene–ethynylene motif was further explored in the development of new switchable and stimuli-responsive materials. Hydrogels were prepared by functionalization of ortho-carboranes with epoxy-terminated phenylene–ethylene–phenylene moieties and subsequent cross-linking of poly(γ-glutamic acid). The hydrogels showed reversible fluorescence switching between swollen and dried states.[344] A terpyridine derivative (**101**) was used in the supramolecular assembly of polymers via metal complexation.[345]

1.27.6 Conclusion

The discussion of boron-functionalized polymers provided in here clearly demonstrates the tremendous advances in this field over the past decade. We have witnessed not only major achievements in the controlled synthesis of boron-containing polymeric materials, but also the discovery of new functional motifs and the development of a thorough understanding of structure-property relations. Most importantly, a host of new applications in areas beyond the more traditional uses of boron polymers have surfaced, for example, as sensory materials for sugars and the fluorescent detection of anions, stimuli-responsive materials, components of lithium ion batteries, precursors to nanostructured ceramics, conjugated materials for organic electronics, luminescent biosensors, and in boron-neutron capture therapy. Since the tools for realizing even the most sophisticated boron polymer architectures and nanostructured materials have been established, we expect further acceleration of discoveries and even more widespread use of boron-containing polymers in materials science, catalysis, and the biomedical field in the coming years.

Acknowledgments

Financial support of our research program by the National Science Foundation (CHE-0956655 and CHE-1112195) is gratefully acknowledged. F. J. thanks all his current and former students and collaborators for their invaluable contributions.

References

1. Abd-El-Aziz, A. S., Carraher, C. E., Pittman, C. U., Zeldin, M., Eds.; In *Boron-Containing Polymers*; John Wiley & Sons Inc.: Hoboken, NJ, 2007.
2. Gabel, D. In In: Kaufmann, D., Matteson, D. S., Eds.; *Science of Synthesis: Houben-Weyl Methods of Molecular Transformations*; Georg Thieme Verlag: Stuttgart/New York, 2005; Vol. 6, pp 1277–1287.
3. Jäkle, F. *Chem. Rev.* **2010**, *110*, 3985–4022.
4. Chung, T. C.; Janvikul, W. J. *J. Organomet. Chem.* **1999**, *581*, 176–187.
5. Chung, T. C. *Functionalization of Polyolefins*. Academic Press: London, San Diego, 2002.
6. Jäkle, F. J. *Inorg. Organomet. Polym. Mater.* **2005**, *15*, 293–307.
7. Boffa, L. S.; Novak, B. M. *Chem. Rev.* **2000**, *100*, 1479–1493.
8. Chung, T. C.; Xu, G.; Lu, Y.; Hu, Y. *Macromolecules* **2001**, *34*, 8040–8050.
9. Chung, T. C. *Progr. Polym. Sci.* **2002**, *27*, 39–85.
10. Zhang, Z. C.; Chung, T. C. M. *Macromolecules* **2006**, *39*, 5187–5189.
11. Zhang, Z. C.; Wang, Z. M.; Chung, T. C. M. *Macromolecules* **2007**, *40*, 5235–5240.
12. Fan, G. Q.; Dong, J. Y.; Wang, Z. G.; Chung, T. C. *J. Polym. Sci. A Polym. Chem.* **2006**, *44*, 539–548.
13. Wang, Z. M.; Hong, H.; Chung, T. C. *Macromolecules* **2005**, *38*, 8966–8970.
14. Dong, J. Y.; Manias, E.; Chung, T. C. *Macromolecules* **2002**, *35*, 3439–3447.
15. Lin, W. T.; Dong, J. Y.; Chung, T. C. M. *Macromolecules* **2008**, *41*, 8452–8457.

Copyright © 2013. Elsevier. All rights reserved.

Comprehensive Inorganic Chemistry II : From Elements to Applications, Elsevier, 2013. ProQuest Ebook Central, http://ebookcentral.proquest.com/lib/inflibnet-ebooks/detail.action?docID=1330977.
Created from inflibnet-ebooks on 2021-02-09 22:27:26.

16. Lin, W.; Niu, H.; Chung, T. C. M.; Dong, J.-Y. *J. Polym. Sci. A Polym. Chem.* **2010**, *48*, 3534–3541.
17. Ramakrishnan, S. *Macromolecules* **1991**, *24*, 3753–3759.
18. Chung, T. C.; Lu, H. L.; Li, C. L. *Macromolecules* **1994**, *27*, 7533–7537.
19. Jo, T. S.; Kim, S. H.; Shin, J.; Bae, C. *J. Am. Chem. Soc.* **2009**, *131*, 1656–1657.
20. Shin, J.; Chang, A. Y.; Brownell, L. V.; Racoma, I. O.; Ozawa, C. H.; Chung, H.-Y.; Peng, S.; Bae, C. *J. Polym. Sci. A Polym. Chem.* **2008**, *46*, 3533–3545.
21. Shin, J.; Jensen, S. M.; Ju, J.; Lee, S.; Xue, Z.; Noh, S. K.; Bae, C. *Macromolecules* **2007**, *40*, 8600–8608.
22. Bae, C.; Hartwig, J. F.; Chung, H.; Harris, N. K.; Switek, K. A.; Hillmyer, M. A. *Angew. Chem. Int. Ed.* **2005**, *44*, 6410–6413.
23. Bae, C.; Hartwig, J. F.; Boaen Harris, N. K.; Long, R. O.; Anderson, K. S.; Hillmyer, M. A. *J. Am. Chem. Soc.* **2005**, *127*, 767–776.
24. Brownell, L. V.; Shin, J.; Bae, C. *J. Polym. Sci. A Polym. Chem.* **2009**, *47*, 6655–6667.
25. Chang, Y.; Brunello, G. F.; Fuller, J.; Hawley, M.; Kim, Y. S.; Disabb-Miller, M.; Hickner, M. A.; Jang, S. S.; Bae, C. S. *Macromolecules* **2011**, *44*, 8458–8469.
26. Shea, K. J. *Eur. J. Chem.* **2000**, *6*, 1113–1119.
27. Luo, J.; Shea, K. J. *Acc. Chem. Res.* **2010**, *43*, 1420–1433.
28. Ramakrishnan, S.; Chung, T. C. *Macromolecules* **1989**, *22*, 3181–3183.
29. Ramakrishnan, S.; Chung, T. C. *Macromolecules* **1990**, *23*, 4519–4524.
30. Chung, T. C.; Ramakrishnan, S.; Kim, M. W. *Macromolecules* **1991**, *24*, 2675–2681.
31. Chung, T. C.; Lu, H. L. J. *J. Mol. Catal. A Chem.* **1997**, *115*, 115–127.
32. Yamamoto, E. H. *Lewis Acids in Organic Synthesis*. Wiley-VCH: New York, 2000.
33. Chen, E. Y.-X.; Marks, T. J. *Chem. Rev.* **2000**, *100*, 1391–1434.
34. Piers, W. E.; Irvine, G. J.; Williams, V. C. *Eur. J. Inorg. Chem.* **2000**, 2131–2142.
35. Hudnall, T. W.; Chiu, C.-W.; Gabbai, F. P. *Acc. Chem. Res.* **2009**, *49*, 388–397.
36. Wade, C. R.; Broomsgrove, A. E. J.; Aldridge, S.; Gabbai, F. P. *Chem. Rev.* **2010**, *110*, 3958–3984.
37. Jäkle, F. *Coord. Chem. Rev.* **2006**, *250*, 1107–1121.
38. Yamaguchi, S.; Akiyama, S.; Tamao, K. *J. Organomet. Chem.* **2002**, *652*, 3–9.
39. Yamaguchi, S.; Wakamiya, A. *Pure Appl. Chem.* **2006**, *78*, 1413–1424.
40. Hudson, Z. M.; Wang, S. *Acc. Chem. Res.* **2009**, *42*, 1584–1596.
41. Nagai, A.; Chujo, Y. *Chem. Lett.* **2010**, *39*, 430–435.
42. Matsumi, N.; Chujo, Y. *Polym. J.* **2008**, *40*, 77–89.
43. Qin, Y.; Cheng, G.; Achara, O.; Parab, K.; Jäkle, F. *Macromolecules* **2004**, *37*, 7123–7131.
44. Qin, Y.; Cheng, G.; Sundararaman, A.; Jäkle, F. *J. Am. Chem. Soc.* **2002**, *124*, 12672–12673.
45. Qin, Y.; Pagba, C.; Piotrowiak, P.; Jäkle, F. *J. Am. Chem. Soc.* **2004**, *126*, 7015–7018.
46. Qin, Y.; Sukul, V.; Pagakos, D.; Cui, C.; Jäkle, F. *Macromolecules* **2005**, *38*, 8987–8990.
47. Qin, Y.; Kiburu, I.; Shah, S.; Jäkle, F. *Macromolecules* **2006**, *39*, 9041–9048.
48. Qin, Y.; Cui, C.; Jäkle, F. *Macromolecules* **2008**, *41*, 2972–2974.
49. Doshi, A.; Jäkle, F. *Main Group Chem.* **2006**, *5*, 309–318.
50. Parab, K.; Venkatasubbaiah, K.; Jäkle, F. *J. Am. Chem. Soc.* **2006**, *128*, 12879–12885.
51. Parab, K.; Jäkle, F. *Macromolecules* **2009**, *42*, 4002–4007.
52. Parab, K.; Doshi, A.; Cheng, F.; Jäkle, F. *Macromolecules* **2011**, *44*, 5961–5967.
53. Qin, Y.; Cui, C.; Jäkle, F. *Macromolecules* **2007**, *40*, 1413–1420.
54. Li, H.; Sundararaman, A.; Pakkirisamy, T.; Venkatasubbaiah, K.; Schödel, F.; Jäkle, F. *Macromolecules* **2011**, *44*, 95–103.
55. Li, H.; Jäkle, F. *Polym. Chem.* **2011**, *2*, 897–905.
56. Li, H.; Sundararaman, A.; Venkatasubbaiah, K.; Jäkle, F. *J. Am. Chem. Soc.* **2007**, *129*, 5792–5793.
57. Zhao, C.; Wakamiya, A.; Yamaguchi, S. *Macromolecules* **2007**, *40*, 3898–3900.
58. Reitzenstein, D.; Lambert, C. *Macromolecules* **2009**, *42*, 773–782.
59. Chujo, Y.; Takizawa, N.; Sakurai, T. *J. Chem. Soc. Chem. Commun.* **1994**, 227–228.
60. Qin, Y.; Cheng, G.; Parab, K.; Achara, O.; Jäkle, F. *Macromolecules* **2004**, *37*, 7123–7131.
61. Scheibitz, M.; Li, H.; Schnorr, J.; Sanchez Perucha, A.; Bolte, M.; Lerner, H.-W.; Jäkle, F.; Wagner, M. *J. Am. Chem. Soc.* **2009**, *131*, 16319–16329.
62. Heilmann, J. B.; Qin, Y.; Jäkle, F.; Lerner, H.-W.; Wagner, M. *Inorg. Chim. Acta* **2006**, *359*, 4802–4806.
63. Matsumi, N.; Naka, K.; Chujo, Y. *J. Am. Chem. Soc.* **1998**, *120*, 5112–5113.
64. Matsumi, N.; Chujo, Y. *Polym. Bull.* **1999**, *43*, 151–155.
65. Matsumi, N.; Miyata, M.; Chujo, Y. *Macromolecules* **1999**, *32*, 4467–4469.
66. Chujo, Y.; Sasaki, Y.; Kinomura, N.; Matsumi, N. *Polymer* **2000**, *41*, 5047–5051.
67. Miyata, M.; Meyer, F.; Chujo, Y. *Polym. Bull.* **2001**, *46*, 23–28.
68. Chujo, Y. *Macromol. Symp.* **1997**, *118*, 111–116.
69. Miyata, M.; Matsumi, N.; Chujo, Y. *Polym. Bull.* **1999**, *42*, 505–510.
70. Nagai, A.; Murakami, T.; Nagata, Y.; Kokado, K.; Chujo, Y. *Macromolecules* **2009**, *42*, 7217–7220.
71. Lorbach, A.; Bolte, M.; Li, H.; Lerner, H.-W.; Holthausen, M. C.; Jäkle, F.; Wagner, M. *Angew. Chem. Int. Ed.* **2009**, *48*, 4584–4588.
72. Chai, J.; Wang, C.; Jia, L.; Pang, Y.; Graham, M.; Cheng, S. Z. D. *Synth. Met.* **2009**, *159*, 1443–1449.
73. Kobayashi, H.; Sato, N.; Ichikawa, Y.; Miyata, M.; Chujo, Y.; Matsuyama, T. *Synth. Met.* **2003**, *135–136*, 393–394.
74. Sato, N.; Ogawa, H.; Matsumoto, F.; Chujo, Y.; Matsuyama, T. *Synth. Met.* **2005**, *154*, 113–116.
75. Cataldo, S.; Fabiano, S.; Ferrante, F.; Previti, F.; Patane, S.; Pignataro, B. *Macromol. Rap. Commun.* **2010**, *31*, 1281–1286.
76. Miyata, M.; Chujo, Y. *Polym. J.* **2002**, *34*, 967–969.
77. Matsumi, N.; Umeyama, T.; Chujo, Y. *Polym. Bull.* **2000**, *44*, 431–436.
78. Matsumi, N.; Naka, K.; Chujo, Y. *J. Am. Chem. Soc.* **1998**, *120*, 10776–10777.
79. Sundararaman, A.; Victor, M.; Varughese, R.; Jäkle, F. *J. Am. Chem. Soc.* **2005**, *127*, 13748–13749.
80. Li, H.; Jäkle, F. *Angew. Chem. Int. Ed.* **2009**, *48*, 2313–2316.
81. Li, H.; Jäkle, F. *Macromol. Rap. Commun.* **2010**, *31*, 915–920.
82. Jäkle, F.; Sundararaman, A.; Venkatasubbaiah, K. *Polym. Mater. Sci. Eng.* **2006**, *94*, 755–756.
83. Bonifácio, V. D. B.; Morgado, J.; Scherf, U. *J. Polym. Sci. A Polym. Chem.* **2008**, *46*, 2878–2883.
84. Braunschweig, H.; Dirk, R.; Müller, M.; Nguyen, P.; Resendes, R.; Gates, D. P.; Manners, I. *Angew. Chem. Int. Ed.* **1997**, *36*, 2338–2340.
85. Berenbaum, A.; Braunschweig, H.; Dirk, R.; Englert, U.; Green, J. C.; Jäkle, F.; Lough, A. J.; Manners, I. *J. Am. Chem. Soc.* **2000**, *122*, 5765–5774.
86. Jäkle, F.; Berenbaum, A.; Lough, A. J.; Manners, I. *Chem. – Eur. J.* **2000**, *6*, 2762–2771.
87. Heilmann, J. B.; Scheibitz, M.; Qin, Y.; Sundararaman, A.; Jäkle, F.; Kretz, T.; Bolte, M.; Lerner, H.-W.; Holthausen, M. C.; Wagner, M. *Angew. Chem. Int. Ed.* **2006**, *45*, 920–925.
88. Pammer, F.; Lalancette, R. A.; Jäkle, F. *Chem. – Eur. J.* **2011**, *17*, 11280–11289.
89. Entwistle, C. D.; Marder, T. B. *Chem. Mater.* **2004**, *16*, 4574–4585.
90. Mutaguchi, D.; Okumoto, K.; Ohsedo, Y.; Moriwaki, K.; Shirota, Y. *Org. Electron.* **2003**, *4*, 49–59.
91. Park, M. H.; Kim, T.; Huh, J. O.; Do, Y.; Lee, M. H. *Polymer* **2011**, *52*, 1510–1514.
92. Yuan, Z.; Collings, J. C.; Taylor, N. J.; Marder, T. B.; Jardin, C.; Halet, J.-F. *J. Solid State Chem.* **2000**, *154*, 5–12.
93. Branger, C.; Lequan, M.; Lequan, R. M.; Large, M.; Kajzar, F.; Barzoukas, M.; Fort, A. *MCLC S&T B Nonlin. Opt.* **1997**, *17*, 281–303.
94. Branger, C.; Lequan, M.; Lequan, R. M.; Large, M.; Kajzar, F. *Chem. Phys. Lett.* **1997**, *272*, 265–270.
95. Thomas III, S. W.; Joly, G. D.; Swager, T. M. *Chem. Rev.* **2007**, *107*, 1339–1386.
96. Elbing, M.; Bazan, G. C. *Angew. Chem. Int. Ed.* **2008**, *47*, 834–838.
97. Zhao, C. H.; Sakuda, E.; Wakamiya, A.; Yamaguchi, S. *Chem. – Eur. J.* **2009**, *15*, 10603–10612.
98. Li, H.; Lalancette, R. A.; Jäkle, F. *Chem. Commun.* **2011**, *47*, 9378–9380.
99. Hoven, C. V.; Wang, H. P.; Elbing, M.; Garner, L.; Winkelhaus, D.; Bazan, G. C. *Nat. Mater.* **2010**, *9*, 249–252.
100. Chaudhuri, D.; Kumar, A.; Nirmala, R.; Sarma, D. D.; Garcia-Hernandez, M.; Chandra, L. S. S.; Ganesan, V. *Phys. Rev. B* **2006**, *73*, 075205.
101. Chaudhuri, D.; Sarma, D. D. *Chem. Commun.* **2006**, 2681–2683.
102. Qian, G.; Wang, Z. Y. *Can. J. Chem.* **2010**, *88*, 192–201.
103. Welch, G. C.; Coffin, R.; Peet, J.; Bazan, G. C. *J. Am. Chem. Soc.* **2009**, *131*, 10802–10803.
104. Welch, G. C.; Bazan, G. C. *J. Am. Chem. Soc.* **2011**, *133*, 4632–4644.
105. Matsumi, N.; Kawaguchi, K.; Hirota, Y.; Aoi, K. *J. Organomet. Chem.* **2009**, *694*, 1776–1779.
106. Revell, J. D.; Dörner, B.; White, P. D.; Ganesan, A. *Org. Lett.* **2005**, *7*, 831–833.
107. Smith, K.; El-Hiti, G. A.; Hou, D. J.; DeBoos, G. A. *J. Chem. Soc. Perkin 1* **1999**, 2807–2812.
108. Roesler, R.; Har, B. J. N.; Piers, W. E. *Organometallics* **2002**, *21*, 4300–4302.
109. Schlögl, M.; Riethmueller, S.; Troll, C.; Möller, M.; Rieger, B. *Macromolecules* **2004**, *37*, 4004–4007.
110. Schubert, U. S.; Eschbaumer, C. *Angew. Chem. Int. Ed.* **2002**, *41*, 2892–2926.
111. Folmer, B. J. B.; Sijbesma, R. P.; Versteegen, R. M.; van der Rijt, J. A. J.; Meijer, E. W. *Adv. Mater.* **2000**, *12*, 874–878.
112. Brunsveld, L.; Folmer, B. J. B.; Meijer, E. W. *MRS Bull.* **2000**, *25*, 49–53.

Copyright © 2013. Elsevier. All rights reserved.

Comprehensive Inorganic Chemistry II : From Elements to Applications, Elsevier, 2013. ProQuest Ebook Central, http://ebookcentral.proquest.com/lib/inflibnet-ebooks/detail.action?docID=1330977.
Created from inflibnet-ebooks on 2021-02-09 22:27:26.

113. Knapp, R.; Schott, A.; Rehahn, M. *Macromolecules* **1996**, *29*, 478–480.
114. Hou, S.; Man, K. Y. K.; Chan, W. K. *Langmuir* **2003**, *19*, 2485–2490.
115. Hofmeier, H.; Schubert, U. S. *Chem. Soc. Rev.* **2004**, *33*, 373–399.
116. Yount, W. C.; Loveless, D. M.; Craig, S. L. *Angew. Chem. Int. Ed.* **2005**, *44*, 2746–2748.
117. Burnworth, M.; Knapton, D.; Rowan, S. J.; Weder, C. *J. Inorg. Organomet. Polym. Mater.* **2007**, *17*, 91–103.
118. Fiore, G. L.; Edwards, J. M.; Payne, S. J.; Klinkenberg, J. L.; Gioeli, D. G.; Demas, J. N.; Fraser, C. L. *Biomacromolecules* **2007**, *8*, 2829–2835.
119. Metera, K. L.; Sleiman, H. *Macromolecules* **2007**, *40*, 3733–3738.
120. Shunmugam, R.; Tew, G. N. *Macromol. Rapid Commun.* **2008**, *29*, 1355–1362.
121. Fontani, M.; Peters, F.; Scherer, W.; Wachter, W.; Wagner, M.; Zanello, P. *Eur. J. Inorg. Chem.* **1998**, 1453–1465.
122. Grosche, M.; Herdtweck, E.; Peters, F.; Wagner, M. *Organometallics* **1999**, *18*, 4669–4672.
123. Dinnebier, R. E.; Wagner, M.; Peters, F.; Shankland, K.; David, W. I. F. *Z. Anorg. Allg. Chem.* **2000**, *626*, 1400–1405.
124. Guo, S. L.; Peters, F.; Fabrizi de Biani, F.; Bats, J. W.; Herdtweck, E.; Zanello, P.; Wagner, M. *Inorg. Chem.* **2001**, *40*, 4928–4936.
125. Ding, L.; Ma, K.; Dürner, G.; Bolte, M.; de Biani, F. F.; Zanello, P.; Wagner, M. *J. Chem. Soc. Dalton Trans.* **2002**, 1566–1573.
126. Ma, K.; Scheibitz, M.; Scholz, S.; Wagner, M. *J. Organomet. Chem.* **2002**, *652*, 11–19.
127. Christinat, N.; Croisier, E.; Scopelliti, R.; Cascella, M.; Röthlisberger, U.; Severin, K. *Eur. J. Inorg. Chem.* **2007**, 5177–5181.
128. Matsumi, N.; Kagata, A.; Aoi, K. *J. Power Sources* **2010**, *195*, 6182–6186.
129. Qin, Y.; Jäkle, F. *J. Inorg. Organomet. Polym. Mater.* **2007**, *17*, 149–157.
130. Krossing, I.; Raabe, I. *Angew. Chem. Int. Ed.* **2004**, *43*, 2066–2090.
131. Roscoe, S. B.; Gong, C.; Fréchet, J. M. J.; Walzer, J. F. *J. Polym. Sci. A Polym. Chem.* **2000**, *38*, 2979–2992.
132. Walzer, J. F.; Dias, A. J.; Fréchet, J. M. J.; Roscoe, S. B. In *WO9855518*; Exxon Chemical Patents Inc., 1998.
133. Roscoe, S. B.; Fréchet, J. M. J.; Walzer, J. F.; Dias, A. J. *Science* **1998**, *280*, 270–273.
134. Schwab, E.; Mecking, S. *Organometallics* **2001**, *20*, 5504–5506.
135. Ono, M.; Hinokuma, S.; Miyake, S.; Inazawa, S. *Eur. Pat. Appl.* **1996** (Japanese Polyolefin Co., Ltd., Japan). Application: EP 0710663.
136. Kanamaru, M.; Fujikawa, S.; Okamoto, T. *Jpn. Kokai Tokkyo Koho* **1999** (Idemitsu Petrochemical Co., Ltd.). Application: JP 11286491.
137. Kanamaru, M.; Okamoto, T.; Okuda, F.; Kamisawa, M. *Jpn. Kokai Tokkyo Koho* **2000** (Idemitsu Petrochemical Co., Ltd.). Application: JP 2000212225.
138. Sivak, A. J.; Zambelli, A.; U.S. Patent (Sunoco, Inc. (R&M), USA), 2002. Application: US 2000502622.
139. Sablong, R.; van der Vlugt, J. I.; Thomann, R.; Mecking, S.; Vogt, D. *Adv. Synth. Catal.* **2005**, *347*, 633–636.
140. Kishi, N.; Ahn, C.-H.; Jin, J.; Uozumi, T.; Sano, T.; Soga, K. *Polymer* **2000**, *41*, 4005–4012.
141. Mager, M.; Becke, S.; Windisch, H.; Denninger, U. *Angew. Chem. Int. Ed.* **2001**, *40*, 1898–1902.
142. Cui, C. Z.; Bonder, E. M.; Jäkle, F. *J. Am. Chem. Soc.* **2010**, *132*, 1810–1812.
143. Camerano, J. A.; Casado, M. A.; Ciriano, M. A.; Oro, L. A. *Dalton Trans.* **2006**, 5287–5293.
144. Wang, S. *Coord. Chem. Rev.* **2001**, *215*, 79–98.
145. Yi, C.; Liu, Q. D.; Bai, D. R.; Jia, W. L.; Ye, T.; Wang, S. N. *Inorg. Chem.* **2005**, *44*, 601–609.
146. Ulrich, G.; Ziessel, R.; Harriman, A. *Angew. Chem. Int. Ed.* **2008**, *47*, 1184–1201.
147. Jäkle, F. *ChemSusChem* **2011**, *4*, 325–326.
148. Matsumoto, F.; Chujo, Y. *J. Organomet. Chem.* **2003**, *680*, 27–30.
149. Niedenzu, K.; Trofimenko, S. *Top. Curr. Chem.* **1986**, *131*, 1–37.
150. Zhang, G.; Evans, R. E.; Campbell, K. A.; Fraser, C. L. *Macromolecules* **2009**, *42*, 8627–8633.
151. Matsumi, N.; Chujo, Y. *Macromolecules* **2000**, *33*, 8146–8148.
152. Nagai, A.; Miyake, J.; Kokado, K.; Nagata, Y.; Chujo, Y. *Macromolecules* **2009**, *42*, 1560–1564.
153. Matsumoto, F.; Matsumi, N.; Chujo, Y. *Polym. Bull.* **2002**, *48*, 119–125.
154. Miyata, M.; Matsumi, N.; Chujo, Y. *Macromolecules* **2001**, *34*, 7331–7335.
155. Matsumi, N.; Umeyama, T.; Chujo, Y. *Macromolecules* **2001**, *34*, 3510–3511.
156. Matsumi, N.; Umeyama, T.; Chujo, Y. *Macromolecules* **2000**, *33*, 3956–3957.
157. Matsumi, N.; Naka, K.; Chujo, Y. *Polym. J.* **1998**, *30*, 833–837.
158. Chujo, Y.; Tomita, I.; Saegusa, T. *Macromolecules* **1994**, *27*, 6714–6717.
159. Trofimenko, S. *J. Am. Chem. Soc.* **1966**, *88*, 1842–1844.
160. Matsumoto, F.; Nagata, Y.; Chujo, Y. *Polym. Bull.* **2005**, *53*, 155–160.
161. Matsumoto, F.; Chujo, Y. *Macromolecules* **2003**, *36*, 5516–5519.
162. Kamaya, E.; Matsumoto, F.; Kondo, Y.; Chujo, Y.; Katagiri, M. *Nucl. Instrum. Methods Phys. Res. A* **2004**, *529*, 329–331.
163. Matsumoto, F.; Chujo, Y. *Pure Appl. Chem.* **2006**, *78*, 1407–1411.
164. Murphree, S. S. *Prog. Heterocycl. Chem.* **2011**, *22*, 21–58.
165. Benstead, M.; Mehl, G. H.; Boyle, R. W. *Tetrahedron* **2011**, *67*, 3573–3601.
166. Zhu, M.; Jiang, L.; Yuan, M.; Liu, X.; Ouyang, C.; Zheng, H.; Yin, X.; Zuo, Z.; Liu, H.; Li, Y. *J. Polym. Sci. A Polym. Chem.* **2008**, *46*, 7401–7410.
167. Donuru, V. R.; Vegesna, G. K.; Velayudham, S.; Green, S.; Liu, H. *Chem. Mater.* **2009**, *21*, 2130–2138.
168. Donuru, V. R.; Vegesna, G. K.; Velayudham, S.; Meng, G.; Liu, H. *J. Polym. Sci. A Polym. Chem.* **2009**, *47*, 5354–5366.
169. Meng, G.; Velayudham, S.; Smith, A.; Luck, R.; Liu, H. *Macromolecules* **2009**, *42*, 1995–2001.
170. Alemdaroglu, F. E.; Alexander, S. C.; Ji, D. M.; Prusty, D. K.; Borsch, M.; Herrmann, A. *Macromolecules* **2009**, *42*, 6529–6536.
171. Cihaner, A.; Algi, F. *React. Funct. Polym.* **2009**, *69*, 62–67.
172. Nagai, A.; Miyake, J.; Kokado, K.; Nagata, Y.; Chujo, Y. *J. Am. Chem. Soc.* **2008**, *130*, 15276–15278.
173. Thivierge, C.; Loudet, A.; Burgess, K. *Macromolecules* **2011**, *44*, 4012–4015.
174. Popere, B. C.; Della Pelle, A. M.; Thayumanavan, S. *Macromolecules* **2011**, *44*, 4767–4776.
175. Gao, L.; Senevirathna, W.; Sauve, G. *Org. Lett.* **2011**, *13*, 5354–5357.
176. Donuru, V. R.; Zhu, S.; Green, S.; Liu, H. *Polymer* **2010**, *51*, 5359–5368.
177. Nagai, A.; Chujo, Y. *Macromolecules* **2010**, *43*, 193–200.
178. Yoshii, R.; Nagai, A.; Chujo, Y. *J. Polym. Sci. A Polym. Chem.* **2010**, *48*, 5348–5356.
179. Amat-Guerri, F.; Liras, M.; Carrascoso, M. L.; Sastre, R. *Photochem. Photobiol.* **2003**, *77*, 577–584.
180. Arbeloa, F. L.; Prieto, J. B.; Arbeloa, I. L.; Costela, A.; Garcia-Moreno, I.; Gomez, C.; Amat-Guerri, F.; Liras, M.; Sastre, R. *Photochem. Photobiol.* **2003**, *78*, 30–36.
181. Costela, A.; Garcia-Moreno, I.; Gomez, C.; Amat-Guerri, F.; Liras, M.; Sastre, R. *Appl. Phys. B* **2003**, *76*, 365–369.
182. Nagai, A.; Kokado, K.; Miyake, J.; Chujo, Y. *J. Polym. Sci. A Polym. Chem.* **2010**, *48*, 627–634.
183. Paris, R.; Quijada-Garrido, I.; Garcia, O.; Liras, M. *Macromolecules* **2011**, *44*, 80–86.
184. Wang, D.; Miyamoto, R.; Shiraishi, Y.; Hirai, T. *Langmuir* **2009**, *25*, 13176–13182.
185. Liras, M.; Garcia-Garcia, J. M.; Quijada-Garrido, I.; Gallardo, A.; Paris, R. *Macromolecules* **2011**, *44*, 3739–3745.
186. Nagai, A.; Kokado, K.; Miyake, J.; Chujo, Y. *Macromolecules* **2009**, *42*, 5446–5452.
187. Kajiwara, Y.; Nagai, A.; Chujo, Y. *J. Mater. Chem.* **2010**, *20*, 2985–2992.
188. Nagai, A.; Yoshii, R.; Otsuka, T.; Kokado, K.; Chujo, Y. *Langmuir* **2010**, *26*, 15644–15649.
189. Tang, C. W.; VanSlyke, S. A. *Appl. Phys. Lett.* **1987**, *51*, 913–915.
190. Tang, C. W.; VanSlyke, S. A.; Chen, C. H. *J. Appl. Phys.* **1989**, *65*, 3610–3616.
191. Kimyonok, A.; Wang, X.-Y.; Weck, M. *J. Macromol. Sci. C Polym. Rev.* **2006**, *46*, 47–77.
192. Wu, Q.; Esteghamatian, M.; Hu, N.-X.; Popovic, Z.; Enright, G.; Tao, Y.; D'Iorio, M.; Wang, S. *Chem. Mater.* **2000**, *12*, 79–83.
193. Cui, Y.; Liu, Q.-D.; Bai, D.-R.; Jia, W.-L.; Tao, Y.; Wang, S. *Inorg. Chem.* **2005**, *44*, 601–609.
194. Qin, Y.; Kiburu, I.; Shah, S.; Jäkle, F. *Org. Lett.* **2006**, *8*, 5227–5230.
195. Pohl, R.; Anzenbacher, P., Jr. *Org. Lett.* **2003**, *5*, 2769–2772.
196. Montes, V. A.; Li, G.; Pohl, R.; Shinar, J.; Anzenbacher, P., Jr. *Adv. Mater.* **2004**, *16*, 2001–2003.
197. Montes, V. A.; Zyryanov, G. V.; Danilov, E.; Agarwal, N.; Palacios, M. A.; Anzenbacher, P. J. *J. Am. Chem. Soc.* **2009**, *131*, 1787–1795.
198. Nagata, Y.; Otaka, H.; Chujo, Y. *Macromolecules* **2008**, *41*, 737–740.
199. Nagata, Y.; Chujo, Y. *Macromolecules* **2007**, *40*, 6–8.
200. Wang, X.-Y.; Weck, M. *Macromolecules* **2005**, *38*, 7219–7224.
201. Moad, G.; Chen, M.; Haussler, M.; Postma, A.; Rizzardo, E.; Thang, S. H. *Polym. Chem.* **2011**, *2*, 492–519.
202. Cheng, F.; Jäkle, F. *Chem. Commun.* **2010**, *46*, 3717–3719.
203. Nagata, Y.; Chujo, Y. *Macromolecules* **2008**, *41*, 2809–2813.
204. Tokoro, Y.; Nagai, A.; Kokado, K.; Chujo, Y. *Macromolecules* **2009**, *42*, 2988–2993.
205. Tokoro, Y.; Nagai, A.; Chujo, Y. *Macromolecules* **2010**, *43*, 6229–6233.
206. Nagai, A.; Kobayashi, S.; Nagata, Y.; Kokado, K.; Taka, H.; Kita, H.; Suzuri, Y.; Chujo, Y. *J. Mater. Chem.* **2010**, *20*, 5196–5201.

Copyright © 2013. Elsevier. All rights reserved.

Comprehensive Inorganic Chemistry II : From Elements to Applications, Elsevier, 2013. ProQuest Ebook Central, http://ebookcentral.proquest.com/lib/inflibnet-ebooks/detail.action?docID=1330977.
Created from inflibnet-ebooks on 2021-02-09 22:27:26.

207. Li, H.; Jäkle, F. *Macromolecules* **2009**, *42*, 3448–3453.
208. Tokoro, Y.; Nagai, A.; Chujo, Y. *Appl. Organomet. Chem.* **2010**, *24*, 563–568.
209. Tokoro, Y.; Nagai, A.; Chujo, Y. *J. Polym. Sci. A Polym. Chem.* **2010**, *48*, 3693–3701.
210. Zhang, G.; Chen, J.; Payne, S. J.; Kooi, S. E.; Demas, J. N.; Fraser, C. L. *J. Am. Chem. Soc.* **2007**, *129*, 8942–8943.
211. Nagai, A.; Kokado, K.; Nagata, Y.; Arita, M.; Chujo, Y. *J. Org. Chem.* **2008**, *73*, 8605–8607.
212. Zhang, G. Q.; Lu, J. W.; Sabat, M.; Fraser, C. L. *J. Am. Chem. Soc.* **2010**, *132*, 2160–2162.
213. Zhang, G. Q.; Singer, J. P.; Kooi, S. E.; Evans, R. E.; Thomas, E. L.; Fraser, C. L. *J. Mater. Chem.* **2011**, *21*, 8295–8299.
214. Zhang, G.; Kooi, S. E.; Demas, J. N.; Fraser, C. L. *Adv. Mater.* **2008**, *20*, 2099–2104.
215. Zhang, G.; St. Clair, T. L.; Fraser, C. L. *Macromolecules* **2009**, *42*, 3092–3097.
216. Zhang, G.; Fiore, G. L.; St. Clair, T. L.; Fraser, C. L. *Macromolecules* **2009**, *42*, 3162–3169.
217. Zhang, G. Q.; Xu, S. P.; Zestos, A. G.; Evans, R. E.; Lu, J. W.; Fraser, C. L. *ACS Appl. Mater. Interf.* **2010**, *2*, 3069–3074.
218. Zhang, G.; Palmer, G. M.; Dewhirst, M. W.; Fraser, C. L. *Nat. Mater.* **2009**, *8*, 747–751.
219. Pfister, A.; Zhang, G.; Zareno, J.; Horwitz, A. F.; Fraser, C. L. *ACS Nano* **2008**, *2*, 1252–1258.
220. Contreras, J.; Xie, J. S.; Chen, Y. J.; Pei, H.; Zhang, G. Q.; Fraser, C. L.; Hamm-Alvarez, S. F. *ACS Nano* **2010**, *4*, 2735–2747.
221. Kersey, F. R.; Zhang, G. Q.; Palmer, G. M.; Dewhirst, M. W.; Fraser, C. L. *ACS Nano* **2010**, *4*, 4989–4996.
222. Fraser, C. L.; Zhang, G. *Mater. Today* **2009**, *12*, 38–40.
223. Nagai, A.; Kokado, K.; Nagata, Y.; Chujo, Y. *Macromolecules* **2008**, *41*, 8295–8298.
224. Piers, W. E.; Bourke, S. C.; Conroy, K. D. *Angew. Chem. Int. Ed.* **2005**, *44*, 5016–5036.
225. Ma, K.; Fabrizi de Biani, F.; Bolte, M.; Zanello, P.; Wagner, M. *Organometallics* **2002**, *21*, 3979–3989.
226. Fox, P. A.; Griffin, S. T.; Reichert, W. M.; Salter, E. A.; Smith, A. B.; Tickell, M. D.; Wicker, B. F.; Cioffi, E. A.; Davis, J. H.; Rogers, R. D.; Wierzbicki, A. *Chem. Commun.* **2005**, 3679–3681.
227. Cui, C.; Jäkle, F. *Chem. Commun.* **2009**, 2744–2746.
228. Cui, C.; Bonder, E. M.; Jäkle, F. *J. Polym. Sci. A Polym. Chem.* **2009**, *47*, 6612–6618.
229. Cui, C.; Heilmann-Brohl, J.; Perucha, A. S.; Thomson, M. D.; Roskos, H. G.; Wagner, M.; Jäkle, F. *Macromolecules* **2010**, *43*, 5256–5261.
230. Hall, D. G., Ed.; *Boronic Acids: Preparation and Applications in Organic Synthesis and Medicine*; Wiley-VCH Verlag GmbH & Co. KGaA: Weinheim, Germany, 2005.
231. Cambre, J. N.; Sumerlin, B. S. *Polymer* **2011**, *52*, 4631–4643.
232. Severin, K. *Dalton Trans.* **2009**, 5254–5264.
233. Mastalerz, M. *Angew. Chem. Int. Ed.* **2008**, *47*, 445–447.
234. Shipp, D. A. *J. Macromol. Sci. Polym. Rev.* **2005**, *45*, 171–194.
235. Kamigaito, M.; Ando, T.; Sawamoto, M. *Chem. Rev.* **2001**, *101*, 3689–3745.
236. Matyjaszewski, K.; Xia, J. H. *Chem. Rev.* **2001**, *101*, 2921–2990.
237. Moad, G.; Rizzardo, E.; Thang, S. H. *Polymer* **2008**, *49*, 1079–1131.
238. Cui, C. Z.; Bonder, E. M.; Qin, Y.; Jäkle, F. *J. Polym. Sci. A Polym. Chem.* **2010**, *48*, 2438–2445.
239. Kim, K. T.; Cornelissen, J. J. L. M.; Nolte, R. J. M.; van Hest, J. C. M. *Adv. Mater.* **2009**, *21*, 2787–2791.
240. Kim, K. T.; Cornelissen, J. J. L. M.; Nolte, R. J. M.; van Hest, J. C. M. *J. Am. Chem. Soc.* **2009**, *131*, 13908–13909.
241. Cambre, J. N.; Roy, D.; Gondi, S. R.; Sumerlin, B. S. *J. Am. Chem. Soc.* **2007**, *129*, 10348–10349.
242. Roy, D.; Cambre, J. N.; Sumerlin, B. S. *Chem. Commun.* **2008**, 2477–2479.
243. Roy, D.; Cambre, J. N.; Sumerlin, B. S. *Chem. Commun.* **2009**, 2106–2108.
244. Nicolas, M.; Fabre, B.; Marchand, G.; Simonet, J. *Eur. J. Org. Chem.* **2000**, 1703–1710.
245. Nicolas, M.; Fabre, B.; Simonet, J. *Chem. Commun.* **1999**, 1881–1882.
246. Deore, B. A.; Braun, M. D.; Freund, M. S. *Macromol. Chem. Phys.* **2006**, *207*, 660–664.
247. Shoji, E.; Freund, M. S. *J. Am. Chem. Soc.* **2002**, *124*, 12486–12493.
248. Shoji, E.; Freund, M. S. *J. Am. Chem. Soc.* **2001**, *123*, 3383–3384.
249. Deore, B. A.; Freund, M. S. *Macromolecules* **2009**, *42*, 164–168.
250. Deore, B. A.; Yu, I.; Woodmass, J.; Freund, M. S. *Macromol. Chem. Phys.* **2008**, *209*, 1094–1105.
251. Ali, S. R.; Ma, Y.; Parajuli, R. R.; Balogun, Y.; Lai, W. Y.-C.; He, H. *Anal. Chem.* **2007**, *79*, 2583–2587.
252. Ali, S. R.; Parajuli, R. R.; Balogun, Y.; Ma, Y.; He, H. *Sensors* **2008**, *8*, 8423–8452.
253. Ma, Y.; Chiu, P. L.; Serrano, A.; Ali, S. R.; Chen, A. M.; He, H. *J. Am. Chem. Soc.* **2008**, *130*, 7921–7928.
254. Ma, Y.; Cheung, W.; Wei, D.; Bogozi, A.; Chiu, P. L.; Wang, L.; Pontoriero, F.; Mendelsohn, R.; He, H. *ACS Nano* **2008**, *2*, 1197–1204.
255. Côté, A. P.; Benin, A. I.; Ockwig, N. W.; O'keeffe, M.; Matzger, A. J.; Yaghi, O. M. *Science* **2005**, *310*, 1166–1170.
256. Doonan, C. J.; Tranchemontagne, D. J.; Glover, T. G.; Hunt, J. R.; Yaghi, O. M. *Nat. Chem.* **2010**, *2*, 235–238.
257. Sheepwash, E.; Krampl, V.; Scopelliti, R.; Sereda, O.; Neels, A.; Severin, K. *Angew. Chem. Int. Ed.* **2011**, *50*, 3034–3037.
258. Spitler, E. L.; Giovino, M. R.; White, S. L.; Dichtel, W. R. *Chem. Sci.* **2011**, *2*, 1588–1593.
259. Lanni, L. M.; Tilford, R. W.; Bharathy, M.; Lavigne, J. J. *J. Am. Chem. Soc.* **2011**, *133*, 13975–13983.
260. Rambo, B. M.; Lavigne, J. J. *Chem. Mater.* **2007**, *19*, 3732–3739.
261. Niu, W.; Smith, M. D.; Lavigne, J. J. *J. Am. Chem. Soc.* **2006**, *128*, 16466–16467.
262. Niu, W. J.; O'Sullivan, C.; Rambo, B. M.; Smith, M. D.; Lavigne, J. J. *Chem. Commun.* **2005**, 4342–4344.
263. Sanchez, J. C.; Trogler, W. C. *J. Mater. Chem.* **2008**, *18*, 5134–5141.
264. Liu, W. J.; Huang, W. J.; Pink, M.; Lee, D. *J. Am. Chem. Soc.* **2010**, *132*, 11844–11846.
265. Liu, W.; Pink, M.; Lee, D. *J. Am. Chem. Soc.* **2009**, *131*, 8703–8707.
266. De, P.; Gondi, S. R.; Roy, D.; Sumerlin, B. S. *Macromolecules* **2009**, *42*, 5614–5621.
267. Korich, A. L.; Iovine, P. M. *Dalton Trans.* **2010**, *39*, 1423–1431.
268. Korich, A. L.; Walker, A. R.; Hincke, C.; Stevens, C.; Iovine, P. M. *J. Polym. Sci. A Polym. Chem.* **2010**, *48*, 5767–5774.
269. Bapat, A. P.; Roy, D.; Ray, J. G.; Savin, D. A.; Sumerlin, B. S. *J. Am. Chem. Soc.* **2011**, *133*, 19832–19838.
270. McBreen, J.; Lee, H. S.; Yang, X. Q.; Sun, X. *J. Power. Sources* **2000**, *89*, 163–167.
271. Sun, X.; Angell, C. A. *Electrochim. Acta* **2001**, *46*, 1467–1473.
272. Xu, W.; Sun, X.-G.; Angell, C. A. *Electrochim. Acta* **2003**, *48*, 2255–2266.
273. Tabata, S.-I.; Hirakimoto, T.; Nishiura, M.; Watanabe, M. *Electrochim. Acta* **2003**, *48*, 2105–2112.
274. Pennarun, P. Y.; Jannasch, P.; Papaefthimiou, S.; Skarpentzos, N.; Yianoulis, P. *Thin Solid Films* **2006**, *514*, 258–266.
275. Matsumi, N.; Sugai, K.; Ohno, H. *Macromolecules* **2003**, *36*, 2321–2326.
276. Matsumi, N.; Sugai, K.; Ohno, H. *Macromolecules* **2002**, *35*, 5731–5732.
277. Zygadło-Monikowska, E.; Florjanczyk, Z.; Słuzewska, K.; Ostrowska, J.; Langwald, N.; Tomaszewska, A. *J. Power. Sources* **2010**, *195*, 6055–6061.
278. Pennarun, P.-Y.; Jannasch, P. *Solid State Ion.* **2005**, *176*, 1849–1859.
279. Shankar, S. R.; Matsumi, N. *Polym. Bull.* **2011**, *68*, 721–727.
280. Lee, J. A.; Lee, J. Y.; Ryou, M. H.; Han, G.-B.; Lee, J.-N.; Lee, D.-J.; Park, J.-K.; Lee, Y. M. *J. Solid State Electrochem.* **2011**, *15*, 753–757.
281. Matsumi, N.; Sugai, K.; Sakamoto, K.; Mizumo, T.; Ohno, H. *Macromolecules* **2005**, *38*, 4951–4954.
282. Mehta, M. A.; Fujinami, T.; Inoue, T. *J. Power Sources* **1999**, *81–82*, 724–728.
283. Nishihara, Y.; Miyazaki, M.; Tomita, Y.; Kadono, Y.; Takagi, K. *J. Polym. Sci. A Polym. Chem.* **2008**, *46*, 7913–7918.
284. Tabata, S.; Hirakimoto, T.; Tokuda, H.; Susan, M. A. B. H.; Watanabe, M. *J. Phys. Chem. B* **2004**, *108*, 19518–19526.
285. Matsumi, N.; Nakamura, Y.; Aoi, K.; Watanabe, T.; Mizumo, T.; Ohno, H. *Polym. J.* **2009**, *41*, 437–441.
286. Herzog, A.; Maderna, A.; Harakas, G. N.; Knobler, C. B.; Hawthorne, M. F. *Chem. – Eur. J.* **1999**, *5*, 1212–1217.
287. Satapathy, R.; Dash, B. P.; Maguire, J. A.; Hosmane, N. S. *Collect. Czechoslov. Chem. Commun.* **2010**, *75*, 995–1022.
288. Dash, B. P.; Satapathy, R.; Maguire, J. A.; Hosmane, N. S. *New J. Chem.* **2011**, *35*, 1955–1972.
289. Welna, D. T.; Bender, J. D.; Wei, X.; Sneddon, L. G.; Allcock, H. R. *Adv. Mater.* **2005**, *17*, 859–862.
290. Borchardt, L.; Kockrick, E.; Wollmann, P.; Kaskel, S.; Guron, M. M.; Sneddon, L. G.; Geiger, D. *Chem. Mater.* **2010**, *22*, 4660–4668.
291. Pender, M. J.; Carroll, P. J.; Sneddon, L. G. *J. Am. Chem. Soc.* **2001**, *123*, 12222–12231.
292. Sneddon, L. G.; Pender, M. J.; Forsthoefel, K. M.; Kusari, U.; Wei, X. *J. Eur. Ceram. Soc.* **2005**, *25*, 91–97.
293. Guron, M.; Wei, X. L.; Carroll, P. J.; Sneddon, L. G. *Inorg. Chem.* **2010**, *49*, 6139–6147.

Copyright © 2013. Elsevier. All rights reserved.

Comprehensive Inorganic Chemistry II : From Elements to Applications, Elsevier, 2013. ProQuest Ebook Central, http://ebookcentral.proquest.com/lib/inflibnet-ebooks/detail.action?docID=1330977.
Created from inflibnet-ebooks on 2021-02-09 22:27:26.

294. Wei, X. L.; Carroll, P. J.; Sneddon, L. G. *Chem. Mater.* **2006**, *18*, 1113–1123.
295. Wei, X.; Carroll, P. J.; Sneddon, L. G. *Organometallics* **2004**, *23*, 163–165.
296. Guron, M. M.; Wei, X.; Welna, D.; Krogman, N.; Kim, M. J.; Allcock, H.; Sneddon, L. G. *Chem. Mater.* **2009**, *21*, 1708–1715.
297. Malenfant, P. R. L.; Wan, J. L.; Taylor, S. T.; Manoharan, M. *Nat. Nanotechnol.* **2007**, *2*, 43–46.
298. Yisgedu, T. B.; Chen, X.; Schricker, S.; Parquette, J.; Meyers, E. A.; Shore, S. G. *Chem. – Eur. J.* **2009**, *15*, 2190–2199.
299. In *Contemporary Boron Chemistry*. Proceedings of the Tenth International Conference on Boron Chemistry, IMEBORON X, held at the University of Durham, United Kingdom, 11–15 July 1999. Davidson, M.; Hughes, A. K.; Marder, T. B.; Wade, K., Eds.; 2000 [In: Spec. Publ. - R. Soc. Chem., 2000; 253].
300. Armistead, J. P.; Houser, E. J.; Keller, T. M. *Appl. Organomet. Chem.* **2000**, *14*, 253–260.
301. Keller, T. M. *Carbon* **2002**, *40*, 225–229.
302. Kolel-Veetil, M. K.; Keller, T. M. *J. Mater. Chem.* **2003**, *13*, 1652–1656.
303. Houser, E. J.; Keller, T. M. *Macromolecules* **1998**, *31*, 4038–4040.
304. Kolel-Veetil, M. K.; Keller, T. M. *J. Polym. Sci. A Polym. Chem.* **2006**, *44*, 147–155.
305. Kolel-Veetil, M. K.; Dominguez, D. D.; Keller, T. M. *J. Polym. Sci. A Polym. Chem.* **2008**, *46*, 2581–2587.
306. Zhang, X. C.; Kong, L. H.; Dai, L. N.; Zhang, X. Z.; Wang, Q.; Tan, Y. X.; Zhang, Z. J. *Polymer* **2011**, *52*, 4777–4784.
307. Park, M. H.; Lee, K. M.; Kim, T.; Do, Y.; Lee, M. H. *Chem. Asian J.* **2011**, *6*, 1362–1366.
308. Liang, L. Y.; Rapakousiou, A.; Salmon, L.; Ruiz, J.; Astruc, D.; Dash, B. P.; Satapathy, R.; Sawicki, J. W.; Hosmane, N. S. *Eur. J. Inorg. Chem.* **2011**, 3043–3049.
309. Simon, Y. C.; Ohm, C.; Zimny, M. J.; Coughlin, E. B. *Macromolecules* **2007**, *40*, 5628–5630.
310. Simon, Y. C.; Coughlin, E. B. *J. Polym. Sci. A Polym. Chem.* **2010**, *48*, 2557–2563.
311. Gratton, S. E. A.; Parrott, M. C.; Adronov, A. *J. Inorg. Organomet. Polym. Mater.* **2005**, *15*, 469–475.
312. Benhabbour, S. R.; Parrott, M. C.; Gratton, S. E. A.; Adronov, A. *Macromolecules* **2007**, *40*, 5678–5688.
313. Sumitani, S.; Oishi, M.; Nagasaki, Y. *React. Funct. Polym.* **2011**, *71*, 684–693.
314. Gonzalez-Campo, A.; Vinas, C.; Teixidor, F.; Nunez, R.; Sillanpaa, R.; Kivekas, R. *Macromolecules* **2007**, *40*, 5644–5652.
315. Parrott, M. C.; Valliant, J. F.; Adronov, A. *Langmuir* **2006**, *22*, 5251–5255.
316. Parrott, M. C.; Marchington, E. B.; Valliant, J. F.; Adronov, A. *J. Am. Chem. Soc.* **2005**, *2005*, 12081–12089.
317. Galie, K. M.; Mollard, A.; Zharov, I. *Inorg. Chem.* **2006**, *45*, 7815–7820.
318. Lerouge, F.; Vinas, C.; Teixidor, F.; Nunez, R.; Abreu, A.; Xochitiotzi, E.; Santillan, R.; Farfan, N. *Dalton Trans.* **2007**, 1898–1903.
319. Nunez, R.; Juarez-Perez, E. J.; Teixidor, F.; Santillan, R.; Farfan, N.; Abreu, A.; Yepez, R.; Vinas, C. *Inorg. Chem.* **2010**, *49*, 9993–10000.
320. Juarez-Perez, E. J.; Vinas, C.; Teixidor, F.; Santillan, R.; Farfan, N.; Abreu, A.; Yepez, R.; Nunez, R. *Macromolecules* **2010**, *43*, 150–159.
321. Hosmane, N. S.; Zhu, Y. H.; Maguire, J. A.; Kaim, W.; Takagaki, M. *J. Organomet. Chem.* **2009**, *694*, 1690–1697.
322. Gonzalez-Campo, A.; Juarez-Perez, E. J.; Vinas, C.; Boury, B.; Sillanpaa, R.; Kivekas, R.; Nunez, R. *Macromolecules* **2008**, *41*, 8458–8466.
323. Muller, J.; Base, K.; Magnera, T. F.; Michl, J. *J. Am. Chem. Soc.* **1992**, *114*, 9721–9722.
324. Grimes, R. N. *Appl. Organomet. Chem.* **1996**, *10*, 209–225.
325. Fox, M. A.; Howard, J. A. K.; MacBride, J. A. H.; Mackinnon, A.; Wade, K. *J. Organomet. Chem.* **2003**, *680*, 155–164.
326. Wedge, T. J.; Hawthorne, M. F. *Coord. Chem. Rev.* **2003**, *240*, 111–128.
327. Dash, B. P.; Satapathy, R.; Maguire, J. A.; Hosmane, N. S. *Org. Lett.* **2008**, *10*, 2247–2250.
328. Dash, B. P.; Satapathy, R.; Gaillard, E. R.; Maguire, J. A.; Hosmane, N. S. *J. Am. Chem. Soc.* **2010**, *132*, 6578–6587.
329. Dash, B. P.; Satapathy, R.; Gaillard, E. R.; Norton, K. M.; Maguire, J. A.; Chug, N.; Hosmane, N. S. *Inorg. Chem.* **2011**, *50*, 5485–5493.
330. Fabre, B.; Chayer, S.; Vicente, M. G. H. *Electrochem. Commun.* **2003**, *5*, 431–434.
331. Fabre, B.; Clark, J. C.; Vicente, M. G. H. *Macromolecules* **2006**, *39*, 112–119.
332. Hao, E.; Fabre, B.; Fronczek, F. R.; Vicente, M. G. H. *Chem. Mater.* **2007**, *19*, 6195–6205.
333. Hao, E.; Fabre, B.; Fronczek, F. R.; Vicente, M. G. H. *Chem. Commun.* **2007**, 4387–4389.
334. Barriere, F.; Fabre, B.; Hao, E. H.; LeJeune, Z. M.; Hwang, E.; Garno, J. C.; Nesterov, E. E.; Vicente, M. G. H. *Macromolecules* **2009**, *42*, 2981–2987.
335. Fabre, B.; Hao, E. H.; LeJeune, Z. M.; Amuhaya, E. K.; Barriere, F.; Garno, J. C.; Vicente, M. G. H. *ACS Appl. Mater. Interf.* **2010**, *2*, 691–702.
336. Simon, Y. C.; Peterson, J. J.; Mangold, C.; Carter, K. R.; Coughlin, E. B. *Macromolecules* **2009**, *42*, 512–516.
337. Peterson, J. J.; Simon, Y. C.; Coughlin, E. B.; Carter, K. R. *Chem. Commun.* **2009**, 4950–4952.
338. Peterson, J. J.; Werre, M.; Simon, Y. C.; Coughlin, E. B.; Carter, K. R. *Macromolecules* **2009**, *42*, 8594–8598.
339. Peterson, J. J.; Davis, A. R.; Werre, M.; Coughlin, E. B.; Carter, K. R. *ACS Appl. Mater. Interf.* **2011**, *3*, 1796–1799.
340. Kokado, K.; Tokoro, Y.; Chujo, Y. *Macromolecules* **2009**, *42*, 9238–9242.
341. Kokado, K.; Tokoro, Y.; Chujo, Y. *Macromolecules* **2009**, *42*, 2925–2930.
342. Kokado, K.; Chujo, Y. *Macromolecules* **2009**, *42*, 1418–1420.
343. Kokado, K.; Tominaga, M.; Chujo, Y. *Macromol. Rapid Commun.* **2010**, *31*, 1389–1394.
344. Kokado, K.; Nagai, A.; Chujo, Y. *Macromolecules* **2010**, *43*, 6463–6468.
345. Kokado, K.; Chujo, Y. *Dalton Trans.* **2011**, *40*, 1919–1923.

Copyright © 2013. Elsevier. All rights reserved.

Comprehensive Inorganic Chemistry II : From Elements to Applications, Elsevier, 2013. ProQuest Ebook Central, http://ebookcentral.proquest.com/lib/inflibnet-ebooks/detail.action?docID=1330977.
Created from inflibnet-ebooks on 2021-02-09 22:27:26.

This page intentionally left blank

Copyright © 2013. Elsevier. All rights reserved.

Comprehensive Inorganic Chemistry II : From Elements to Applications, Elsevier, 2013. ProQuest Ebook Central, http://ebookcentral.proquest.com/lib/inflibnet-ebooks/detail.action?docID=1330977.
Created from inflibnet-ebooks on 2021-02-09 22:27:26.

1.28 Phosphorus-Containing Polymers

Y-y Carpenter and T Baumgartner, University of Calgary, Calgary, AB, Canada

© 2013 Elsevier Ltd. All rights reserved.

Nomenclature

CD	Circular dichroism
COD	1,5-Cyclooctadiene
DABCO	1,4-Diazabicyclo[2.2.2]octane
DFT	Density-functional theory
DP	Degree of polymerization
DSC	Differential scanning calorimetry
E_{bg}	Bandgap energy
EDX	Energy-dispersive x-ray analysis
$E_{p(\ldots)}$	Electrochemical oxidation potential measures at the (onset) or (peak)
E_{pa}	Anodic (oxidation) peak potential
Fc	Ferrocene or ferrocenyl
FRET	Fluorescence resonance energy transfer
GPC	Gel-permeation chromatography
M/I	Monomer/initiator ratio
MALDI-TOF	Matrix-assisted laser desorption ionization – time of flight (mass spectrometry)
M_n	Number-average molecular weight
M_w	Weight-average molecular weight
PDI	Polydispersity index
PE	Polyethylene
PI	Polyisoprene
PMP	Poly(methylenephosphane)
PPV	Poly(*p*-phenylenevinylene)
PS	Polystyrene
ROP	Ring-opening polymerization
SCE	Saturated calomel electrode
TD	Time-dependent
T_d	Decomposition temperature
TEM	Transmission electron microscope
TGA	Thermogravimetric analysis
Tht	Tetrahydrothiophene
TMP	2,4,4-Trimethylpentyl
VAZO	1,1′-Azobis(cyclohexanecarbonitrile)
λ_{abs}	Absorption maximum wavelength
λ_{em}	Fluorescence emission maximum wavelength
ϕ_{PL}	Photoluminescence quantum yield

1.28.1 Introduction

The chemistry of phosphorus is quite diverse and in many aspects significantly different from that of its pnictogen congener, nitrogen. In fact, phosphorus recently has been dubbed a carbon copy[1] because many phosphorus compounds show structures and behavior similar to their related carbon-based compounds, due to their diagonal relationship in the periodic table. For more than 50 years, researchers have recognized the complexity and high value of phosphorus chemistry, and a plethora of exciting results in terms of structure, bonding, and reactivity have since resulted from this research, including many essential industrial applications. However, it is remarkable that the majority of this work has been confined to the molecular scale, and only recently have phosphorus-containing building blocks been systematically considered for

Copyright © 2013. Elsevier. All rights reserved.

Comprehensive Inorganic Chemistry II : From Elements to Applications, Elsevier, 2013. ProQuest Ebook Central, http://ebookcentral.proquest.com/lib/inflibnet-ebooks/detail.action?docID=1330977.
Created from inflibnet-ebooks on 2021-02-09 22:27:26.

polymer chemistry.[2] It is now well established that the incorporation of phosphorus centers into polymers can result in materials with unique physical and chemical properties. This chapter highlights pertinent developments in the area of phosphorus-containing polymers, with an emphasis on the new millennium, a period during which a rich chemistry has been developed, resulting in highly diverse, value-added materials. Practical applications will receive particular attention. In terms of the classes of materials explored, organophosphorus-based polymers will be the exclusive focus of this chapter, that is, organic polymers that contain phosphorus-functional groups either as part of their backbone or as a side chain.

1.28.2 Polymers with Phosphate- and Phosphonate-Functional Groups

The introduction of phosphorus centers into polymers has been found to improve the thermostability of polymers and engineering plastics significantly, as well as their oxygen and ultraviolet (UV) plasma resistance. Because they can be very effective flame retardants, phosphorus-containing polymers have received significant attention from engineers in recent years. Consequently, recent patent and technical literature indicates a growing interest in halogen-free solutions centering on phosphorus-based flame-retardants.[3] Considering that printed wiring boards currently comprise the largest market for flame-retardant polymeric materials, phosphorus-containing polymers now play a substantial role within this industry. The majority of the materials employed to date rely on organophosphate or organophosphonate architectures, in which the phosphorus-functional groups are either incorporated in the backbone of the polymers or appended as side chains to an exclusively organic polymer backbone.[4–12] In all cases, the presence of the phosphate/phosphonate units significantly increases the thermal stability of the polymers and decreases their volatility. Notably, the materials tend to char rather than burn, thereby providing a favorable diffusion barrier of gaseous products to the flame, shielding the polymer surface from heat and oxygen and reducing the production of combustible gasses during polymer degradation.

One particularly successful phosphorus building block with proven potential in flame-retardant polymers is 9,10-dihydro-9-oxa-10-phosphaphenanthrene-10-oxide (DOPO, **1**). In the past few years, it has been the topic of several research articles because it can easily be introduced as a side chain via its reactive P—H functional group.[4–7] Its polar P═O group and bulky structure generally provide polymers with good solubility, improved thermal oxidative stability, good adhesion, and low birefringence. Multiple research groups have reported polyesters or polyester imides with DOPO-functional groups appended to an aromatic diol.[4,5] The monomeric building block is generally accessible through addition of the DOPO P—H bond to a suitable quinone **2** (Scheme 1). The resulting diols **3** can then be polymerized with appropriate difunctionalized carboxylic acid chlorides and other diol monomers to afford a variety of polyesters **4–6** with aromatic and aliphatic backbones.

The effect of the phosphorus content on the thermal properties and flame retardancy of polymers is commonly evaluated by means of thermogravimetric analysis (TGA). Polymers with fully aromatic backbone architectures were found to be stable above 340 °C, and the observed char yields at 700 °C increased with the content of phosphorus-containing diphenol, reaching values as high as 45%.[4] In addition to their flame-retardant properties, the polyesters **4–6** were also found to exhibit thermotropic liquid crystalline behavior that involved nematic phases in the melt (usually between 200 and 350 °C). The liquid-crystalline behavior could be further addressed by variation of the aromatic/aliphatic monomer diol ratio. The mesomorphic transition temperatures decreased with the increase of the aliphatic molar ratio in the polymer backbone.[4–6]

It is notable that Sun and Wang have already reported similar bisphenolic DOPO building blocks **7a–c** in 2001 for a completely different purpose, namely, as components in organic light-emitting diodes (OLEDs).[7] Copolymers of DOPO-functionalized units with functionalized 1,3,4-oxadiazole units (Scheme 2) were found to show blue light–emitting features that depend on the nature of the backbone. It also is notable that the light-emitting properties were accompanied by useful electron-transport capabilities. The latter proved an early indication of the high value of organophosphorus electronic materials, a feature that has been broadly recognized only recently and has developed into a very active field of research.[2,13]

Incorporation of organophosphate building blocks as a major polymer component leads to desirable features similar to those obtained with the DOPO-based materials.[8–12] Polymers with the structural motifs **I** and **II**, depicted in Figure 1, also provide highly flame-retardant materials with the added benefit that they are potentially also biodegradable.[9,10] In addition, the free valence at the phosphorus center allows for the introduction of further functional groups or crosslinks that can significantly impact the overall properties of the materials. The latter includes liquid crystalline behavior for polymers of type **8**.[12]

One recent review highlights a variety of hydrogels accessible by crosslinking appropriate polymeric phosphates and phosphonates to yield biologically compatible and degradable materials with good swelling properties.[10] These materials can be employed in diverse practical applications, including medical device coatings, contact lenses, controlled-release applications, and, most recently, potential tissue engineering applications.

In a similar context, poly(vinylphosphonic acid) not only has found commercial application as a binder in bone and dental concrete,[14] but also has proven effective as a corrosion inhibition agent in cooling and boiler water systems because of its ability to inhibit the formation of $CaSO_4$, $CaCO_3$, and $Ca_3(PO_4)_2$.[15] Details of other prospective uses for this material such as membranes in fuel cells or flame-retardants in commodity polymers are summarized in a recent review and will, therefore, not be covered in this chapter.[11]

1.28.3 Polymeric Phosphorus Ligands

1.28.3.1 Polymer-Supported Systems

Organic transformations involving transition metal-based catalyst systems are a staple of many chemical processes, and specific catalyst properties can be designed selectively and economically.[16] In homogeneous catalysis, organophosphorus

Copyright © 2013. Elsevier. All rights reserved.

Comprehensive Inorganic Chemistry II : From Elements to Applications, Elsevier, 2013. ProQuest Ebook Central, http://ebookcentral.proquest.com/lib/inflibnet-ebooks/detail.action?docID=1330977.
Created from inflibnet-ebooks on 2021-02-09 22:27:26.

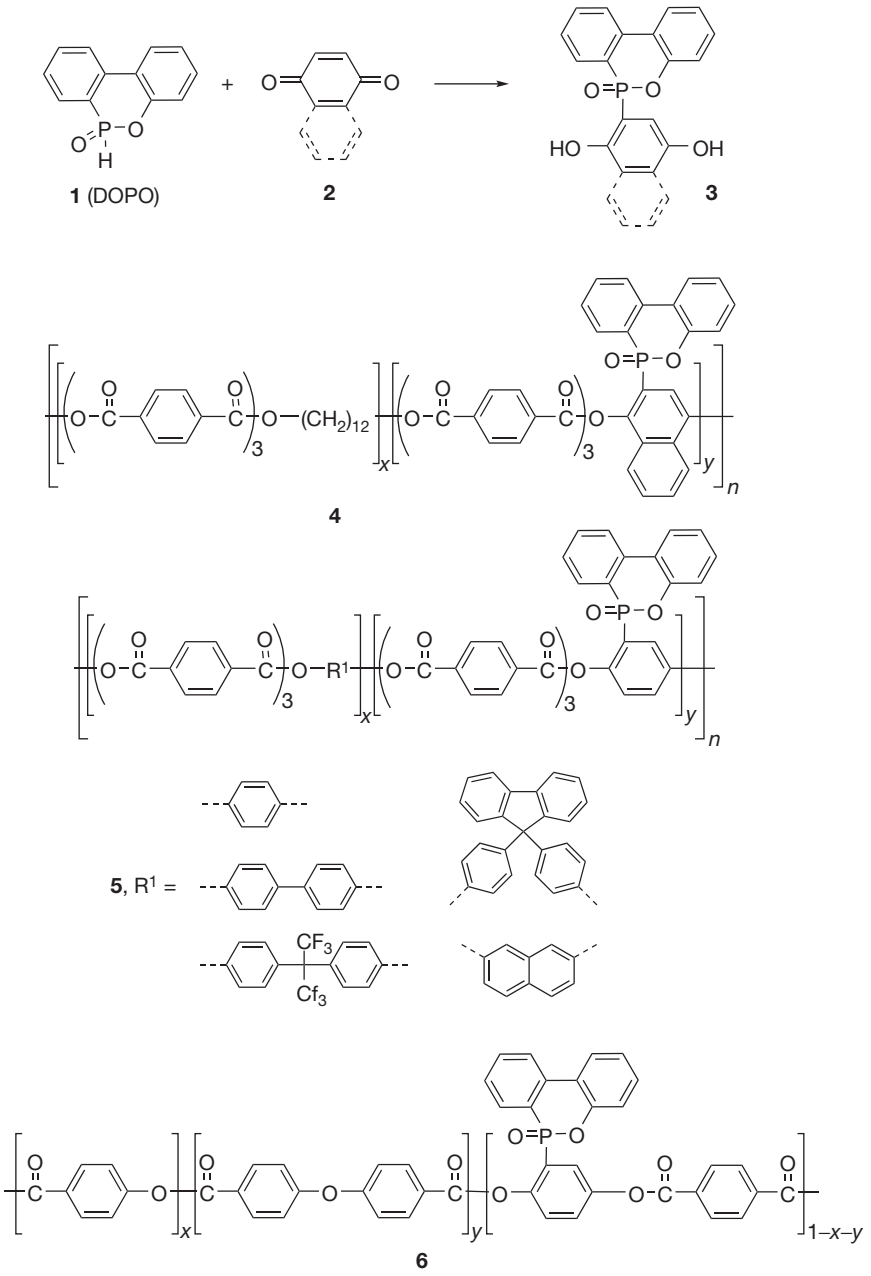

Scheme 1 Synthesis of DOPO-containing polymers.

compounds represent an almost infinite pool of ligands from which to draw, providing an opportunity for tailor-made catalyst systems.[17] While molecular systems are arguably the most successful and are therefore already used in a plethora of catalytic processes, there recently has been a growing interest in developing polymer-bound ligands and the corresponding catalyst systems. Among the major advantages of polymer-supported ligands are the ease of purification during compound synthesis and the ability to recover the catalyst for reuse in subsequent processes.[18] Moreover, the immobilization of synthetic catalysts has enabled the rapid development of combinatorial chemistry, wherein high-throughput synthesis of large numbers of organic molecules by solution-phase catalysis is becoming a useful methodology.[19] An important benefit in this context is the provision of efficient methods for compound purification after catalysis. Polymer-supported catalysts can, for example, be readily removed by simple filtration from a solution-phase reaction mixture. Uozumi has recently reviewed the great versatility of polymer-supported ligands with a representative focus on Pd catalysts,[20] so the discussion of polymer-supported phosphanes in this section will be brief.

Polystyrene (PS) is among the most popular scaffolds for polymer-supported phosphane ligands, as it is generally soluble and inert under the catalysis conditions most commonly employed and can easily be functionalized at the 4-position of the benzene ring in order to anchor corresponding organophosphorus units directly to the aromatic ring or

Copyright © 2013. Elsevier. All rights reserved.

Comprehensive Inorganic Chemistry II : From Elements to Applications, Elsevier, 2013. ProQuest Ebook Central, http://ebookcentral.proquest.com/lib/inflibnet-ebooks/detail.action?docID=1330977.
Created from inflibnet-ebooks on 2021-02-09 22:27:26.

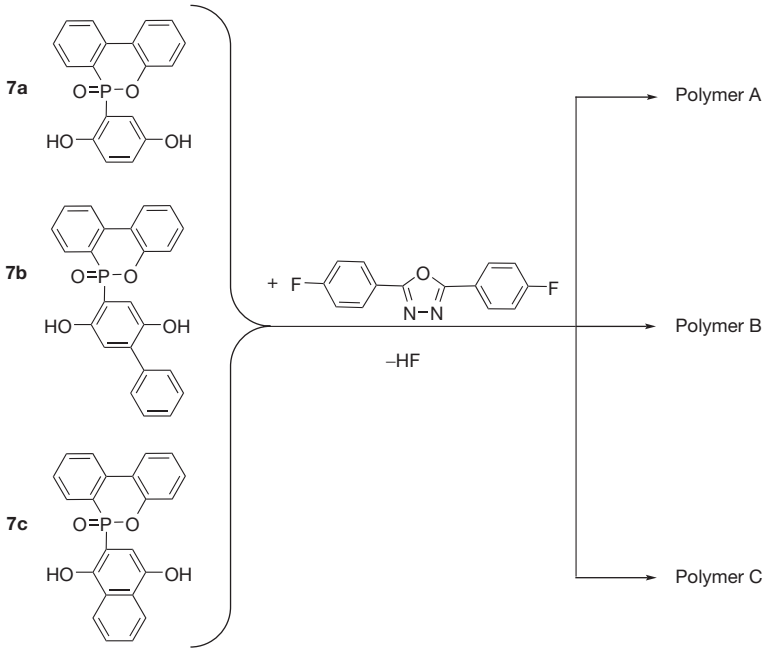

Scheme 2 Synthesis of light-emitting DOPO-containing polymers.

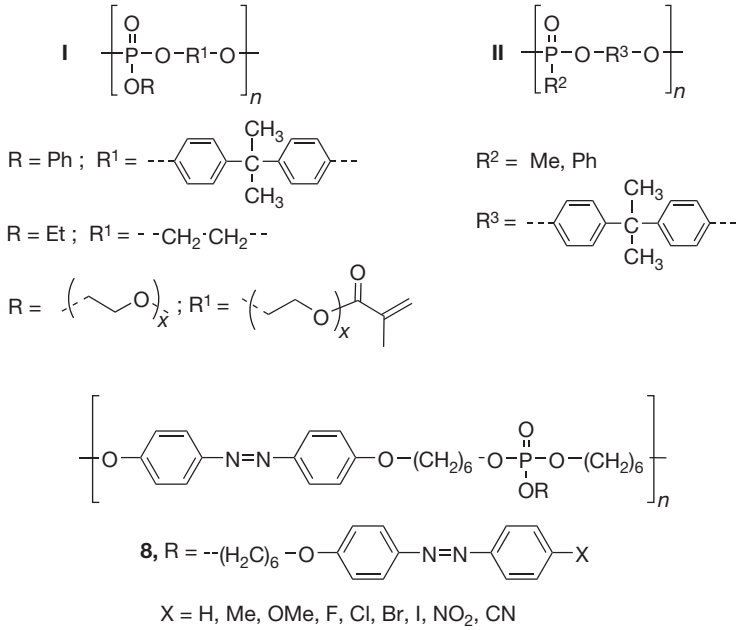

Figure 1 Poly(organophosphate)s.

via aliphatic spacer groups. Some general ligand/catalyst architectures are shown in Figure 2.[20]

The functionalization of the styrene units can typically be performed either pre- or post-polymerization, providing a very flexible basis for the design of tailored ligand systems. The countless opportunities for ligand design involve the chemical nature of the phosphorus centers, but also their distribution along the polymer backbone, that is, high or low phosphane concentrations. The latter can also be addressed by the nature of the polymer backbone, for example, through copolymerization of ethylene and (functionalized) styrene (**D** and **E**, Figure 2; PE = polyethylene). The use of polyethylene glycol as support (**F**) provides the opportunity for biphasic catalysis, wherein catalyst can be recovered from an aqueous phase after use, while the product remains in the organic phase.[20]

Kamer and coworkers have recently reported the use of a polystyrene-based support in P-stereogenic aminophosphane-phosphinite/phosphite ligands **11** for Rh-catalyzed asymmetric hydrogenation.[21] Molecular ligands of this type can be built up in modular fashion, and the aforementioned researchers were able to illustrate the large potential for ligand fine-tuning (Scheme 3) that could be further exploited in a combinatorial catalysis

Copyright © 2013. Elsevier. All rights reserved.

Comprehensive Inorganic Chemistry II : From Elements to Applications, Elsevier, 2013. ProQuest Ebook Central, http://ebookcentral.proquest.com/lib/inflibnet-ebooks/detail.action?docID=1330977.
Created from inflibnet-ebooks on 2021-02-09 22:27:26.

protocol. These solid-phase procedures allowed for the rapid synthesis and screening of the new resin-bound ligands. It was found that the ligands form active hydrogenation catalysts displaying moderate to good enantioselectivity.

1.28.3.2 Dendrimer-Supported Systems

Dendrimers constitute a unique class of well-defined hyperbranched polymers, and phosphorus-containing species have thus also garnered some interest as supports for selective and recoverable homogeneous catalysts. Due to the very versatile synthetic strategies toward dendrimers in general, which involve convergent or divergent approaches, the phosphorus centers can be introduced either at the core and/or at internal branching points (Figure 3).

Since several recent review articles have illustrated the benefits and applications of phosphorus-containing dendrimers,[22] this section will only provide a brief overview of this area of

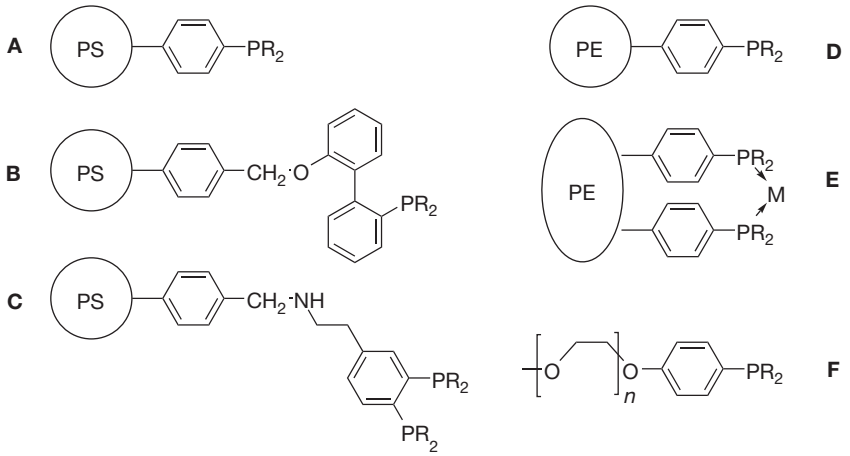

Figure 2 Structural motifs for polymer-supported phosphane catalysts.

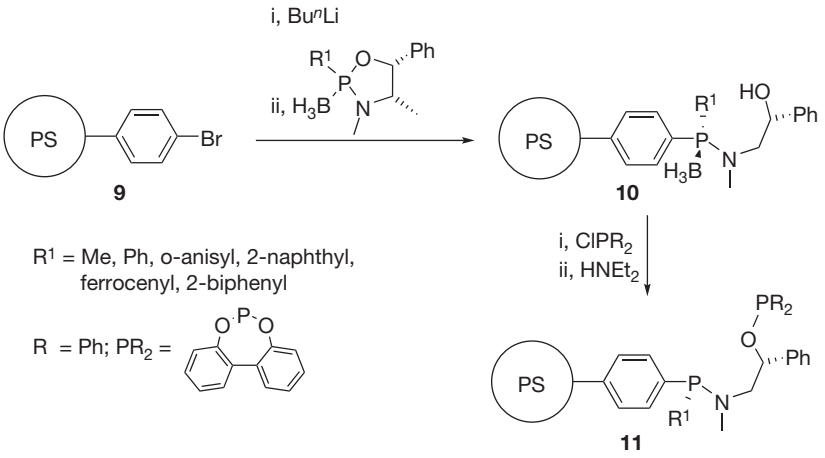

Scheme 3 Synthesis of PS-supported chiral aminophosphane ligands.

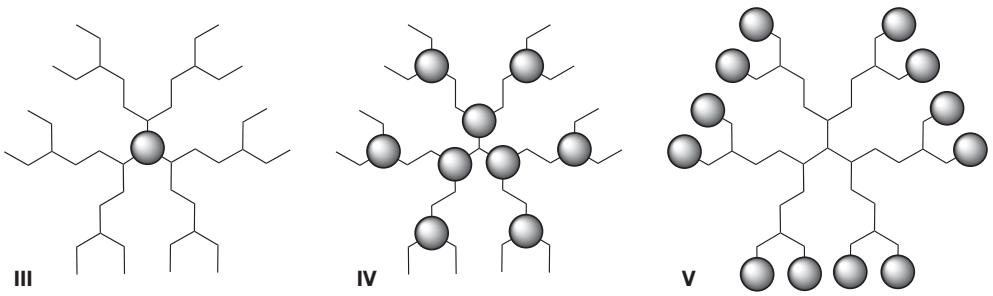

Figure 3 Schematic architectures of phosphorus-containing dendrimers (spheres represent location of the P-functional groups).[22]

Copyright © 2013. Elsevier. All rights reserved.

Comprehensive Inorganic Chemistry II : From Elements to Applications, Elsevier, 2013. ProQuest Ebook Central, http://ebookcentral.proquest.com/lib/inflibnet-ebooks/detail.action?docID=1330977.
Created from inflibnet-ebooks on 2021-02-09 22:27:26.

research. From a practical point of view, surface functionalization of the dendrimers (**V**, **Figure 3**) is the most feasible in terms of catalysis, but the versatile nature of phosphorus lends itself to internal incorporation as well. The easy access to dendrons from phosphorus reagents allows easy diversification of ways in which a variety of multidendritic macromolecules are synthesized. In this context, Majoral et al. have reported several P-containing dendrimers with internal P-groups that act as both branching points and coordination sites for transition metals.[22]

In 1993, Engel and coworkers reported the first example of a metal-containing phosphorus-based dendrimer (**12**), which exhibited the metal at the core (**Figure 4**).[23] Although the dendrimer contained several other P-centers, all but the core

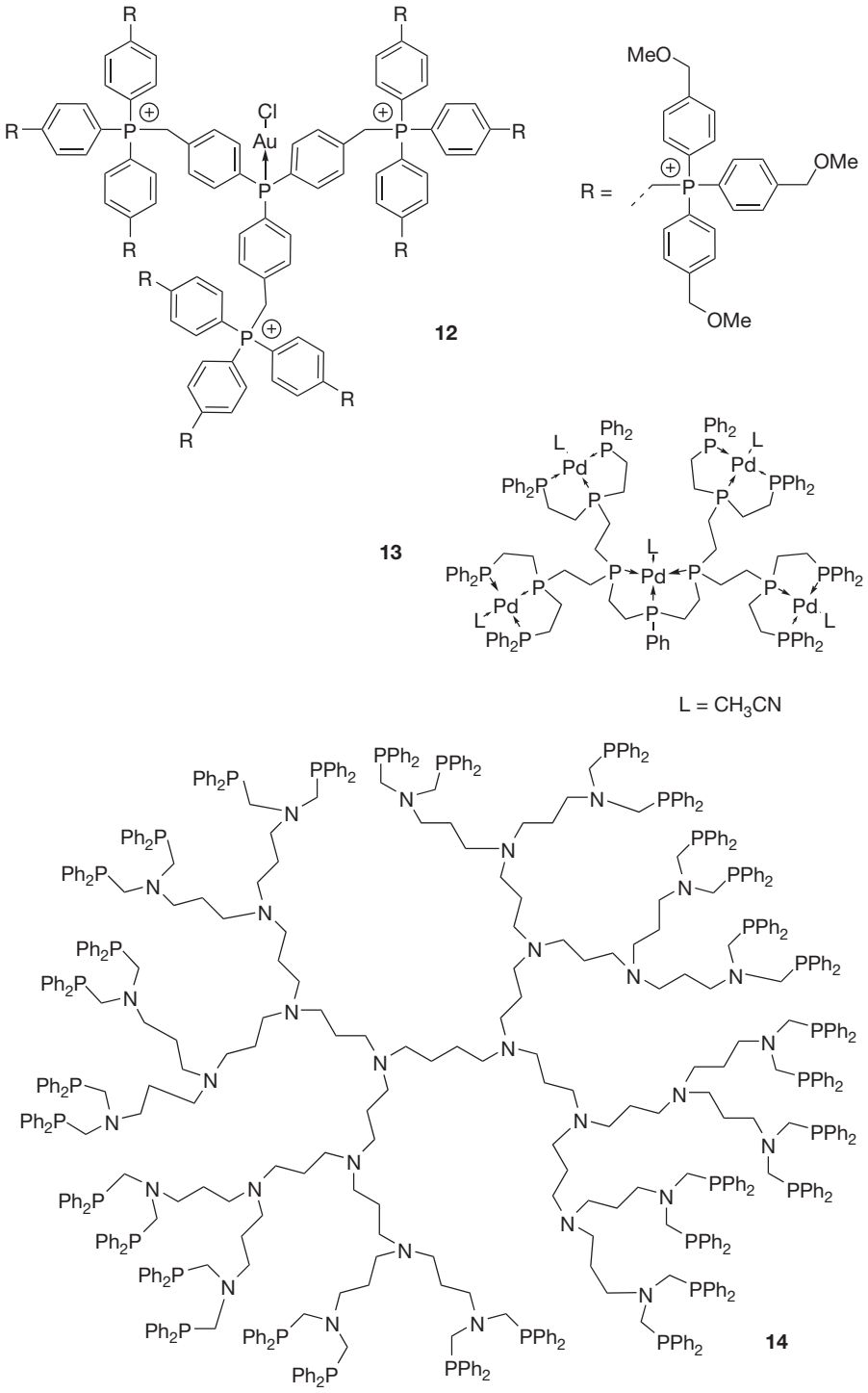

Figure 4 Dendrimeric phosphorus ligands with different architectures.

Copyright © 2013. Elsevier. All rights reserved.

Comprehensive Inorganic Chemistry II : From Elements to Applications, Elsevier, 2013. ProQuest Ebook Central, http://ebookcentral.proquest.com/lib/inflibnet-ebooks/detail.action?docID=1330977.
Created from inflibnet-ebooks on 2021-02-09 22:27:26.

phosphorus atom were quaternized, precluding the possibility of metal complexation at these sites. The first example of a dendrimer with metal centers throughout the structure (**13**) was reported by DuBois et al. in 1994 (Figure 4).[24] This material highlights the flexibility of these structures, as complexation of Pd involves the participation of phosphorus centers from different dendrimer generations in a chelating fashion. One example of a periphery P-functionalized dendrimer (**14**) was reported by Reetz and coworkers in 1997 (Figure 4).[25] It is accessible by double phosphinomethylation of the terminal primary amino groups of the commercially available 1,4-diaminobutane-cored and propyleneimine-based dendrimer with CH_2O/Ph_2PH. Subsequent complexation of Pd or Rh provides recoverable catalyst systems that were employed in Heck and hydroformylation reactions, respectively. Notably, the catalytic activity of the Pd dendrimer was increased in comparison to its corresponding molecular systems, while the Rh-system provided results comparable to those of its molecular analogues.

The well-defined and precise control over the structure of dendrimers has commonly been touted as the major advantage of these systems over polymer-supported catalysts. However, Reek and coworkers have recently shown that the structural precision of a dendritic support is not critical for all catalytic applications, and so, simple hyperbranched polymers may provide interesting and cheap alternatives as recyclable catalyst supports. In their study, hyperbranched poly(ethyleneimine) (PEI) polymers with P-functional surface groups (**15**) were obtained from a simple one-pot synthesis, yielding globular polymeric structures with broader molecular weight distributions compared to their dendritic analogues (Scheme 4). Corresponding Pd-complexes of **15** were used to catalyze allylic substitution reactions, revealing that, although the PEI-functionalized polymers appear more sensitive to small changes in the P/Pd ratio than commercial dendrimeric propyleneimine analogues, the catalysts were more active.[26]

Besides their application as supported catalysts, phosphorus-based dendrimer systems can also be utilized in a variety of other applications. Within this scope lie biological applications, such as the production of water-soluble systems for transfection experiments, the generation of vesicles with anti-HIV activity in vitro, and the formation of hydrogels.[22] Moreover, these dendrimers can contribute to materials science via modification of inorganic surfaces making them biocompatible, or for the fabrication of metallic/nonmetallic hybrid materials.[22]

1.28.4 Polymers with Phosphorus in the Backbone

While the attachment of phosphorus-based side chain-functionalities in polymers can result in some interesting materials properties, as highlighted in the preceding sections, implementation of these units as a central component of the polymer backbone provides considerably more opportunities toward functional and tunable materials. The following sections highlight a variety of organophosphorus polymers in which phosphorus has been incorporated as part of the backbone. We will illustrate that the functionalization of trivalent P-centers provides a particularly unique approach toward value-added, smart materials with potential uses in catalysis and electronic or optical/photophysical applications. In the past, the major challenges revolved around the limited synthetic procedures available to access the corresponding phosphorus-containing polymers. However, in recent years, significant progress has been made in this regard, which is evidenced by the increasing number of intriguing and diverse materials that are being reported in contemporary literature.

1.28.4.1 Chiral Alkylphosphane-Based Polymers

Despite the fact that there are countless examples of optically active organic polymers, the number of polymers with chiral

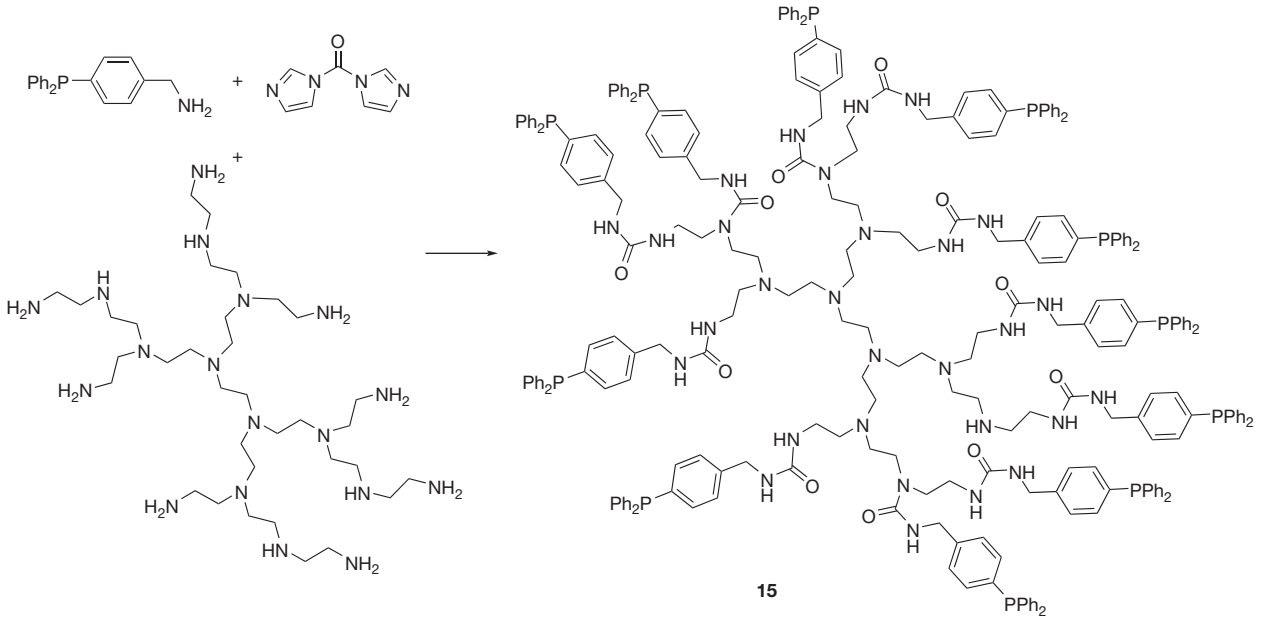

Scheme 4 Synthesis of a hyperbranched polymeric P-ligand.

Copyright © 2013. Elsevier. All rights reserved.

Comprehensive Inorganic Chemistry II : From Elements to Applications, Elsevier, 2013. ProQuest Ebook Central, http://ebookcentral.proquest.com/lib/inflibnet-ebooks/detail.action?docID=1330977.
Created from inflibnet-ebooks on 2021-02-09 22:27:26.

inorganic heteroatoms remains severely limited to date. In a series of publications starting in 2007, Chujo and coworkers have reported optically active polymers with chiral phosphorus centers in the backbone.[27] This work relies upon the low tendency for racemization of chiral trialkylphosphanes, attributable to their high-energy inversion barrier. The development of a variety of different chiral copolymers was facilitated by the group's successful syntheses, building upon the earlier work by Wild et al.[29], of a series of chiral oligomers with up to eight chiral phosphorus centers.[28] The chiral oligomers **18–20** are accessible by the stepwise oxidative coupling of (*S*,*S*)-1,2-bis(boranato-(*t*-butyl)methyl-phosphino)ethane **17** using ^{s}BuLi and $CuCl_2$ in the presence of the chiral base (−)-sparteine (**Scheme 5**). The optically pure starting material is available through oxidative coupling of boranato-(*t*-butyl)dimethylphosphane **16** in a similar protocol. Based on the observed solution dynamics, the authors could confirm the transition from small molecule to polymer behavior occurred between the hexamer and octamer.[28]

By reacting enantiomerically pure (*S*,*S*)-1,2-bis(boranato-(*t*-butyl)methylphosphino)ethane **17** with ^{s}BuLi in the presence of (−)-sparteine and using appropriately functionalized benzyl bromides instead of $CuCl_2$, access to a variety of different copolymers is provided (**Scheme 6**). Symmetric, bifunctional comonomers, such as α,α′-dibromoxylenes (*o*, *m*, or *p*) and 4,4′-bis(bromomethyl)azobenzene, provide polymeric materials **22** and **23**, respectively, with low-molecular-weights of approximately $M_w = 2000–5000$ g mol^{-1} (PDI = 1.3–3.1). The use of 4-iodobenzyl bromide gave a bifunctional chiral P-monomer **24** that could be used in Sonogashira cross-coupling with 1,4-diethynylbenzene to provide a higher-molecular-weight polymer **25** with $M_w = 10\,000$ g mol^{-1} (PDI = 1.8).

The polymers were soluble in common organic solvents and were characterized by multinuclear NMR spectroscopy. Differential scanning calorimetry (DSC) and circular dichroism (CD) confirmed that the chiral nature of the phosphorus centers, in conjunction with the flexibility of the various comonomers, has significant impact on the higher-order structure (helical conformation) of the polymers, as the chirality of the P-containing monomers is retained upon polymerization. Further control over the higher-order structure is available with the azobenzene-containing copolymer **23** (**Scheme 6**), which showed unique stimuli-responsive behavior. The latter property is a consequence of reversible switching of the N=N bond configuration upon irradiation with UV light (*trans* to *cis*) or thermal treatment (*cis* to *trans*). More importantly, trivalent phosphorus centers could be generated in polymer **23** via reduction with CF_3SO_3H and KOH, subsequently allowing for complexation of the trivalent species with $Pt(COD)Cl_2$. Once coordinated to Pt, the isomerization of the diazobenzene unit upon exposure to UV light resulted in a helical structure for the polymer, illustrating the cooperative effects that stem from the phosphane units' chirality, the rigidification of the structure through complexation, and the conformation of the diazo units.

Replacement of the *t*-butyl groups at the phosphorus centers with phenyl substituents in (*S*,*S*)-1,2-bis(boranatomethyl(phenyl)phosphino)ethane reduces the Lewis basicity of the phosphorus centers, which allows for milder reduction conditions for subsequent metal complexation without compromising the stability of the configuration at the chiral P-centers.[30] As in their earlier studies on the *t*-butyl species, Morisaki and Chujo have reported an extended bis(iodo)monomer that was copolymerized with a 1,3-bisethynylarene to provide for a chiral polymer **26** with *meta*-aryl linkages ($M_w = 16\,000$ g mol^{-1}; PDI = 2.3).[31] Reduction of the phosphorus centers with 1,4-diazabicyclo[2.2.2]octane (DABCO) cleanly provided trivalent species **27** that could be complexed with $PdCl_2$, and the resulting polymer **28** (**Scheme 7**) again confirmed the chirality transfer of the P-centers onto the polymer as a whole, which fails in the noncomplexed state. The authors conclude that the structural rigidity of the chiral Pd-complex is crucial for the generation of higher-order structure.[31]

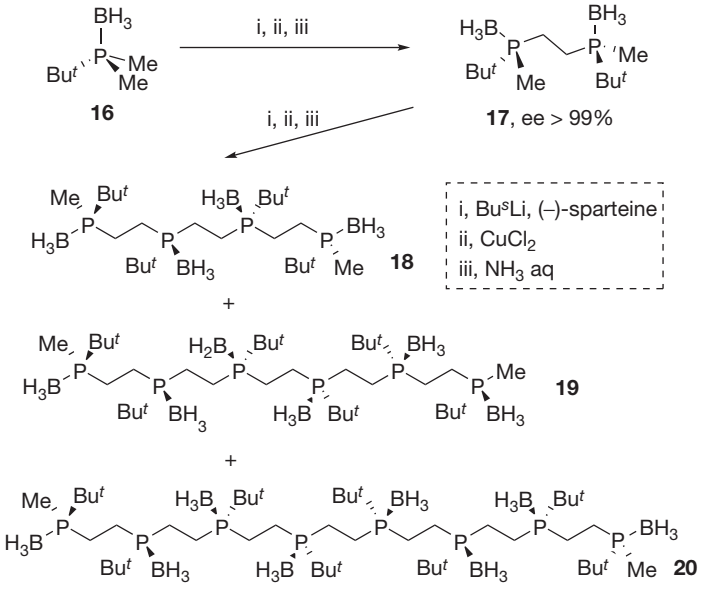

Scheme 5 Synthesis of oligomers with chiral P-centers.

Copyright © 2013. Elsevier. All rights reserved.

Comprehensive Inorganic Chemistry II : From Elements to Applications, Elsevier, 2013. ProQuest Ebook Central, http://ebookcentral.proquest.com/lib/inflibnet-ebooks/detail.action?docID=1330977.
Created from inflibnet-ebooks on 2021-02-09 22:27:26.

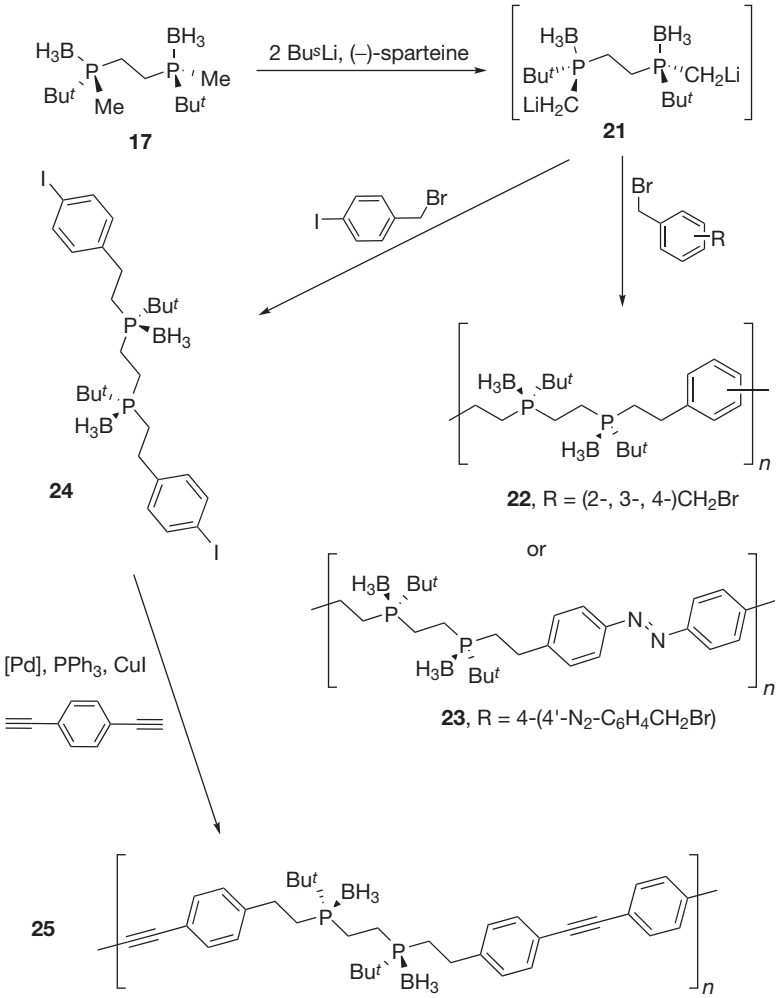

Scheme 6 Synthesis of polymers with optically pure P-centers.

Recently, the same authors reported the functionalization of their modified (*S*,*S*)-1,2-bis(boranatomethyl(phenyl) phosphino)ethane building block with azide groups (**29**) that allow for the formation of a high-molecular-weight polymer ($M_w = 42\,000\ g\ mol^{-1}$) using a copper-catalyzed Huisgen ('click') cycloaddition polymerization (Scheme 7).[31] Reduction of the P-centers with DABCO resulted in the formation of the trivalent species **30**, which was subsequently complexed with $PtCl_2$ and Cu^+, respectively. The preferred coordination sphere of the metal centers was found to have a drastic impact on the overall conformation of the polymer. While Pt^{2+} is satisfied by the coordination to the two phosphorus centers in **31**, as it is balanced with the two chlorides, Cu^+ (employed as $Cu(MeCN)_4PF_6$) requires two additional ligands for a tetradentate environment. These ligands are provided by the two nitrogen atoms of the neighboring triazole units in **32**. To accommodate such a coordination sphere, the polymer backbone experiences a significantly bent structure, while coordination to $PtCl_2$ allows for a relatively linear backbone. The successful coordination in both polymers was confirmed via multinuclear NMR spectroscopy. These results nicely illustrate the benefits of incorporating phosphorus atoms along the polymer backbone, as materials with highly tunable structures can be obtained by complexation to transition metal species. On the other hand, no use of these polymers in asymmetric catalysis processes has been reported to date.

1.28.4.2 Ferrocene-Based Polymers

In search of efficient methods towards inorganic, high-molecular-weight polymers, Manners and coworkers have developed the ring-opening polymerization (ROP) of strained ferrocenophanes with main group elements or transition metals in the *ansa*-position.[32] Studies by Seyferth et al. conducted in the 1980s had indicated that the treatment of corresponding phospha[1]ferrocenophanes with ^{n}BuLi affords a mixture of oligomers and polymers.[33] Based on these initial results, Manners et al. have optimized the reaction conditions and established several routes towards high-molecular-weight poly(ferrocenyl)phosphanes. In terms of properties, the benefits of these polymers are twofold: the presence of the ferrocene units provides for stable redox-switching, while the P-centers can be chemically modified through functionalization with a variety of different functional groups (O, S, BR_3, Me^+, and transition metals), and the specific nature of both functionalities has significant impact on the polymer properties as a whole.

Copyright © 2013. Elsevier. All rights reserved.

Comprehensive Inorganic Chemistry II : From Elements to Applications, Elsevier, 2013. ProQuest Ebook Central, http://ebookcentral.proquest.com/lib/inflibnet-ebooks/detail.action?docID=1330977.
Created from inflibnet-ebooks on 2021-02-09 22:27:26.

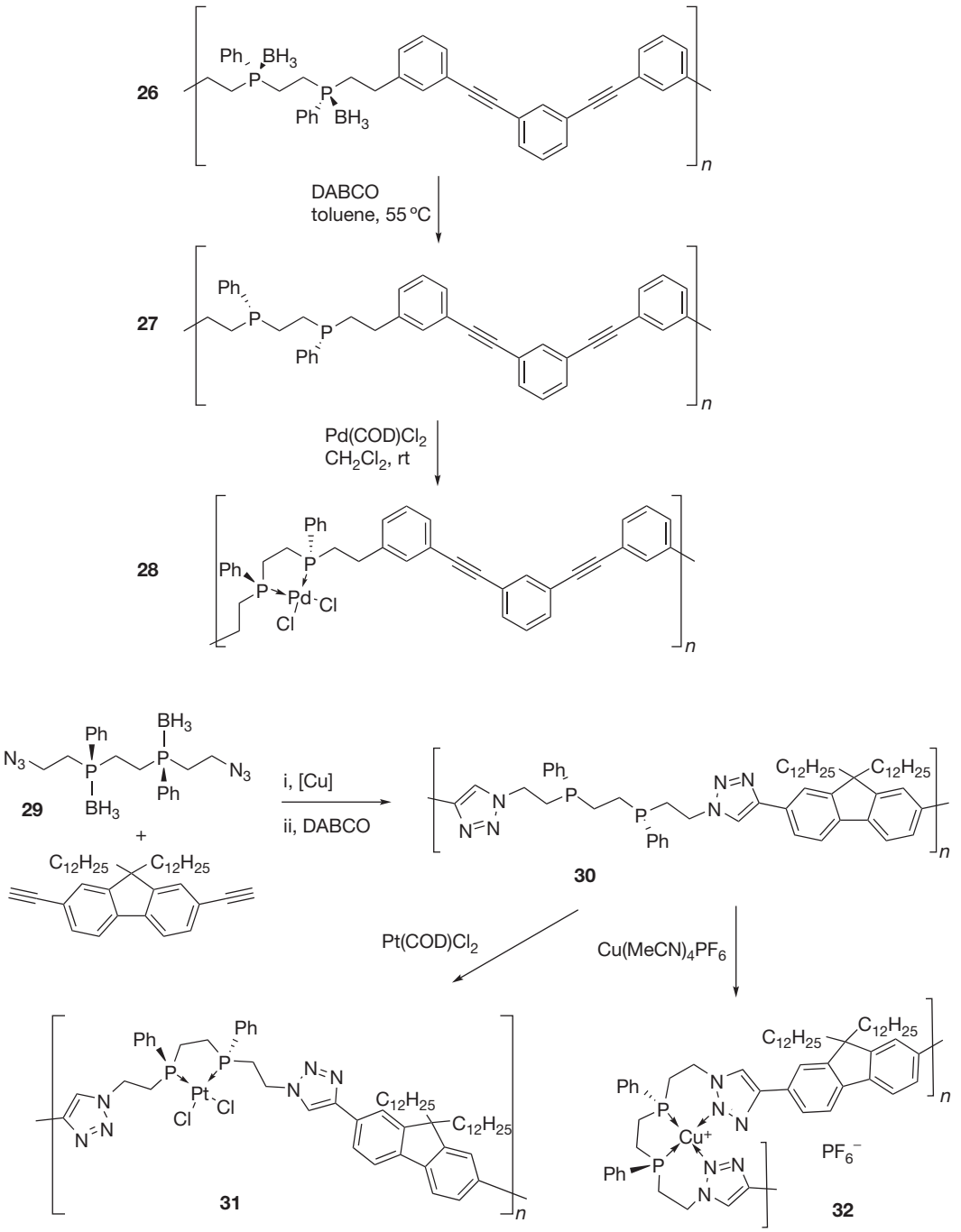

Scheme 7 Synthesis of P-chiral polymers and their utility as polymeric ligands.

In their first report in 1995,[34] the Manners group utilized thermal ROP conditions (i.e., $T > 120\,^{\circ}C$, Scheme 8), which had previously been successfully employed in the synthesis of the corresponding silicon-based polymers,[32] to access a variety of differently P- and Cp-substituted polymers of type **34** and establish the general accessibility of such systems. Notably, the molecular-weight distributions ranged from $M_w = 18\,000$–$65\,000\ g\ mol^{-1}$ with relatively low polydispersities from PDI = 1.5–2.3. To further demonstrate the flexibility of the approach, trivalent as well as pentavalent P-ferrocenophanes were probed under these conditions, and both resulted in high-molecular-weight polymers. However, the pentavalent sulfurized (P=S) polymer partially decomposed under the thermal conditions employed. Access to higher molecular-weight polymers with pentavalent phosphorus centers (**35**) was nevertheless possible by post-polymerization functionalization of the trivalent polymer **34** (Scheme 8).

In a subsequent paper, living anionic ROP was established to be an effective alternative toward high-molecular-weight poly(ferrocenylphosphanes) with trivalent P-centers.[35] In this case, polymerization was induced via addition of ^{n}BuLi at room temperature to yield monodisperse poly(ferrocenylphosphane) **37**

Copyright © 2013. Elsevier. All rights reserved.

Comprehensive Inorganic Chemistry II : From Elements to Applications, Elsevier, 2013. ProQuest Ebook Central, http://ebookcentral.proquest.com/lib/inflibnet-ebooks/detail.action?docID=1330977.
Created from inflibnet-ebooks on 2021-02-09 22:27:26.

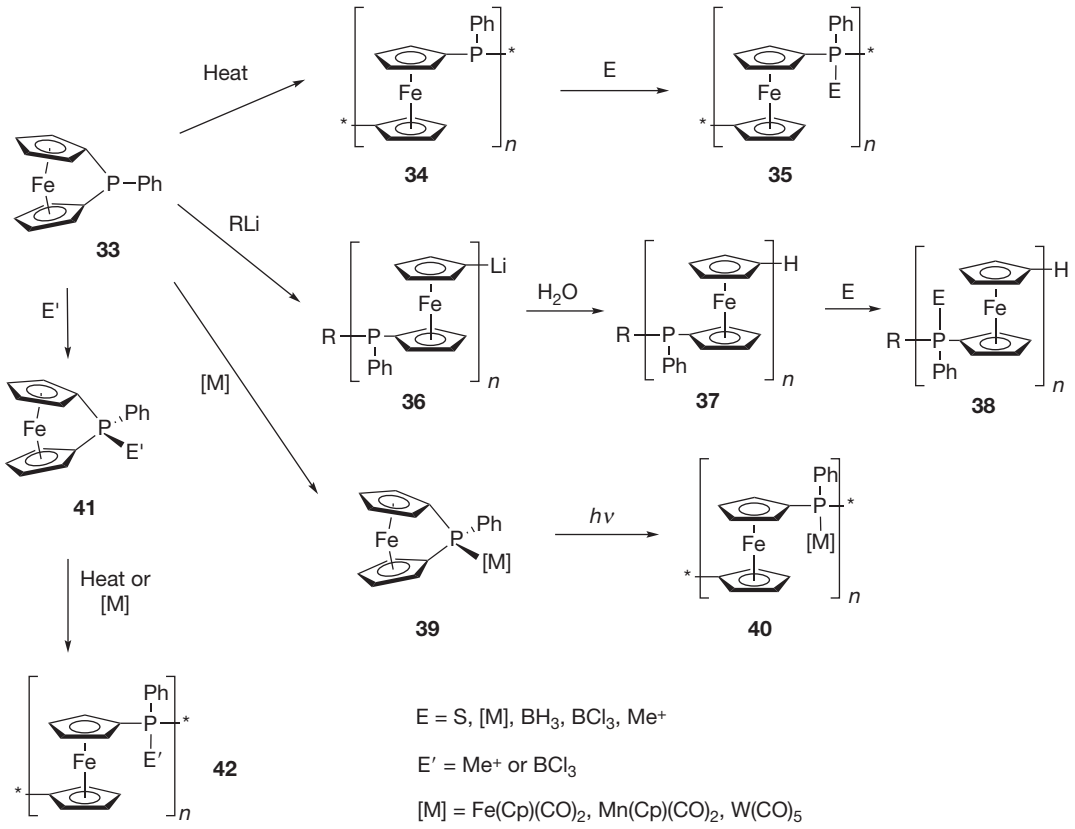

Scheme 8 Synthesis and P-modification of poly(ferrocenylphosphane)s.

of controlled molecular mass that depended on the amount of ^{n}BuLi employed. The molecular weights of the polymer **37** could be controlled from $M_n = 2400–36\,000$ g mol^{-1} with narrow polydispersities (PDI = 1.08–1.25) by varying the ^{n}BuLi:ferrocenophane ratio from 1:11 to 1:100. The preservation of the trivalent state of the P-centers in the polymers was confirmed by ^{31}P NMR spectroscopy, which showed a resonance at $\delta = -28.8$ ppm for the internal chain, as well as a resonance at $\delta = -31.1$ ppm for the terminal P-groups (in shorter polymers). Due to the living nature of the polymerization process, the active (i.e., lithiated) end of the growing polymer chain (**36**) could also be used for the synthesis of corresponding block copolymers (see below).

A third avenue toward high-molecular-weight poly(ferrocenylphosphane)s relies on a transition metal catalyzed ROP process. Miyoshi and coworkers reported that complexation of the trivalent phosphorus center in phospha[1]ferrocenophanes to a variety of transition metals (e.g., $FeCp(CO)_2$, $MnCp(CO)_2$, or $W(CO)_5$) results in species of type **39** that can be ring-opened upon irradiation with UV light (Scheme 8).[36] The initial step involves the insertion of the metal species into one of the P—C_{Cp} bonds. Similar results were reported by Manners et al. using sila[1]ferrocenophanes.[32] The polymers reported by Miyoshi (**40**) ranged in molecular weight from $M_w = 3700–22\,000$ g mol^{-1} and showed narrow polydispersities between PDI = 1.0 and 1.9, with the variations in the latter due primarily to variation in monomer purity. Importantly, irradiation of the noncomplexed ferrocenophane **33** only resulted in a mixture of short chains ($M_w = 1100$ g mol^{-1}), as well as the cyclic dimer and trimer, highlighting the necessity of the transition metal for successful high-molecular-weight polymer syntheses. On the other hand, transition-metal-catalyzed ROP is also possible using nonmetal, P-functionalized precursors **41** in the presence of a suitable Pt-catalyst, while trivalent species do not undergo ROP under the same conditions.[37] Both methylphosphonio[1]ferrocenophane and the related trichloroborane congener undergo transition-metal-catalyzed ROP (Scheme 8), although several side products, including the cyclic dimer, were also observed. It should be noted that both species of type **41** can also be polymerized using thermal ROP and that similar polymers are equally accessible using a postpolymerization approach with the trivalent P-polymer. Importantly, the latter route provides for flexible functionalization of the phosphorus centers in the polymers, depending on the amount of quaternizing agent (MeOTf) added.[37] Variation of the amount of borane reagent (BCl_3, BH_3) has not been reported, but complete conversion of all P-centers of the polymer was observed in the stoichiometric reaction.[37] Since the different environments of the phosphorus centers have significant impact on the photophysical and redox properties of the resulting polymers, pre- and post-polymerization functionalization in these systems clearly highlight the benefits of exploiting the versatile chemistry of phosphorus in the context of polymer chemistry.

As mentioned earlier, living anionic ROP of phospha[1]ferrocenophanes provides well-defined high-molecular-weight polymers that moreover possess an active terminus (**36**, Scheme 8). Manners and coworkers were able to exploit the living nature of the growing polymer chain to access a variety

Copyright © 2013. Elsevier. All rights reserved.

Comprehensive Inorganic Chemistry II : From Elements to Applications, Elsevier, 2013. ProQuest Ebook Central, http://ebookcentral.proquest.com/lib/inflibnet-ebooks/detail.action?docID=1330977.
Created from inflibnet-ebooks on 2021-02-09 22:27:26.

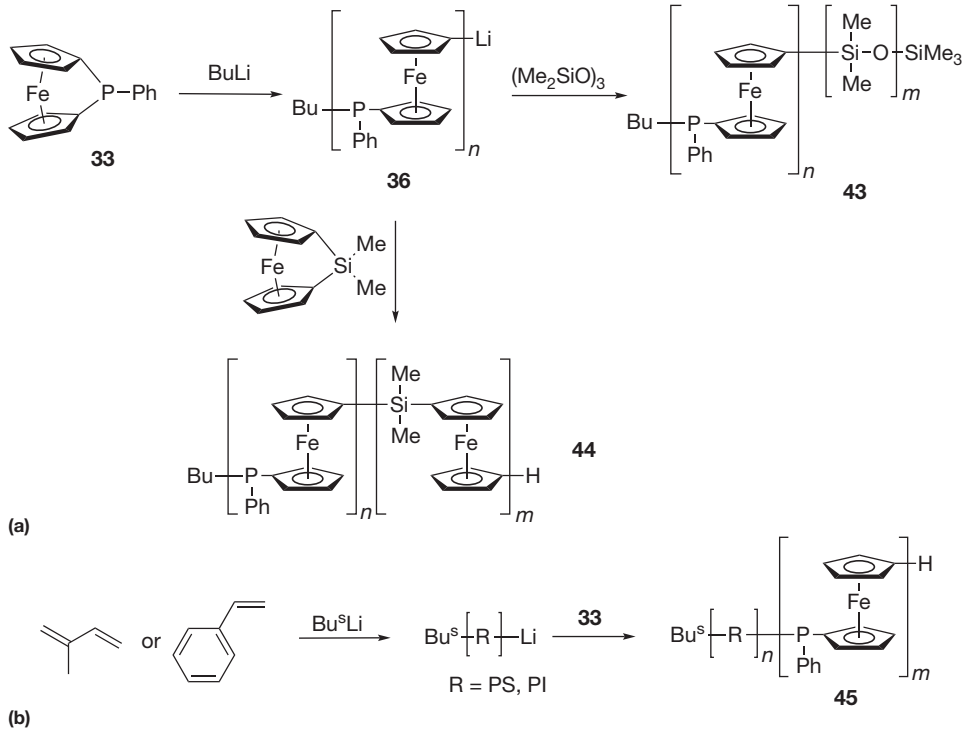

Scheme 9 Synthesis of poly(ferrocenylphosphane)-based block copolymers.

of block copolymers (Scheme 9).[38] It is well known that block copolymers will self-assemble into a variety of morphologies in solution and in the solid state due to the immiscibility of the constituting blocks, which makes them a particularly intriguing class of materials among polymers. Ferrocenylphosphane-containing block copolymers are accessible by either starting with the phosphorus-containing (PFP) block (Scheme 9(a)), as shown by the use of secondary dimethylsiloxane (PDMS) blocks for polymer **43** and ferrocenylsilane (PFS) blocks for polymer **44**[38] or by starting with an organic polystyrene (PS)[38] or polyisoprene (PI)[38] block (Scheme 9(b)) and continuing with the ferrocenylphosphane (PFP) as a secondary block to afford polymer **45**.

Both approaches successfully exploit the benefits of block copolymers by allowing for variation of the block length ratio, which has significant impact on the self-assembly behavior of such systems. For example, the PI-*b*-PFP block copolymers (**45**, R = PI) assemble into spherical micelles that can further be cross-linked with UV light due to the presence of additional double bonds in the PI block (Figure 5).[38]

Moreover, the trivalent nature of the phosphorus centers in **43** and **45** was shown to allow for post-polymerization functionalization with transition metals in the PFP block copolymers. However, according to ^{31}P NMR spectroscopy,[38] treatment of PFP-*b*-PDMS copolymers **43** with $Pd(COD)Cl_2$ and $Fe(CO)_4(THF)$ only resulted in ~20% coordination of the P-centers in the backbone. On the other hand, complexation of a PI-*b*-PFP block copolymer **45** with Au(CO)Cl was found to be quantitative (via ^{31}P NMR spectroscopy), and the resulting self-assembled micelles showed a significantly different morphology from those without coordinated-Au, again highlighting the high value of P-functionalization for polymeric systems.[38]

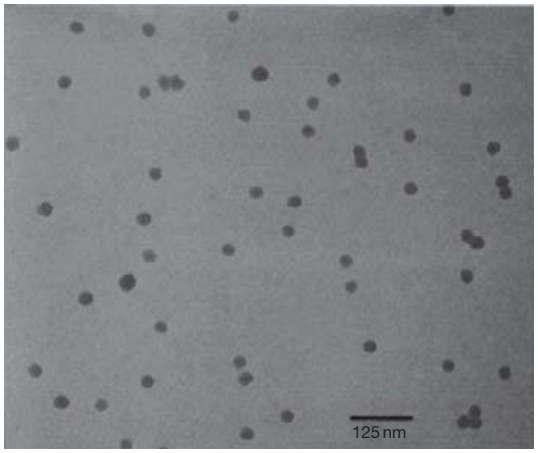

Figure 5 TEM image of PI_{140}-*b*-PFP_{82} micelles. Reprinted from Cao, L.; Winnik, M. A.; Manners, I. *Macromolecules* **2001**, *34*, 3353–3360. Copyright 2001 American Chemical Society.

1.28.4.3 Organophosphorus Polymers with π-Conjugation

Organic π-conjugated materials have a wealth of potential applications, not only in electronic devices such as molecular or polymer-based light-emitting diodes (OLEDs/PLEDs) for display or lighting applications, solar cells (OPV), field-effect transistors (FET), nonlinear optical (NLO) devices, but also in a variety of sensor applications.[39] The field of organic electronics is growing at a high pace, spurred by the sustained demand for new and improved electronics that are environmentally friendly. In the search for new avenues toward energy-efficient and tunable organic electronics, the incorporation of inorganic

Copyright © 2013. Elsevier. All rights reserved.

Comprehensive Inorganic Chemistry II : From Elements to Applications, Elsevier, 2013. ProQuest Ebook Central, http://ebookcentral.proquest.com/lib/inflibnet-ebooks/detail.action?docID=1330977.
Created from inflibnet-ebooks on 2021-02-09 22:27:26.

main-group elements into π-conjugated materials has recently created a promising, state-of-the-art perspective for the field.[40] Phosphorus-containing polymers represent one interesting facet of the diverse main group element-based materials currently being developed for this purpose. Beyond the unique properties expected from these materials, convenient access to such species continues to be a major focal point in research, as highlighted in the subsequent subsections.

1.28.4.3.1 Poly(arylphosphane)s

Polyaniline is one of the most intensively studied organic π-conjugated polymers and has long been known for its electroactive properties, as it can be reversibly doped to afford an electronically conductive state. Consequently, researchers have uncovered many interesting applications for polyaniline, including hole-transport layers in OLEDs and electrodes for rechargeable batteries, to name only a few.[39] Since the influence of the heteroatom is typically the result of the incorporation of a lone pair of electrons into the delocalized electronic system, researchers were interested in replacing the nitrogen atoms of polyaniline with its heavier congener phosphorus.

While Lucht and coworkers were the first to investigate the access and properties of phosphorus-analogue polyanilines systematically,[41] the first record of such polymers was actually reported by Novak et al. in 1997.[42] Their accidental discovery of phosphorus-containing polyphenylenes (**46**, **Scheme 10**) was a result of a failed Suzuki–Miyaura cross-coupling process involving functionalized biphenyl monomers in the presence of a triphenylphosphane-ligated Pd catalyst, which led to the interchange of P-phenyl moieties with the Pd-bound aryl moieties during the catalysis. Due to the relatively uncontrolled nature of this process, the materials obtained were ill-defined,

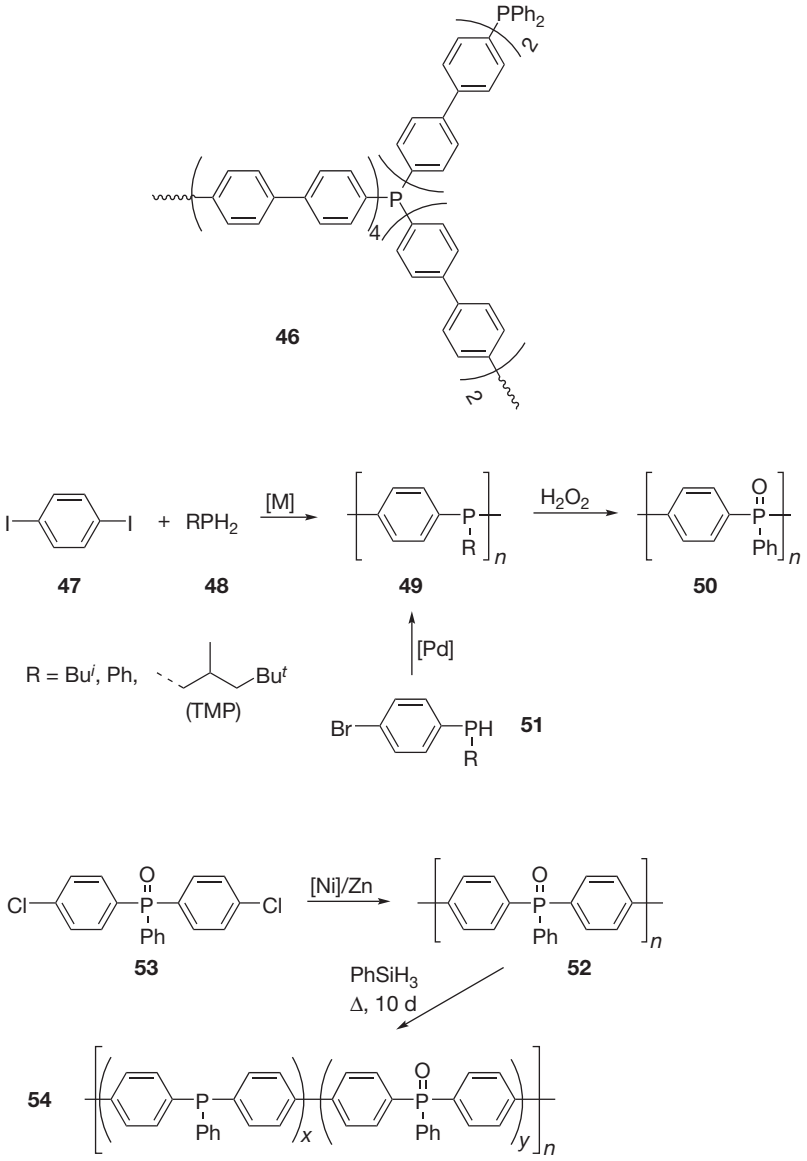

Scheme 10 Synthesis of poly(phenylenephosphane)s.

Copyright © 2013. Elsevier. All rights reserved.

Comprehensive Inorganic Chemistry II : From Elements to Applications, Elsevier, 2013. ProQuest Ebook Central, http://ebookcentral.proquest.com/lib/inflibnet-ebooks/detail.action?docID=1330977.
Created from inflibnet-ebooks on 2021-02-09 22:27:26.

but nevertheless showed some interesting properties in terms of their molecular weight and viscosity.[42]

Well-defined poly(aryl-*P*-alkylphosphane)s, on the other hand, were prepared by Lucht and coworkers via transition metal (Pd, Ni)-mediated coupling reactions, and the photophysical and electrochemical properties of the polymers were investigated (Scheme 10).[41]

Their initial study involved Buchwald–Hartwig-based conditions that provided low-molecular-weight polymers ($M_n = 1700–3100$ g mol^{-1}; PDI = 1.3–1.5) by the condensation polymerization of 1,4-diiodobenzene **47** with primary alkylphosphanes **48** (R = ^{i}Bu, Ph, 2,4,4-trimethylpentyl; TMP). The identity of the soluble polymers **49** was supported by ^{1}H, ^{31}P, and ^{13}C NMR spectroscopy and the broad resonances were consistent with the polymer structures anticipated. Notably, the trivalent P-species were found to be mildly sensitive toward oxidation in air, while the P-phenyl polymer could also deliberately be oxidized (**50**) via addition of H_2O_2. Higher molecular-weight, soluble polymers of type **49** were obtained via slightly modified polymerization conditions using hetero-bifunctional monomers **51** and a Pd catalyst in a Buchwald-type cross-coupling process, particularly without the presence of a solvent ($M_n = 1000–14\,000$ g mol^{-1}; PDI = 1.8–2.1).[41] The properties of the polymers were investigated with UV–vis–NIR spectroscopy, which suggested some degree of electronic delocalization along the polymer backbone through phosphorus by virtue of the red-shifted optical absorptions (R = ^{i}Bu, $\lambda_{max} = 274$ nm; R = TMP, $\lambda_{max} = 273$ nm; R = Ph, $\lambda_{max} = 291$ nm) compared with corresponding diphenyl model compounds (R = ^{i}Bu, TMP, $\lambda_{max} = 252$ nm; R = Ph, $\lambda_{max} = 263$ nm). Exposure to atmospheric oxygen shifts the absorption of polymer **49** (R = ^{i}Bu) bathochromically, as evidenced by the occurrence of shoulders at $\lambda_{max} = 370$ and 434 nm. Upon deliberate oxidation of the polymer (**50**, R = Ph), the absorption maximum clearly shifts to $\lambda_{max} = 434$ nm. Although cyclic voltammetry provided additional support for the electronic delocalization in the polymers via conjugation through phosphorus, the degree and type of overlap between the lone pair on phosphorus and the adjacent aromatic groups could not fully be determined from these studies.[41]

The synthesis of the peripherally related biphenyl-based polymers of type **52** (Scheme 10) has also been reported by the Lucht group.[41] Polymerization using *p*-bromophenyl-(alkyl)phosphanes (R = ^{i}Bu, TMP) as polymer precursors and Ni as a catalyst for a Yamamoto-type protocol, was found to be unsuccessful, leading only to mostly insoluble solids. Similarly, slight variation of the protocol/precursors involving the palladium-catalyzed cross-coupling of 4,4′-diiodobiphenyl with $TMPPH_2$ resulted in a poorly soluble low-molecular-weight polymer ($M_n = 3100$ g mol^{-1}). On the other hand, the use of the dichlorinated precursor bis(4-chlorophenyl) phenylphosphane oxide **53** in a Ni-catalyzed protocol, as reported by McGrath and Ghassemi, provided a high-molecular-weight polymer of type **52** with relatively narrow weight distribution ($M_n = 15\,300$ g mol^{-1}; PDI = 1.65).[43] The results are remarkable insofar as the latter polymer does not exhibit a solubilizing group at the P-center and the polar nature of the P═O bond adjacent to the sterically hindered P-center seemed to provide sufficient solubility despite the rigidity of the polymer backbone. Moreover, it is possible to reduce the phosphorus centers in the polymer with an excess of $PhSiH_3$. However, even after 10 days at 110 °C, conversion to the trivalent polymer was incomplete; according to ^{31}P NMR spectroscopy, only ~34% of the phosphorus centers in **54** were reduced. In terms of optical properties, the polymer showed comparable features as those previously reported by Lucht et al.[41] The fully oxidized species **52** showed an absorption maximum at $\lambda_{max} = 280$ nm that shifted bathochromically in the mixed P(III)/P(V) polymer **54** ($\lambda_{max} = 300$ nm) due to the donor–acceptor nature of these centers. Again, the relatively high-energy absorption values indicate that the polymer does not demonstrate efficient delocalization of the π-electrons along the polymer backbone. In line with the polymers described in Section 1.28.2, polymer **52** is quite robust thermally, exhibiting a glass transition temperature around 365 °C and 5% weight loss around 550 °C in nitrogen and air. Upon heating to 750 °C in air, the polymer produces a significant amount of char (35%).[43]

In a subsequent publication in 2005, Jin and Lucht have reported hybrid-systems that include aniline and phenylphosphane building blocks (**55–57**), which were expected to show improved electronic delocalization (Scheme 11).[41] The synthesis of these polymers involved a variety of differently (symmetrically or unsymmetrically) functionalized monomer precursors that resulted in a set of polymers with slightly different P/N-sequences. A Pd-catalyzed Buchwald-type protocol with DABCO as base provided the polymers in decent to high-molecular-weights with narrow polydispersities (**55**: $M_w = 3000$, PDI = 1.5; **56**: $M_w = 5000$, PDI = 1.6; **57**: $M_w = 11\,000$, PDI = 1.9) in low to moderate yields (30–50%). However, these polymers were obtained next to significant amounts of insoluble material.

The identity of the soluble polymers was confirmed by multinuclear NMR spectroscopy, and their ^{31}P NMR spectra support the presence of trivalent phosphorus centers ($\delta^{31}P \approx -22$ ppm). Consequently, Pd-catalyzed P–C coupling appears to be an efficient synthetic methodology toward polyanilines bearing P(III) moieties in the main conjugated chain. The spectroscopic and electronic properties of the materials were investigated via UV–vis–NIR spectroscopy and cyclic voltammetry. The P/N-aniline hybrid copolymers **55–57** exhibit electronic and spectroscopic features that resemble those of *p*-phenylene diamines with aryl substituents. While copolymers containing two neighboring P-centers between the amino-bridged units (**57**) show evidence for weak electronic delocalization along the polymer chain, the electrochemical and spectroscopic properties support strong electronic delocalization in copolymers containing consistently alternating P/N repeat units (**55**, **56**). Cyclic voltammetry of copolymers **55**, **56** and **57** provides evidence for multiple oxidations and revealed that the N-atoms are oxidized at lower potentials than the trivalent P-atoms. In other words, the presence of a single diphenylphosphane bridge between nitrogen centers provides an efficient mode of electronic delocalization between nitrogen centers.

Moreover, the trivalent P-centers can be further modified, as exemplified by their oxidation with H_2O_2 (Scheme 11), for which complete conversion was confirmed by ^{31}P NMR spectroscopy ($\delta^{31}P \approx 32$ ppm). Cyclic voltammetry revealed a resemblance of the P-oxidized copolymers to isolated *p*-phenylene diamines or triarylamines, as equivalence of the

Copyright © 2013. Elsevier. All rights reserved.

Comprehensive Inorganic Chemistry II : From Elements to Applications, Elsevier, 2013. ProQuest Ebook Central, http://ebookcentral.proquest.com/lib/inflibnet-ebooks/detail.action?docID=1330977.
Created from inflibnet-ebooks on 2021-02-09 22:27:26.

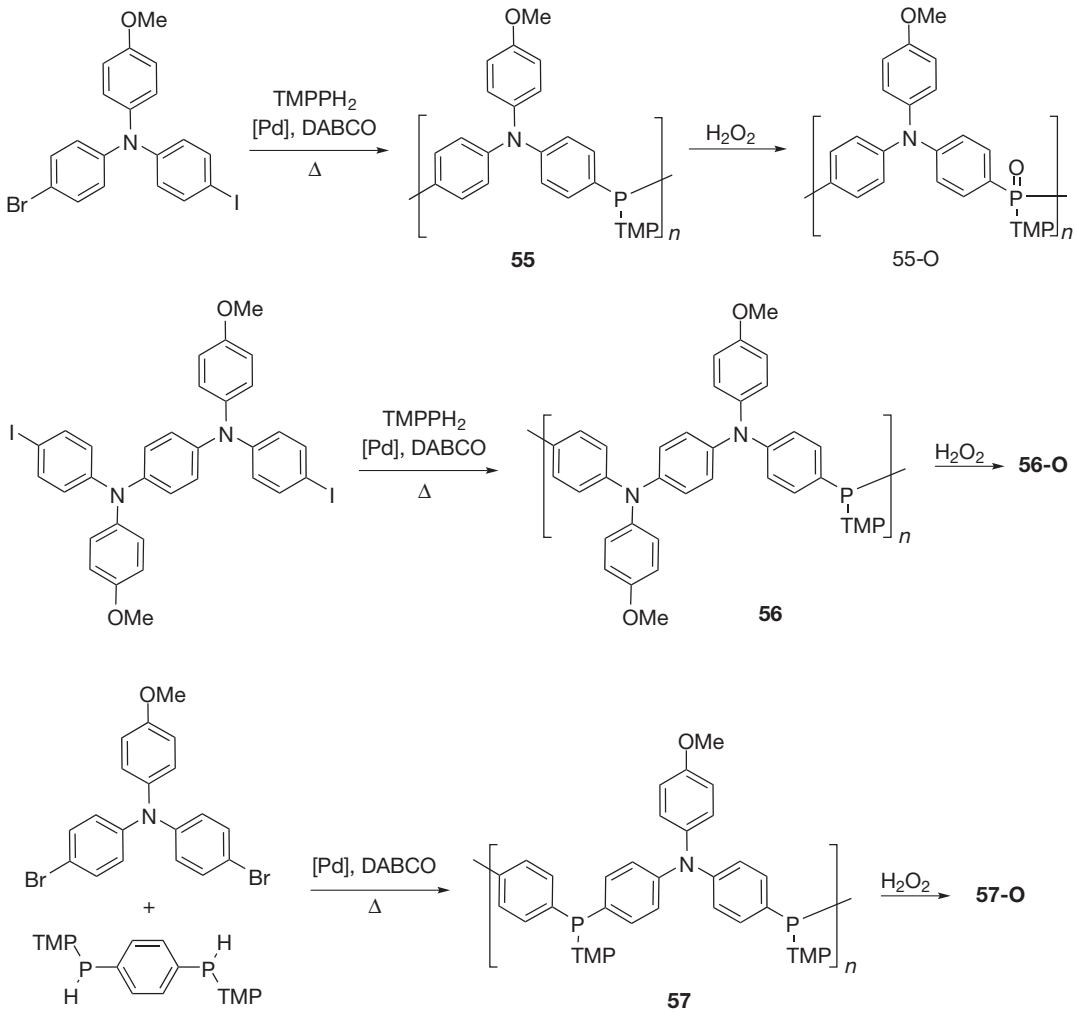

Scheme 11 Synthesis and oxidation of aniline-phenylphosphane hybrid polymers.

oxidation potentials of the other oxidized polymers **56-O** and **57-O** suggests electronic isolation of the amine fragments in the polymer. The conversion of the P(III) centers to P(V) centers inhibits electronic delocalization through phosphorus, as evidenced by the large shift in oxidation potentials observed upon its conversion to **55-O**. This observation clearly supports the delocalization of the lone pair of electrons on phosphorus in copolymers with trivalent P-centers. Optical spectroscopy studies further support the conclusions drawn from the electrochemical studies: Conversion of P(III) phosphane centers to P(V) phosphane oxides switches off electronic delocalization through the P-moieties.

Furthermore, the versatile chemistry of phosphorus allows access to poly(arylphosphane)s via quaternization of functionalized bisphosphanes, as shown by Smith and coworkers in 2010.[44] This strategy bears several benefits: in addition to phosphonium linkages commonly being formed in high yield, the resulting phosphonium salts are generally air-stable, thermally robust, and even water-soluble. Furthermore, corresponding polyelectrolytes are intriguing candidates for application in biomedical sensing and optoelectronics, as well as for building blocks in layer-by-layer self-assembled materials.[45]

Using the phenyleneethynylene–diphosphane chromophore **58**, polymerization can be induced by reaction with an appropriate dibromoxylene **59** used in 10% excess to limit the polymer molecular weight and favor the material's overall solubility for further studies (Scheme 12).[44]

Formation of the polymer **60** was monitored by ^{31}P NMR spectroscopy via the disappearance of the monomer signal at $\delta = -4.6$ ppm and the emergence of the phosphonium signal, with a typical low field-shifted resonance at $\delta = 22.1$ ppm. The broad ^{31}P NMR signal further indicated the presence of a polymeric material, confirmed by GPC, which indicated a molecular weight of $M_n = 24\,000$ g mol^{-1}. The bright orange polymer **60** was found to form highly fluorescent films readily and was soluble in both a diverse set of organic solvents, as well as water, due to its amphiphilic nature. The amphiphilic character of the polymer was further evidenced by its solvatochromism. Depending on the solvent polarity, the absorption maxima showed small shifts between $\lambda_{max} = 390$–396 nm, while the intense fluorescence emission covered a larger range between $\lambda_{em} = 475$–510 nm. Moreover, the polymer showed excellent layer-by-layer self-assembly features when paired with polyacrylic acid, forming uniform bilayer films with low

Copyright © 2013. Elsevier. All rights reserved.

Comprehensive Inorganic Chemistry II : From Elements to Applications, Elsevier, 2013. ProQuest Ebook Central, http://ebookcentral.proquest.com/lib/inflibnet-ebooks/detail.action?docID=1330977.
Created from inflibnet-ebooks on 2021-02-09 22:27:26.

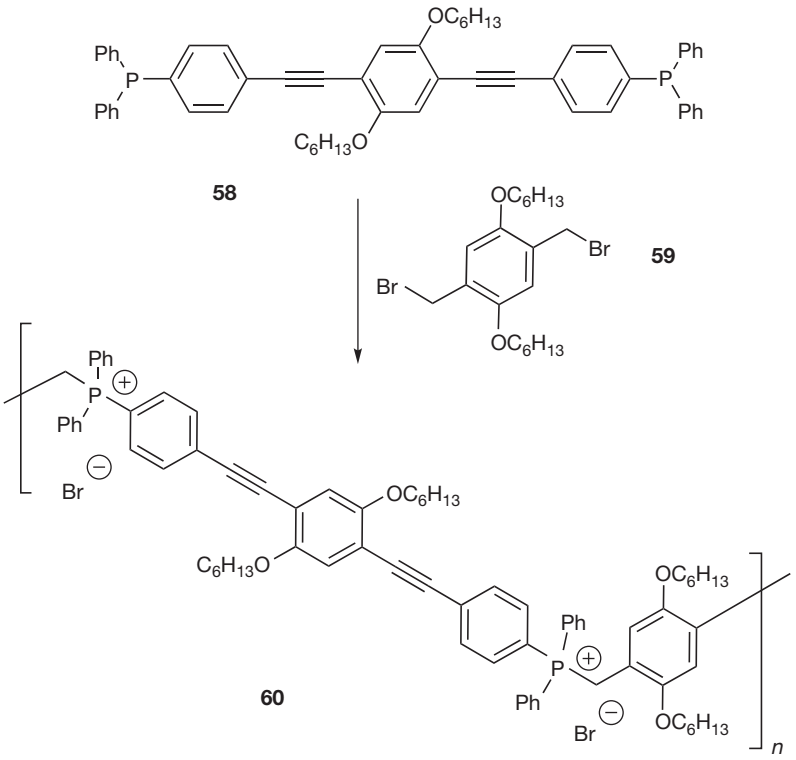

Scheme 12 Synthesis of a poly(arylphosphane) via quaternization of phosphorus.

root mean square roughness and without observable point defects as determined by atomic force microscopy (AFM).

1.28.4.3.2 Poly(vinylphosphane)s

Poly(vinylphosphane)s and their oxidized P(V) congeners have been the topic of a series of recent papers primarily focused on their general accessibility, as the resulting polymers are expected potentially to benefit from extended conjugation and, in consequence, interesting electronic properties. In this context, two major routes have been recognized to lead successfully to this type of polymer: hydrophosphorylation/phosphination or ring-opening/ring-collapsed polymerization of suitable organophosphorus precursors. The first record of poly(vinylphosphane)s, made by Han et al.,[46] uses hydrophosphorylation, which has also been established to be a powerful route toward several phosphorus-containing molecular conjugated ring systems in recent years.[47] Corresponding polymers **61a/b** are accessible using appropriately functionalized bisphosphorylated building blocks **62** with a variety of aromatic spacer units in conjunction with suitable diynes **63** in the presence of a catalyst (Scheme 13).

Notably, depending on the metal used in the catalysis, the P—H bond undergoes either 1,2-addition (i.e., Markovnikov; via $RhBr(PPh_3)_3$) or 2,1-addition (i.e., anti-Markovnikov; via $Ni(PPhMe_2)_4/Ph_2P(O)OH$) to the alkynes yielding polymers **61a/b** with high-molecular-weights of $M_n = 19\,500$–$101\,700$ g mol^{-1} and relatively narrow polydispersities (PDI = 1.21–2.43). The regioselectivity of the addition was unambiguously supported using terminal acetylenes to afford corresponding monomeric model compounds. The study furthermore confirmed that the resulting polymers exhibited good thermal stability, with 5% weight losses above 350 °C.

A more sophisticated approach using hetero-bifunctional monomers for the synthesis of poly(vinylphosphane)s was reported Greenberg and Stephan.[48] In their studies, they were able to show that a bulky secondary phosphane with an alkynyl substituent (**64**) could also undergo polymerization via hydrophosphination (Scheme 14). However, among the products of the room-temperature, ^{n}BuLi-initiated reaction were cyclic systems with up to eight repeat units, as confirmed by MALDI-TOF mass spectrometry. Gel permeation chromatography using a light scattering detector further supported the identification of additional higher-molecular-weight fractions within the product mixture, with $M_n = 21\,000$ g mol^{-1} (~70 repeat units). Since corresponding end-groups could not be detected via NMR spectroscopy, the molecular weight distributions led the authors to conclude that the products of the hydrophosphination were ring systems (**65**) of varying size.

However, the disappearance of the ^{31}P NMR resonance at $\delta = -99$ ppm and the emergence of a broad signal at $\delta = -20$ ppm not only confirmed the polymerization in solution, but also showed that the phosphorus centers remain in their trivalent state under these conditions. The trivalent P-centers in **65** could subsequently be reacted with elemental sulfur to provide the P(V)-species **65-S**, with minimal chain degradation as indicated MALDI-TOF mass spectrometry and GPC. Hydrophosphination could be proposed to follow either radical or ionic pathways; as such, the mechanism of the polymerization was probed experimentally, as well as by means of DFT calculations. A radical mechanism was

Copyright © 2013. Elsevier. All rights reserved.

Comprehensive Inorganic Chemistry II : From Elements to Applications, Elsevier, 2013. ProQuest Ebook Central, http://ebookcentral.proquest.com/lib/inflibnet-ebooks/detail.action?docID=1330977.
Created from inflibnet-ebooks on 2021-02-09 22:27:26.

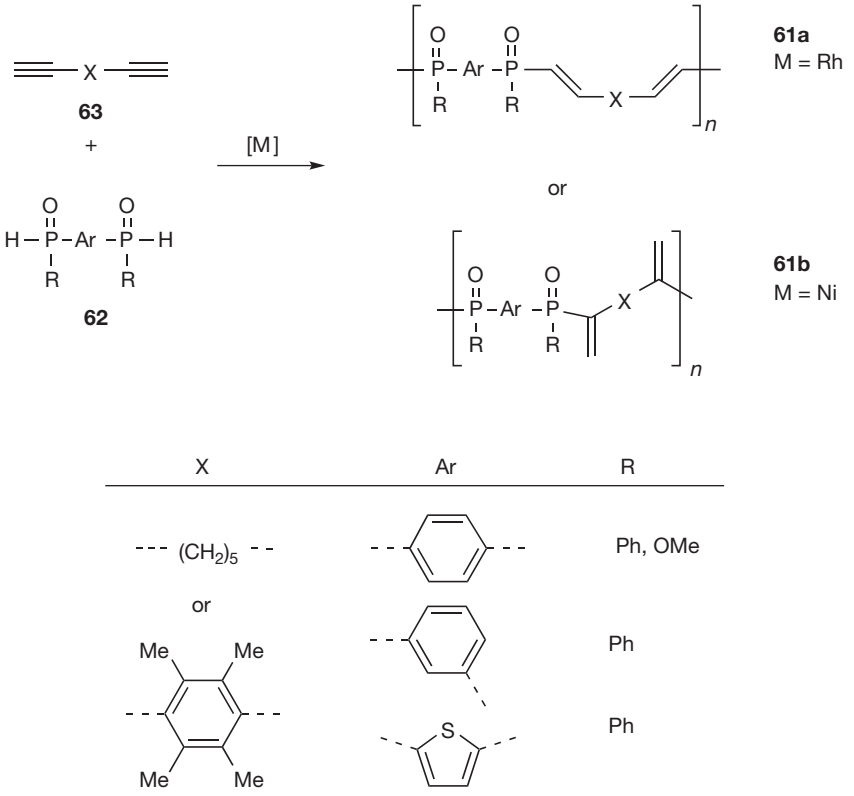

Scheme 13 Synthesis of poly(vinylphosphane)s via hydrophosphorylation.

eliminated based on the absence of detectable polymerization in the presence of the radical initiator azobis(isobutyronitrile) (AIBN). A more likely scenario, supported by DFT models, is an ionic route involving attack of a phosphide on the alkyne, with subsequent protonation of the resulting β-carbanion by a second phosphane, to regenerate the phosphide.

Manners, Lammertsma and coworkers have reported the synthesis of poly(vinylphosphane) **66** via ROP of strained phosphirene **67** that can be ring-opened anionically upon exposure to a catalytic amount of ^{n}BuLi at room temperature (Scheme 14).[49] Notably, the stoichiometric version of this reaction had been previously reported by Mathey in the 1980s.[50] From those studies it was known that the ring-opening reaction does not proceed under stereochemical control, and both *cis*- and *trans*-configured double bonds are formed, despite the well-defined architecture of the ring system; as such, the mechanism likely involves an allene intermediate.[50] While reaction of 1,2,3-triphenylphosphirene did not proceed beyond the ring-opened monomer due to the steric bulk of its substituents, the corresponding P-phenyl dimethylphosphirene (**67**) underwent ROP to provide a polymer (**66**) with molecular weights up to $M_n = 18\,000$ g mol^{-1} and narrow polydispersities (PDI = 1.23–1.58) that both depended on the monomer/initiator ratio. Molecular weights were determined for the air-stable sulfurized polymer (**66-S**), accessed through quantitative sulfurization of the trivalent polymer. In terms of microstructure, both *cis*- and *trans*-configured double bonds could be found in the trivalent polymer, as indicated by the two distinct ^{31}P NMR resonances at $\delta = -5.1$ and -9.6 ppm in a ratio of 0.65/0.35 (*cis*/*trans*), in line with the monomeric species reported earlier.

In a somewhat related approach, Naka and coworkers have reported access to poly(vinylphosphane)s using ring-collapsed radical alternating copolymerization (RCRAC) of pentamethylcyclopentaphosphane cyclo-(PMe)$_5$ and phenylacetylene (Scheme 14).[51] This work builds upon earlier studies by the same group that involved the corresponding cycloarsanes and stibanes.[52] In a radical protocol initiated by AIBN, cyclo-(PMe)$_5$ (**68**) and phenylacetylene (**69**) were refluxed in benzene to provide the polymer **70** as light yellow powder in the absence of air. GPC analysis indicated a low-molecular-weight of $M_n = 2500$ g mol^{-1} with a PDI of 1.25; despite the low weight, the degree of polymerization (DP) still corresponds to 16 repeat units. The ^{31}P NMR resonance for the polymer at $\delta = -28$ ppm supports the preservation of the trivalent P-centers, and ^{1}H NMR spectroscopy indicated that predominantly *trans*-configured double bonds were formed in the process. While the polymer was found to be reasonably stable to air and moisture in the solid state, its $CHCl_3$-solution showed a significant degree of oxidation after 12 h. Longer exposure even led to the degradation of the polymer backbone, as indicated by GPC. Sulfurization, on the other hand, could be performed to provide **70-S** without the degradation of the polymer backbone. The trivalent polymer **70** was furthermore examined by optical spectroscopy and showed a blue/green fluorescence emission at $\lambda_{em} = 470$ nm with a shoulder at 500 nm upon excitation at $\lambda_{ex} = 430$ nm, indicating some degree of delocalization along the polymer backbone. These results are in line with those for the corresponding

Copyright © 2013. Elsevier. All rights reserved.

Comprehensive Inorganic Chemistry II : From Elements to Applications, Elsevier, 2013. ProQuest Ebook Central, http://ebookcentral.proquest.com/lib/inflibnet-ebooks/detail.action?docID=1330977.
Created from inflibnet-ebooks on 2021-02-09 22:27:26.

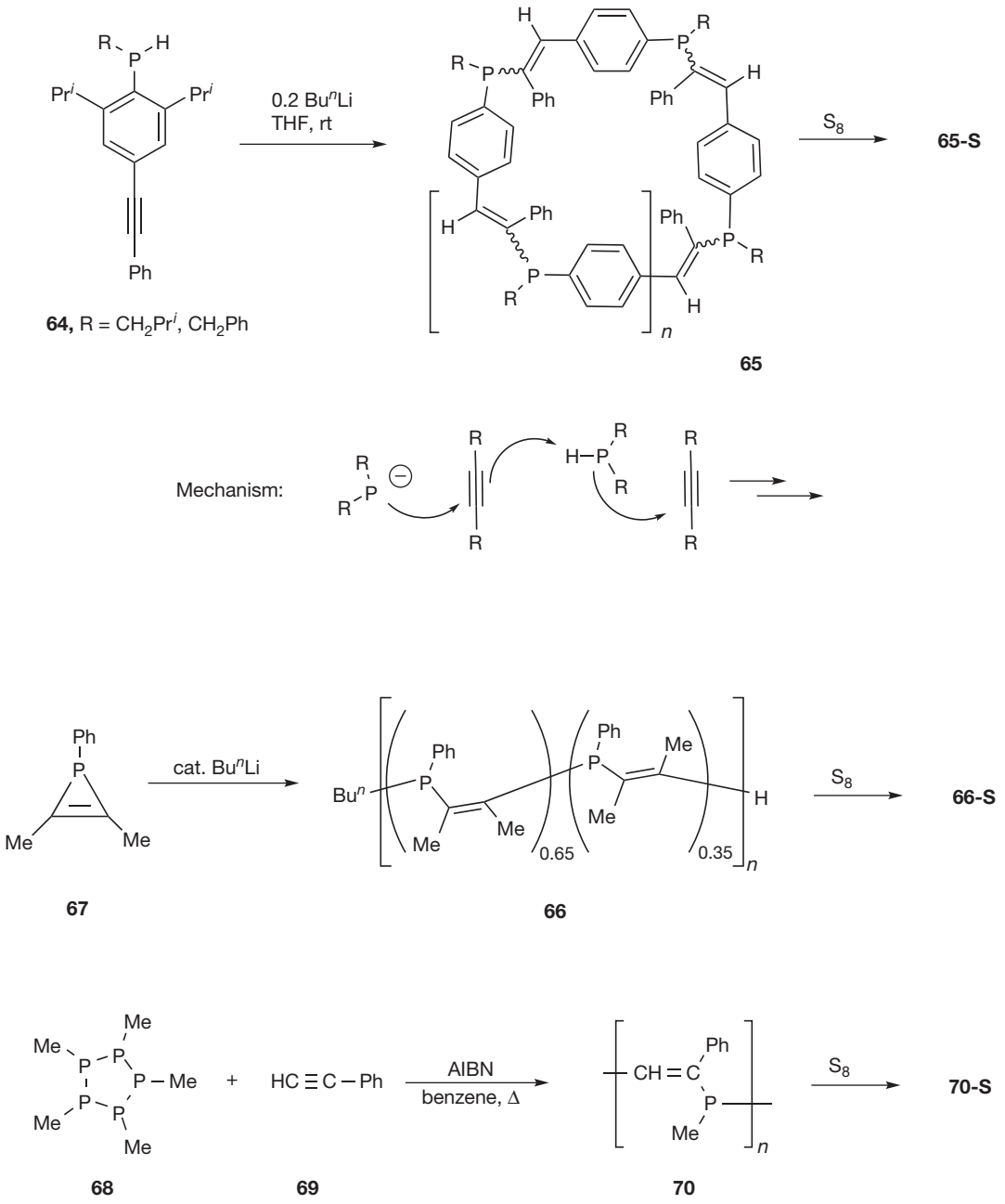

Scheme 14 Synthesis of poly(vinylphosphane)s via hydrophosphination (top), ring-opening (center), and ring-collapsing (bottom) polymerizations.

As-based polymer.[51] Extension of this polymerization method to other unsaturated monomers, particularly electron-withdrawing acetylenes that had been used successfully with the heavier congeners, did not yield any useful results in the case of the phosphorus species.

1.28.4.3.3 Polymers with low-coordinate phosphorus units

While the chemistry of tricoordinate, trivalent phosphorus still shows many parallels to that of its congener, nitrogen, the chemistry of low-coordinate phosphorus compounds deviates sharply from this behavior. Extensive research over the past 40 years has clearly established that low-coordinate phosphorus species mimic the chemistry of carbon more closely, a fact that ultimately led to the aforementioned designation of phosphorus as a carbon copy.[1] To emphasize this dramatic change, the chemistry of such compounds is now often referred to as phosphaorganic rather than organophosphorus.[2] In this context, studies involving molecular systems have, for example, established that alkenes and the corresponding phosphaalkenes with P=C double bond exhibit quite similar frontier orbitals, despite the bond energy of P=C (180 kJ mol^{-1}) being somewhat weaker that C=C (272 kJ mol^{-1}).[2] This similarity has recently been identified as an intriguing entry point into phosphaorganic polymer chemistry.

Copyright © 2013. Elsevier. All rights reserved.

Comprehensive Inorganic Chemistry II : From Elements to Applications, Elsevier, 2013. ProQuest Ebook Central, http://ebookcentral.proquest.com/lib/inflibnet-ebooks/detail.action?docID=1330977.
Created from inflibnet-ebooks on 2021-02-09 22:27:26.

Among the most successful conjugated organic polymers for organic electronics are poly(*p*-phenylenevinylene)s (PPVs) that are highly luminescent and thus of interest for a variety of practical applications.[39] The P—C analogy thus prompted the research groups of Gates and Protasiewicz to investigate the synthesis and properties of corresponding phospha-PPV systems independently.[53,54] In 2002, the Gates group reported the first example of a phospha-PPV (**71**), utilizing a strategy developed by Becker et al. for the synthesis of molecular phosphaalkenes.[53]

The protocol makes use of a [1,3]-silatropic rearrangement of an acyl phosphane at elevated temperatures (Scheme 15, inset). In order to access the corresponding polymeric systems, Gates and coworkers developed appropriately difunctionalized monomers **72** and **73** that balance reactivity with the necessity for kinetic stabilization of the product polymer (Scheme 15).[53] The synthesis was found to proceed best without the addition of a solvent in a vacuum-sealed pyrex tube held just above the melting point of the two starting materials. The viscous polymer **71** that was obtained was characterized by multinuclear NMR

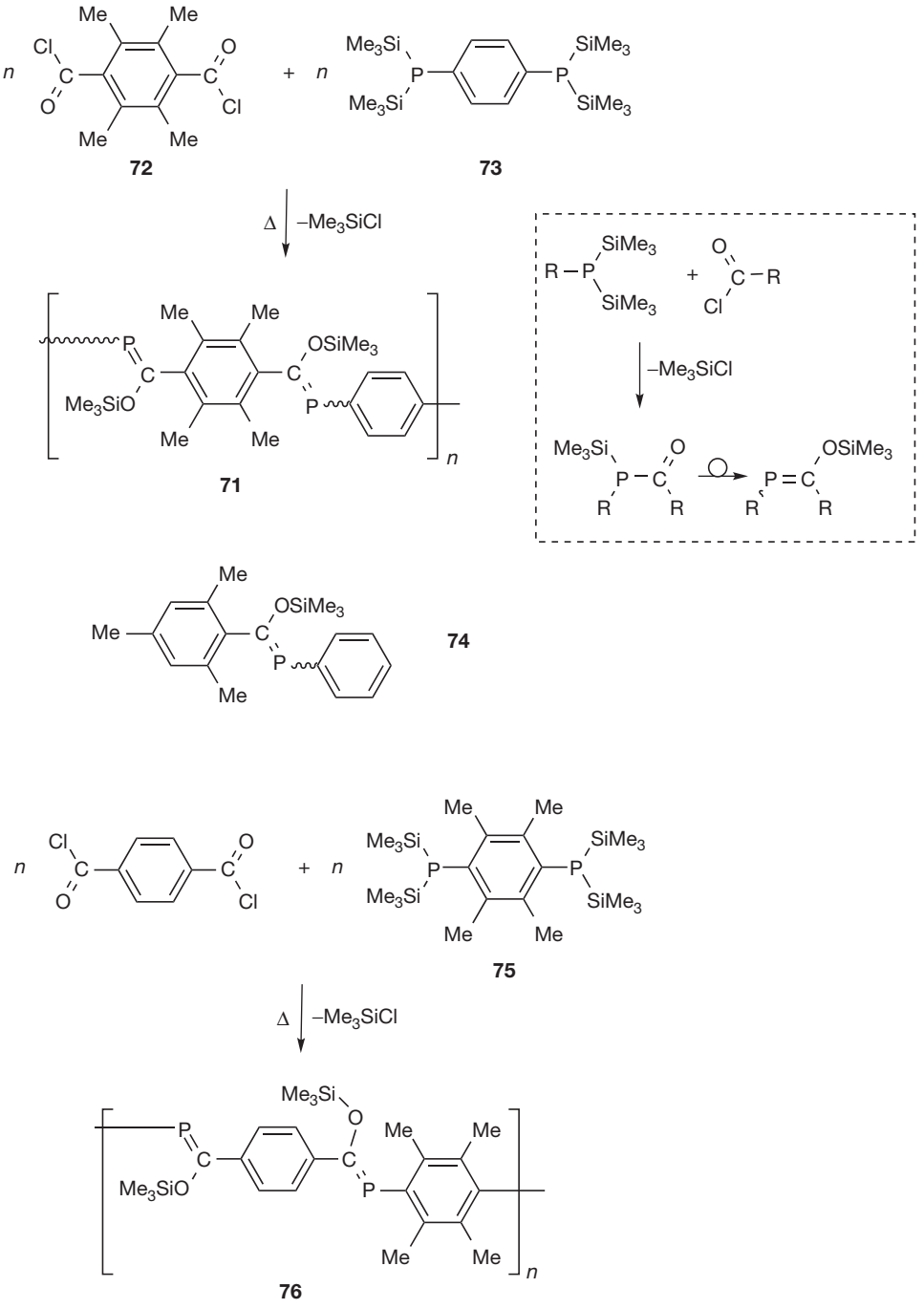

Scheme 15 Synthesis of phospha-PPVs via the Gates route.

Copyright © 2013. Elsevier. All rights reserved.

Comprehensive Inorganic Chemistry II : From Elements to Applications, Elsevier, 2013. ProQuest Ebook Central, http://ebookcentral.proquest.com/lib/inflibnet-ebooks/detail.action?docID=1330977.
Created from inflibnet-ebooks on 2021-02-09 22:27:26.

spectroscopy, indicating molecular weights of up to $M_n = 10\,500$ g mol^{-1} estimated though end-group analysis using ^{31}P NMR spectroscopy. Multinuclear NMR spectroscopy further revealed the presence of both *Z*- and *E*-configured P═C bonds, as evidenced by the two broad overlapping signals for the phosphorus- as well as silicon-functional groups. UV–vis spectroscopy indicated some degree of conjugation in the polymer, as the absorption maximum for the polymer ($\lambda_{max} = 333$ nm) was red-shifted with respect to corresponding monomer model compound **74** ($\lambda_{max} = 310$ nm). However, the red shift was much less pronounced than that observed for the native, carbon-based PPV congener (cf. $\Delta\lambda_{max} = 119$ nm vs. stilbene). More detailed studies involving corresponding model compounds with well-defined configurations revealed that the positioning of the bulky substituents is crucial for stereochemical control and, consequently, the degree of conjugation. When placing the bulky *ortho*-dimethylated subsituent at the P-center (**75**), the *Z*-isomer (with both aryl groups *trans* to each other) is formed exclusively, a feature which is also successfully transferred to the corresponding polymer architecture in **76** (Scheme 15). Importantly, the stereospecific, *Z*-configured model compounds and the polymer **76** show significantly red-shifted absorption maxima relative to the *E*/*Z*-mixture of **71**, suggesting improved conjugation in the former. In comparison to the monomeric model compound **74**, the exclusively *Z*-configured polymer shows a red shift of $\Delta\lambda_{max} = 70$ nm, suggesting extended conjugation along its backbone.

In 2003, Protasiewicz and coworkers reported a different strategy towards phospha-PPVs, which builds instead upon the phospha-Wittig reaction that this group had developed previously.[54] Starting from an appropriately substituted dichlorophosphane **77**, reaction with elemental Zn and PMe_3 provides access to a bis(phosphinidenephosphorane) **78** that undergoes near quantitative exchange reactions with aldehyde species, as first confirmed by the synthesis of bis(phosphaalkene)s **79** (Scheme 16).[54]

For the generation of corresponding polymeric systems (**80**), suitably functionalized conjugated dialdehydes **81** were used, resulting in highly colored polymers.[54] However, only the orange-colored hexyloxy-substituted phenyl species (**80d**) showed any appreciable solubility in common organic solvents to allow for comprehensive characterization. The existence of two broad resonances in the ^{31}P NMR spectrum of the polymer **80d**, representing internal as well as terminal P═C signals, supported the polymeric nature of the obtained material. End-group analysis of the phosphaalkene ^{1}H NMR resonances versus the terminal aldehyde protons supported a low-molecular-weight of M_n 6500 g mol^{-1}, corresponding to a degree of polymerization of 6. Significantly, the phospha-Wittig reaction selectively provides *E*-configured phosphaalkenes, that is, species with both aryl groups oriented *trans* to each other, which offered significant benefits in terms of conjugation, as established by Gates et al.[53] The increased conjugation along the polymer backbone of **80d** was supported by optical spectroscopy that showed a substantial red shift of the π–π^* transition ($\lambda_{max} = 445$ nm), compared to the *Z*-configured phospha-PPV **76** reported by Gates ($\lambda_{max} = 394$ nm)[53] and even to native carbon-based PPV systems ($\lambda_{max} = 426$ nm).[55] Notably, while the absorption maximum of the polymer **80d** is similar to that of a related model compound, its broader absorption has a significantly bathochromically shifted onset, which is responsible for the bright coloration of the polymer. Although the model compound and the polymer showed some fluorescence, both were much weaker than that of the all-carbon analogues, an effect attributed to quenching by the phosphorus lone pair.[54] Due to the kinetic stabilization of the low-coordinate phosphorus units with bulky substituents, the polymer showed a good degree of air stability in the solid state, as confirmed via ^{31}P NMR spectroscopy. Even after exposure to air for 1 week, no oxidation could be detected.

To improve the molecular weights of the phospha-PPV polymers, Smith and Protasiewicz developed a second-generation phospha-Wittig reagent **82**, which incorporates a π-conjugated oligo(phenylenevinylene) unit with built-in solubility by virtue of two hexyloxy groups (Scheme 16, bottom).[54] Reaction of the extended monomer with appropriately conjugated aldehydes **83** provided good yields (76-85%) of three orange or violet polymers **84** that were thermally stable in the absence of air and water. Polymer molecular weights were again estimated via NMR end-group analysis, revealing moderate chain lengths ($M_n = 5000$–7300 g mol^{-1}). Due to the nature of the constituent monomers, the resulting polymers exhibited around 18–26 phenylenevinylene repeat units, corresponding roughly to the effective conjugation length commonly observed in the PPV system.[39] In other words, extension of the polymer chain is unlikely to yield materials with smaller bandgaps, although this theory has not been confirmed to date. The absorption maxima at $\lambda_{max} = 416$–435 nm for the three polymers are blue-shifted to that of the phospha-PPV reported earlier by the same group.[54] In line with their earlier observations, the new polymers also showed some weak fluorescence ($\lambda_{em} = 481$–486 nm). Remarkably, however, the second-generation extended phospha-Wittig reagent **82** can also be used for the (near) quantitative synthesis of P═P-bridged homopolymers **85** via dimerization of transient phosphinidene species.[54] The latter can either be generated photolytically or thermolytically, with thermal conditions providing a more defined polymer and fewer side products in a very fast reaction (complete conversion after ~2 min). The molecular weight of the diphospha-PPV **85** was estimated via end-group analysis as $M_n = 6500$ g mol^{-1}. The P═P-PPV polymer **85** was found to show a red-shifted absorption at $\lambda_{max} = 445$ nm compared to that of the other three P═C-PPV polymers of type **84**, and the fluorescence emission intensity ($\lambda_{em} = 545$ nm) was further reduced due to the presence of additional P-centers.

To gain deeper insight into the effect of the phosphorus atoms on the photophysical properties and the degree of conjugation in the PPV-analogues, Smith and Protasiewicz have subsequently synthesized a series of oligomeric systems **86** with an increasing number of repeat units, as well as variation in the quantity and position of phosphorus centers in the vinylene bridges (Figure 6).[54]

This structure–property study revealed that low-coordinate P-centers could indeed support conjugation across extended systems. As can be seen in Table 1, there is a noticeable red shift in the materials that correlates with the increasing number of phosphorus centers. The notable differences that can also be observed between the native organic systems and their phosphorus-analogs can largely be attributed to the steric

Copyright © 2013. Elsevier. All rights reserved.

Comprehensive Inorganic Chemistry II : From Elements to Applications, Elsevier, 2013. ProQuest Ebook Central, http://ebookcentral.proquest.com/lib/inflibnet-ebooks/detail.action?docID=1330977.
Created from inflibnet-ebooks on 2021-02-09 22:27:26.

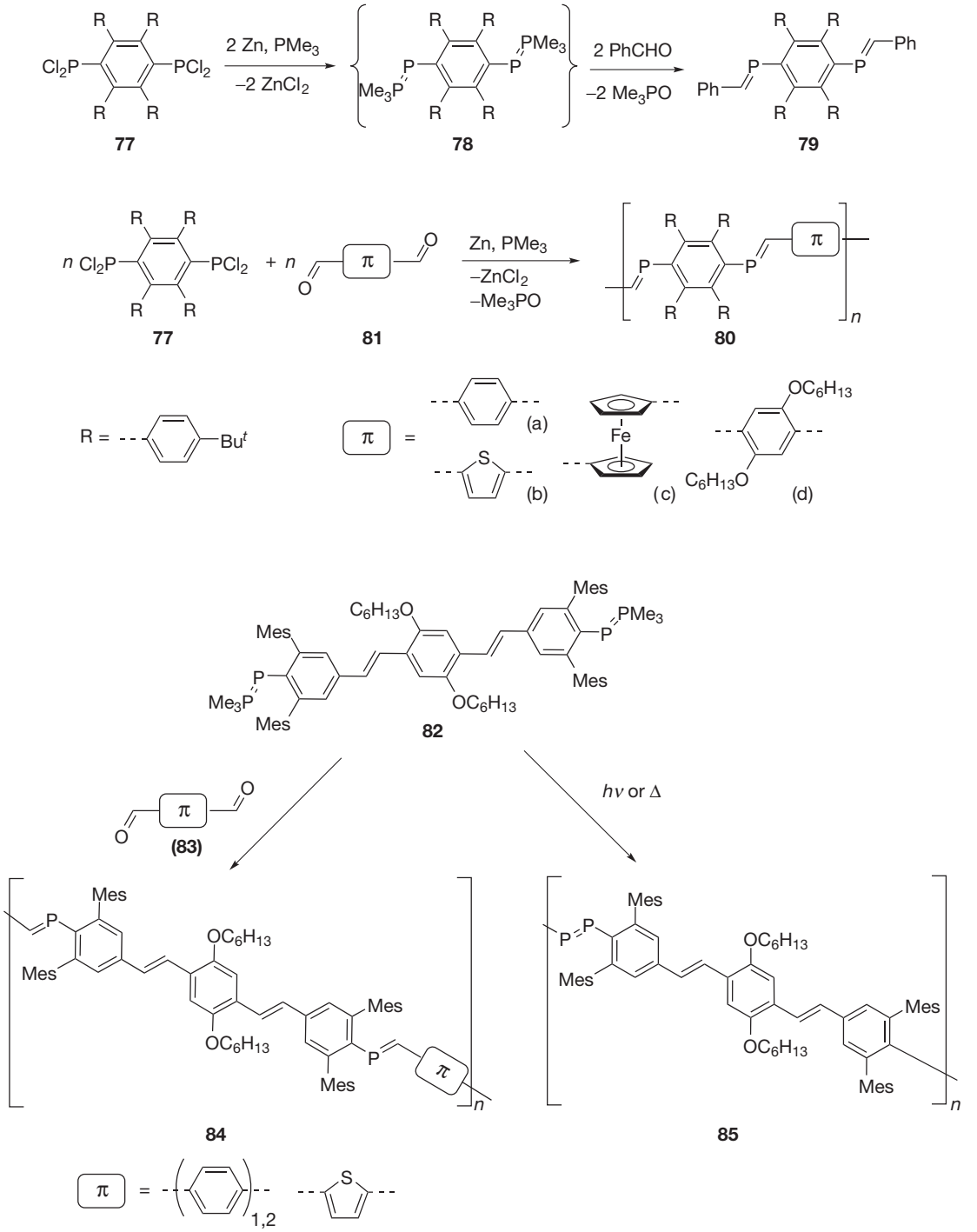

Scheme 16 Synthesis of phospha-PPVs via the Protasiewicz route.

bulk present in the latter systems that is necessary to stabilize these species.

These proof-of-principle studies have clearly established that the incorporation of low-coordinate phosphorus centers into the backbone of conjugated materials can yield materials with properties that are noticeably different from those of the native carbon-based materials. While the photophysical properties of the phospha-PPV systems described here ultimately could not compete with those of the genuine PPV systems, the results nevertheless illustrate that phosphorus is capable of adding a new dimension to polymer chemistry, and, as such, further research into low-coordinate phosphorus-containing polymers can indeed be very rewarding (see next Section 1.28.4.4). Further avenues in phosphaorganic polymer chemistry have been suggested by the computational studies of Nguyen and coworkers concerning phosphaethyene polymers that can be considered analogues of *cis*-polyacetylene and graphane.[56]

Copyright © 2013. Elsevier. All rights reserved.

Comprehensive Inorganic Chemistry II : From Elements to Applications, Elsevier, 2013. ProQuest Ebook Central, http://ebookcentral.proquest.com/lib/inflibnet-ebooks/detail.action?docID=1330977.
Created from inflibnet-ebooks on 2021-02-09 22:27:26.

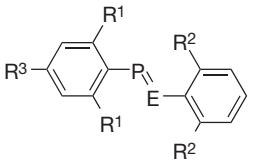

86a: E = CH, R^1 = Mes, R^2 = R^3 = H

86b: E = P, R^1 = R^2 = Mes, R^3 = H

86c: E = CH, R^1 = Mes, R^2 = H, R^3 = 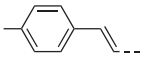

86d: E = P, R^1 = R^2 = Mes, R^3 = 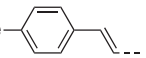

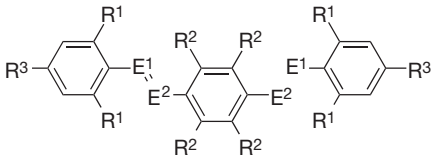

86e: E^1 = CH, E^2 = P, R^1 = R^3 = H, R^2 = Bu^t 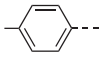

86f: E^1 = E^2 = P, R^1 = Mes, R^3 = H, R^2 = Bu^t 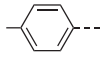

86g: E^1 = P, E^2 = CH, R^1 = Mes, R^2 = R^3 = H

86h: E^1 = P, E^2 = CH, R^1 = Mes, R^2 = R^3 = Me 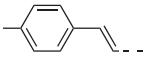

86i: E^1 = E^2 = P, R^1 = Mes, R^2 = Bu^t 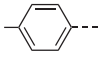 , R^3 = Me 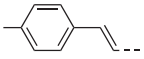

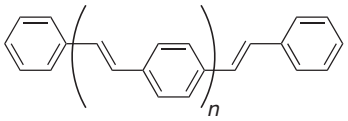

87; *n* = 0, 1, 2, 3

Figure 6 Oligomeric model compounds for phospha-PPVs.

Table 1 Photophysical data of carbon and phosphorus-based oligo (phenylenevinylene)s (**Figure 6**)[54]

C=C	$\lambda_{\pi-\pi^*}$ (nm; log ε)	P=C	$\lambda_{\pi-\pi^*}$ (nm; log ε)	P=P	$\lambda_{\pi-\pi^*}$ (nm; log ε)
87 (*n* = 0)	317 (4.53)	**86a**	334 (4.59)	**86b**	372 (3.63)
87 (*n* = 1)	354 (4.77)	**86c**	341 (4.54)	**86f**	398 (3.88)
		86e	349 (4.60)		
		86g	411 (4.68)		
87 (*n* = 2)	384 (4.92)			**86d**	407 (4.68)
87 (*n* = 3)	385 (5.10)	**86h**	417 (4.30)	**86i**	422 (4.64)

1.28.4.4 Poly(methylenephosphane)s

In addition to the aforementioned work on phospha-PPV systems, the Gates group has also recently begun to investigate the addition polymerization of low-coordinate phosphaalkenes comprehensively. In a series of publications beginning in 2003, several landmark discoveries have been made that lift methylenephosphane-based polymers from obscurity to an intriguing class of applied materials with a promising future.[57–59] From the early molecular phosphaorganic work, it was well known that insufficient kinetic stabilization of low-coordinate centers often led to undesired polymer-like side products, which were usually discarded uncharacterized.[60] In their initial communication, Gates and coworkers set out to balance the kinetic stabilization of phosphaalkenes in order to allow both the isolation, purification, and controlled investigation of the polymerization behavior of these species.[57a] Addition polymerization was targeted, as it ranks among the most general and industrially important methods for organic commodity polymers, such as polyethylene, polypropylene, and polystyrene. Remarkably, this process had been previously ruled out for inorganic polymers, due to the absence of suitable precursors.[61] However, by installing a mesityl (2,4,6-

Copyright © 2013. Elsevier. All rights reserved.

Comprehensive Inorganic Chemistry II : From Elements to Applications, Elsevier, 2013. ProQuest Ebook Central, http://ebookcentral.proquest.com/lib/inflibnet-ebooks/detail.action?docID=1330977.
Created from inflibnet-ebooks on 2021-02-09 22:27:26.

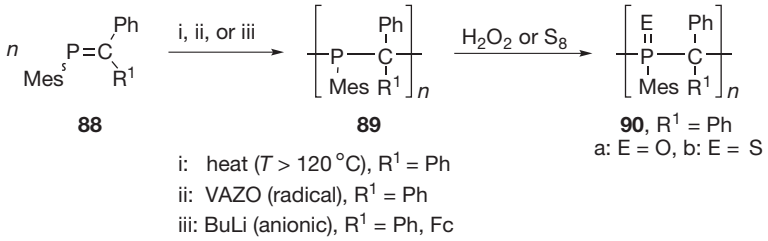

Scheme 17 Addition polymerization of methylenephosphanes.

trimethylphenyl, Mes) group at the phosphorus center, phosphaalkene **88** can be isolated and polymerized in controlled fashion.[57] The Gates group was able to illustrate this successfully for thermal, radical, and anionic polymerization processes (Scheme 17).

Distillation of the monomer **88** (R^1 = Ph) resulted in a brown gummy residue that could be purified by precipitation, yielding 7% of the desired polymer **89**, whose identity was confirmed by multinuclear NMR spectroscopy. A broad ^{31}P NMR resonance at $\delta = -10$ ppm confirmed the trivalent nature of the P-centers. GPC analysis revealed a molecular weight of $M_n = 11\,500$ g mol^{-1} with relatively narrow distribution (PDI = 1.25). Notably, the trivalent polymer **89** is reasonably air- and moisture-stable in the solid state, but can be oxidized with H_2O_2 or elemental sulfur to provide the pentavalent polymers **90** in good yields (**90a**: 60%, δ^{31}P = 47 ppm; **90b**: 84%, δ^{31}P = 52 ppm). Furthermore, this chemical transformation of the phosphorus centers does not noticeably degrade the backbone, as supported by via GPC results (**90a**: $M_n = 8800$ g mol^{-1}, PDI = 1.27; **90b**: $M_n = 11\,900$ g mol^{-1}, PDI = 1.24). However, it should be noted that the molecular weights for these phosphorus-containing polymers, obtained via standard GPC methods (i.e., vs. a polystyrene standard), generally underestimate the actual molecular weight significantly, as confirmed by light scattering, which revealed a true molecular weight of $M_w = 35\,000$ g mol^{-1} for **90b**. The low-molecular-weights obtained via standard GPC can be rationalized by the interaction of the phosphorus units with the column materials, retarding their flow. Moreover, the presence of the phosphorus centers again lends some degree of thermal stability to the three poly(methylenephosphane)s, which showed 5% weight loss at 265 °C (**89**, R^1 = Ph), 320 °C (**90a**), and 220 °C (**90b**), respectively. In addition to thermal polymerization, monomer **88** (R^1 = Ph) can also be polymerized in a radical fashion by the use of 1,1′-azobis(cyclohexanecarbonitrile) (VAZO) as a catalyst. However, the polymer obtained via this route averaged a molecular weight of only $M_n = 5700$ g mol^{-1} (PDI = 1.10) and also exhibited an ill-defined microstructure with several distinct phosphorus environments, as determined by ^{31}P NMR spectroscopy. Use of an anionic initiator (0.05 equiv, of MeLi or ^{n}BuLi) was also found to result in the formation of polymeric materials ($M_n = 5000$–$10\,000$ g mol^{-1}, PDI = 1.15–1.55).

Due to the similarity of P═C and C═C bonds, the corresponding polystyrene-poly(methylenephosphane) random copolymers are also accessible (Scheme 18). The initial study targeted a radical protocol due to the less stringent purity requirements for the monomers employed (compared with anionic polymerization).[57] A mixture of monomer **88** (R^1 = Ph) and styrene **91** was heated in the presence of VAZO for 14 h at 140 °C, resulting in a polymer **92** that was stable toward hydrolysis and showed only slow oxidation in air. Complete oxidation could again be achieved via straightforward treatment with H_2O_2. Analysis of the trivalent polymer via GPC (vs. polystyrene) indicated molecular weights of $M_w = 3600$–9000 g mol^{-1}, with monomodal distributions (PDI = 1.4–1.7) that support the formation of a single copolymer, rather than two separate homopolymers. However, two major broad signals in the ^{31}P NMR spectrum at $\delta = -9$ and 4 ppm, respectively, suggested partial regioirregular enchainment.

In four subsequent publications, the Gates group turned their focus toward anionic polymerization conditions to assess the specific nature of the various mechanistic steps.[57] To gain deeper insight into the initiation and propagation steps in the polymerization of methylenephosphanes relative to those of the purely carbon-based systems, ambient-temperature oligomerization with anionic initiators was investigated by means of MALDI-TOF mass spectrometry.[57] Oligomers were selected as model compounds, since they allow for the clear detection of terminal groups and are substantially easier to ionize for study under the MALDI-TOF conditions. While the study supported the hypothesis that P═C polymerization indeed proceeds in analogy to the C═C system, yielding linear chains with observable CH_3 and H termini, MALDI-TOF mass spectrometry also revealed the presence of two distinct series of oligomers (3–11 repeat units), separated by a mass difference of only 166 Da, that is, half a monomer unit. The authors concluded that the second set of oligomers results from backbiting during the polymerization via nucleophilic attack of the growing anionic chain-end on either a P- or C-center of the backbone, thereby splitting the repeat unit in half. This process, however, results cyclic in species that were only observed for a maximum of five repeat units. These observations notwithstanding, the overall process clearly supports the premise that anionic polymerization of methylenephosphanes can indeed be achieved at low temperatures. This therefore permitted extension of this protocol toward a living polymerization process, which had been unprecedented for inorganic multiple bond systems.[57] In general, living polymerization is a very intriguing process for the construction of exceptionally well-defined polymers with explicitly designed properties and architectures, as is known for a plethora of organic polymers. However, this process necessitates highly purified monomers, solvents, and initiators to avoid any undesired impurities that result in early or uncontrolled chain termination.[62]

Methylenephosphane monomers **88** (R^1 = Ph) that have been carefully purified by distillation and recrystallization

Copyright © 2013. Elsevier. All rights reserved.

Comprehensive Inorganic Chemistry II : From Elements to Applications, Elsevier, 2013. ProQuest Ebook Central, http://ebookcentral.proquest.com/lib/inflibnet-ebooks/detail.action?docID=1330977.
Created from inflibnet-ebooks on 2021-02-09 22:27:26.

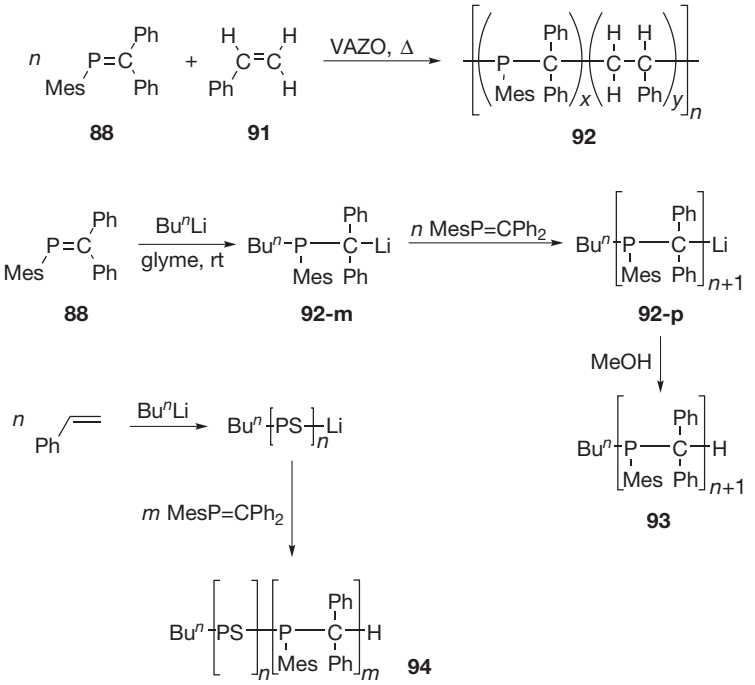

Scheme 18 Synthesis of poly(methylenephosphane) copolymers.

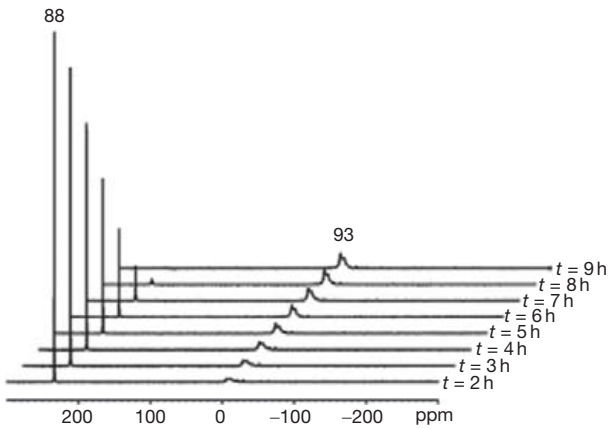

Figure 7 ^{31}P NMR spectra (glyme 296.3 K) of the anionic polymerization of **88** (R^1 = Ph; M/I = 50:1). Adapted from Noonan, K. J. T.; Gates, D. P. *Macromolecules* **2008**, *41*, 1961–1965. Copyright 2008 American Chemical Society.

methods can be polymerized in a living fashion using 2 mol% of an ^{n}BuLi initiator at 25 °C in a glyme solution (Scheme 18).[57] The initiation of the polymerization can be easily followed via the deep red color of the solution caused by the living, anionic polymer end in **92-p**, as well as the gradual decrease of the ^{31}P NMR resonance at δ = 234 ppm (i.e., the monomer **88**) with the concomitant increase of the broad resonance for the polymer (δ^{31}P = −7 ppm). Importantly, no other species can be detected via ^{31}P NMR spectroscopy, indicating the very clean nature of the polymerization process (Figure 7).

The molecular weight for the polymer **93** was determined to be M_n = 15 900 g mol^{-1}, matching the theoretical value of M_n = 14 800 g mol^{-1}quite well, and the very narrow distribution of PDI = 1.04 is typical for living polymerization processes. Furthermore, the polymerization also showed the expected linear change of the polymer molecular weight depending on the monomer-initiator (M/I) ratio (Table 2).

Table 2 Polymer molecular weights and polydispersities of **93** upon variation of M/I ratio[57]

M/I	M_n *(calcd) [g mol^{-1}]*	M_n *(abs) [g mol^{-1}]*	*PDI*
25:1	8000	8900	1.08
33:1	10 500	10 500	1.08
50:1	15 900	14 800	1.04
100:1	31 700	29 600	1.15

Moreover, establishment of the living nature of the polymerization process for **88** (R^1 = Ph) also allowed for the synthesis of a well-defined polystyrene–poly(methylenephosphane) block copolymer **94** in 60% yield (Scheme 18).[57] The polystyrene-*block*-poly(methylenephosphane) **94** had a molecular weight of M_n = 29 600 g mol^{-1} (PDI = 1.06) corresponding to n = 100 and m = 50, as anticipated (M_n(calcd) = 26 300 g mol^{-1}). Monomodal GPC traces, as well as ^{13}C and ^{1}H NMR spectra, support the assigned block copolymer structure. A detailed investigation of the polymerization kinetics revealed that the steric nature of the methylenephosphane significantly affected the process.[57] While typical alkene polymerizations have half-lives of seconds to minutes, the phosphaalkene was found to have a half-life of several hours, which allowed for the convenient monitoring of the reaction via ^{31}P NMR spectroscopy. From the rate-constant data an activation energy of E_a = 14.0 ± 0.9 kcal mol^{-1} was determined for **88** (R^1 = Ph), which is substantially higher than that observed for styrene (E_a = 5.9 kcal mol^{-1}) or even the more

Copyright © 2013. Elsevier. All rights reserved.

Comprehensive Inorganic Chemistry II : From Elements to Applications, Elsevier, 2013. ProQuest Ebook Central, http://ebookcentral.proquest.com/lib/inflibnet-ebooks/detail.action?docID=1330977.
Created from inflibnet-ebooks on 2021-02-09 22:27:26.

sterically crowded α-methylstyrene ($E_a = 7.2$ kcal mol^{-1}). This result was explained by the increased steric bulk surrounding the P=C double bond, as well as the substantial stabilization of the carbanion intermediate by both phenyl rings. However, the rate of polymerization also increased at high concentration, which is unknown for C=C bonds and therefore suggests additional subtle complexity in the P=C polymerization mechanisms.

To investigate the utility of the copolymer **92** and homopolymer **89** ($R^1 = Ph$) further, Gates et al. employed both materials as polymer-supported ligands for Pd complexes in a simple Suzuki cross-coupling protocol (**Scheme 19(a)**).[57] While the homopolymer **89** only provided the biphenyl product in low yield (23%), tuning of the amount of ligand/Pd in reactions of copolymer **92** offered yields as high as 90%, supporting the utility of such systems for catalysis.

Expanding on this concept, the introduction of a ferrocenyl substituent at the C-atom of the P=C bond of the monomer **88** ($R^1 = Fc$) would afford bimetallic polymers with interesting electronic, magnetic, or catalytic properties. In analogy to the diphenyl-substituted monomers, anionic polymerization of the ferrocenyl-substituted species at room temperature in glyme provided a golden-colored polymer **89** ($R^1 = Fc$) with $M_n = 9500$ (PDI = 1.21) (absolute molecular weight, **Scheme 17**).[58] However, despite a prolonged reaction period of 7 days, only ~50–60% of the monomer was converted to the polymer, as determined by ^{31}P NMR spectroscopy ($\delta = -5$ ppm). On the other hand, the polymer **89** ($R^1 = Fc$) showed redox features consistent with the reversible oxidation of electronically isolated ferrocene units ($\Delta E_{1/2} = 0.41$ V; vs. SCE). The utilization of this polymer as a supported ligand for Pd-catalysis, however, has not been reported to date.

To exploit the inherent functionality of the phosphorus backbone and its impact on the polymer properties, Gates and coworkers have also investigated the post-polymerization modification of the trivalent center with Lewis acids (BH_3 and CH_3^+) and, with a view toward materials applications, AuCl (**Scheme 19(b)**).[59] Simple borane-adducts of phosphanes are of interest as potential protecting groups that impart significant environmental stability on the polymer, while quaternization with methyl groups provides convenient access to cationic polyelectrolytes, with the ionic centers incorporated into the backbone in a manner similar to that observed with respect to the polymer reported by Smith et al. (**Section 1.28.4.3.1**).[44] Potential applications for the corresponding ionomers could range from drug delivery to fuel cell membranes.[63] To verify

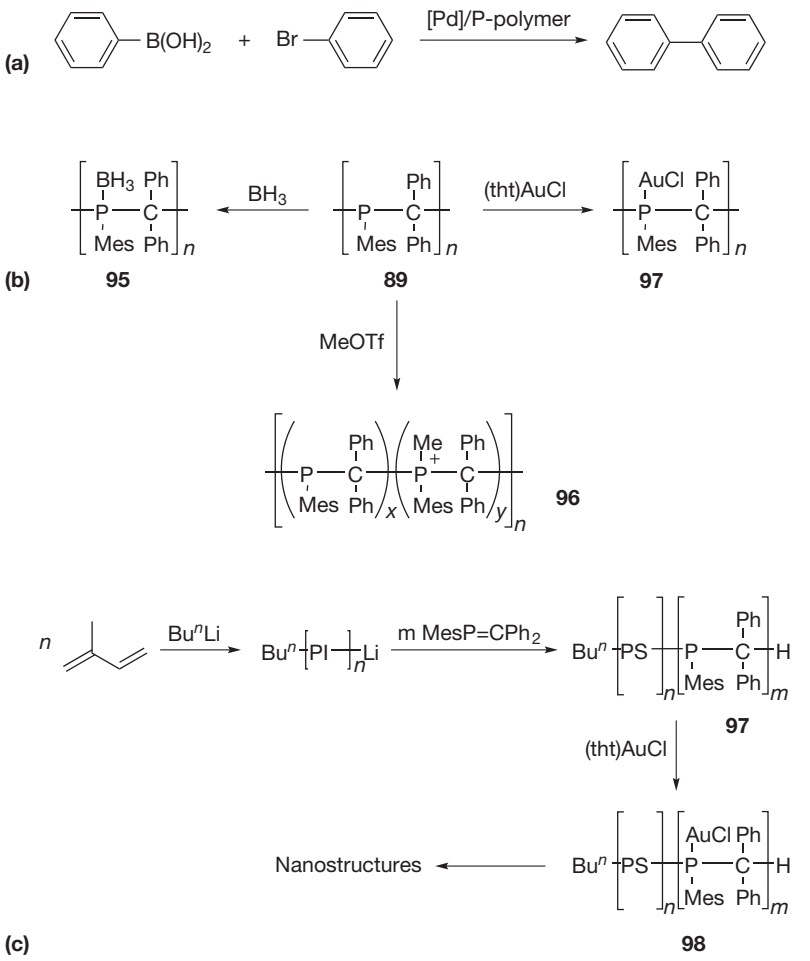

Scheme 19 Functionalization and utility of poly(methylenephosphane) homo- and block copolymers.

Copyright © 2013. Elsevier. All rights reserved.

Comprehensive Inorganic Chemistry II : From Elements to Applications, Elsevier, 2013. ProQuest Ebook Central, http://ebookcentral.proquest.com/lib/inflibnet-ebooks/detail.action?docID=1330977.
Created from inflibnet-ebooks on 2021-02-09 22:27:26.

the degree of P-functionalization, corresponding monomeric model compounds were targeted first as references.[59] However, the net functionalization of the polymeric systems was met with mixed success. While treatment of a sample trivalent poly(methylenephosphane) **89** ($M_n = 38\,900$ g mol^{-1}; PDI = 1.34) provided complete conversion of all P-centers to the corresponding borane-adduct species **95**, methylation was found to proceed only to a maximum of 50% conversion, even after prolonged reaction times, elevated temperatures, or an excess of MeOTf.[59] While the ^{31}P NMR spectrum of the borane-adduct polymer **95** showed two broad signals at $\delta = 26.8$ (major) and 32.4 (minor) ppm that were assigned to the varying tacticity of the polymer backbone, the methylated polymer **96** showed two signals at $\delta = 31.0$ and -10.0 ppm, respectively, in a 1:1 ratio, corresponding instead to methylated and nonmethylated P-centers. The absence of methylation at adjacent sites has been attributed to the deactivating character of each phosphonium center on the methylation of its direct neighbors, presumably due to the repulsion of concentrated cationic charges. Importantly, however, both of the modified polymers showed similar molecular weights and distributions as the trivalent polymer, confirming again that backbone degradation does not occur during the postpolymerization modification. Moreover, addition of excess NEt_3 to the borane-adduct **95** permitted reversion to the trivalent P-polymer **89** with retention of backbone integrity, illustrating the protecting-group character of the borane.

Full conversion of the trivalent P-centers can also be achieved with AuCl (**Scheme 19(b)**).[59] Gold-containing polymers are of particular interest for applications in nanochemistry, catalysis, and as sensory materials, to offer only a partial list.[61,64] Treatment of the trivalent polymer sample with an excess of Au(tht)Cl at room temperature in CH_2Cl_2 resulted in complete coordination, as determined by ^{31}P NMR spectroscopy showing a low field shift of the ^{31}P resonance to $\delta = 25.0$ ppm, which corresponds to the monomeric reference compound. GPC analysis of the gold-containing polymer **96** revealed the expected increase in molecular weight ($M_n = 71\,600$ g mol^{-1}; PDI = 1.29), supporting both the high degree of metalation and the continued integrity of the polymer backbone. Moreover, complexation with AuCl significantly improved the thermal stability of the polymer, as confirmed via TGA showing decomposition only above 325 °C (cf. 265 °C for the trivalent polymer). These post-polymerization modifications were subsequently extended successfully to the corresponding block copolymers, thus opening up the application of these materials in the context of nanoscience, particularly with regards to self-assembling Au nanostructures (**Scheme 19(c)**).[59] As mentioned earlier, self-organization of block copolymers is an important tool for the generation of highly ordered nanoscopic structures that can be modified by the nature of the block lengths in the polymer. In this context, metallic and other inorganic nano-assemblies are of particular interest because they can show intriguing electronic, magnetic, and optical properties.[61] To assess the potential for such structures using poly(methylenephosphane)s (PMPs), Gates and coworkers have prepared polyisoprene-poly(methylenephosphane) block copolymers **97** and subsequently modified the P-containing block with AuCl post-polymerization.[59] Remarkably, depending on the block lengths in the corresponding block copolymers of type **98**, a variety of nanostructures could be verified by TEM. The polymer with the shortest PMP block (PI_{404}-*b*-PMP_{35}) resulted in the formation of spherical morphologies with diameters of 28–32 nm. Elongation of this block and shortening of the PI-block (i.e., PI_{222}-*b*-PMP_{77}, PI_{164}-*b*-PMP_{85}) induced significant morphological changes that resulted in oblong, worm-like structures, imparting dimensionality on the nano-assemblies (**Figure 8**). These results nicely underscore the potential of a bottom-up approach toward gold nanostructures that use PMPs as central, well-defined templating agents.

1.28.5 Phosphole-Containing Polymers

The phosphole system is a member of the five-ring heterocycle family that includes pyrrole and thiophene.[65] The latter two units have been extensively studied for their very intriguing physical and chemical properties, which have made them exceptionally valuable building blocks for organic conjugated materials and thus application in organic electronics.[39] In contrast to these highly aromatic rings, the phosphole unit shows considerably different properties, as already established in the late twentieth century. Due to the increased inversion

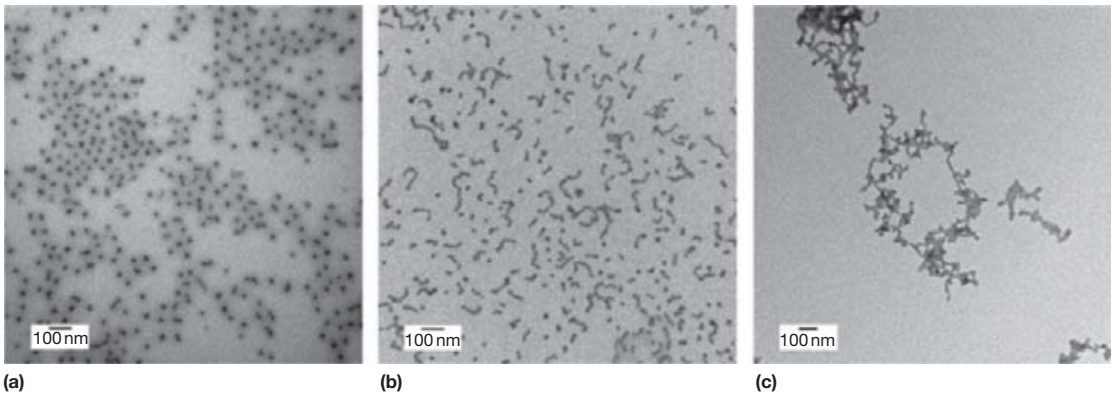

Figure 8 TEM images of the Au-polymer nanostructures: (a) PI_{404}-*b*-PMP_{35}·AuCl, (b) PI_{222}-*b*-PMP_{77}·AuCl, (c) PI_{164}-*b*-PMP_{85}·AuCl. Reprinted from Noonan, K. J. T.; Gillon, B. H.; Cappello, V.; Gates, D. P. *J. Am. Chem. Soc.* **2008**, *130*, 12876–12877. Copyright 2008 American Chemical Society.

Copyright © 2013. Elsevier. All rights reserved.

Comprehensive Inorganic Chemistry II : From Elements to Applications, Elsevier, 2013. ProQuest Ebook Central, http://ebookcentral.proquest.com/lib/inflibnet-ebooks/detail.action?docID=1330977.
Created from inflibnet-ebooks on 2021-02-09 22:27:26.

barrier of phosphorus, compared to that of nitrogen (16 kcal mol^{-1}, vs. 7 kcal mol^{-1} for pyrrole), phospholes are generally not planar, which reduces the orbital overlap of the lone pair with the conjugated system and, in consequence, lowers the aromaticity of the P-ring system.[65] Furthermore, it is well established that phospholes generally have low-lying LUMO levels due to a peculiar interaction of the σ*-orbital of the exocyclic P—H (or P—R) bond with the π*-orbital of the ring system, which presents an intriguing prospect for organic electronics.[2,40] More importantly, the lone pair at the phosphorus center is again available for chemical modifications which could have significant impact on the electronic properties of the π-system. As a result, phospholes have recently been identified as powerful building blocks for organophosphorus π-conjugated materials.[2] In the past 10 years, research involving functional materials based on phospholes has gained increasing popularity due to the unique properties of these materials,[13] and polymeric systems are no exception in this context.

1.28.5.1 Polymers Involving Simple Phosphole Units

Three computational studies on a variety of poly(heteroles) dating from 2002 have concluded that the electronic features of phospholes, as elaborated above, would provide an excellent entry point for the corresponding polymers in the context of conjugated materials.[66] It was calculated that the bandgaps of polymers based on phospholes would be significantly smaller than those of the polypyrrole or polythiophene congeners. These theoretical studies also touched on the possibility of the modulation of the phosphorus centers via standard P-chemistry to generate materials with significantly altered electronic properties.[66]

The first synthetic account of a phosphole-based conjugated polymer was reported by Tilley and coworkers in 1997.[67] The investigation on the potential of zirconocene diyne-coupling for the synthesis of ziroconocene-based polymers included the conversion of the latter into a series of heterole-based polymers via metal-element exchange reactions (Scheme 20).

Initial studies using corresponding model compounds revealed that the diyne coupling is not regioselective, affording an 80/20 mixture of 1,2- and 2,1-coupled products that could not be separated, particularly in the case of the polymeric system. Furthermore, the model studies indicated that the 80/20 ratio of the regioisomers prevailed during the metal-element exchange and, moreover, that the latter does not proceed in a quantitative manner. Consequently, the resulting polymer **99** contained 2,4- as well as 2,5-phosphole linkages, as well as butadiene defect sites due to incomplete conversion. The ill-defined polymer mixture **99** was isolated as an air-sensitive yellow powder and its molecular weight was estimated to be $M_w = 16\,000$ g mol^{-1} with a broad distribution (PDI = 2.59). ^{31}P NMR spectroscopy confirmed the presence of 2,4- as well as 2,5-phosphole-linked units with resonances at $\delta = 11.3$ and 14.9 ppm, respectively. The photophysical characterization of the phosphole polymer indicated an absorption maximum at $\lambda_{abs} = 308$ nm and a fluorescence emission at $\lambda_{em} = 470$ nm; however, the quantum yield of photoluminescence was very low ($\phi_{PL} = 9\%$). A marginally

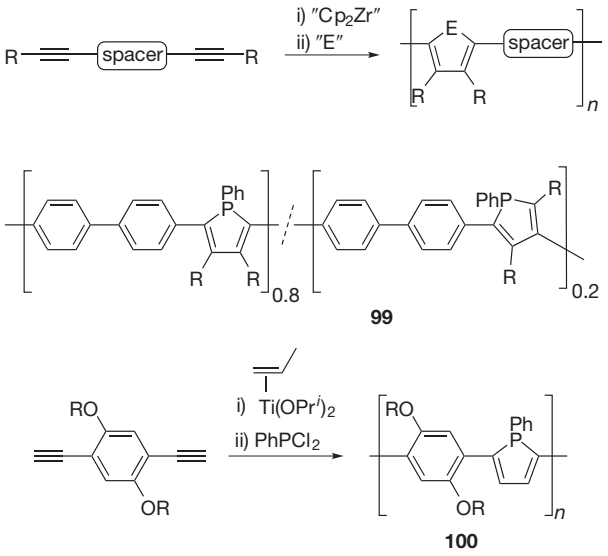

Scheme 20 Zr- and Ti-mediated syntheses of phosphole polymers.

related approach toward the analogous phosphole-based polymer **100** using titanium as coupling agent was reported by Tomita et al. in 2003 (Scheme 20).[68] The polymer was found to exhibit an absorption maximum at $\lambda_{em} = 500$ nm and showed fluorescence at $\lambda_{em} = 600$ nm. Further details on the polymer have not been reported.

Despite the fact that well-defined oligophospholes had been reported in the 1990s by Mathey et al.,[2,65] Réau and coworkers were the first to investigate phosphole-based conjugated materials systematically in the context of organic electronics.[69] Their comprehensive studies on molecular and oligomeric species, starting in the late 1990s, revealed important structure–property relationships that could be used to optimize these (molecular) materials toward practical applications, including OLEDs.[69] Corresponding molecular species of type **101** are accessible, in a fashion similar to the polymers reported by Tilley, via the Fagan–Nugent method involving the intramolecular coupling of two appropriately functionalized dialkynes with zirconocene and subsequent metal-phosphorus exchange (Scheme 21). This method was applied to a series of different conjugated molecular materials with phenyl, thienyl, and/or pyridinyl end-groups.[69,70] The thienyl-substituted species displayed the smallest bandgap in this series, due to the pronounced donor–acceptor character of the thiophene and phosphole units, respectively.[70]

The latter was further substantiated by DFT-calculations.[71] Importantly, the phosphorus center in these species can efficiently be manipulated by simple chemical modifications (Scheme 21) from the established phosphorus chemistry repertoire, resulting in significantly altered photophysical properties of the materials (Table 3).[70] This once again illustrates the unique intrinsic benefits of phosphorus-based conjugated materials that allow access to a whole family of species from one well-defined central precursor. The 2,5-bis(thienyl) phospholes **101-E** were subjected to electrochemical oxidation to prepare π-conjugated polymers as thin films on a platinum electrode (Scheme 22). Notably, the films proved insoluble in

Copyright © 2013. Elsevier. All rights reserved.

Comprehensive Inorganic Chemistry II : From Elements to Applications, Elsevier, 2013. ProQuest Ebook Central, http://ebookcentral.proquest.com/lib/inflibnet-ebooks/detail.action?docID=1330977.
Created from inflibnet-ebooks on 2021-02-09 22:27:26.

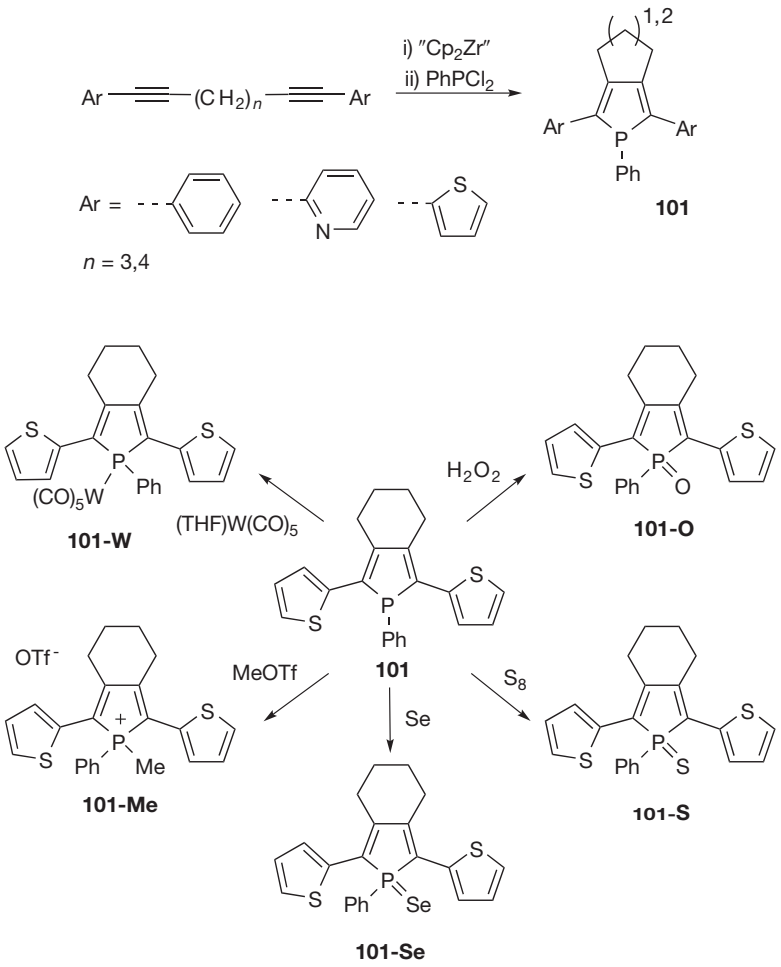

Scheme 21 Synthesis and modification of conjugated phospholes via the Réau route.

Table 3 Photophysical data of molecular phosphole derivatives (**Scheme 21**)[70]

Compound	λ_{max} *(nm; log ε)*	λ_{onset} *(nm)*	λ_{em} *(nm)*
101	412 (3.93)	468	501
101-O	434 (3.97)	500	556
101-S	432 (3.98)	496	548
101-Se	423 (4.09)	503	547
101-W	408 (4.04)	475	506
101-Me	442 (3.92)	528	593

common organic solvents, therefore precluding the verification of their polymeric nature via GPC or other standard spectroscopies.[70] However, the polymers were electroactive and could be studied using cyclic voltammetry. While polymers with neutral phosphorus centers (E = lone pair, O, S) exhibited *p*- and *n*-doping processes with good reversibility (>70%), the cationic phospholium-based polymer (E = Me^+) only demonstrated *p*-doping reproducibly. Significantly, these doping processes appeared at lower potentials than those of the corresponding monomeric species, suggesting a decrease in the polymer bandgap due to extended conjugation. The latter premise was also supported by UV–vis spectroscopy, with polymers showing red-shifted absorption onsets when compared to the corresponding monomers/model compounds ($\Delta\lambda_{onset}$ = 162 nm (**poly-101**), 280 nm (**poly-101-O**), 254 nm (**poly-101-S**), 385 nm (**poly-101-Me**)). More importantly, the photophysical features of the polymers showed significant dependence upon the functionalization of the phosphorus centers, much like the corresponding monomers (λ_{max} = 463 nm (**poly-101**), 568 nm (**poly-101-O**), 529 nm (**poly-101-S**), 627 nm (**poly-101-Me**)). To solidify the conclusions from the study of the insoluble polymers, the Réau group targeted a series of soluble alternating phosphole–thiophene oligomers **102a**,**b** with increasing numbers of repeat units that confirm the corresponding decrease in the optical bandgap with increasing number of repeat units, and the dependence of the photophysical properties of the systems on the nature of the P-center (**Scheme 22**).[72]

The absorption maxima were observed to increase from the trivalent dimer **102a** (λ_{max} = 490 nm) to the pentavalent trimer **102b** (λ_{max} = 550 nm), with the pentavalent dimer **102a-S** falling in between (λ_{max} = 508 nm). As the end-groups of these oligomers are thiophenes, subsequent electropolymerization could also be accomplished using a similar protocol to the monomeric congeners. The polymers could likewise be deposited as insoluble, electroactive films by repeated cycling of the

Copyright © 2013. Elsevier. All rights reserved.

Comprehensive Inorganic Chemistry II : From Elements to Applications, Elsevier, 2013. ProQuest Ebook Central, http://ebookcentral.proquest.com/lib/inflibnet-ebooks/detail.action?docID=1330977.
Created from inflibnet-ebooks on 2021-02-09 22:27:26.

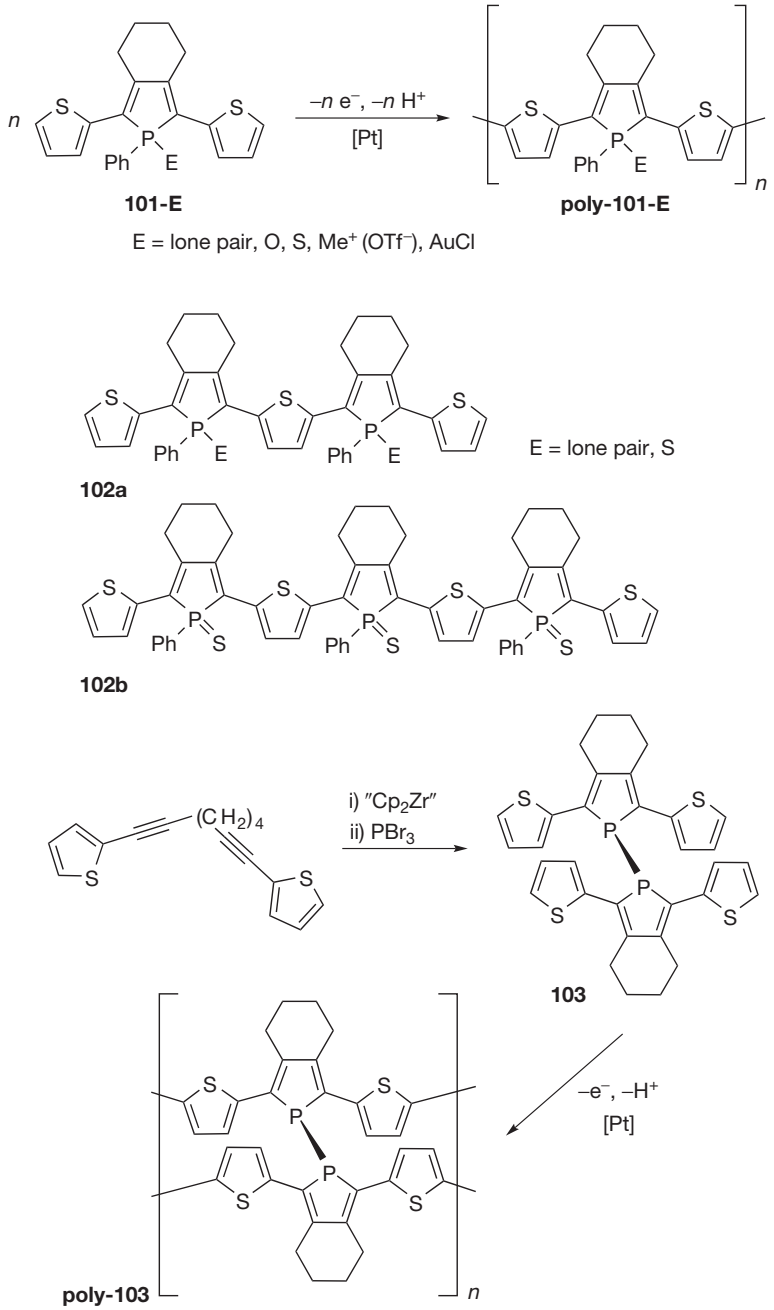

Scheme 22 Electropolymerization of conjugated bis(thienyl)phospholes and related model compounds.

potential between −0.1 V and +1.0 V (vs. Fc/Fc^+), yielding increasing currents with each cycle. The polymers likewise exhibited p- and n-doping; however, only the p-doping showing an appreciable degree of reversibility (>90%).[72]

In addition to the ready modification of the trivalent P-center via functionalization with oxidizing agents, Lewis acids, or transition metals, the phosphole unit offers an additional intriguing opportunity for creating a unique electronic structure with a reduced bandgap.[65] Direct linkage of two phosphole units via their P-centers results in a highly polarizable P—P bond perpendicular to the ring planes, allowing for σ–π conjugation, that is, considerable orbital overlap with the π-system.[2] Such 1,1′-bisphospholes are commonly accessed via reductive cleavage of an exocyclic P-phenyl substituent and subsequent oxidation of the phospholyl-anion intermediate with iodine.[2,65] However, Réau and coworkers found that dimerization could also be achieved in situ when the metal-phosphorus exchange during the Fagan–Nugent reaction is performed with PBr_3, as the 1-bromophosphole intermediate spontaneously dimerizes under these reaction conditions (Scheme 22).[73] UV–vis spectroscopy and TD-DFT calculations revealed that the HOMO–LUMO gap of the bisphosphole **103** is indeed smaller than that of the P-phenyl species **101**, as evidenced by the red-shifted absorption maxima ($\Delta\lambda_{max}$ ~130 nm) attributable to the addition of σ–π conjugation between the two phosphole units. Since the dimer **103**

Copyright © 2013. Elsevier. All rights reserved.

Comprehensive Inorganic Chemistry II : From Elements to Applications, Elsevier, 2013. ProQuest Ebook Central, http://ebookcentral.proquest.com/lib/inflibnet-ebooks/detail.action?docID=1330977.
Created from inflibnet-ebooks on 2021-02-09 22:27:26.

still exhibits thiophene end-groups, electropolymerization was readily achieved by scanning in a potential range between −0.5 and +0.8 V (vs. Fc/Fc^+). The increasing current with each cycle, in analogy to earlier results, indicated that the insoluble film of **poly-103** depositing on the electrode was indeed conductive and showed reversible p-doping processes.[73] The UV–vis absorption is considerably red-shifted (λ_{max} = 590 nm [onset: 730 nm]) compared to that of the monomer (cf. λ_{max} = 445 nm), indicating a significantly decreased bandgap for the polymer.

In a subsequent publication, Réau and coworkers illustrated that the polymers obtained via electropolymerization can be utilized in a sensory materials context that takes advantage of the post-polymerization functionalization of the phosphorus centers (Scheme 23).[74] As the nature of the P-centers is strongly coupled with the conjugated π-system,

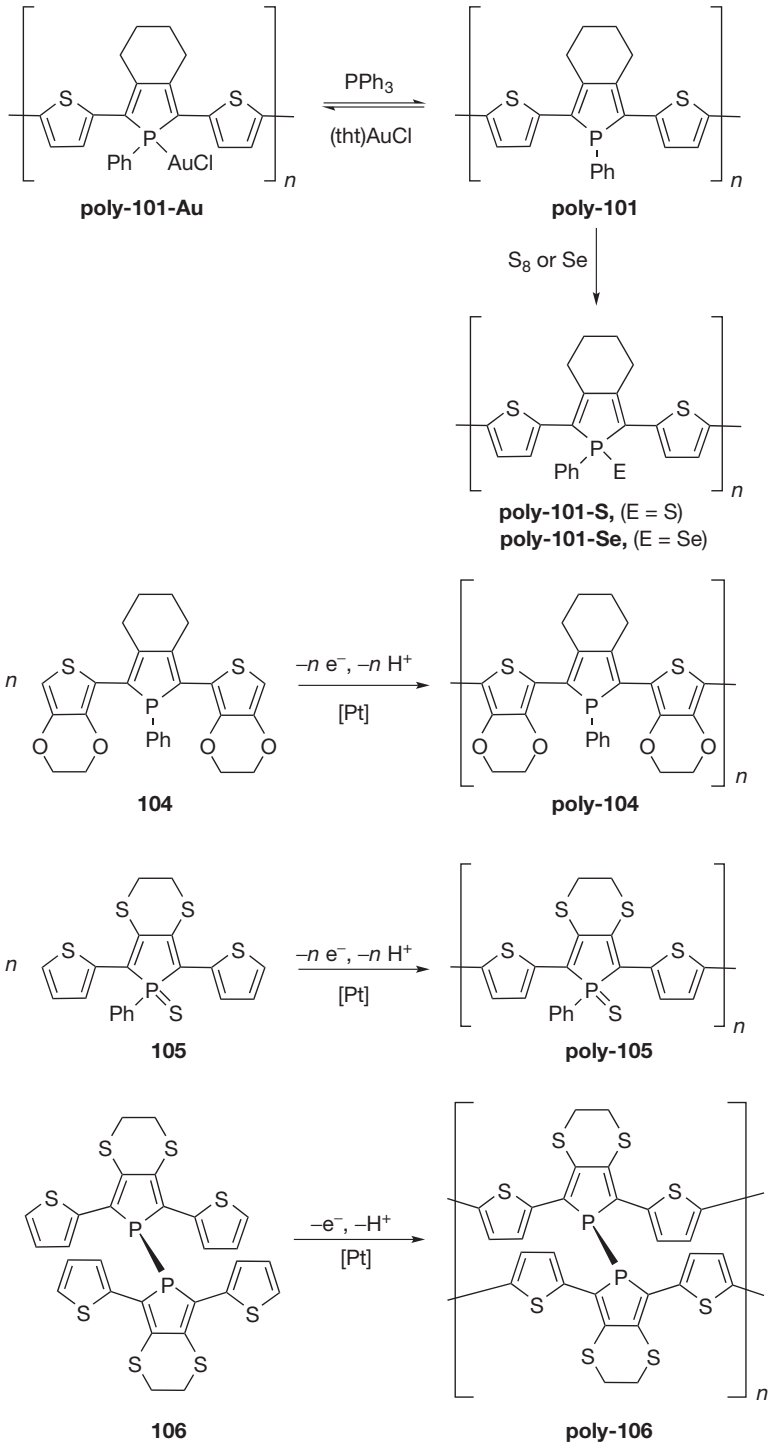

Scheme 23 Post-polymerization functionalization of poly-**101**-Au used as sensory material (top), and electropolymerization of electron-rich monomers **104–106** (bottom).

Copyright © 2013. Elsevier. All rights reserved.

Comprehensive Inorganic Chemistry II : From Elements to Applications, Elsevier, 2013. ProQuest Ebook Central, http://ebookcentral.proquest.com/lib/inflibnet-ebooks/detail.action?docID=1330977.
Created from inflibnet-ebooks on 2021-02-09 22:27:26.

changes at these sites can be detected through altered properties of the material as a whole, an essential prerequisite for functional sensory materials. Trivalent phosphorus centers are ideal candidate components in sensory materials, as modification using standard P-chemistry provides for potentially diverse applicability. However, using the thienyl-capped trivalent phosphole **101** (or even the borane-protected species **101-B**; E = BH_3), electropolymerization was found to be impossible under the oxidative conditions, as it negatively affected the integrity of the P-center. On the other hand, electropolymerization of the corresponding AuCl-complex **101-Au** (Scheme 23) was viable without complication. The air- and moisture-stable, insoluble film of **poly-101-Au** formed on the electrode showed again some reversible *p*-doping processes between −0.5 and +0.85 V (vs. Fc/Fc^+), as well as a red-shifted UV–vis absorption ($\Delta\lambda_{max} = 175$ nm; $\Delta\lambda_{onset} = 290$ nm). Furthermore, the elemental composition of the film was confirmed by energy-dispersive x-ray analysis (EDX), and solid-state high-resolution ^{31}P MAS NMR spectroscopy revealed a resonance at $\delta = 45$ ppm (cf. 39 ppm for the monomer),[74] in addition to a resonance corresponding to the decomplexed species at $\delta = 16$ ppm (<10%; via integration of the ^{31}P NMR signals). Since the model molecular species could efficiently be decomplexed with PPh_3, the film of **poly-101-Au** was treated under the same conditions (CH_2Cl_2, room temperature) resulting in the immediate formation of the trivalent polymer **poly-101** (Scheme 23). The expected loss of mass was confirmed with a gravimetric quartz-crystal microbalance, and EDX confirmed a low gold content (Au/P < 0.1), whereas ^{31}P MAS NMR exhibited a high field-shifted resonance at $\delta = 15$ ppm with a small residual peak for remaining complexed P-centers ($\delta = 45$ ppm). UV–vis spectroscopy confirmed the expected blue shift of the absorption upon reduction of the P-centers ($\Delta\lambda_{onset} = -41$ nm).

Notably, the trivalent phosphole polymer **poly-101** is air- and moisture-stable and can be handled without special care and used in further post-polymerization reactions. In a proof-of-principle approach, the AuCl-functionalized polymer **poly-101-Au** could be regenerated from the trivalent species (as monitored by cyclic voltammetry), thus satisfying another prerequisite for successful sensory materials. The sensing capabilities of the trivalent phosphole polymer **poly-101** were probed via reaction with sulfur and selenium, two essential oligoelements. Exposure of the polymer, deposited on a Pt electrode, to S_8 or Se (in toluene) resulted in a large positive shift of the oxidation current onset ($\Delta E_{pa} = 230$ mV) and a red shift of the absorption ($\Delta\lambda_{onset} = 38$ nm), providing a real-time response to the reaction with sulfur, while the reaction with selenium was slower due to its reduced solubility in toluene. These promising results clearly show that, despite their insolubility in organic media, these phosphorus-containing polymers can nevertheless offer a variety of opportunities with regard to practical applications.

In an effort to tune the electronic properties of the 2,5-dithienylphospholes for direct access to trivalent phosphole polymers via electropolymerization, the corresponding bis(ethylenedioxothiophene)-capped (EDOT) phosphole **104** was synthesized (Scheme 23).[75] The EDOT group is known to exhibit a very low oxidation potential due to the strongly electron-donating nature of the dioxo-substituent.[39] A suitably functionalized dialkyne could be converted into the phosphole-species using standard approaches, which could successfully be electropolymerized to provide **poly-104** without affecting the integrity of the trivalent phosphorus center.[75] The onset and peak potentials of the bis(EDOT)-phosphole **104** at $E_{p(onset)} = 0.10$ V and $E_{p(ox)} = 0.22$ V (vs. Fc/Fc^+) are much lower than those of the simple thienyl-capped species **101** ($E_{p(onset)} = 0.33$ V; $E_{p(ox)} = 0.80$ V), allowing for successful electropolymerization upon repeated cycling between −0.32 and +0.58 V. In line with earlier observations, the obtained film of **poly-104** was insoluble in organic solvents but conductive. To confirm the conservation of the trivalent phosphorus centers during the electropolymerization process, the polymer was subsequently exposed to (tht)AuCl for 20 min, resulting in a shift in the oxidation potential of about 170 mV upon complexation.[75]

The successful transfer of these promising results was then probed in the most recent account by the Réau group dealing with the synthesis of 3,4-ethylenedithio-functionalized P-phenyl phospholes **105**, as well as corresponding P—P dimers **106** (Scheme 23).[76] However, electropolymerization of the trivalent P-phenyl species did not result in any polymer formation, and only the pentavalent sulfurized species **105-S** could be converted. This behavior was rationalized by the fact that the remote S-atoms in the 3- and 4-position of the phosphole ring do not impart the necessary stability on the radical formed during the electropolymerization, as the latter is mainly located on the terminal thienyl ring, which can nonetheless be stabilized by an increased acceptor character of the phosphorus center. On the other hand, the trivalent P—P dimer **106** did form a polymeric species upon electrochemical oxidation. Both polymer films obtained in the context of this study were dark blue and insoluble in common organic solvents. Notably, the presence of the ethylenedithio-group shifted the oxidation potentials of polymers **poly-105-S** and **poly-106** to lower values than those of the all-carbon analogues **poly-101-S** and **poly-103**, which is consistent with lowered LUMO-levels in the 3,4-ethylenedithio-bridged phospholes. This is also evident in the UV–vis absorptions of the polymers at $\lambda_{max} = 600$ nm (**poly-105-S**) and $\lambda_{max} = 611$ nm (**poly-106**) that are significantly red-shifted to those of the corresponding monomers, but more importantly, red-shifted to those of the analogous all-carbon-bridged polymers as well (cf. $\lambda_{max} = 529$ nm (**poly-101-S**) and $\lambda_{max} = 594$ nm (**poly-103**)).

Based on the molecular phosphole species developed by Réau et al., Chujo and coworkers have reported a series of corresponding soluble polymers (Scheme 24).[77] Installation of 4-bromophenyl groups at the terminal positions of the alkyne starting materials afforded functional phospholes of type **107** that could be utilized in a Heck–Cassar–Sonogashira cross-coupling protocol with a variety of rigid, solubilized bis(alkynes) of type **108**. Surprisingly, the trivalent phosphorus center appears not to be affected by the employed Pd-catalyst, and the resulting polymers only show a ^{31}P NMR resonance for uncomplexed trivalent P-centers at around $\delta = 13$ ppm.[77] All polymers **109** are soluble in a variety of common solvents (THF, $CHCl_3$, CH_2Cl_2, toluene) and could thus be characterized by GPC showing moderate molecular weights and relatively narrow distributions that mainly depended on the solubility of the bis(alkyne) spacer (Table 4, **109a–f**).

Copyright © 2013. Elsevier. All rights reserved.

Comprehensive Inorganic Chemistry II : From Elements to Applications, Elsevier, 2013. ProQuest Ebook Central, http://ebookcentral.proquest.com/lib/inflibnet-ebooks/detail.action?docID=1330977.
Created from inflibnet-ebooks on 2021-02-09 22:27:26.

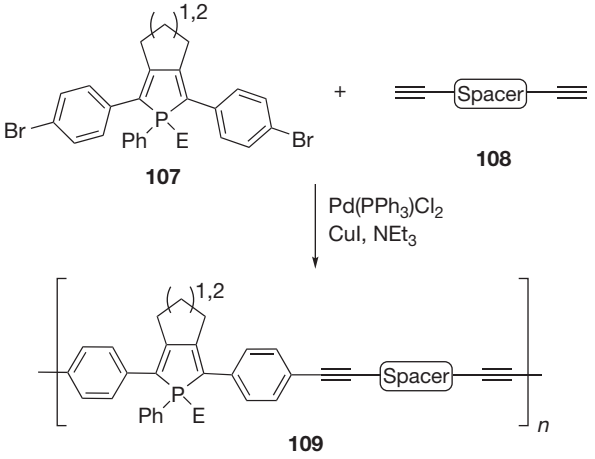

	n	E	spacer	ref.
a	2	lone pair	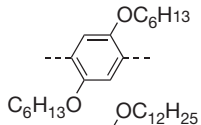	77a
b	2	lone pair	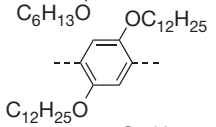	77a
c	2	lone pair	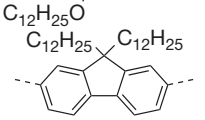	77a
d	1	lone pair	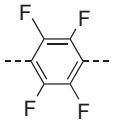	77b
e	1	lone pair	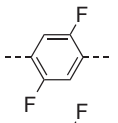	77b
f	1	lone pair	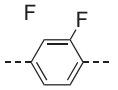	77b
g	1	lone pair	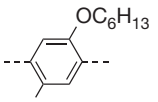	77c
h	1	O		77c
i	1	S		77c

Scheme 24 Solution-polymerization of functionalized phosphole monomers.

Table 4 Molecular weights, polydispersities, and photophysical data for polymers **109**

Polymer	M_w	*PDI*	λ_{max} *(nm; log ε)*	λ_{em} *(nm;* ϕ_{PL}*)*
109a[77]	15 400	1.5	410 (4.53)	490 (0.09)
109b[77]	14 000	1.4	414 (4.52)	487 (0.14)
109c[77]	9000	1.3	382 (4.80)	435 (0.08)
109d[77]	7000	1.03	395 (4.00)	470 (0.18)
109e[77]	3900	1.96	388 (4.20)	461 (0.30)
109f[77]	2100	1.50	396 (4.09)	502 (0.21)
109g[77]	5000	1.4	398 (4.39)	466 (0.39)
109h[77]	6600	2.4	408 (4.29)	523 (0.15)
109i[77]	14 100	2.3	431 (4.17)	522 (0.13)

The alkyne spacer also impacts the electronic nature of the polymers, showing absorption maxima from $\lambda_{max}=382–410$ nm and fluorescence emission between $\lambda_{em}=435–502$ nm. Photoluminescence quantum yields are modest, ranging from $\phi_{PL}=8–39\%$. The polymers were found to be stable in air as solids, but slowly oxidized in solution when exposed to atmospheric oxygen. It should be noted in this context that pentavalent phosphole monomers **107** (E = O, S) could also be used for the synthesis of corresponding polymers. The photophysical properties of the polymers mirror the features observed for molecular species, with the pentavalent polymers showing red shifts for their absorption and emission wavelengths in comparison to the corresponding trivalent species (Table 4, **109g–i**).

In 2010, Matano and coworkers reported the first successful synthesis of a dark blue phosphole oxide homopolymer **110** accessible from the 2,5-stannylphosphole precursor **111**. The latter is also the basis for the complementary 2,5-iiodophosphole oxide **112** that permits the use of a Stille cross-coupling protocol for the synthesis of oligomers and a soluble polymer with $M_n=13\,000$ g mol^{-1} (PDI = 2.3), by virtue of the solubilizing group at the P-center (Scheme 25).[78]

Notably, due to the low solubility of the polymer, polymerization of the corresponding P-phenyl phosphole species led only to low-molecular-weights. The alkoxy-solubilized polymer **110** exhibited a set of broad ^{31}P NMR resonances ($\delta=51–57$ ppm), likely due to the diastereomeric nature of the P-centers, as well as an absorption at $\lambda_{max}=655$ nm, significantly red-shifted in comparison to the phenyl-capped monomer (cf. $\lambda_{max}=386$ nm). The absorption onset at $\lambda_{onset}=850$ nm translates to a small bandgap of $E_{bg}=1.46$ eV, illustrating the significantly extended conjugation of the π-system. The electrochemical properties of the polymers also strongly supported the enhanced electron-accepting character over those of the monomer and oligomeric phospholes. The latter is in stark contrast to the ubiquitous polypyrroles and thiophenes, which are commonly employed as electron donors, and highlights the electronic benefits resulting from the presence of the phosphorus centers in the polymer.

1.28.5.2 Polymers Involving Fused Phosphole Units

Fusion of ring systems has been identified as a powerful approach for tuning the electronic properties of conjugated materials for organic electronics, as it significantly reduces the

Copyright © 2013. Elsevier. All rights reserved.

Comprehensive Inorganic Chemistry II : From Elements to Applications, Elsevier, 2013. ProQuest Ebook Central, http://ebookcentral.proquest.com/lib/inflibnet-ebooks/detail.action?docID=1330977.
Created from inflibnet-ebooks on 2021-02-09 22:27:26.

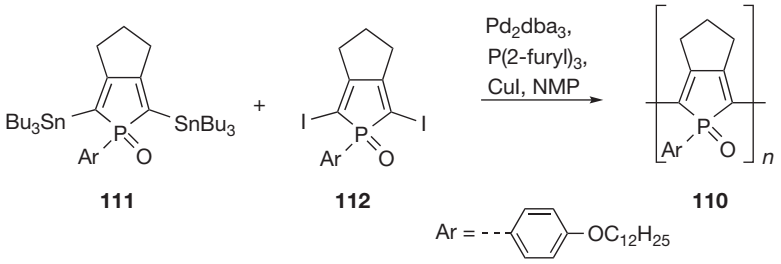

Scheme 25 Synthesis of the first phosphole homopolymer by Matano et al.[78]

HOMO–LUMO gap of a material by the formation of a rigidified, planar π-conjugated scaffold.[79] In this context, Baumgartner and coworkers have established the dithieno[3,2-*b*:2′,3′-*d*]phosphole system as an intriguing building block for a variety of molecular and polymeric organophosphorus materials.[80,81] The dithienophosphole is a powerful chromophore with highly tunable electronic/photophysical properties that result from the modification of the phosphorus center and the molecular backbone (Figure 9). In line with the work of the Réau group, the modification of the phosphorus center provides access to whole families of materials with altered properties that can easily be monitored via ^{31}P NMR and optical spectroscopies.

However, in contrast to simple phospholes, the rigid scaffold of fused dithienophospholes results in dramatically improved photoluminescence quantum yields that range from 50 to 90% for the parent system, thereby making it a promising building block for organic electronics.[13,80] In an effort to explore desirable processability for these materials, Baumgartner et al. have reported a diverse series of polymeric species.[80,81] The first account reports polystyrene-based polymers **113** and **114** that showcase dithienophosphole units as side chain functionalities, thus preserving the desirable highly efficient blue light-emitting features of the system.[80] The high-molecular-weight polymer (M_n = 147 650 g mol^{-1}; PDI = 2.46) is accessible by furnishing the P-center of the monomer **115** with a styryl-group that was used in the radical polymerization (Scheme 26) of a 1:30 mixture of phosphole to styrene (**91**).

Despite the low concentration of the phosphole, the polymer **113** was found to retain the photophysical properties of the monomer, showing an absorption maximum at λ_{max} = 352 nm with an intense blue fluorescence emission at λ_{max} = 424 nm (ϕ_{PL} = 75%). Furthermore, the presence of the organophosphorus units led to improved thermal stability with a glass-transition temperature of 114.2 °C (cf. polystyrene: <100 °C) and a decomposition temperature of 428 °C. The polymer was found to be air- and moisture-stable in the solid state, but slowly oxidized in solution. Like many other organophosphorus polymers reported herein, polymer **113** can also be deliberately oxidized with H_2O_2 without compromising the polymer backbone, resulting in a polymer (**114**) with red-shifted photophysics that match those of the monomer perfectly (λ_{max} = 374 nm; λ_{em} = 453 nm; ϕ_{PL} = 57%).

In addition to furnishing the exocyclic substituent with a polymerizable group, the dithienophosphole scaffold can also be functionalized in the 2,6-position to afford polymers

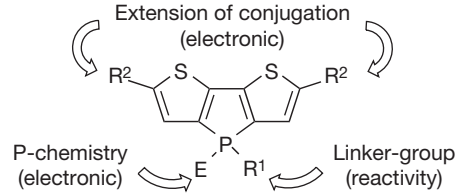

Figure 9 Potential sites for the tuning of dithienophospholes.[40]

(Scheme 26).[80,81] The latter approach allows for incorporation of the system as part of the polymer backbone, with correspondingly larger impact on the electronics of the polymer. In a proof-of-principle study, Baumgartner et al. installed tributyltin groups at the 2,6-positions of the dithienophosphole scaffold (**115**) to provide a conjugated polymer via a Stille-coupling protocol with a solubilized dialkoxyphenylene dibromide **116** (Scheme 26).[80] Although the reduced solubility of the polymer **117** precluded characterization by GPC or NMR spectroscopy, strongly red-shifted photophysics (λ_{max} = 456, 502 nm; λ_{em} = 555 nm) confirmed the successful formation of a conjugated dithienophosphole-based polymer (cf. monomer: λ_{max} = 379 nm; λ_{em} = 463 nm). In an effort to improve the access toward conjugated polymers, inversion of the functional groups, that is, the use of halogenated dithienophosphole building blocks, was found to be more advantageous, as it allowed for a more flexible approach to polymerization, covering Stille as well as Suzuki cross-coupling conditions. Initial studies on a series of molecular species with different emission colors via modification of the aromatic end-groups confirmed the feasibility of both protocols.[80] Using a 2,7-diborylated fluorene comonomer **118** with the dibrominated dithienophosphole oxide **119** (E = O) under Suzuki-conditions confirmed the general feasibility of the polymerization approach (Scheme 26); however, the reduced solubility of the polymer **120** again complicated its comprehensive characterization. Polymer **120** was only partially soluble in common organic solvents, and a soluble (minor) fraction revealed only a low-molecular-weight of M_w = 3200 g mol^{-1} (PDI = 1.37). Optical spectroscopy confirmed the extended conjugation in the polymer, with a demonstrated absorption maximum at λ_{max} = 507 nm, an orange emission at λ_{em} = 546 nm, and a reasonable quantum yield of ϕ_{PL} = 48% (c.f. monomer: λ_{max} = 366 nm; λ_{em} = 453 nm; ϕ_{PL} = 57%). Remarkably, the Suzuki approach, which uses borylated dithienophospholes and brominated arylenes, had been previously proven unsuccessful, resulting exclusively in deborylated dithienophospholes.[82]

Copyright © 2013. Elsevier. All rights reserved.

Comprehensive Inorganic Chemistry II : From Elements to Applications, Elsevier, 2013. ProQuest Ebook Central, http://ebookcentral.proquest.com/lib/inflibnet-ebooks/detail.action?docID=1330977.
Created from inflibnet-ebooks on 2021-02-09 22:27:26.

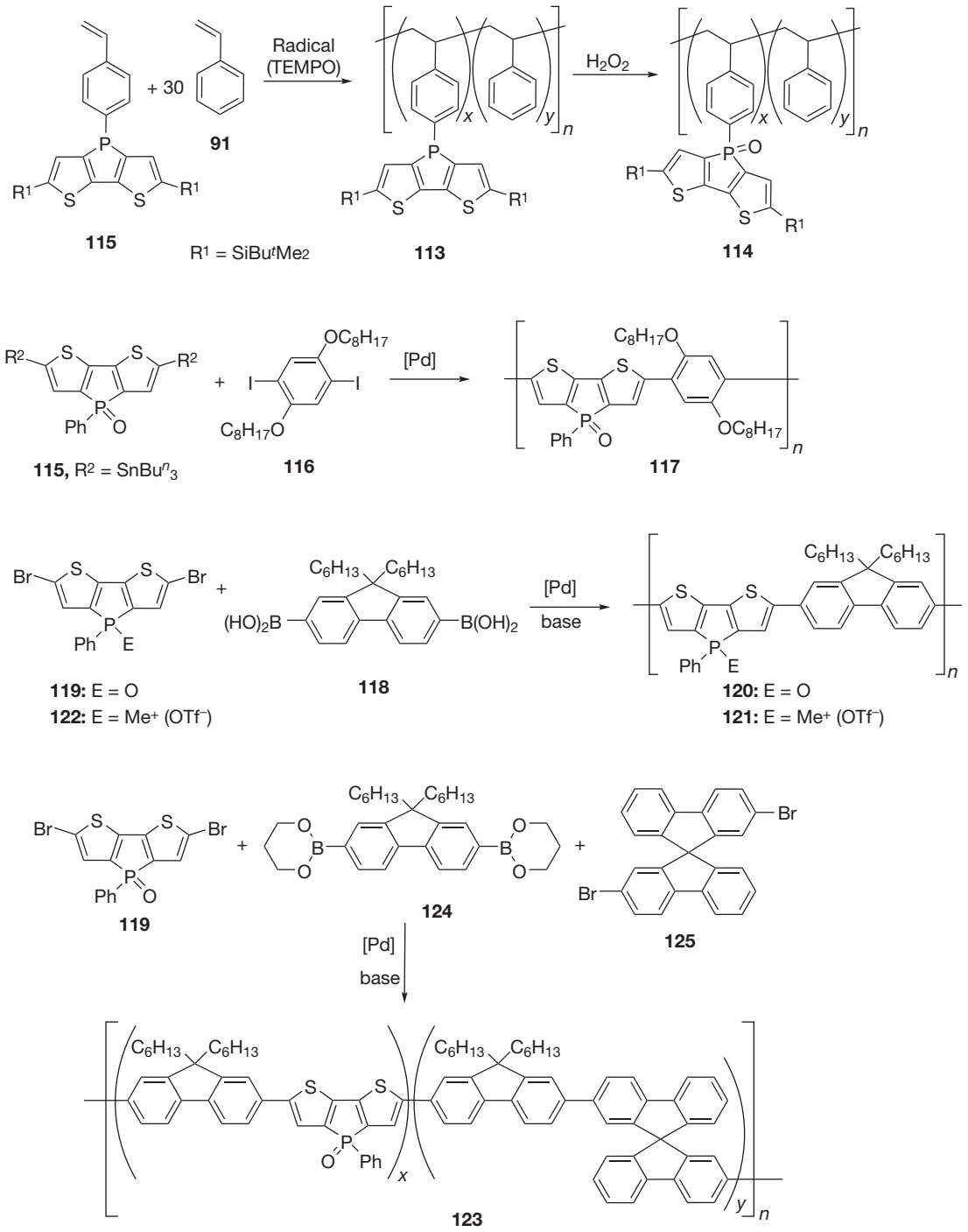

Scheme 26 Synthesis of dithienophosphole-based polymers.

A similar fluorene copolymer **121** with improved solubility features was obtained by modifying the dithienophosphole building block via formation of a cationic phospholium monomer **122** (E = Me^+, Scheme 26).[80] The resulting conjugated polyelectrolyte (CPE) **121** could be isolated in 69% yield as a yellow powder that was soluble in polar organic solvents ($CHCl_2$, CH_2Cl_2, THF) but not in water, due to the non-polar hexyl groups of the fluorene unit. A broad ^{31}P NMR resonance at $\delta = 23.2$ ppm and similarly broad ^1H- and ^{13}C NMR resonances confirmed the polymeric nature of the material. GPC revealed a moderate molecular weight of $M_w = 9800$ g mol^{-1} and narrow polydispersity (PDI = 1.7), which was nonetheless sufficient for the formation of thin films. The photophysical data of polymer **121** showed a red shift ($\lambda_{max} = 345$, 485 nm; $\lambda_{em} = 509$, 540 nm; $\phi_{PL} = 47\%$) when compared to those of the phospholium monomer ($\lambda_{max} = 276$, 376 nm; $\lambda_{em} = 467$ nm; $\phi_{PL} = 53\%$), which confirmed the extended conjugation in the polymer. Remarkably, the photophysics of the CPE **121** are also red-shifted relative to those of the related native poly(9,9-dihexyl) fluorene ($\lambda_{max} = 388$ nm; $\lambda_{em} = 445$ nm),[39] illustrating the

Copyright © 2013. Elsevier. All rights reserved.

Comprehensive Inorganic Chemistry II : From Elements to Applications, Elsevier, 2013. ProQuest Ebook Central, http://ebookcentral.proquest.com/lib/inflibnet-ebooks/detail.action?docID=1330977.
Created from inflibnet-ebooks on 2021-02-09 22:27:26.

strong acceptor-character of the phosphole unit, which resulted in a decreased LUMO-level for the polymer as a whole. The very small Stokes shift of only 15 nm and the occurrence of vibrational side band in the emission spectrum supported the rigidity of the polymer structure.[39] Moreover, the phosphole-based CPE showed significant luminescence in the solid state, which is highly unusual for polyelectrolytes, as their fluorescence is commonly quenched due to solid-state interactions, often referred to as 'superquenching'.[83]

Li and coworkers have reported dithienophosphole-doped polyfluorenes **123** that also showcase spirobifluorene units, which were expected to suppress unfavorable intermolecular interactions by virtue of the steric bulk of this building block (**Scheme 26**).[84] Besides quenching effects, solid-state interactions can also include formation of excimers with shifted emission and can, moreover, impact the thermal stability of the polymers.[39] Using the dibrominated dithienophosphole **119** and a related diborylated fluorene **124** next to a dibromospirobifluorene unit (**125**), two ABC copolymers (**123**) with low phosphole content (10% or 20%) were accessible, both of which showed a ^{31}P NMR resonance at $\delta = 20.1$ ppm. The polymers were soluble in common organic solvents and GPC confirmed high-molecular-weights of $M_n = 48\,000$–$53\,000$ g mol^{-1} (PDI = 1.23–1.30). High thermal stability was confirmed via TGA, showing a 5% weight loss at ~410 °C, and both polymers were found to be highly green/yellow luminescent in solution and the solid state, confirming the beneficial features of both the dithienophosphole and spirobifluorene units for the polymers.

Notably, the simple combination of dithienophosphole and fluorene units affords polymers with green to orange emission features. With a view toward improved efficiencies for organic photovoltaics (OPVs), however, it is desirable for a conjugated polymer to exhibit a bandgap that would absorb in the red or near-IR region of the optical spectrum, that is, $E_{bg} = 1.4$–1.9 eV.[39] Baumgartner and coworkers therefore targeted a series of ABC-copolymers **126** with an additional monomer adjacent to the dithienophosphole and fluorene units (**Scheme 27**).[81a] In this study, the exocyclic phenyl at the P-center was furnished with a 2-ethylhexyloxy (EtHexO) group for improved solubility (**127**). For reference, the solubilized dithienophosphole-fluorene AB-copolymer **126a** was also synthesized, and it was found that the EtHexO group indeed provided the desired improvement in terms of solubility.

Polymer molecular weights were determined to be $M_w = 14\,220$ g mol^{-1} (**126a**, PDI = 1.55), $M_w = 11\,380$ g mol^{-1} (**126b**, PDI = 1.91), and $M_w = 12\,490$ g mol^{-1} (**126c**, PDI = 1.85). As expected, the photophysical data of the AB-copolymer **126a** were similar to those of the earlier phosphole–fluorene copolymer,[80] with $\lambda_{max} = 505$ nm and $\lambda_{em} = 550$ nm. However, polymer **126b** showed surprisingly similar features ($\lambda_{max} = 460$ nm; $\lambda_{em} = 550$ nm; $\phi_{PL} = 60\%$), despite the strongly electron-donating nature of the EDOT comonomer.[39] This observation was attributed to steric congestion along the polymer backbone, which forced the repeat units in the polymer out of planarity and, consequently, disrupted the conjugation. The benzothiadiazole-containing copolymer **126b**, on the other hand, showed a significantly red-shifted emission at $\lambda_{em} = 658$ nm in solution. The absorption maximum, however, was measured at only $\lambda_{max} = 522$ nm.[81] Notably, the absorption experienced a dramatic red shift in the solid state, showing a maximum at $\lambda_{max} = 645$ nm ($\lambda_{em} = 695$ nm) that was in a suitable range for application in organic photovoltaics ($E_{bg} = 1.7$ eV). The latter was further confirmed via the emission quenching in the presence of C_{60}, which supported an efficient electron-transfer from the excited-state polymer to the fullerene acceptor in solution. Efficient electron-transfer from the donor-component to the acceptor component is a crucial process in organic bulk-heterojunction (BHJ) solar cells. Among the most popular materials for this application are poly(3-hexyl) thiophene (P3HT; donor) and 1-(3-methoxycarbonyl)propyl-1-phenyl[6,6]C_{61} (PCBM; acceptor).[39] In an effort to tune the electronic features of P3HT-like systems for improved interaction with PCBM, Baumgartner, Sutherland, and coworkers have synthesized a series of polythiophenes **129** with small amounts of dithienophosphole to be used a dopant for LUMO-level tuning (**Scheme 27**).[81] Via adjustment of the three comonomers **130**, **131**, and **132**, the amount of dithienophosphole could be varied from 0% to 17% providing polymers **129** with molecular weights ranging from $M_w = 2200$ to $12\,000$ g mol^{-1} with moderate polydispersities (PDI = 1.1–2.2). Thermal stabilities were determined to be high, in general showing decomposition only above 370 °C. While the energy levels of the phosphole-doped polymers were quite constant at $E_{HOMO} = -5.4$ eV and $E_{LUMO} = -3.4$ eV, an increasing amount of dithienophosphole was found to have a strong effect on the stability of the polymers, resulting in improved resistance toward oxidation that often hampers the application of P3HT. The observed stabilization was attributed to the lowered LUMO-levels of the polymers due to the presence of the organophosphorus component, while the thiophene components dominate the HOMO-levels. These results further highlight the favorable electron-acceptor features that can be achieved using organophosphorus building blocks.

In an extension of the work on dithienophosphole-based polystyrenes, Baumgartner and coworkers reported a white light-emitting polymer **133** in 2009 (**Scheme 28**).[81] The white light is generated by the mixing of three different color components (blue, green, orange) that are all based on the dithienophosphole scaffold. While the blue component **115** was provided from their earlier studies,[80] the orange component **134** was accessible through a 2,6-extended scaffold with 4-aminophenyl groups. Remarkably, the green component can be generated upon simple protonation of the amino groups of the orange species. Polymer **135**, which exhibited the blue and orange component, was accessible in analogy to earlier studies involving a radical protocol that used the styrene-functionalized **119** and **134** components in the presence of styrene (**91**) in a 1.6:1:2600 ratio and involved subsequent oxidation of the P-centers post-polymerization. The molecular weight of polymer **135** was determined to be 322 500 g mol^{-1}, with relatively broad distribution (PDI = 2.70) observed. The polymer was highly luminescent, despite the very small amounts of dithienophosphole incorporated. In the nonprotonated form of **135**, the photophysical data at $\lambda_{max} = 350$, 460, and 500 nm, as well as $\lambda_{em} = 456$ and 600 nm, confirmed the presence of the blue and orange components, respectively. After partial protonation of the amino groups of the orange component, white light-emission could be generated showing Commission Internationale de L'Eclairage (CIE) coordinates (0.34, 0.36) very close to those for pure white light (0.33, 0.33). White-light emission is a

Copyright © 2013. Elsevier. All rights reserved.

Comprehensive Inorganic Chemistry II : From Elements to Applications, Elsevier, 2013. ProQuest Ebook Central, http://ebookcentral.proquest.com/lib/inflibnet-ebooks/detail.action?docID=1330977.
Created from inflibnet-ebooks on 2021-02-09 22:27:26.

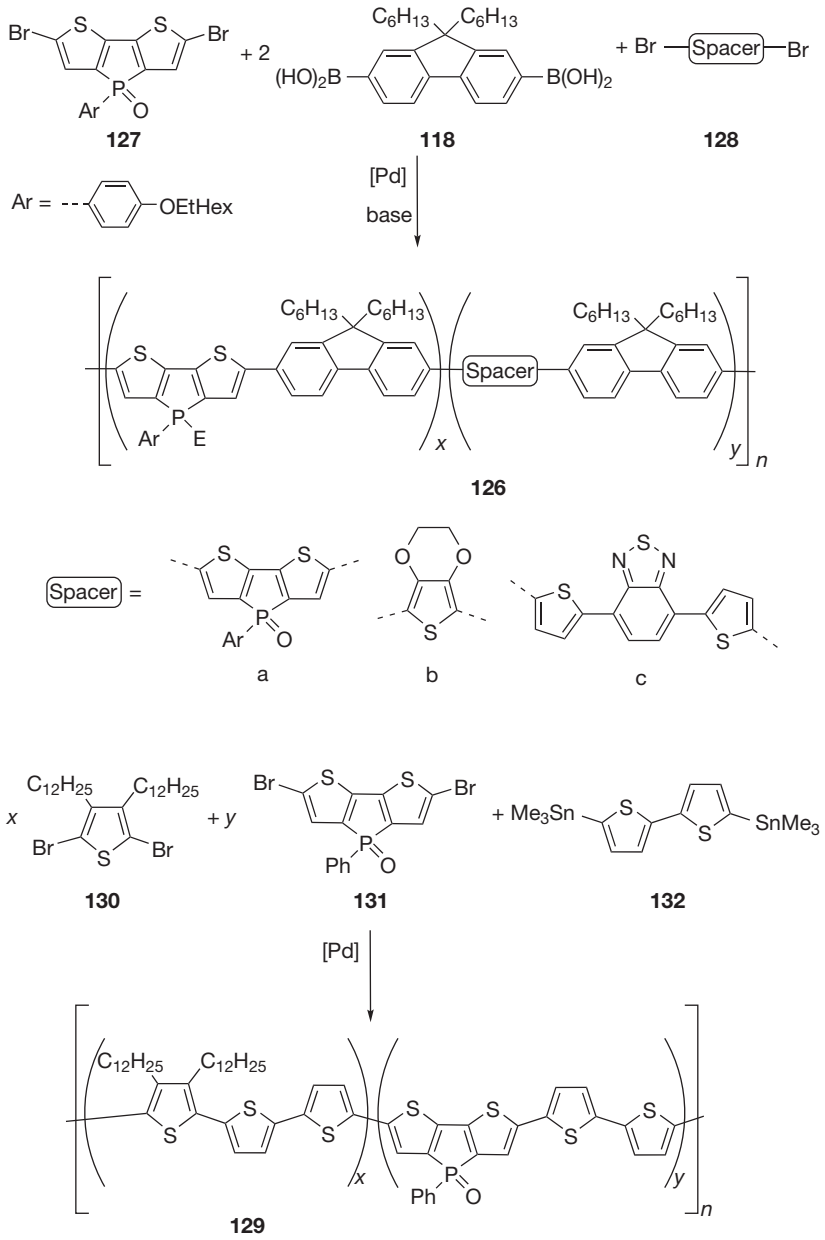

Scheme 27 Synthesis of low-bandgap polymers with dithienophosphole units.

result of Fluorescence Resonance Energy Transfer (FRET) from the three components (blue → green → orange).

White-light emission was also reported in 2008 by Huang and coworkers from another phosphole-based polymer.[85] In an effort to generate polyfluorene-analogue polymers with stabilized emission features, the group has reported two dibenzophosphole-fluorene copolymers of type **136** that are accessible via Suzuki cross-coupling of 2,7-dibrominated dibenzophospholes **137** with different P-centers and appropriately functionalized fluorenes **138** and **139**. Molecular weights were determined to be $M_n = 15\,400$ g mol^{-1} (PDI = 2.3) for **136a** and $M_n = 9500$ g mol^{-1} (PDI = 1.1) for **136b**. From the ^{1}H NMR signal of the methoxy groups, the levels of phosphole content were estimated to be 8% and 11%, respectively, suggesting the polymerization reactivity of the comonomers was decreasing in the following order: **137b** > **139** > **137a** (Scheme 29).

The polymers **136a/b** showed good solubility in common organic solvents, as well as high thermal stabilities ($T_d > 400$ °C). The photoluminescence features of both polymers in solution and the solid state were quite similar, despite the different nature of the P-centers (P(III) vs. P(V)), indicating that the fluorene units dominate the photophysical properties of the polymers. Cyclic voltammetry revealed lower energy levels for HOMO and LUMO when compared to those of native polyfluorene, suggesting improved electron-injection and -transport ability of the phosphole-based polymers. Moreover, the application of both polymers in preliminary devices confirmed the utility of the two polymers as emitters in OLEDs. However, their electroluminescence was surprisingly quite

Copyright © 2013. Elsevier. All rights reserved.

Comprehensive Inorganic Chemistry II : From Elements to Applications, Elsevier, 2013. ProQuest Ebook Central, http://ebookcentral.proquest.com/lib/inflibnet-ebooks/detail.action?docID=1330977.
Created from inflibnet-ebooks on 2021-02-09 22:27:26.

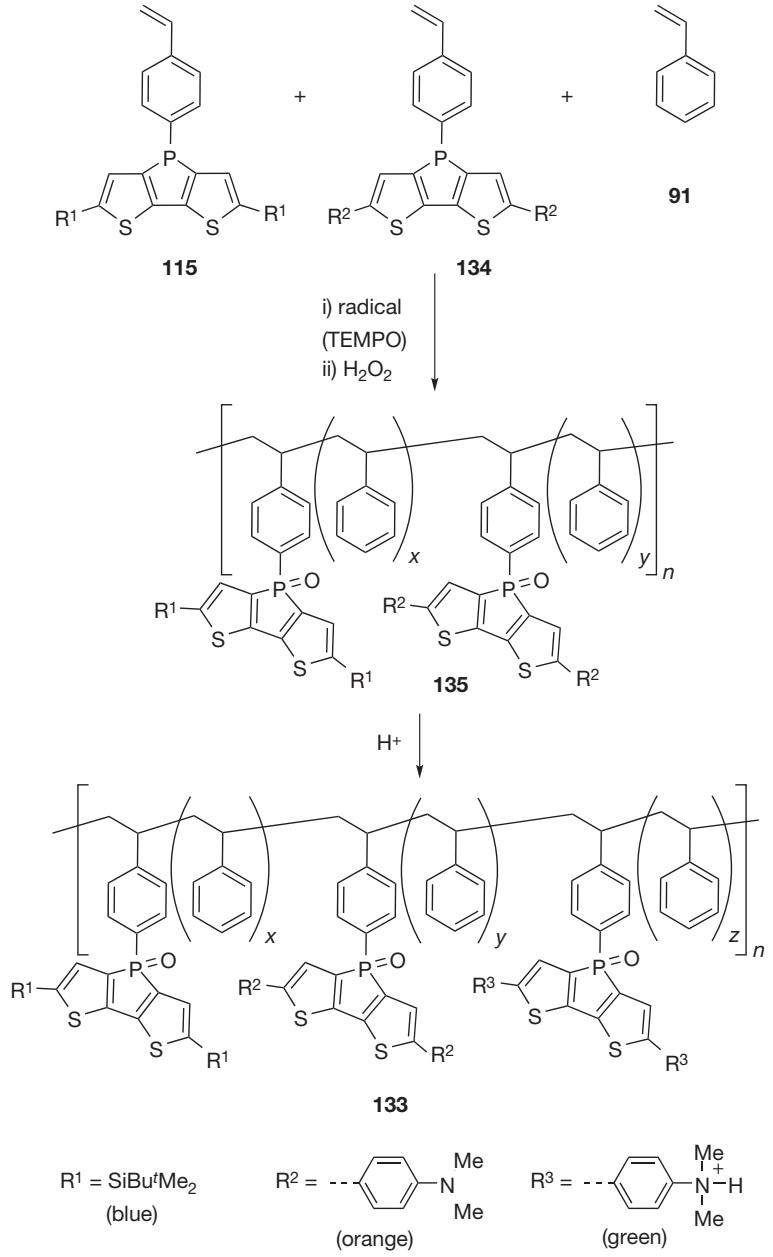

Scheme 28 Synthesis of a white light-emitting polystyrene with dithienophosphole side-groups.

different. While **136a** showed a blue emission in the device, **136b** actually exhibited white-light emission (CIE: 0.34, 0.36) under the same device setting. The reason for this difference in behavior has not been reported to date.

An interesting hybrid polymer was obtained by Baumgartner and coworkers in the context of their studies on the reactivity of 2,6-Si-H-capped dithienophospholes of type **140**.[81] While the Pt-catalyzed reaction with alkynes provided the expected hydrosilation polymer **141** selectively as *cis*-configured 1,2-addition products, as confirmed via reaction with 1,7-octadiyne, the analogous reaction with alkenes did not occur. Instead of the hydrosilation product, the resulting polymer **142** was the product of a dehydrogenative homocoupling via elimination of H_2, resulting in disilane-bridges between the dithienophosphole units. The same product was obtained simply by stirring the monomer in the presence of the Pt-catalyst. This result is remarkable insofar as quantitative dehydrocoupling of tertiary silanes had not been observed previously; more importantly, the reaction occurs even at room temperature. The molecular weight of polymer **142** confirmed chain lengths with up to 20 repeat units and the presence of two sets of ^{29}Si satellites in the ^{1}H NMR spectrum confirmed the exclusive nature of the dehydrogenative homocoupling; ^{29}Si NMR spectroscopy revealed only one resonance at $\delta = -4.7$ ppm. Both polymers, the hydrosilation product **141** as well as the dehydro-coupling product **142**, exhibited quite similar photophysical properties with absorptions at $\lambda_{max} = 378$ nm (**141**) and $\lambda_{max} = 393$ nm (**142**) and emission at $\lambda_{max} = 459$ and

Copyright © 2013. Elsevier. All rights reserved.

Comprehensive Inorganic Chemistry II : From Elements to Applications, Elsevier, 2013. ProQuest Ebook Central, http://ebookcentral.proquest.com/lib/inflibnet-ebooks/detail.action?docID=1330977.
Created from inflibnet-ebooks on 2021-02-09 22:27:26.

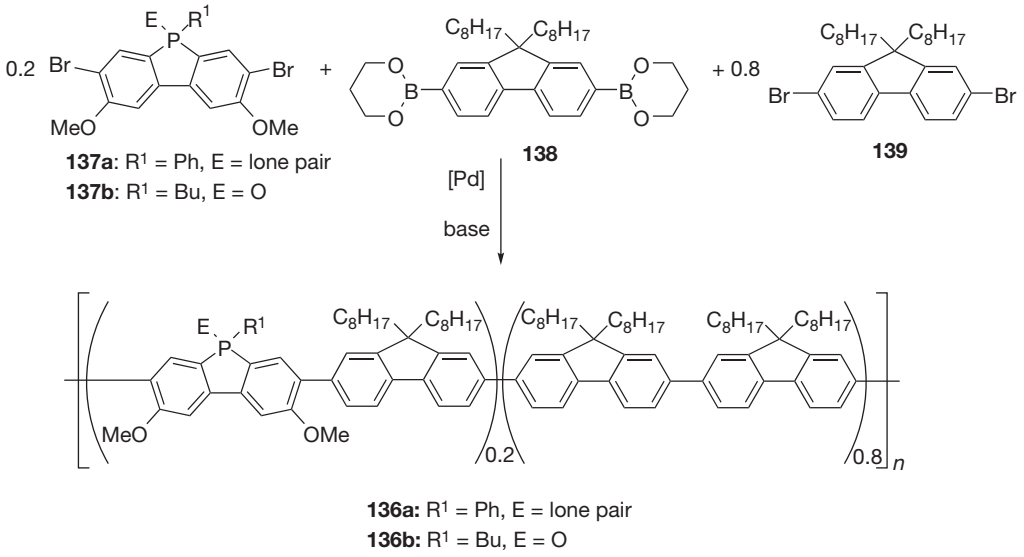

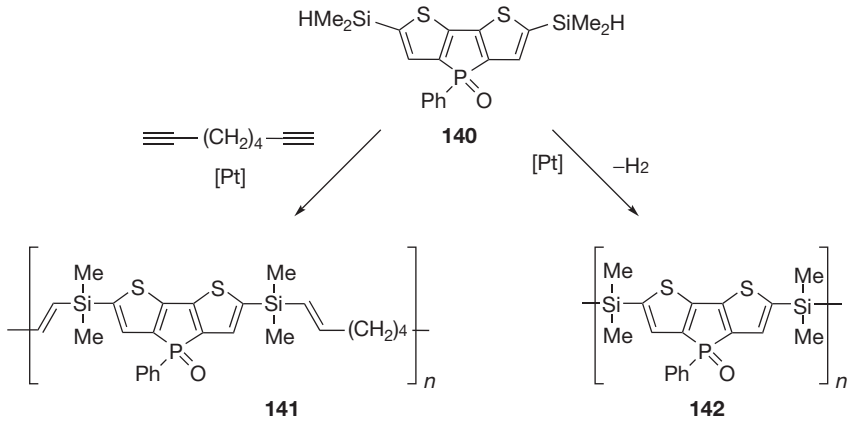

Scheme 29 Synthesis of dibenzophosphole-containing polyfluorenes (top), and poly(dithienophosphole silane)s (bottom).

460 nm, respectively, indicating that the fluorescence likely originates from the (isolated) dithienophosphole core.

1.28.6 Conclusion

While the exploration of phosphorus-containing polymers is a relatively new entry in the area of materials science, the diverse potential of these systems has led to rapid growth in this field. Beyond their well-known thermal stability, phosphorus-containing polymers are now becoming recognized for their potential application as electronic device materials. Numerous recent advances in synthetic methods toward extended π-conjugated organophosphorus systems emphasize the potential for the production of polymers with novel, desirable physical and electronic properties. In particular, the incorporation of trivalent phosphorus moieties into the backbone of diverse phosphaorganic polymers opens straightforward avenues to pre- or post-polymerization modification of these materials and, accordingly, easy access to new and diverse architectures. For related chapters in this Comprehensive, we refer to Chapters 1.02, 1.07, and 1.26.

References

1. Dillon, K., Mathey, F., Nixon, J. F., Eds.; In *Phosphorus: The Carbon Copy*; John Wiley and Sons Ltd: Chichester, 1998.
2. (a) Mathey, F. *Angew. Chem. Int. Ed.* **2003**, *42*, 1578–1604; (b) Baumgartner, T.; Réau, R. *Chem. Rev.* **2006**, *106*, 4681–4727 (correction: Baumgartner, T.; Réau, R., *Chem. Rev.* **2007**, *107*, 303); (c) Bates, J. I.; Dugal-Tessier, J.; Gates, D. P. *Dalton Trans.* **2010**, *39*, 3151–3159.
3. Levchik, S. V.; Weil, E. D. *J. Fire Sci.* **2006**, *24*, 345–364.
4. (a) Serbezeanu, D.; Vlad-Bubulac, T.; Hamciuc, C.; Aflori, M. *J. Polym. Sci. Part A: Polym. Chem.* **2010**, *48*, 5391–5403; (b) Serbezeanu, D.; Vlad-Bubulac, T.; Hamciuc, C.; Aflori, M. *Macromol. Chem. Phys.* **2010**, *211*, 1460–1471; (c) Hamciuc, C.; Vlad-Bubulac, T.; Sava, I.; Petreus, O. *J. Macromol. Sci. Part A: Pure Appl. Chem.* **2006**, *43*, 1355–1364.
5. (a) Zhao, C.-S.; Chen, L.; Wang, Y.-Z. *J. Polym. Sci. Part A: Polym. Chem.* **2008**, *46*, 5752–5759; (b) Bian, X.-C.; Chen, L.; Wang, J.-S.; Wang, Y.-Z. *J. Polym. Sci.*

Copyright © 2013. Elsevier. All rights reserved.

Comprehensive Inorganic Chemistry II : From Elements to Applications, Elsevier, 2013. ProQuest Ebook Central, http://ebookcentral.proquest.com/lib/inflibnet-ebooks/detail.action?docID=1330977.
Created from inflibnet-ebooks on 2021-02-09 22:27:26.

Part A: Polym. Chem. **2010**, *48*, 1182–1189; (c) Yang, M.; Chen, L.; Zhao, C.-S.; Huang, H.-Z.; Wang, J.-S.; Wang, Y.-Z. *Polym. Adv. Technol.* **2009**, *20*, 378–383.
6. Petreus, O.; Avram, E.; Lisa, G.; Serbezeanu, D. *J. Appl. Polym. Sci.* **2010**, *115*, 2084–2092.
7. (a) Lin, C. H.; Chang, S. L.; Cheng, P. W. *J. Polym. Sci. Part A: Polym. Chem.* **2011**, *49*, 1331–1340; (b) Lin, C. H.; Hwang, T. Y.; Taso, Y. R.; Lin, T. L. *Macromol. Chem. Phys.* **2007**, *208*, 2628–2641; (c) Lin, C. H.; Chang, S. L.; Wei, T. P. *Macromol. Chem. Phys.* **2011**, *212*, 455–464.
8. Sun, Y.-M.; Wang, C.-S. *Polymer* **2001**, *42*, 1035–1045.
9. Vlase, T.; Vlase, G.; Doca, N.; Iliescu, S.; Ilia, G. *High Perf. Polym.* **2010**, *22*, 863–875.
10. Ilia, G. *Polym. Adv. Technol.* **2009**, *20*, 707–722.
11. Macarie, L.; Ilia, G. *Prog. Polym. Sci.* **2010**, *35*, 1078–1092.
12. (a) Kumaresan, S.; Kannan, P. *J. Polym. Sci. Part A: Polym. Chem.* **2003**, *41*, 3188–3196; (b) Senthil, S.; Kannan, P. *J. Polym. Sci. Part A: Polym. Chem.* **2001**, *39*, 2396–2403.
13. (a) Fukazawa, A.; Hara, M.; Son, E.-C.; *et al. Org. Lett.* **2008**, *10*, 913–916; (b) Fukazawa, A.; Ichihashi, Y.; Kosaka, Y.; Yamaguchi, S. *Chem. Asian J.* **2009**, *4*, 1729–1740; (c) Saito, A.; Miyajima, T.; Nakashima, M.; Fukushima, T.; Kaji, H.; Matano, Y.; Imahori, H. *Chem. Eur. J.* **2009**, *15*, 10000–10004; (d) Miyajima, T.; Matano, Y.; Imahori, H. *Eur. J. Org. Chem.* **2008**, 255–259; (e) Matano, Y.; Miyajima, T.; Fukushima, T.; Kaji, H.; Kimura, Y.; Imahori, H. *Chem. Eur. J.* **2008**, *14*, 8102–8115; (f) Dienes, Y.; Eggenstein, M.; Kárpáti, T.; Sutherland, T. C.; Nyulászi, L.; Baumgartner, T. *Chem. Eur. J.* **2008**, *14*, 9878–9889; (g) Ren, Y.; Dienes, Y.; Hettel, S.; Parvez, M.; Hoge, B.; Baumgartner, T. *Organometallics* **2009**, *28*, 734–740; (h) Tsuji, H.; Sato, K.; Nakamura, E. *J. Mater. Chem.* **2009**, *19*, 3364–3366; (i) Von Ruden, A. L.; Cosimbescu, L.; Polikarpov, E.; Koech, P. K.; Swensen, J. S.; Wang, L.; Darsell, J. T.; Padmaperuma, A. B. *Chem. Mater.* **2010**, *22*, 5667–5671.
14. Ellis, J.; Wilson, A. D. *Dent. Mater.* **1992**, *8*, 79–84.
15. Becker, L. W. (Betz Laboratories Inc.) U.S. Patent 4,446,046, 1984.
16. Hagen, J. *Industrial Catalysis - A Practical Approach*, 2nd ed.; Weinheim: Wiley-VCH, 2002.
17. (a) Le Floch, P. *Coord. Chem. Rev.* **2006**, *250*, 627–681; (b) Mathey, F.; Sevin, A. *Molecular Chemistry of the Transition Metals*. Wiley: Chichester, 1996.
18. (a) Guinó, M.; Hii, K. K. *Chem. Soc. Rev.* **2007**, *36*, 608–617; (b) McNamara, C. A.; Dixon, M. J.; Bradley, M. *Chem. Rev.* **2002**, *102*, 3275–3300; (c) Bergbreiter, D. E. *Chem. Rev.* **2002**, *102*, 3345–3384; (d) Leadbeater, N. E.; Marco, M. *Chem. Rev.* **2002**, *102*, 3217–3274.
19. (a) Nicolaou, K. C., Hanko, R., Hartwig, W., Eds.; *Handbook of Combinatorial Chemistry,* Wiley-VCH: Weinheim, 2002; (b) Jäkel, C.; Paciello, R. Chem. Rev. 2006, 106, 2912–2942.
20. Uozumi, Y. *Top. Curr. Chem.* **2004**, *242*, 77–112.
21. den Heeten, R.; Swennenhuis, B. H. G.; van Leeuwen, P. W. N. M.; de Vries, J. G.; Kamer, P. C. J. *Angew. Chem. Int. Ed.* **2008**, *47*, 6602–6605.
22. (a) Dasgupta, M.; Peori, M. B.; Kakkar, A. K. *Coord. Chem. Rev.* **2002**, 233–234, 223–235; (b) Majoral, J.-P.; Caminade, A.-M. *Top. Curr. Chem.* **2003**, *223*, 111–159; (c) Caminade, A.-M.; Majoral, J.-P. *Coord. Chem. Rev.* **2005**, *249*, 1917–1926; (d) Caminade, A.-M.; Servin, P.; Laurent, R.; Majoral, J.-P. *Chem. Soc. Rev.* **2008**, *37*, 56–67.
23. Engel, R.; Rengan, K.; Chan, C. S. *Heteroatom Chem.* **1993**, *4*, 181–184.
24. Miedaner, A.; Curtis, C. J.; Barkley, R. M.; DuBois, D. L. *Inorg. Chem.* **1994**, *33*, 5482–5490.
25. Reetz, M. T.; Lohmer, G.; Schwickardi, R. *Angew. Chem. Int. Ed Engl.* **1997**, *36*, 1526–1529.
26. Ribaudo, F.; van Leeuwen, P. W. N. M.; Reek, J. N. H. *Israel J. Chem.* **2009**, *49*, 79–98.
27. (a) Morisaki, Y.; Ouchi, Y.; Tsurui, K.; Chujo, Y. *J. Polym. Sci. Part A: Polym. Chem.* **2007**, *45*, 866–872; (b) Morisaki, Y.; Ouchi, Y.; Tsurui, K.; Chujo, Y. *Polym. Bull.* **2007**, *58*, 665–671; (c) Ouchi, Y.; Morisaki, Y.; Ogoshi, T.; Chujo, Y. *Chem. Asian J.* **2007**, *2*, 397–402.
28. (a) Morisaki, Y.; Ouchi, Y.; Fukui, T.; Naka, K.; Chujo, Y. *Tetrahedron Lett.* **2005**, *46*, 7011–7014; (b) Morisaki, Y.; Ouchi, Y.; Naka, K.; Chujo, Y. *Tetrahedron Lett.* **2007**, *48*, 1451–1455.
29. Bowyer, P. K.; Vernon, C. C.; Nahid, G.-N.; *et al. Proc. Natl. Acad. Sci.* **2002**, *99*, 4877–4882.
30. Morisaki, Y.; Imoto, H.; Tsurui, K.; Chujo, Y. *Org. Lett.* **2009**, *11*, 2241–2244.
31. (a) Morisaki, Y.; Suzuki, K.; Imoto, H.; Chujo, Y. *Macromol. Rapid Commun.* **2010**, *31*, 1719–1724; (b) Imoto, H.; Morisaki, Y.; Chujo, Y. *Chem. Commun.* **2010**, *46*, 7542–7544.
32. (a) Foucher, D. A.; Tang, B. Z.; Manners, I. *J. Am. Chem. Soc.* **1992**, *114*, 6246–6248; (b) Foucher, D. A.; Honeyman, C. H.; Nelson, J. M.; Tang, B. Z.; Manners, I. *Angew. Chem. Int. Ed.* **1993**, *32*, 1709–1711; (c) Gómez-Elipe, P.; Resendes, R.; Macdonald, P. M.; Manners, I. *J. Am. Chem. Soc.* **1998**, *120*, 8348–8356; (d) Kulbaba, K.; Manners, I. *Macromol. Rapid Commun.* **2001**, *22*, 711–724; (e) Tanabe, M.; Vandermeulen, G. W. M.; Chan, W. Y.; Cyr, P. W.; Vanderark, L.; Rider, D. A.; Manners, I. *Nature Mater.* **2006**, *5*, 467–470; (f) Eloi, J. C.; Chabanne, L.; Whittell, G. R.; Manners, I. *Materials Today* **2008**, *11*, 28–36; (g) Whittell, G. R.; Manners, I. *Adv. Mater.* **2007**, *19*, 3439–3468; (h) Bellas, V.; Rehahn, M. *Angew. Chem. Int. Ed.* **2007**, *46*, 5082–5104; (i) Matas, I.; Whittell, G. R.; Partridge, B. M.; Holland, J. P.; Haddow, M. F.; Green, J. C.; Manners, I. *J. Am. Chem. Soc.* **2010**, *132*, 13279–13289.
33. Withers, H. P.; Seyferth, D.; Fellmann, J. D.; Garrou, P. E.; Martin, S. *Organometallics* **1982**, *1*, 1283–1288.
34. Honeyman, C. H.; Foucher, D. A.; Dahmen, F. Y.; Rulkens, R.; Lough, A. J.; Manners, I. *Organometallics* **1995**, *14*, 5503–5512.
35. Honeyman, C. H.; Peckham, T. J.; Massey, J. A.; Manners, I. *Chem. Commun.* **1996**, 2589–2590.
36. Mizuta, T.; Onishi, M.; Miyoshi, K. *Organometallics* **2000**, *19*, 5005–5009.
37. (a) Peckham, T. J.; Lough, A. J.; Manners, I. *Organometallics* **1999**, *18*, 1030–1040; (b) Evans, C. E. B.; Lough, A. J.; Grondey, H.; Manners, I. *New. J. Chem.* **2000**, *24*, 447–453.
38. (a) Peckham, T. J.; Massey, J. A.; Honeyman, C. H.; Manners, I. *Macromolecules* **1999**, *32*, 2830–2837; (b) Cao, L.; Winnik, M. A.; Manners, I. *J. Inorg. Organomet. Polym.* **1998**, *4*, 215–224; (c) Cao, L.; Winnik, M. A.; Manners, I. *Macromolecules* **2001**, *34*, 3353–3360.
39. (a) Skotheim, T. A., Reynolds, J. R., Eds.; *Handbook of Conducting Polymers*, 3rd ed.; CRC-Press: Boca Raton, 2007; (b) Müllen, K., Scherf, U., Eds.; *Organic Light Emitting Devices;* Wiley-VCH: Weinheim, 2006; (c) Perepichka, I. F., Perepichka, D. F., Eds.; *Handbook of Thiophene-Based Materials*; Wiley: Chichester, 2009; Vols. 1 and 2; (d) Thompson, B. C.; Fréchet, J. M. J. *Angew. Chem. Int. Ed.* **2008**, *47*, 58–77; (e) Facchetti, A. *Chem. Mater.* **2011**, *23*, 733–758; (f) Boudreault, P.-L.; Najari, A.; Leclerc, M. *Chem. Mater.* **2011**, *23*, 456–469; (g) Thomas, S. W., III; Joly, G. D.; Swager, T. M. *Chem. Rev.* **2007**, *107*, 1339–1386
40. (a) Elbing, M.; Bazan, G. C. *Angew. Chem. Int. Ed.* **2008**, *47*, 834–838; (b) Bosdet, M. J. D.; Piers, W. E. *Can. J. Chem.* **2009**, *87*, 8–29; (c) Ohshita, J. *Macromol. Chem. Phys.* **2009**, *210*, 1360–1370; (d) Matano, Y.; Imahori, H. *Org. Biomol. Chem.* **2009**, *7*, 1258–1271; (e) Crassous, J.; Réau, R. *Dalton Trans.* **2008**, 6865–6876; (f) Hobbs, M. G.; Baumgartner, T. *Eur. J. Inorg. Chem.* **2007**, 3611–3628; (g) Fukazawa, A.; Yamaguchi, S. *Chem. Asian J.* **2009**, *15*, 1386–1400.
41. (a) Lucht, B. L.; St Onge, N. O. *Chem. Commun.* **2000**, 2097–2098; (b) Jin, Z.; Lucht, B. L. *J. Organomet. Chem.* **2002**, *653*, 167–176; (c) Jin, Z.; Lucht, B. L. *J. Am. Chem. Soc.* **2005**, *127*, 5586–5595.
42. (a) Goodson, F. E.; Wallow, T. I.; Novak, B. M. *Macromolecules* **1998**, *31*, 2047–2056; (b) Goodson, F. E.; Wallow, T. I.; Novak, B. M. *J. Am. Chem. Soc.* **1997**, *119*, 12441–12453.
43. Ghassemi, H.; McGrath, E. *Polymer* **1997**, *38*, 3139–3143.
44. Tennyson, E. G.; He, S.; Osti, N. C.; Perahia, D.; Smith, R. C. *J. Mater. Chem.* **2010**, *20*, 7984–7989.
45. (a) Duarte, A.; Pu, K.-Y.; Liu, B.; Bazan, G. C. *Chem. Mater.* **2011**, *23*, 501–515; (b) Jiang, H.; Taranekar, P.; Reynolds, J. R.; Schanze, K. S. *Angew. Chem. Int. Ed.* **2009**, *48*, 4300–4316; (c) An, L.; Liu, L.; Wang, S.; Bazan, G. C. *Angew. Chem. Int. Ed.* **2009**, *48*, 4372–4375.
46. Han, L.-B.; Huang, Z.; Matsuyama, S.; Ono, Y.; Zhao, C.-Q. *J. Polym. Sci. Part A: Polym. Chem.* **2005**, *43*, 5328–5336.
47. (a) Tsuji, H.; Sato, K.; Illies, L.; Itoh, Y.; Sato, Y.; Nakamura, E. *Org. Lett.* **2008**, *10*, 2263–2265; (b) Sanji, T.; Shiraishi, K.; Kashiwabara, T.; Tanaka, M. *Org. Lett.* **2008**, *10*, 2689–2692; (c) Han, L.-B.; Zhang, C.; Yazawa, H.; Shimada, S. *J. Am. Chem. Soc.* **2004**, *126*, 5080–5081.
48. (a) Greenberg, S.; Gibson, G. L.; Stephan, D. W. *Chem. Commun.* **2009**, 304–306; (b) Greenberg, S.; Stephan, D. W. *Inorg. Chem.* **2009**, *48*, 8623–8631.
49. Vanderark, L. A.; Clark, T. J.; Rivard, E.; Manners, I.; Slootweg, J. C.; Lammertsma, K. *Chem. Commun.* **2006**, 3332–3333.
50. (a) Marinetti, A.; Mathey, F. *J. Am. Chem. Soc.* **1985**, *107*, 4700–4706; (b) Nief, F.; Mathey, F. *Tetrahedron* **1991**, *47*, 6673–6680.
51. Nake, K.; Umeyama, T.; Nakahashi, A.; Chujo, Y. *Macromolecules* **2007**, *40*, 4854–4858.
52. (a) Naka, K.; Umeyama, T.; Chujo, Y. *J. Am. Chem. Soc.* **2002**, *124*, 6600–6603; (b) Umeyama, T.; Naka, K.; Nakahashi, A.; Chujo, Y. *Macromolecules* **2004**, *37*, 1271–1275; (c) Naka, K.; Nakahashi, A.; Chujo, Y. *Macromolecules* **2006**, *39*, 8257–8262.

Copyright © 2013. Elsevier. All rights reserved.

Comprehensive Inorganic Chemistry II : From Elements to Applications, Elsevier, 2013. ProQuest Ebook Central, http://ebookcentral.proquest.com/lib/inflibnet-ebooks/detail.action?docID=1330977.
Created from inflibnet-ebooks on 2021-02-09 22:27:26.

53. (a) Wright, V. A.; Gates, D. P. *Angew. Chem. Int. Ed*. **2002**, *41*, 2389–2392; (b) Wright, V. A.; Patrick, B. O.; Schneider, C.; Gates, D. P. *J. Am. Chem. Soc.* **2006**, *128*, 8836–8844.
54. (a) Shah, S.; Concolino, T.; Rheingold, A. L.; Protasiewicz, J. D. *Inorg. Chem.* **2000**, *39*, 3860–3867; (b) Shah, S.; Eichler, B. E.; Smith, R. C.; Power, P. P.; Protasiewicz, J. D. *New J. Chem*. **2003**, *27*, 442–445; (c) Smith, R. C.; Chen, X.; Protasiewicz, J. D. *Inorg. Chem*. **2003**, *42*, 5468–5470; (d) Smith, R. C.; Protasiewicz, J. D. *J. Am. Chem. Soc*. **2004**, *126*, 2268–2269; (e) Smith, R. C.; Protasiewicz, J. D. *Eur. J. Inorg. Chem*. **2004**, 998–1006; (f) Gudimetla, V. B.; Ma, L.; Washington, M. P.; Payton, J. L.; Simpson, M. C.; Protasiewicz, J. D. *Eur. J. Inorg. Chem*. **2010**, 854–865.
55. Simmons, W. W. *The Stadtler Handbook of Ultraviolet Spectra*. Stadtler Research Laboratories: Philadelphia, 1979.
56. Höltzl, T.; Veszprémi, T.; Nguyen, M. T. *C. R. Chimie* **2010**, *13*, 1173–1179.
57. (a) Tsang, C.-W.; Yam, M.; Gates, D. P. *J. Am. Chem. Soc*. **2003**, *125*, 1480–1481; (b) Tsang, C.-W.; Baharloo, B.; Riendel, D.; Yam, M.; Gates, D. P. *Angew. Chem. Int. Ed*. **2004**, *43*, 5682–5685; (c) Gillon, B. H.; Gates, D. P. *Chem. Commun*. **2004**, 1868–1869; (d) Noonan, K. J. T.; Gates, D. P. *Angew. Chem. Int. Ed*. **2006**, *45*, 7271–7274; (e) Gillon, B. H.; Noonan, K. J. T.; Feldscher, B.; Wissenz, J. M.; Kam, Z. M.; Hsieh, T.; Kingsley, J. J.; Bates, J. I.; Gates, D. P. *Can. J. Chem*. **2007**, *85*, 1045–1052; (f) Noonan, K. J. T.; Gates, D. P. *Macromolecules* **2008**, *41*, 1961–1965.
58. Noonan, K. J. T.; Patrick, B. O.; Gates, D. P. *Chem. Commun*. **2007**, 3658–3660.
59. (a) Noonan, K. J. T.; Feldscher, B.; Bates, J. I.; Kingsley, J. J.; Yam, M.; Gates, D. P. *Dalton Trans*. **2008**, 4451–4457; (b) Gillon, B. H.; Patrick, B. O.; Gates, D. P. *Chem. Commun*. **2008**, 2161–2163; (c) Noonan, K. J. T.; Gillon, B. H.; Cappello, V.; Gates, D. P. *J. Am. Chem. Soc*. **2008**, *130*, 12876–12877.
60. Gaumont, A.-C.; Denis, J.-M. *Chem. Rev*. **1994**, *94*, 1413–1439.
61. (a) Manners, I. *Angew. Chem. Int. Ed Engl*. **1996**, *35*, 1602–1621; (b) Manners, I. *Synthetic Metal-Containing Polymers*. Wiley-VCH: Weinheim, 2004;.
62. (a) Webster, O. W. *Science* **1991**, *251*, 887–893; (b) Odian, G. *Principles of Polymerization*. Wiley: New York, 1991;.
63. (a) Park, K., Mrsny, R. J., Eds.; *Controlled Drug Delivery: Designing Technologies for the Future;* ACS Symposium Series 752 American Chemical Society: Washington, DC, 2000; (b) Hickner, M. A.; Ghassemi, H.; Kim, Y. S.; Einsla, B. R.; McGrath, J. E. *Chem. Rev*. **2004**, *104*, 4587–4612
64. Puddephatt, R. J. *Coord. Chem. Rev*. **2001**, *216–217*, 313–332.
65. (a) Mathey, F., Ed.; *Phosphorus-Carbon Heterocyclic Chemistry: The Rise of a New Domain;* Elsevier Science Ltd: Oxford, 2001; (b) Mathey, F. *Chem. Rev*. **1988**, *88*, 429–453; (c) Quin, L. D. In *Comprehensive Heterocyclic Chemistry*; Katritzky, A. R., Ed.; Pergamon: Oxford, 1996; pp 757–856
66. (a) Ma, J.; Li, S.; Jiang, Y. *Macromolecules* **2002**, *35*, 1109–1115; (b) Delaere, D.; Nguyen, M. N.; Vanquickenborne, L. G. *Phys. Chem. Chem. Phys*. **2002**, *4*, 1522–1530; (c) Delaere, D.; Nguyen, M. T.; Vanquickenborne, L. G. *J. Organomet. Chem*. **2002**, *643*, 194–201.
67. Mao, S. S. H.; Tilley, T. D. *Macromolecules* **1997**, *30*, 5566–5569.
68. Ueda, M.; Tomita, I. *Polym. Prep. Jpn*. **2003**, *52*, 1255–1257.
69. (a) Le Vilain, D.; Hay, C.; Deborde, V.; Toupet, L.; Réau, R. *Chem. Commun*. **1999**, 345–346; (b) Hay, C.; Fischmeister, C.; Hissler, M.; Toupet, L.; Réau, R. *Angew. Chem. Int. Ed Engl*. **2000**, *10*, 1812–1815; (c) Fave, C.; Cho, T. Y.; Hissler, M.; Chen, C. W.; Luh, T. Y.; Wu, C. C.; Réau, R. *J. Am. Chem. Soc*. **2003**, *125*, 9254–9255; (d) Su, H.-C.; Fadhel, O.; Yang, C.-J.; Cho, T.-Y.; Fave, C.; Hissler, M.; Wu, C.-C.; Réau, R. *J. Am. Chem. Soc*. **2006**, *128*, 983–995; (e) Zhang, L.; Hissler, M.; Bu, H.-B.; Bäuerle, P.; Lescop, C.; Réau, R. *Organometallics* **2005**, *24*, 5369–5376; (f) Fadhel, O.; Gras, M.; Lemaitre, N.; Deborde, V.; Hissler, M.; Geffory, B.; Réau, R. *Adv. Mater*. **2009**, *21*, 1261–1265; (g) Joly, D.; Tondelier, D.; Deborde, V.; Geffroy, B.; Hissler, M.; Réau, R. *J. New Chem*. **2010**, *34*, 1603–1611.
70. Hay, C.; Hissler, M.; Fischmeister, C.; *et al*. *Chem. Eur. J*. **2001**, *7*, 4222–4236.
71. Delaere, D.; Nguyen, M. T.; Vanquickenborne, L. G. *J. Phys. Chem. A* **2003**, *107*, 838–846.
72. Hay, C.; Fave, C.; Hissler, M.; Rault-Berthelot, J.; Réau, R. *Org. Lett*. **2003**, *5*, 3467–3470.
73. Fave, C.; Hissler, M.; Karpati, T.; *et al*. *J. Am. Chem. Soc*. **2004**, *126*, 6058–6063.
74. Sebastian, M.; Hissler, M.; Fave, C.; Rault-Berthelot, J.; Odin, C.; Réau, R. *Angew. Chem. Int. Ed*. **2006**, *16*, 6152–6155.
75. Lemau de Talancé, V.; Hissler, M.; Zhang, L.-Z.; *et al*. *Chem. Commun*. **2008**, 2200–2202.
76. Fadhel, O.; Benkö, Z.; Gras, M.; *et al*. *Chem. Eur. J*. **2010**, *16*, 11340–11356.
77. (a) Morisaki, Y.; Aiki, Y.; Chujo, Y. *Macromolecules* **2003**, *36*, 2594–2597; (b) Morisaki, Y.; Na, H.-S.; Aiki, Y.; Chujo, Y. *Polym. Bull*. **2007**, *58*, 777–784; (c) Na, H.-S.; Morisaki, Y.; Aiki, Y.; Chujo, Y. *J. Polym. Sci Part A: Polym. Chem*. **2007**, *45*, 2867–2875.
78. Saito, A.; Matano, Y.; Imahori, H. *Org. Lett*. **2010**, *12*, 2675–2677.
79. Baumgartner, T. *J. Inorg. Organomet. Poly. Mater*. **2005**, *15*, 389–409.
80. (a) Baumgartner, T.; Neumann, T.; Wirges, B. *Angew. Chem. Int. Ed*. **2004**, *43*, 6197–6201; (b) Baumgartner, T.; Bergmans, W.; Kárpáti, T.; Neumann, T.; Nieger, M.; Nyulászi, L. *Chem. Eur. J*. **2005**, *11*, 4687–4699; (c) Dienes, Y.; Durben, S.; Kárpáti, T.; Neumann, T.; Englert, U.; Nyulászi, L.; Baumgartner, T. *Chem. Eur. J*. **2007**, *13*, 7487–7500; (d) Durben, S.; Dienes, Y.; Baumgartner, T. *Org. Lett*. **2006**, *8*, 5893–5896; (e) Romero-Nieto, C.; Merino, S.; Rodríguez-López, J.; Baumgartner, T. *Chem. Eur. J*. **2009**, *15*, 4135–4145; (f) Romero-Nieto, C.; Kamada, K.; Cramb, D. T.; Merino, S.; Rodríguez-López, J.; Baumgartner, T. *Eur. J. Org. Chem*. **2010**, 5225–5231; (g) Ren, Y.; Baumgartner, T. *J. Am. Chem. Soc*. **2011**, *133*, 1328–1340.
81. (a) Durben, S.; Nickel, D.; Krüger, R. A.; Sutherland, T. C.; Baumgartner, T. *J. Polym. Sci. Part A: Polym. Chem*. **2008**, *46*, 8179–8190; (b) Krüger, R. A.; Gordon, T. J.; Sutherland, T. C.; Baumgartner, T. *J. Polym. Sci. Part A: Polym. Chem*. **2011**, *49*, 1201–1209; (c) Romero-Nieto, C.; Durben, S.; Kormos, I. M.; Baumgartner, T. *Adv. Funct. Mater*. **2009**, *14*, 3625–3631; (d) Wilk, W.; Baumgartner, T. *Org. Lett*. **2006**, *8*, 503–506.
82. Neumann, T.; Dienes, Y.; Baumgartner, T. *Org. Lett*. **2006**, *8*, 495–497.
83. Achyuthan, K. E.; Bergstedt, T. S.; Chen, L.; *et al*. *J. Mater. Chem*. **2005**, *15*, 2648–2656.
84. Zhang, Z.; Li, J.; Huang, B.; Qin, J. *Chem. Lett*. **2006**, *35*, 958–959.
85. Chen, R.-F.; Zhu, R.; Fan, Q.-L.; Huang, W. *Org. Lett*. **2008**, *10*, 2913–2916.

Copyright © 2013. Elsevier. All rights reserved.

Comprehensive Inorganic Chemistry II : From Elements to Applications, Elsevier, 2013. ProQuest Ebook Central, http://ebookcentral.proquest.com/lib/inflibnet-ebooks/detail.action?docID=1330977.
Created from inflibnet-ebooks on 2021-02-09 22:27:26.

1.29 Coordination Polymers with Group 15/16 Element Building Blocks

J Wachter, Universität Regensburg, Regensburg, Germany

© 2013 Elsevier Ltd. All rights reserved.

Abbreviations and Nomenclature

bipy	4,4′-Bipyridine
Cp	Any substituted cyclopentadienyl
Cp*	Pentamethylcyclopentadienyl (C_5Me_5)
Cp°	1-*tert*-Butyl-3,4-dimethylcyclopentadienyl
Cp^{Et}	Tetramethylethylcyclopentadienyl (C_5Me_4Et)
DFT	Density functional theory
dppe	Bis(diphenylphosphino)ethane
ESI	Electrospray spray ionization
MAS	Magic angle spinning
MOF	Metal–organic framework
NMR	Nuclear magnetic resonance
OTf	Trifluorosulfonate
pyz	Pyrazine
Q	Chalcogen (S, Se)
SBU	Secondary building unit
THF	Tetrahydrofurane
tri	1,3,5-Triazine
triphos	1,1,1-*Tris*(diphenylphosphinomethyl)ethane
WCA	Weakly coordinating anion
X	Halogen (Cl, Br, I)

1.29.1 Introduction

The construction of solid-state materials with infinite structures from metal ions and organic spacer ligands has become an explosively growing field of research in the past decade.[1] The properties of the supramolecular networks depend on the coordination geometry of the metal center and the functionality and donor properties of the organic ligands. Within the rich pool of organic ligands, polycarboxylates[2] and/or multifunctional N donor ligands[3] are of particular importance for the construction of metal–organic frameworks (MOFs).

This article is centered on the chemistry of copper(I) halides and mixed ligands of higher substituent free group 15 and group 16 elements. The interest in copper(I) halide coordination chemistry is based on its versatility to form aggregates with organic donor ligands.[4] Initial examples of group 15 ligands L included tertiary phosphanes, phosphites, and arsines, most frequently expressed as structural motif $Cu_4Hal_4L_4$ cubane tetramers[5] or stepped cubanes.[6] The first landmark in polymer chemistry of phosphorus complexes was the synthesis of $[Cu_6Br_6\{(triphos)CoP_3\}_2]$, which adopts a macrocyclic Cu_6Br_6 structure between two $[(triphos)Co(\eta^3\text{-}P_3)]$ units.[7]

Copyright © 2013. Elsevier. All rights reserved.
Comprehensive Inorganic Chemistry II : From Elements to Applications, Elsevier, 2013. ProQuest Ebook Central, http://ebookcentral.proquest.com/lib/inflibnet-ebooks/detail.action?docID=1330977.
Created from inflibnet-ebooks on 2021-02-09 22:27:26.

Another Cu_6X_6 aggregate has been realized in the capped adamantane-like cage of $[Cu_6I_6(m\text{-}tolyl_3P)_4(CH_3CN)_2]$.[8] Further examples are listed in the review of Peng et al.[4]

The potential of organometallic complexes bearing naked phosphorus ligands, the so-called P_n ligand complexes, as supramolecular building blocks was discovered in 2002 by Scheer et al. Oligomers and polymers have been formed by connecting P_n ligand complexes like $[(C_5H_5)_2(CO)_4Mo_2P_2]$[9] and $[Cp^*FeP_5]$,[10] with Cu(I), Ag(I), and Tl(I) salts (**Scheme 1**). The formation of spherical fullerene-like nanoclusters from $[Cp^*FeP_5]$ and CuCl under carefully controlled diffusion conditions opened new dimensions in coordination chemistry.[11] Many of these compounds exhibit dynamic behavior in solution as a consequence of dissociation–association equilibria.[12] Recent examples show that As_n ligand complexes may have a similar coordination potential.[13]

The aggregation of S- and Se-organic compounds with copper halides has also been intensively studied.[14,15] Bifunctional organic linkers with different donor sites are still rare, although recent developments have shown that bifunctional organic S,N ligands give organic–inorganic hybrid materials with interesting properties.[16]

An overview of coordination polymers containing building blocks from mixed group 15/16 elements has first to consider the 'normal' coordination chemistry of intact cage molecules of the element combinations P/S, P/As/S, As/S, and P/Se, and then the assembly of polymers by copper(I) halides. Accordingly, the chemistry of the coordination polymers is at the borderline of molecular and solid-state chemistry. The coordination chemistry of E_nQ_m ligand complexes, which arises from fragmentation reactions of cage molecules, has also to be considered before turning to the chemistry of coordination polymers. Then, the question, whether unsaturated metal centers coordinate to both the pnictogen and chalcogen atoms or whether there is a preference for one element type, may be addressed.

1.29.2 The Renaissance of Group 15/16 Element Cage Chemistry

1.29.2.1 Metal Complexes of the Intact Cage Molecules

1.29.2.1.1 Complexes with the P_4Q_3 cage (Q = S, Se)

Cage molecules composed of group 15 (E = P, As) and group 16 elements (Q = S, Se) are small inorganic clusters, and among them molecules of the nortricyclane type are ideal targets for molecular chemists. As the solubility in organic solvents decreases in the order $P_4S_3 > P_4Se_3 > As_4S_3$, the addition of Lewis acidic metal fragments to P_4S_3 has been the most intensively studied reaction type since more than 30 years. Addition reactions to one of the P atoms, insertion reactions into one of the cage bonds, or the replacement of one cage atom have been the subject of numerous reviews.[17,18] β-P_4S_4 may be regarded as a structural derivative of P_4S_3, but it is relatively unstable in solution (see later discussion).[19] The P_4S_4 cage exists in two isomeric forms (**Scheme 2**).

The coordination chemistry of P_4S_3 has, for a long time, focused on the addition reaction of a Lewis acidic complex fragment L either at the apical or the basal phosphorus (**I**, **II**; **Scheme 3**).[17] The first crystal structure of a metal carbonyl monoadduct was that of $P_4S_3{\cdot}Mo(CO)_5$ (type **I**), already published by Cordes in 1974,[21] but only recently $P_4S_3{\cdot}W(CO)_5$ (type **I**), $P_4S_3\{W(CO)_5\}_2$ (type **III**), and $P_4S_3\{W(CO)_5\}_4$ (type **V**) have been prepared.[22] In all cases, the $W(CO)_5$ fragments coordinate to the phosphorus sites of the cage (**Scheme 3**).

The adduct formation in the system of P_4Q_3 (Q = S, Se) with BX_3 (X = Br, I) provided evidence for the existence of monoadducts belonging to types **I** and **II**. Density functional theory (DFT) calculations on the B3LYP level have predicted similar energies for coordination modes **I** and **II**, whereas according to thermodynamic data the formation of basal adducts in the gas phase is favored.[23] Because of the weak nature of the P–B bonds the compounds only exist in the solid state. The structures of $BX_3(P_4S_3)$ (type **I**) and $BI_3(P_4Se_3)$ (type **II**) were solved by x-ray powder diffraction and solid-state ^{31}P magic angle spinning (MAS) NMR spectroscopy.

Considerable efforts were dedicated to the simultaneous apical and basal coordination (type **III**) of 16-electron Re, Ru, or Rh fragments. Thus, the reaction of $(triphos)Re(CO)_2(OTf)$ with P_4Q_3 yields the dinuclear species $[\{(triphos)Re(CO)_2\}_2P_4Q_3](OTf)_2$, which are first examples of an intact P_4Q_3 molecule bridging two transition metal fragments in coordination mode **III**.[24] No thermodynamic reason has been found for the preference of one coordination mode over the other, and from a theoretical analysis of electronic properties of the free cage the participation of sulfur lone pairs has not been excluded. The stepwise reaction of $[Cp^*Ru(dppe)]^+$ or $(C_5H_5)Fe(dppe)Cl$ with P_4Q_3 proceeds in a similar way.[25] The first crystal structure of a basal–apical adduct of type **III** was that of $[\{(C_5H_5)Ru(PPh_3)_2\}_2(\mu\text{-}P_4S_3)][CF_3SO_3]_2$ (**1**), published in 2007 (**Figure 1**).[26]

A new strategy in the coordination chemistry of P_4S_3 has been introduced by using Ag(I) salts with weakly coordinating anions (WCAs) $[Al(OR^F)_4]^-$ (OR^F = poly- or perfluorinated alkoxide).[27] Depending on the size of the anion, the formed cations are of dimeric or polymeric nature. Whereas smaller aluminates form polymeric species, for example, $[Ag(P_4S_3)_2]$

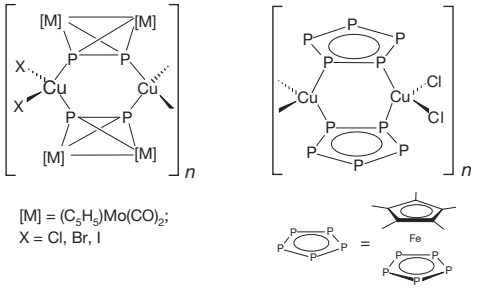

Scheme 1 Building principle of 1D polymeric structures generated from $[(C_5H_5)_2Mo_2(CO)_4P_2]$ and $[Cp^*FeP_5]$, respectively, and various copper(I) halides. Adapted from Scheer, M. *Dalton Trans.* **2008**, 4372.

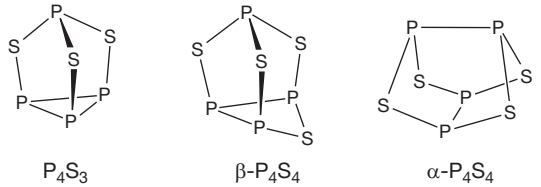

Scheme 2 Molecular structures of P_4S_3, α-P_4S_4,[20] and β-P_4S_4.

Copyright © 2013. Elsevier. All rights reserved.

Comprehensive Inorganic Chemistry II : From Elements to Applications, Elsevier, 2013. ProQuest Ebook Central, http://ebookcentral.proquest.com/lib/inflibnet-ebooks/detail.action?docID=1330977.
Created from inflibnet-ebooks on 2021-02-09 22:27:26.

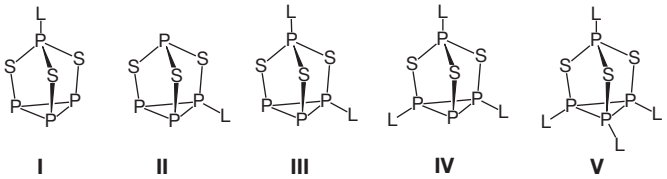

Scheme 3 Various coordination sites of the P_4S_3 cage (L = Lewis acidic fragment).

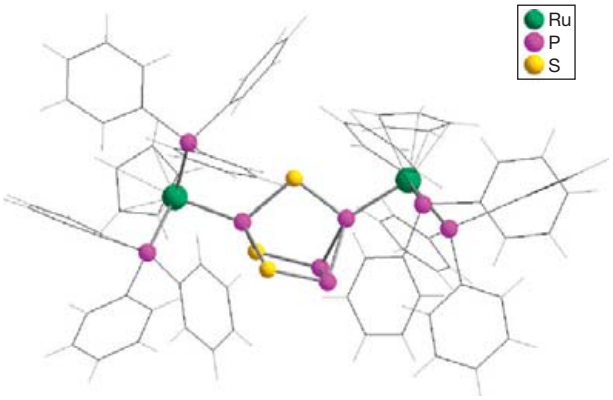

Figure 1 Structure of the dication $[\{(C_5H_5)Ru(PPh_3)_2\}_2(\mu\text{-}P_4S_3)]^{2+}$ in **1**. Adapted from Barbaro, P.; Di Vaira, M.; Peruzzini, M.; Seniori Costantini, S.; Stoppioni, P. *Chem. Eur. J.* **2007**, *13*, 6682.

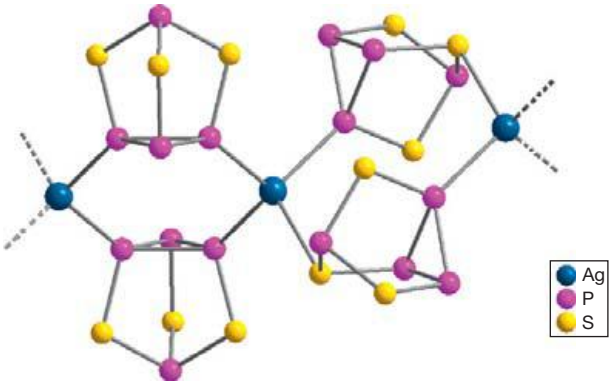

Figure 2 Section of the polymeric cation $[Ag(P_4S_3)_2]^+$ in **2**. Adapted from Adolf, A.; Gonsior, M.; Krossing, I. *J. Am. Chem. Soc.* **2002**, *124*, 7111; Raabe, I.; Antonijevic, S.; Krossing, I. *Chem. Eur. J.* **2007**, *13*, 7510.

$\{Al[OC(CF_3)_3]_4\}$ (**2**) (Figure 2), the largest anion forms $[Ag_2(P_4S_3)_6][(\{(CF_3)_3CO\}_3Al)_2F]_2$ (**3**) containing the dimeric dication $[Ag_2(P_4S_3)_6]^{2+}$ (Scheme 4). A common structural feature of both compounds is P_4S_3 bridging two Ag centers through sulfur with the assistance of basal P atoms. The pending cages in **3** coordinate either through sulfur or phosphorus. NMR studies and DFT calculations prove the adduct character of the compounds, which is manifested by a highly dynamic behavior in solution.

1.29.2.1.2 Coordination chemistry of the P_4Q_4 cage (Q = S, Se)

As already mentioned, phosphorus chalcogenide cages with higher S or Se content than P_4Q_3 are difficult to prepare.

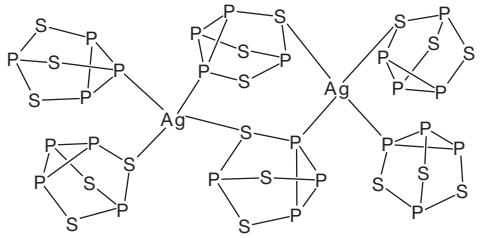

Scheme 4 Schematic structure of the dication $[Ag_2(P_4S_3)_6]^{2+}$ in **3**.

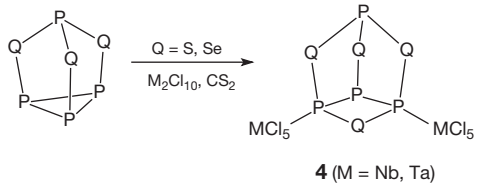

Scheme 5 Reaction of P_4Q_3 (Q = S, Se) with M_2Cl_{10} (M = Nb, Ta).

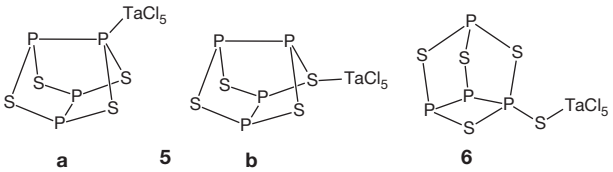

Scheme 6 Structures of $TaCl_5$ adducts of **5** and **6**.

However, the reaction of M_2Cl_{10} (M = Nb, Ta) with P_4Q_3 in CS_2/hexane gives $[(MCl_5)_2(\beta\text{-}P_4Q_4)]$ (**4**) in low yields (Scheme 5).[28] The surprising incorporation of chalcogen in the P_3 base of the original cage may be a consequence of redox processes between P_4Q_3 and the Lewis acidic metal halides ($M^V \rightarrow M^{IV}$). The adduct character of compounds **4** has been established by crystal structures and Raman spectroscopy.[29]

Addition of $TaCl_5$ to $\alpha\text{-}P_4S_4$ occurs at phosphorus, giving $[(TaCl_5)(\alpha\text{-}P_4S_4)]$ (**5a**). Ab initio electronic structure calculations found the hypothetical structure **5b** (coordination through one of the sulfur atoms) to be ca. 11.5 kJ mol^{-1} less stable than **5a** (Scheme 6). However, coordination of $TaCl_5$ to terminal sulfur sites like in $\alpha\text{-}P_4S_5$ is possible, thus giving **6** (Scheme 6).[29]

1.29.2.1.3 Solution chemistry of As_4S_n cages (n = 3,4)

Among binary arsenic sulfides, As_4S_3[30] (isotypic with P_4S_3) and realgar As_4S_4[31] exhibit molecular cage structures. While the solid-state chemistry of binary arsenic sulfides is well explored, their coordination chemistry in solution is poorly developed. Attempts to increase the solubility of As_4S_3 or As_4S_4

Copyright © 2013. Elsevier. All rights reserved.

Comprehensive Inorganic Chemistry II : From Elements to Applications, Elsevier, 2013. ProQuest Ebook Central, http://ebookcentral.proquest.com/lib/inflibnet-ebooks/detail.action?docID=1330977.
Created from inflibnet-ebooks on 2021-02-09 22:27:26.

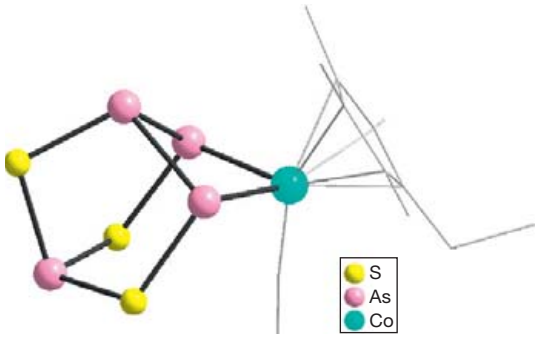

Figure 3 Molecular structure of $[Cp^{Et}Co(CO)(\eta^2\text{-}As_4S_3)]$ (**7**). Hydrogen atoms are omitted. Adapted from Brunner, H.; Kauermann, H.; Poll, L.; Nuber, B.; Wachter, J. *Chem. Ber.* **1996**, *129*, 657.

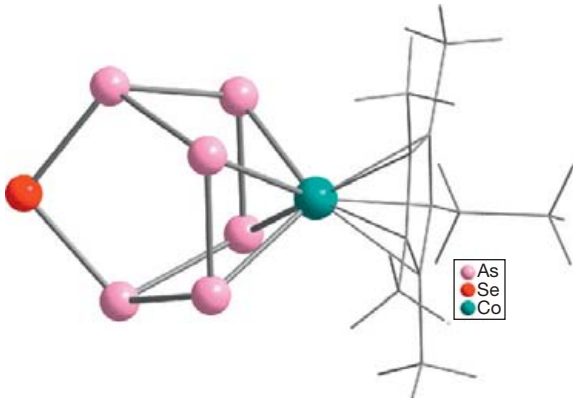

Figure 4 Molecular structure of $[Cp^{Et}Co(\eta^4\text{-}As_6Se)]$ (**8**). Adapted from Brunner, H.; Leis, F.; Nuber, B.; Wachter, J. *Polyhedron* **1999**, *18*, 347.

by heating their solutions in the presence of reactive organometallic or Lewis acidic substrates led to the extrusion of small homo- or heteroatomic E_n or E/S ligands. Relevant examples will be given in Section 1.29.2.2.

Transition metal complexes containing nearly intact cage molecules are still rare. Examples include $[Cp^{Et}Co(CO)(\eta^2\text{-}As_4S_3)]$ (**7**; Figure 3) and $[Cp^{Et}Co(CO)(\eta^2\text{-}As_4S_4)]$. Formally, both compounds are insertion products of the 16-electron $Cp^{Et}Co(CO)$ fragment in As–As bonds of the respective cage molecules.[32] That transition metal-induced cage fragmentation and ligand recombination processes may also play an important role is demonstrated by the formation of $[Cp^{Et}Co(\eta^4\text{-}As_6Se)]$ (**8**; Figure 4) from As_4Se_4 and $[Cp^{Et}Co(CO)]_2$ in boiling xylene.[33]

A group 6 metal carbonyl adduct of As_4S_3 can be prepared under mild conditions upon stirring its suspension in THF with $Cr(CO)_5THF$. The formed $As_4S_3{\cdot}Cr(CO)_5$ (**9**) is considerably more soluble than the free cage.[34] The $Cr(CO)_5$ fragment is fixed at the apical As atom,[18] which corresponds to type **I** of P_4S_3 adducts (Scheme 3).

Surprisingly, compound **9** is also a product of the reaction of β-As_4S_4(α- and β-As_4S_4 stand for high- and low-temperature modifications of realgar,[31] while α- and β-P_4S_4 signify different cage molecules) and $Cr(CO)_5THF$ in THF (Scheme 7).[35] The reaction requires the presence of light and parallels therefore to some extent the light-induced structural change of crystalline

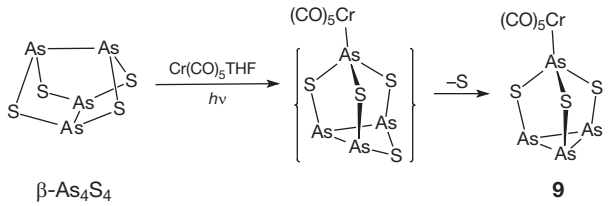

Scheme 7 Possible pathway for the reaction of β-As_4S_4 with $Cr(CO)_5THF$ in the presence of light.

α-As_4S_4 into pararealgar,[36] the molecular structure of which is related to that of β-P_4S_4 (Scheme 2).

1.29.2.2 Cage Fragmentation Reactions

1.29.2.2.1 General remarks

As already mentioned, the degradation of mixed E_nQ_m cage molecules by reactive organometallic complexes is one method for the synthesis of metal complexes with heteroatomic E/Q ligands. Other synthetic strategies include the reduction of binary E/Q phases by nucleophilic coordination compounds or the insertion of metal complex fragments into neutral or anionic cage molecules, which has been reviewed in detail.[17,18,37,38] The advantage of fragmentation reactions is that they produce stable hybrid clusters with inorganic cores, which exhibit coordination properties corresponding to group 15 and/or group 16 ligand complexes, and peripheral organometallic groups that are responsible for solubility and kinetic stabilization.

1.29.2.2.2 Triple-decker-like complexes with mixed group 15/16 ligands

One important subgroup from these fragmentation reactions are triple-decker-like complexes with a middle deck consisting of group 15/16 ligands. The interest in group 15 triple-decker sandwich complexes has been stimulated by the isolobal relationship between the heavier group 15 elements and carbon.[39] Prominent examples with aromatic middle decks are $[Cp^*_2Cr_2P_5]$ (**10**),[40] $[(C_5H_5)_2Mo_2As_5]$ (**11**), which contains a distorted middle deck,[41] and $[Cp^*_2Mo_2P_6]$ (**12**)[42] (Scheme 8).

Formal substitution of one (**13**) or three (**14**) group 15 ligands in the elusive $[Cp^*_2Mo_2P_5]$[43] by group 16 ligands causes loss of aromaticity, but may give rise to new and interesting properties depending on the chalcogen content (Scheme 8). The displacement of two E15 atoms has not yet been realized, but complete substitution of phosphorus by chalcogens produces $[Cp^*_2Mo_2Q_4]$ complexes in different isomeric forms.[44] A related ligand exchange can be carried out for the As_5 triple-decker **11**.

1.29.2.2.3 Isomerism and ligand rearrangement in dimolybdenum complexes

The first mixed phosphorus- and sulfur-containing molybdenum complexes are $[Cp^*_2Mo_2P_4S]$ (**13**) and $[Cp^*_2Mo_2P_2S_3]$ (**14**), which were prepared in 1987 by the reaction of P_4S_3 and $[Cp^*Mo(CO)_2]_2$.[45] The CO-containing and phosphorus-rich products $[Cp^*(CO)_2Mo(\eta^3\text{-}P_3)]$[42] (**15**) and $[Cp^*_2(CO)_4Mo_2(\mu,\eta^2\text{-}P_2)]$[42] (**16**) are formed (Scheme 9) as by-products. The reactions of P_4Se_3 or As_4S_4 give similar results and produce $[Cp^*_2Mo_2P_2Se_3]$[46] (**18**) or $[Cp^*_2Mo_2As_2S_3]$[47] (**21**) as the main products (Scheme 9). The structure of **13** was solved by a

Copyright © 2013. Elsevier. All rights reserved.

Comprehensive Inorganic Chemistry II : From Elements to Applications, Elsevier, 2013. ProQuest Ebook Central, http://ebookcentral.proquest.com/lib/inflibnet-ebooks/detail.action?docID=1330977.
Created from inflibnet-ebooks on 2021-02-09 22:27:26.

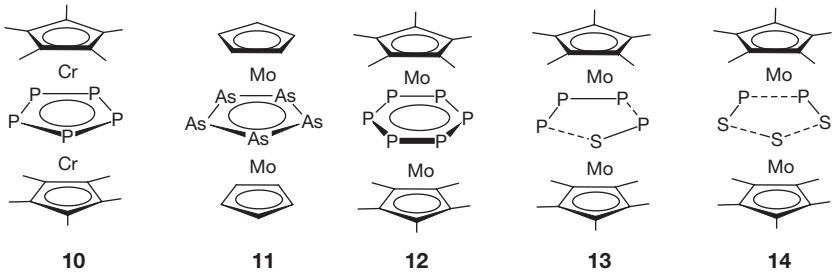

Scheme 8 Comparison of homo- and heteroligand triple-decker-like complexes of group 6 metals.

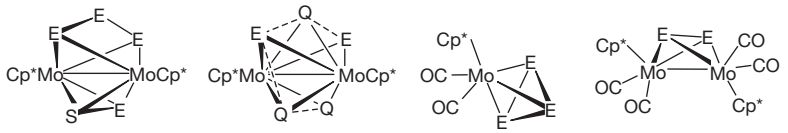

13: E = P
17: E = As
14: E = P; Q = S
18: E = P; Q = Se
21: E = As; Q = S
15: E = P
19: E = As
16: E = P
20: E = As

Scheme 9 Products from the reactions of $[Cp^*Mo(CO)_2]_2$ with P_4S_3, P_4Se_3, and As_4S_3, respectively, in boiling toluene.

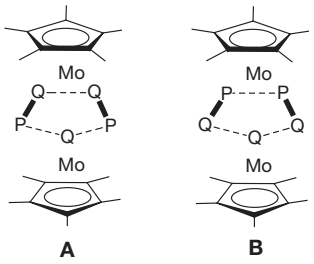

Scheme 10 Energetically favored distributions of P and Q (Q = S, Se) within the P_2Q_3 middle deck of triple-decker complexes **14** and **18**.

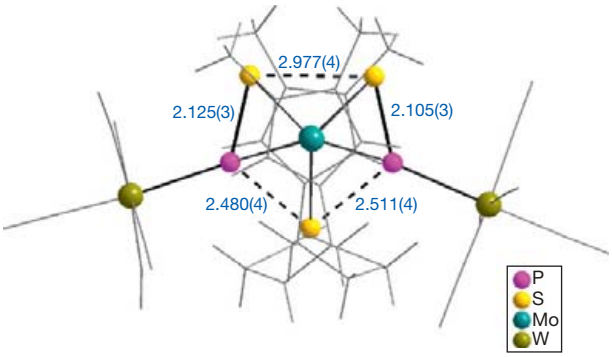

Figure 5 Molecular structure of $[Cp^\circ{}_2Mo_2P_2S_3\{W(CO)_5\}_2]$ (**24**) and selected distances (Å). Adapted from Gröger, C.; Kubicki, M. M.; Meier, W.; Pronold, M.; Wachter, J.; Zabel, M. *Organometallics* **2009**, *28*, 5633.

combination of ^{31}P NMR spectroscopy and x-ray crystallography of a $Cr(CO)_5$ adduct: The triple-decker-like molecule contains a *cyclo*-P_4S middle deck composed of μ,η^3-P_3 and μ,η^2-PS ligands.[45] However, the structures of **14**, **18**, and **21** remained elusive until very recently because of the difficulty in distinguishing between phosphorus and sulfur atoms in the presence of heavy atoms in x-ray diffraction experiments. Disorder problems within the inorganic middle deck are typical of As_nS_m ligand complexes.[48]

It may be noted that the use of substituted cyclopentadienyl ligands enhances both kinetic stability and solubility of the E_nQ_m ligand complexes. For this reason $[Cp^\circ{}_2Mo_2P_2S_3]$ (**22**) and $[Cp^\circ{}_2Mo_2P_4S]$ (**23**) bearing the Cp° ligand were synthesized.[49]

DFT calculations and ^{31}P NMR spectroscopy (including solid-state ^{31}P MAS NMR) showed that **14** contains a P_2S_3 middle deck composed of two η^2-PS dumbbells and one singly bridging sulfur ligand. The energetically favored distributions and connections of phosphorus and sulfur are those found in the positional isomers **14A** and **14B** (Scheme 10) and calculated total energies reveal **14A** to be more stable by 12–13 kcal·mol^{-1} than **14B**. Successful crystallographic studies require the addition of $W(CO)_5$ fragments to the P_2S_3 middle deck. Correlation of crystal structures and ^{31}P NMR spectra of the stable diadduct $[Cp^\circ{}_2Mo_2P_2S_3\{W(CO)_5\}_2]$ (**24**) (Figure 5) confirms the exclusive presence of a P_2S_3 middle deck analogous to positional isomer **A**.[50]

The distribution of P and Se in **18** is analogous to that in **14A**,[46] but the distribution of As and S in **21** can only be deduced from the structures of the coordination polymers formed with Cu(I) halides. Thus, the crystal structure of $[(CuCl)_2(Cp^*{}_2Mo_2As_2S_3)]_n$ (see Figure 19) unequivocally shows an element distribution in the As_2S_3 middle deck corresponding to that in positional isomer **B** (Scheme 10).

1.29.2.2.4 Diiron complexes with $(AsQ)_n$ (n = 1, 2; Q = S, Se) ligands

The chemistry of triple-decker-like complexes can be extended to dimeric iron complexes with arsenic chalcogenide ligands. The synthesis of $[Cp^*{}_2Fe_2As_2Q_2]$ complexes (Q = S: **25**[51]; Q = Se: **26**[52]) from As_4Q_4 and $[Cp^*{}_2Fe_2(CO)_4]$ in boiling toluene is outlined in Scheme 11. The formation of related

Copyright © 2013. Elsevier. All rights reserved.

Comprehensive Inorganic Chemistry II : From Elements to Applications, Elsevier, 2013. ProQuest Ebook Central, http://ebookcentral.proquest.com/lib/inflibnet-ebooks/detail.action?docID=1330977.
Created from inflibnet-ebooks on 2021-02-09 22:27:26.

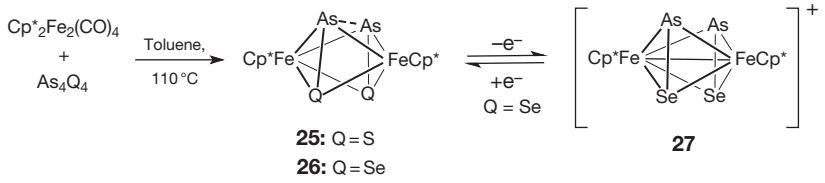

Scheme 11 Reaction of $[Cp^*_2Fe_2(CO)_4]$ with As_4Q_4 (Q = S, Se).

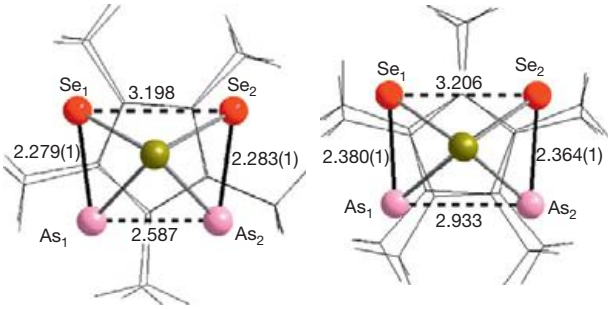

Figure 6 Molecular structures of $[Cp^*_2Fe_2As_2Se_2]$ (**26**) (left) and the cation $[Cp^*_2Fe_2As_2Se_2]^+$ in [**27**][PF_6] (right) and selected distances (Å). Adapted from Blacque, O.; Brunner, H.; Kubicki, M. M.; Leis, F.; Lucas, D.; Mugnier, Y.; Nuber, B.; Wachter, J. *Chem. Eur. J.* **2001**, *7*, 1342.

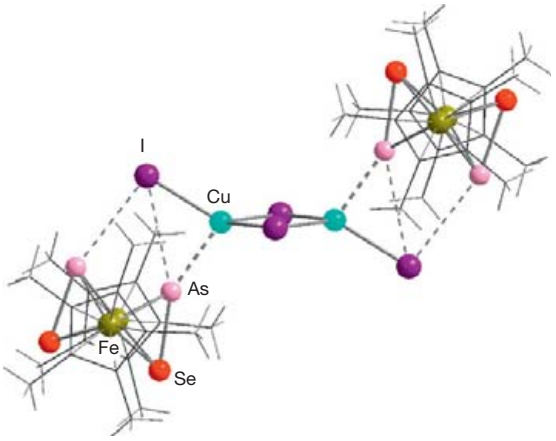

Figure 7 Molecular structure of $[Cp^*_2Fe_2As_2Se_2][Cu_2I_4]$ (**28**). Selected distances (Å): As···I_{mean} 3.462(2), As···Cu 2.528(2).

P/S containing compounds using the thermal degradation of P_4S_3 was tried without success in our laboratories.

The 30-electron complex **26** contains a trapezoid $\mu,\eta^{4:4}$-As_2Se_2 ligand, which behaves according to DFT and extended Hückel molecular orbital calculations as a four-electron π donor (Figure 6). Complex **26** can be reversibly oxidized into the cation $[Cp^*_2Fe_2As_2Se_2]^+$ (**27**) (Scheme 11). This process is accompanied by a shortening of the Fe–Fe distance by more than 0.3 Å and by breaking of the weak As–As bond of 2.587 Å. Thus, the geometry of the middle deck of **27** consists of an approximately rectangular core with two separate η^2-AsSe dumbbells (Figure 6). The calculations also reveal that during oxidation an electron is removed from an occupied Fe—Fe orbital of antibonding character.[52]

The elusive dication $[Cp^*_2Fe_2(AsSe)_2]^{2+}$ can be electrochemically generated by further one-electron oxidation ($E_{1/2}$ = +0.72 V) of **27**, but is unstable on the timescale of cyclovoltammetry. This species may be related to the isolobal [(1,3-*tert*-$Bu_2C_5H_3$)Fe_2P_4],[53] which exhibits a trapezoid middle deck in the solid state, whereas ^{31}P NMR solution spectra are in agreement with a $Fe_2(\mu,\eta^{2:2}\text{-}P_2)_2$ core.[54]

The reaction of **26** with CuI gives $[Cp^*_2Fe_2As_2Se_2][Cu_2I_4]$ (**28**), which is the result of a redox reaction between **26** and CuI. The structure of **28** contains two $[Cp^*_2Fe_2As_2Se_2]^+$ cations that are bridged by a $Cu_2I_4^{2-}$ dianion (Figure 7). In this compound a rare Cu···As interaction is observed (see later discussion), probably supported by As···I interactions and electrostatic attraction forces.[55]

1.29.2.3 Coordination Polymers from E_nQ_m Ligand Complexes and Copper(I) Halides

1.29.2.3.1 General remarks

The versatility of organometallic E_n ligand complexes as building blocks in supramolecular chemistry has been reviewed recently.[12] For practical reasons it has been proposed in this chapter to distinguish between the reactivity of E_n ligand complexes with noncoordinated Lewis acidic cations, for example, Ag^+ or Cu^+, and Lewis acidic coordination compounds containing at least one terminal ligand, like copper(I) halides. In this way oligomers and polymers may be formed depending on the nature of the cation, while the anion determines the supramolecular properties.

Among E_2 ligand complexes the reaction of $[(C_5H_5)_2(CO)_4Mo_2(\mu,\eta^2\text{-}P_2)]$ with CuX (X = Cl, Br, I) is relatively straightforward. The structure of the insoluble linear polymer 1D-$[(CuBr)\{(C_5H_5)_2(CO)_4Mo_2(\mu,\eta^2\text{-}P_2)\}]_n$ (**29**) consists of a strand composed of planar six-membered Cu_2P_4 rings, which are orthogonally connected by four-membered Cu_2Br_2 rings (Figure 8).[9]

While the incorporation of an As_2 ligand complex like **20** into coordination polymers could not yet be realized, $[Cp^*(CO)_2Mo(\eta^3\text{-}As_3)]$ (**19**) reacts with CuX (X = Cl, Br, I) under formation of the dimeric compounds $[CuX\{Cp^*(CO)_2Mo(\eta^3\text{-}As_3)\}]_2$ (**30**).[13] The structure of **30** is characterized by a side-on coordination of the $(CuX)_2$ bridge to the *cyclo*-As_3 unit [d(Cu-As)$_{mean}$ 2.474 Å] (Figure 9). Interestingly, the product of the reaction of the Sb_2 ligand complex $[(C_5H_5)_2(CO)_4Mo_2(\mu,\eta^2\text{-}Sb_2)]$ with CuX follows the same coordination mode.[56]

Although the coordination properties of the *cyclo*-P_5 ligand in pentaphosphaferrocene have been widely established,[11,12] the potential of triple-decker complexes with P_5 or P_6 middle deck as building blocks is still unexplored. However, it has been shown in Section 1.29.2.2.2 that substitution of phosphorus by chalcogens produces a series of triple-decker-like E_nQ_m complexes. In these compounds, group 15 and group

Copyright © 2013. Elsevier. All rights reserved.

Comprehensive Inorganic Chemistry II : From Elements to Applications, Elsevier, 2013. ProQuest Ebook Central, http://ebookcentral.proquest.com/lib/inflibnet-ebooks/detail.action?docID=1330977.
Created from inflibnet-ebooks on 2021-02-09 22:27:26.

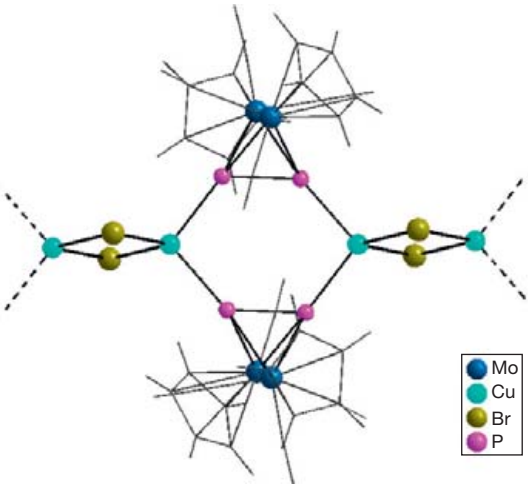

Figure 8 Section of the structure of 1D-$[(CuBr)\{(C_5H_5)_2(CO)_4Mo_2P_2\}]_n$ (**29**). Adapted from Bai, J.; Leiner, E.; Scheer, M. *Angew. Chem. Int. Ed.* **2002**, *41*, 783; Scheer, M.; Gregoriades, L. J.; Zabel, M.; Sierka, M.; Zhang, L.; Eckert, H. *Eur. J. Inorg. Chem.* **2007**, 2775.

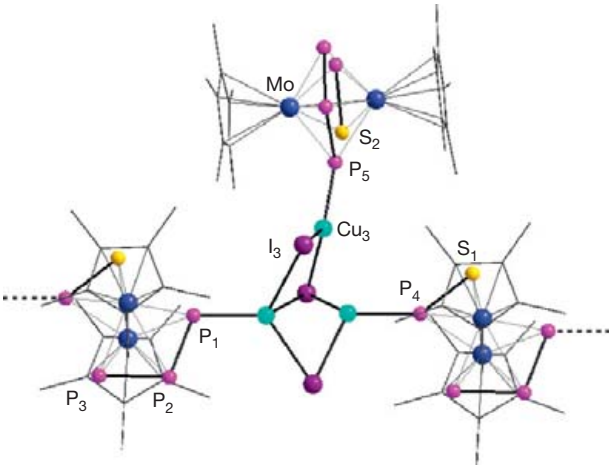

Figure 10 Section of 1D-$[(CuI)_3(Cp^*_2Mo_2P_4S)_2]_n$ (**31**). Hydrogen atoms are omitted for clarity. Adapted from Gregoriades, L. J.; Balázs, G.; Brunner, E.; Gröger, C.; Wachter, J.; Zabel, M.; Scheer, M. *Angew. Chem. Int. Ed.* **2007**, *46*, 5966.

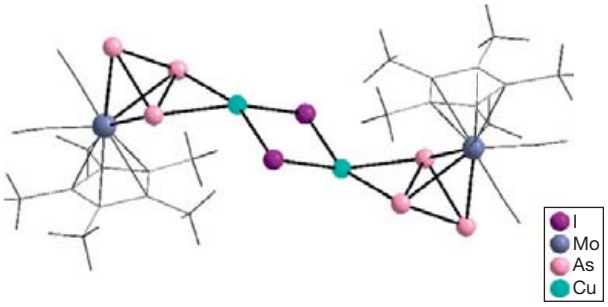

Figure 9 Molecular structure of $[(CuBr)\{(C_5H_5)(CO)_2MoAs_3\}]_2$ (**30**). Adapted from Gregoriades, L. J.; Krauss, H.; Wachter, J.; Virovets, A. V.; Sierka, M.; Scheer, M. *Angew. Chem. Int. Ed.* **2006**, *45*, 4189.

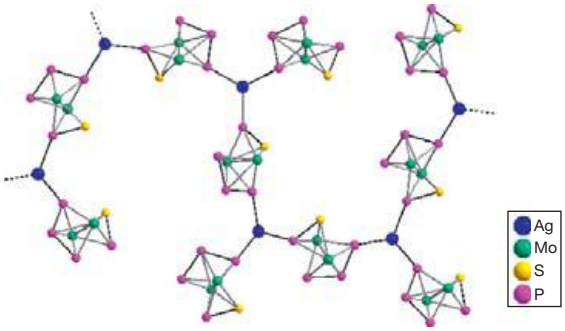

Figure 11 Section of the S-shaped polycationic chain of 1D-$[Ag(Cp^*_2Mo_2P_4S)_2]_n^{n+}$ in **32**. Cp* ligands are omitted for clarity. Adapted from Gregoriades, L. J.; Balázs, G.; Brunner, E.; Gröger, C.; Wachter, J.; Zabel, M.; Scheer, M. *Angew. Chem. Int. Ed.* **2007**, *46*, 5966.

16 elements may either compete for coordination sites or may both coordinate, which makes them suitable candidates for the construction of coordination polymers. In the following sections, E_nQ_m ligand complexes containing the building blocks P_4S, P_2S_3, P_2Se_3, and As_2S_3 will be considered in their reactions with copper(I) halides. Unfortunately, reactions of $[Cp^*_2Mo_2E_2Q_3]$ complexes with Ag^+ salts are prevented by the precipitation of silver mirrors because of the low oxidation potentials of **14**, **18**, and **21**, respectively, between 0.10 and 0.19 V.

1.29.2.3.2 The $[Cp_2Mo_2P_4S]$ building block

Reaction of **13** with CuI gives the polymer $[(CuI)_3(Cp^*_2Mo_2P_4S)_2]_n$ (**31**), the solid-state structure of which follows from x-ray crystallography and ^{31}P MAS NMR spectroscopy. The structure consists of stacks of distorted bicyclic $(CuI)_3$ rings bridged by units of **13**, with a further molecule of **13** being coordinated to Cu3 of each $(CuI)_3$ ring as a pending ligand (Figure 10).[57] Solid-state NMR spectroscopy is an important diagnostic tool because of the low solubility of **31**. The ^{31}P NMR MAS spectrum of **31** allows the assignment of phosphorus sites bearing copper (P1, P4, P5) and also distinguishes between pendent and bridging dimolybdenum units. In agreement with the observed $^{31}P-^{63/65}Cu$ couplings, the bridging P_4S middle deck employs P1 of the $\mu,\eta^{3:3}$-P_3 ligand ($^1J_{P-Cu}=1200$ Hz) and P4 of the μ,η^2-PS dumbbell ($^1J_{P-Cu}=1500$ Hz), while the terminal P_4S middle deck coordinates through P5 ($^1J_{P-Cu}=1500$ Hz). It is important to note that the data exclude coordination of sulfur.

The reaction of **13** with the Ag(I) salt of the WCA $[Al\{OC(CF_3)_3\}_4]^-$ leads to the polymeric compound $[Ag(Cp^*_2Mo_2P_4S)_2][Al\{OC(CF_3)_3\}_4]$ (**32**). The structure of **32** contains S-shaped polycationic chains $[Ag(\mathbf{13})]_n^{n+}$ in which nearly trigonal-planar Ag(I) centers are surrounded by three units of **13** (Figure 11). The chain is formed by an alternating arrangement of Ag(I) and bridging organometallic building blocks, while a pending unit of **13** coordinates via a lateral P atom of the P_3 ligand. The assignment of P atoms by ^{31}P MAS NMR spectroscopy is handicapped because of the lack of resolvable coupling to $^{107/109}Ag$, but sulfur coordination has been excluded by comparing the observed ^{31}P chemical shifts with those of **13** and **31**. ^{31}P NMR and ESI mass spectra of solutions

Copyright © 2013. Elsevier. All rights reserved.

Comprehensive Inorganic Chemistry II : From Elements to Applications, Elsevier, 2013. ProQuest Ebook Central, http://ebookcentral.proquest.com/lib/inflibnet-ebooks/detail.action?docID=1330977.
Created from inflibnet-ebooks on 2021-02-09 22:27:26.

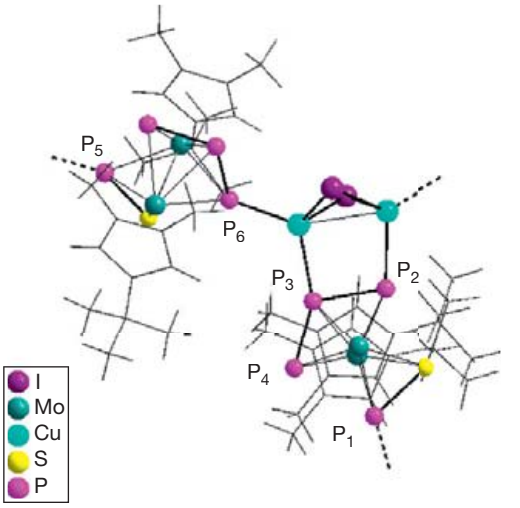

Figure 12 Section of the crystal structure of 3D-$[(CuI)_4(Cp^{\circ}{}_2Mo_2P_4S)_3]_n$ (**33a**). Adapted from Gröger, C.; Kalbitzer, H. R.; Pronold, M.; Piryazev, D.; Scheer, M.; Wachter, J.; Virovets, A.; Zabel, M. *Eur. J. Inorg. Chem.* **2011**, 785.

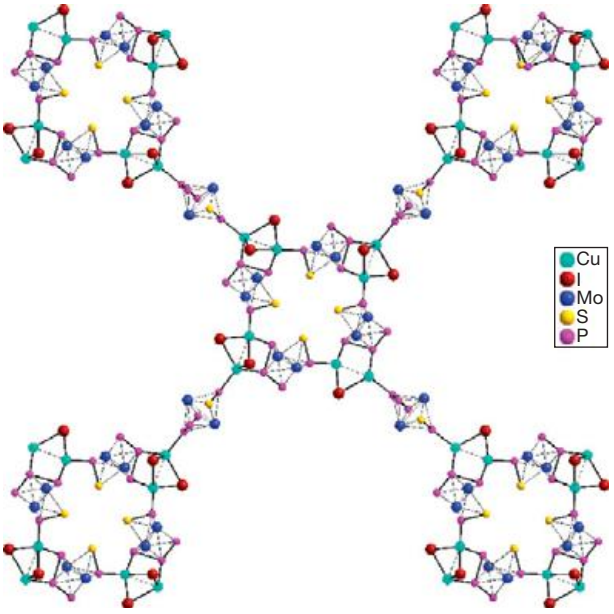

Figure 13 Assembly of left-handed helices of **33a** in the lattice. Cp° rings are omitted for clarity. Adapted from Gröger, C.; Kalbitzer, H. R.; Pronold, M.; Piryazev, D.; Scheer, M.; Wachter, J.; Virovets, A.; Zabel, M. *Eur. J. Inorg. Chem.* **2011**, 785.

in CH_3CN reveal the presence of $[Ag(\mathbf{13})_2]^+$ cations, in which Ag^+ is 'sandwiched' between the P_3 ligands of two units of **13**, while the η^2-PS dumbbell does not participate in bonding.[57]

The influence of substituents at the cyclopentadienyl ligand on the nature of the polymeric network is demonstrated by the reaction of $[Cp^{\circ}{}_2Mo_2P_4S]$ (**23**) with CuI. Initially, $[(CuI)_4(Cp^{\circ}{}_2Mo_2P_4S)_3]_n$ (**33a**) formed, which when stored under CH_2Cl_2 incorporates solvent molecules under formation of [**33a**·0.55CH_2Cl_2] (**33b**). The crystal structures of **33a** and **33b** consist of helical substructures of opposed chirality. These are formed by the coordination of two vicinal atoms P2 and P3 of the μ,η^3-P_3 ligand and P1 of the μ,η^2-PS dumbbell of one of the P_4S middle decks of **23** to twofolded $(CuI)_2$ rings (Figure 12). The resulting helix is connected with four helices of the same chirality through η^2-PS (P5) and μ,η^3-P_3 (P6) coordination of another triple-decker unit (Figure 13).[49]

Crystals of **33a** can reversibly include or release CH_2Cl_2 molecules without losing their crystalline character. Concomitantly, the unit cell volume of **33a** increases by 113.6 Å^3 per formula unit, while in high vacuum the unit cell volume of **33b** decreases by the same value. Overall, compound **33** represents a new type of dynamic helical porous MOF, what has been ascribed to the steric influence of the Cp° ligand.[49]

1.29.2.3.3 The system $[Cp^*{}_2Mo_2P_2Q_3]$/CuX (Q = S, Se; X = Cl, Br, I)

The building block $[Cp^*{}_2Mo_2P_2S_3]$ (**14**) is part of the two-dimensional (2D) coordination polymers $[(CuCl)_4(Cp^*{}_2Mo_2P_2S_3)]$ (**34**), $[(CuBr)_3(Cp^*{}_2Mo_2P_2S_3)]$ (**35**), and $[(CuI)_3(Cp^*{}_2Mo_2P_2S_3)]$ (**36**). Of particular interest in all structures is that the distribution and connectivity of main group atoms in the P_2S_3 middle deck, which follows from correlation of ^{31}P MAS NMR spectra with x-ray crystallographic data, correspond to that of the positional isomer **14B**.[58] Thus, the structure of **34** (Figure 14) is distinguished by coordination of two η^2-PS dumbbells with P1 and P2 in neighboring positions at both sides of a hexameric Cu_6Cl_6 ladder, while the singly bridging sulfur atom S1 is part of an eight-membered $Cu_4S_2Cl_2$ ring. The structure of **35** (and isotypic **36**) contains folded bicyclic Cu_3Br_3 clusters, which are connected by the single sulfur bridge. Only the phosphorus atom of one η^2-PS dumbbell coordinates, but to a copper atom of the next Cu_3Br_3 unit (Figure 15).

A possible reason for the preference of the energetically less favored middle deck **14B** over that of **14A** may be the role of the singly bridging sulfur (S1 in Figure 14), which provides two lone pairs for the coordination of copper halide units. This 'lone pair effect' is also found in related coordination polymers starting from $[Cp^*{}_2Mo_2As_2S_3]$ (see later discussion). Alternatively, a coordinatively induced dynamic behavior of the main group ligands within the E_2Q_3 middle deck has been discussed.[50]

The reaction of $[Cp^*{}_2Mo_2P_2Se_3]$ (**18**) with CuBr gives $[(CuBr)_2(Cp^*{}_2Mo_2P_2Se_3)_2]$ (**37**), and that with CuI forms 2D-$[(CuI)_3(Cp^*{}_2Mo_2P_2Se_3)(CH_3CN)]_n$ (**38**). The structure of **37** is distinguished by a central planar $(CuBr)_2$ ring to which on each side a triple-decker complex coordinates through one of its P atoms (Figure 16). In spite of its oligomeric character, **37** is insoluble in common solvents. This unexpected property may be explained by weak attractive forces between Se atoms [d(Se···Se) = 3.79 Å] of neighboring molecules, which form a 2D network (Figure 17). An isostructural CuCl analog exists, but only as a few crystals.[46]

The crystal structure of **38** can be described by a 2D polymer, which is formed by ribbons containing short twisted chains of three planar edge-connected $(CuI)_2$ rings bearing P, Se-attached $[Cp^*{}_2Mo_2P_2Se_3]$ molecules (Figure 18).[46] These chains are bridged by the P atoms of one η^2-PSe dumbbell and the singly bridging Se atoms of two opposite units **18**. Contrary to the sulfur bridges in polymers **34**–**36**, the selenium

Copyright © 2013. Elsevier. All rights reserved.

Comprehensive Inorganic Chemistry II : From Elements to Applications, Elsevier, 2013. ProQuest Ebook Central, http://ebookcentral.proquest.com/lib/inflibnet-ebooks/detail.action?docID=1330977.
Created from inflibnet-ebooks on 2021-02-09 22:27:26.

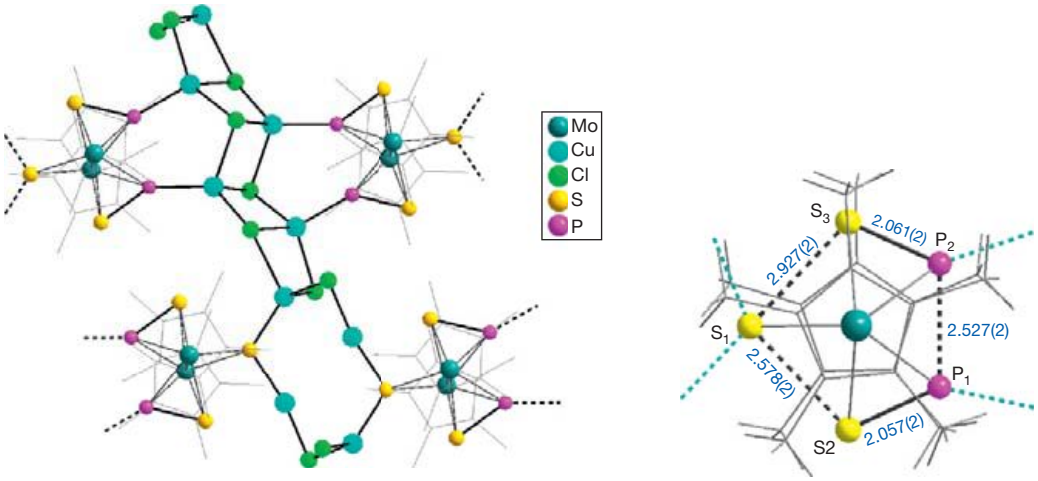

Figure 14 Section of the structure of 2D-[$(CuCl)_4(Cp^*_2Mo_2P_2S_3)$] (**34**) (left) and distances (Å) within the P_2S_3 middle deck (right). Adapted from Gröger, C.; Kalbitzer, H. R.; Meier, W.; Pronold, M.; Scheer, M.; Wachter, J.; Zabel, M. *Inorg. Chim. Acta* **2011**, *370*, 191.

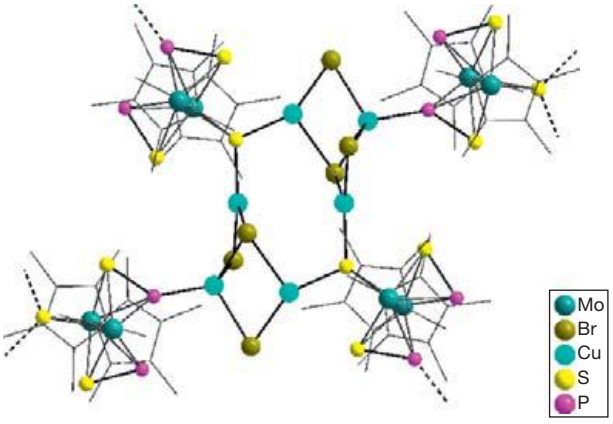

Figure 15 Section of the structure of 2D-[$(CuBr)_3(Cp^*_2Mo_2P_2S_3)$] (**35**). Hydrogen atoms are omitted for clarity. Adapted from Gröger, C.; Kalbitzer, H. R.; Meier, W.; Pronold, M.; Scheer, M.; Wachter, J.; Zabel, M. *Inorg. Chim. Acta* **2011**, *370*, 191.

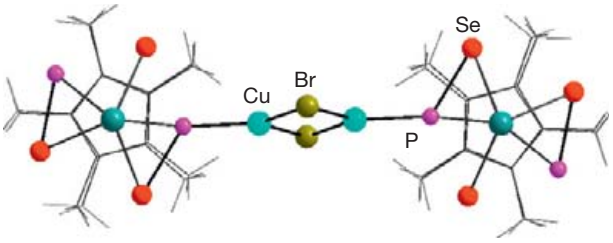

Figure 16 Molecular structure of [$(CuBr)_2(Cp^*_2Mo_2P_2Se_3)_2$] (**37**). Adapted from Bodensteiner, M.; Dušek, M.; Kubicki, M. M.; Pronold, M.; Scheer, M.; Wachter, J.; Zabel, M. *Eur. J. Inorg. Chem.* **2010**, 5298.

bridge provides only one of its lone pairs for coordination. The second η^2-PSe dumbbell of the same molecule coordinates to trigonal-planar copper of a new chain. The resulting strands are arranged into stepped layers by weak Se···Se interactions [d(Se···Se) = 3.67 Å]. By this way all main group atoms of the five-membered middle deck are involved in coordination either to Cu or to Se.

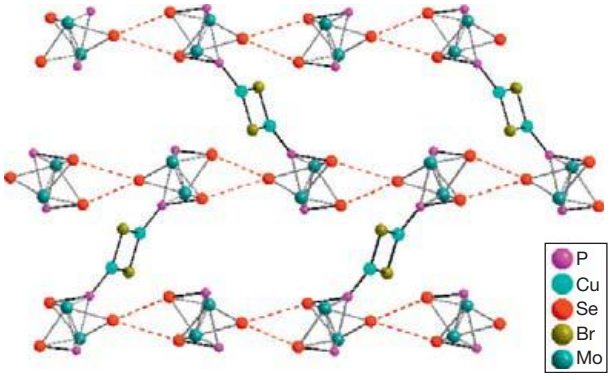

Figure 17 Intermolecular Se···Se interactions (dashed lines) in the crystal structure of **37**. Cp* ligands are omitted for clarity. Adapted from Bodensteiner, M.; Dušek, M.; Kubicki, M. M.; Pronold, M.; Scheer, M.; Wachter, J.; Zabel, M. *Eur. J. Inorg. Chem.* **2010**, 5298.

1.29.2.3.4 The system [$Cp^*_2Mo_2As_2S_3$]/CuX (X = Cl, Br, I)

Starting from the [$Cp^*_2Mo_2As_2S_3$] (**21**) building block, copper (I) halides form one-dimensional (1D) polymers [$(CuX)_2(Cp^*_2Mo_2As_2S_3)]_n$ (X = Cl: **39**; Br: **40**) and the oligomer [$(CuI)_7(Cp^*_2Mo_2As_2S_3)_3$] (**41**). Compounds **39** and **40** are isostructural. The structures contain 1D S-shaped chains with alternating planar and folded $(CuX)_2$ rings (Figure 19), which are connected by sulfur.[59] In analogy to the polymers **34**–**36** the structures of **39** and **40** (and also **41**, see later discussion) exhibit As_2S_3 middle decks consisting of two trapezoidal η^2-AsS dumbbells with vicinal arsenic atoms As1 and As2 and one monosulfide ligand (Figure 19). Probably, the folding of one of the $(CuCl)_2$ rings is caused by very weak As···Cl interactions [$d(As–Cl)_{mean} = 3.79(4)$ Å].

The structure of **41** contains a $(CuI)_7$ aggregate, which forms a flat $Cu_6I_3S_3$ bowl together with the singly bridging sulfur atoms of three [$Cp^*_2Mo_2As_2S_3$] building blocks (Figure 20). The oligomeric substructures fit into a flat sheet by attractive As–I interactions [$d(As–I_{mean}) = 3.751(4)$ Å]. Like in the sulfur-containing compounds **34**–**36** the assembly of the building blocks in **39**–**41** is promoted by the singly

Copyright © 2013. Elsevier. All rights reserved.

Comprehensive Inorganic Chemistry II : From Elements to Applications, Elsevier, 2013. ProQuest Ebook Central, http://ebookcentral.proquest.com/lib/inflibnet-ebooks/detail.action?docID=1330977.
Created from inflibnet-ebooks on 2021-02-09 22:27:26.

bridging sulfur. In consequence, the arrangement of main group elements corresponds to that in positional isomer **14B** (Scheme 10).

A comparison of the coordination behavior of the triple-decker complexes **14**, **18**, and **21** with that of the related sulfur rich complex $[Cp^*_2Mo_2S_4]$[60] shows that compounds with mixed E15/E16 ligands do not have the same tendency for cluster formation as organometallic sulfido complexes. Thus, $[Cp^*_2Mo_2(\mu,\eta^2\text{-}S_2)(\mu\text{-}S)_2]$ forms with CuCl the 62-electron cubane-like cluster $[Cp^*_2Mo_2(CuCl)_2(\mu_3\text{-}S)_4]$,[61] while trans-$[Cp^*_2Mo_2S_2(\mu\text{-}S)_2]$[60] reacts with $[Cu(MeCN)_4][PF_6]_2$ under formation of $[Cp^*_2Mo_2(CuMeCN)_2(\mu_3\text{-}S)_4]^{2+}$.[62] A more attractive way to get coordination polymers of sulfido complexes is to react of unsaturated organometallic trisulfido complex anions like $[Cp^*MS_3]^-$ (M = Mo, W) with AgBr[63] or CuNCS.[64]

oligomeric main group molecules.[65] Examples cover the preparation of new phosphorus nanorods in compounds like $(CuI)_8P_{12}$ or $(CuI)_3P_{12}$ by a typical high-temperature synthesis. In these polymers copper iodide functions as a solid solvent ('matrix') for phosphorus.[66] These solid-state techniques can also be applied to the synthesis of a series of phosphorus chalcogenide cage adducts, among them $(CuI)_3P_4S_4$ (**42**)[67] and $(CuI)_3P_4Se_4$ (**43**) containing the hitherto unknown β-P_4Se_4 cage.[68] In these compounds β-P_4Q_4 cage molecules are embedded between hexagonal $(Cu_3I_3)_n$ columns (Figure 21). Three of the four phosphorus atoms are weakly coordinated to copper, which has been found by correlation of x-ray crystallographic data with ^{31}P and $^{63,65}Cu$ solid-state MAS NMR spectroscopy. On the basis of these data only weak interactions between the metal and the cage atoms have been postulated.[69]

1.29.3 Coordination Polymers of Intact Group 15/16 Cage Molecules

1.29.3.1 The Copper Iodide Matrix

Copper(I) halides are a useful tool in solid-state reactions for the synthesis of adduct compounds with new polymeric and

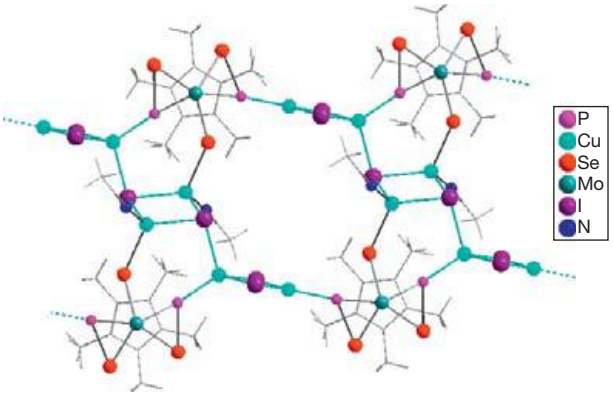

Figure 18 Section of 2D-$[(CuI)_3(Cp^*_2Mo_2P_2Se_3)(CH_3CN)]_n$ (**38**). Adapted from Bodensteiner, M.; Dušek, M.; Kubicki, M. M.; Pronold, M.; Scheer, M.; Wachter, J.; Zabel, M. *Eur. J. Inorg. Chem.* **2010**, 5298.

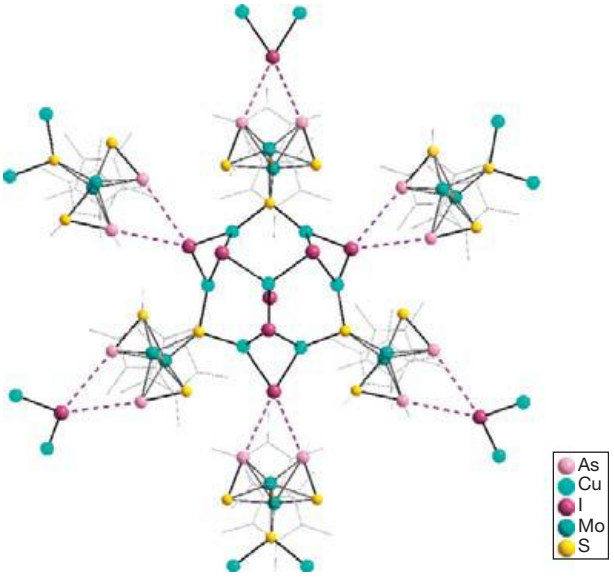

Figure 20 Section of the structure of $[(CuI)_7(Cp^*_2Mo_2As_2S_3)_3]$ (**41**) with As···I interactions between 3.692(4) and 3.839(4) Å. Hydrogen atoms are omitted for clarity. Adapted from Pronold, M.; Scheer, M.; Wachter, J.; Zabel, M. *Inorg. Chem.* **2007**, *46*, 1396.

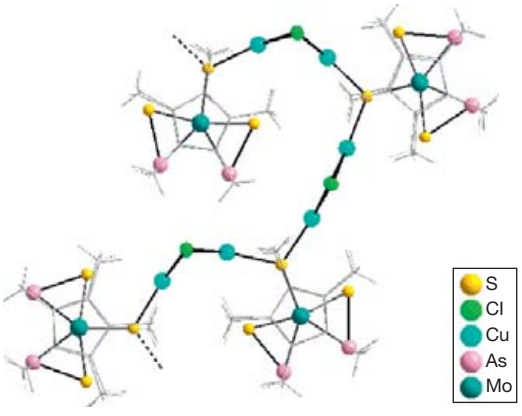

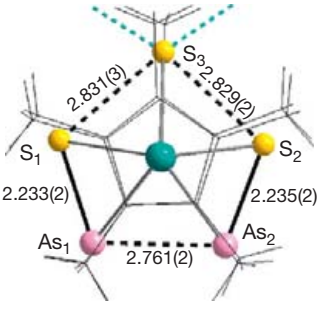

Figure 19 Section of the structure of 1D-$[(CuCl)_2(Cp^*_2Mo_2As_2S_3)]_n$ (**39**) (left) and distances (Å) within the As_2S_3 middle deck (right). Adapted from Pronold, M.; Scheer, M.; Wachter, J.; Zabel, M. *Inorg. Chem.* **2007**, *46*, 1396.

Copyright © 2013. Elsevier. All rights reserved.

Comprehensive Inorganic Chemistry II : From Elements to Applications, Elsevier, 2013. ProQuest Ebook Central, http://ebookcentral.proquest.com/lib/inflibnet-ebooks/detail.action?docID=1330977.
Created from inflibnet-ebooks on 2021-02-09 22:27:26.

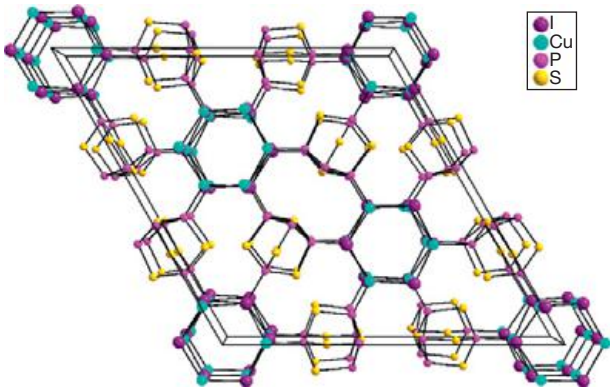

Figure 21 Section of the crystal structure of $(CuI)_3P_4S_4$ (**42**). Adapted from Reiser, S.; Brunklaus, G.; Hong, J. H.; Chan, J. C. C.; Eckert, H.; Pfitzner, A. *Chem. Eur. J.* **2002**, *8*, 4228.

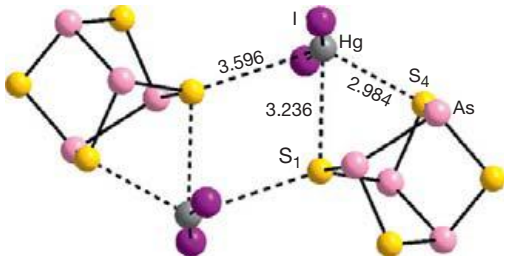

Figure 22 Structure of $HgI_2{\cdot}As_4S_4$ (**45**), distances *d*(Hg-S) in Å. Adapted from Bräu, M.; Pfitzner, A. *Angew. Chem. Int. Ed.* **2006**, *45*, 4464.

It is one of the great advantages of the high-temperature method that the reaction products are usually obtained as pure samples. However, the method can neither be used for the synthesis of polymers containing the P_4Q_3 cage nor for the reagents CuCl and CuBr, which give in the presence of phosphorus-containing substrates the corresponding phosphorus trihalides.

Very recently it has been shown that $(CuI)_3(As_4Q_4)_2$ (Q = S, Se) (**44**) can be prepared from the elements and CuI at 300 °C.[70] Both structures consist of As_4Q_4 cage molecules and disordered CuI dumbbells, the copper atoms being coordinated to chalcogen atoms of the cage.

1.29.3.2 Adduct Compounds from As_4S_4 and HgX_2 (X = Br, I)

A new type of realgar adduct is formed by the reaction of HgI_2, elemental arsenic and sulfur at 400 °C, followed by annealing at 200 °C. The orange crystals of $HgI_2{\cdot}As_4S_4$ (**45**) consist of dimerized units, in which sulfur atoms of As_4S_4 cradles are bridged by nearly linear HgI_2 units.[71] The relatively long Hg–S distances indicate weak bonding interactions between Hg and S1 and Hg and S4, respectively. Coordination of HgI_2 to the second cage results in still longer Hg–S distances (Figure 22). A similar bond situation has been found in $(HgBr_2)_3(As_4S_4)_2$ (**46**).[72] As in compound **45**, weakly bound $HgBr_2$ units serve as bridges between sulfur of two As_4S_4 cages.

As it is known that α-As_4S_4 undergoes a light-induced structural change into pararealgar (see also Scheme 7),[36] $HgI_2{\cdot}As_4S_4$ (**45**) has been subjected to single-crystal x-ray diffraction analysis under photochemical conditions. Upon light exposure, single crystals of **45** slowly increase their unit-cell volume (up to 59%), which more slowly decreases when keeping the crystal in the dark. This 'light-induced molecular change' has been ascribed to the transient partial formation of pararealgar followed by a very slow re-formation of β-As_4S_4.[73]

1.29.3.3 Polymers Assembled by P_4Q_3 (Q = S, Se) and Cu(I) Halide Building Blocks

It has already been shown that it seems to be impossible to prepare coordination polymers with P_4Q_3 building blocks by solid-state techniques. However, it is known since 1977 that P_4S_3 reacts with Cu(I) halides in polar solvents under formation of insoluble microcrystalline precipitates. These were proposed to be of polymeric nature.[74] Progress in crystallization came from application of interdiffusion techniques. An important condition for this method is the solubility of the respective cage molecule in CH_2Cl_2 or toluene. The resulting solution is then carefully layered by the solution of the copper(I) halide in CH_3CN. Other conditions influencing the nature of the product are the polarity of the employed solvents and the concentration of the CuX solution. The latter controls the diffusion rate and often the selectivity of the reaction. The yields span the wide range from 'a few crystals' up to 80% depending on the system.

If one also considers the coordination polymers comprising the As_4S_3 building block (see later discussion), the structural diversity of the compounds is impressive, although they contain only a limited set of copper halide building blocks. These include the well-known structural motifs of diatomic (CuX) dumbbells, planar or folded four-membered $(CuX)_2$ rings, planar or twisted 1D castellated $(CuX)_n$ chains, 1D zigzag $(CuX)_n$ chains, undulated $(Cu_3X_3)_n$ layers, and hexagonal $(Cu_3X_3)_n$ columns.[4,75] It is clear that the structural variety arises from the combination of these substructures with two and three P atoms like in P_4Se_3, or even up to four phosphorus atoms in P_4S_3, while the chalcogen atoms are only involved in the case of As_4S_3. In the following sections some typical examples are described, others have already been described in a recent review article.[75]

$(CuX)_7(P_4S_3)_3$ (X = Cl: **47-Cl**[76]; X = Br: **47-Br**[77]). The three-dimensional (3D) structure of **47-Cl** (**47-Br** is isostructural) consists of hexagonal $(Cu_3Cl_3)_n$ columns, castellated $(CuCl)_n$ chains, and stacks of diatomic (CuCl) dumbbells. The latter contains a threefold crystallographic axis (Figure 23). The various components are linked by all P atoms of the P_4S_3 ligand. While hexagonal $(Cu_3Cl_3)_n$ columns seem to be unique, $(Cu_3Br_3)_n$ columns have been described in $[(Cu_3Br_3)(tri)]_n$ and $[(Cu_2Br_2)(tri)]_n$.[78] Contrary to the planar triazine linkers, the P_4S_3 cage possesses C_{3v} geometry.

The polymers 1D-$(CuX)P_4S_3$ (X = Br: **48-Br**; X = I: **48-I**) belong to the 1D structural type, in which planar four-membered $(CuX)_2$ rings and bridging cage molecules form linear chains (Figure 24). $(CuI)P_4Se_3$ (**49**) is of the same structural type.[79] The resulting chains are stacked along the *a*-axis and there are no apparent contacts between the stacks in the crystal. All these compounds exhibit a remarkable downfield shift of the apical ^{31}P resonance signal in the ^{31}P MAS

Copyright © 2013. Elsevier. All rights reserved.

Comprehensive Inorganic Chemistry II : From Elements to Applications, Elsevier, 2013. ProQuest Ebook Central, http://ebookcentral.proquest.com/lib/inflibnet-ebooks/detail.action?docID=1330977.
Created from inflibnet-ebooks on 2021-02-09 22:27:26.

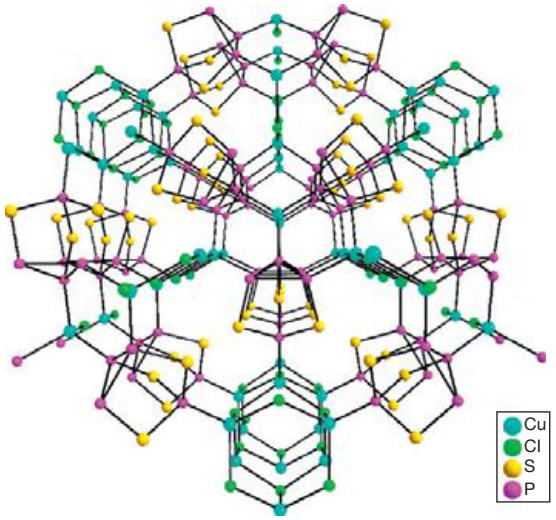

Figure 23 Section of the crystal structure of 3D-$(CuCl)_7(P_4S_3)_3$ (**47-Cl**). In this view, a crystallographic axis passes through the central stacks of (CuCl) dumbbells. Adapted from Biegerl, A.; Brunner, E.; Gröger, C.; Scheer, M.; Wachter, J.; Zabel, M. *Chem. Eur. J.* **2007**, *17*, 9270.

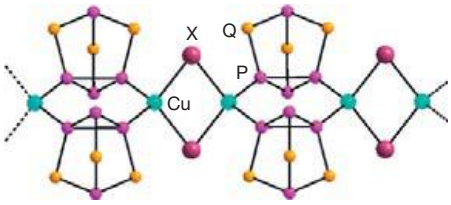

Figure 24 Section of the crystal structure of 1D-$(CuX)P_4Q_3$ (**48:** Q = S, X = Br, I; **49:** Q = Se, X = I). Adapted from Biegerl, A.; Brunner, E.; Gröger, C.; Scheer, M.; Wachter, J.; Zabel, M. *Chem. Eur. J.* **2007**, *17*, 9270.

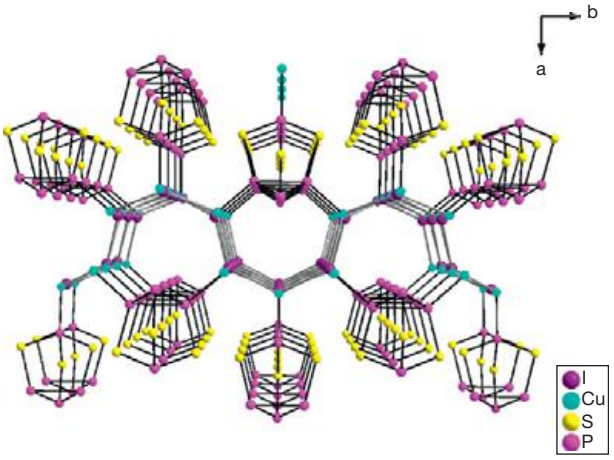

Figure 25 Section of the crystal structure of 3D-$(CuI)_3P_4S_3$ (**50-I**). Adapted from Biegerl, A.; Brunner, E.; Gröger, C.; Scheer, M.; Wachter, J.; Zabel, M. *Chem. Eur. J.* **2007**, *17*, 9270.

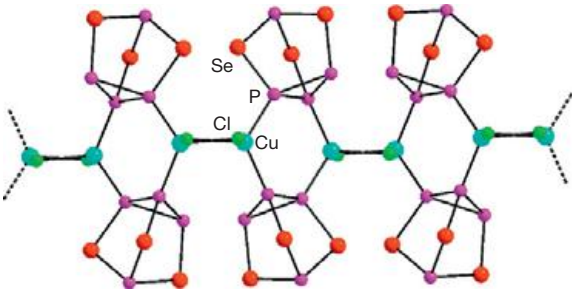

Figure 26 Section of the structure of $(CuCl)P_4Se_3$ (**51**), projection on *ab* plane. Adapted from Biegerl, A.; Gröger, C.; Kalbitzer, H. R.; Pfitzner, A.; Wachter, J.; Weihrich, R.; Zabel, M. *J. Solid State Chem.* **2011**, *184*, 1719.

NMR spectra compared with the free cage molecules and all the other polymers of this section, although they bear no metal atom. This phenomenon is in agreement with a decrease of 3 s orbital electron distribution of the apical P atom as has been found by Mulliken population analyses carried out in the crystalline phase with DFT programs adapted for the solid state.[22] The same programs have allowed the calculation and assignment of Raman vibrations, providing very reliable results.

$(CuX)_3P_4S_3$ (X = Br: **50-Br**; X = I: **50-I**). In both compounds, parallel undulated $(Cu_3I_3)_n$ layers are linked by tridentate P_4S_3 cage molecules (Figure 25), thus giving seven-membered columns in which two atoms of the cage P_3 basis are incorporated.[76,77] Compounds that contain similar hexagonal $(Cu_3X_3)_n$ networks are still extremely rare.[4,78,80]

The incorporation of the P_4Se_3 cage into polymers follows the same synthetic procedure as for P_4S_3. However, the obtained structures are, with the exception of **49**, slightly different, although the set of CuX building blocks is limited to planar $(CuX)_2$ rings and 1D-$(CuX)_n$ chains. The structure of $(CuCl)P_4Se_3$ (**51**) contains slightly twisted (torsion angle 11°) castellated $(CuCl)_n$ chains. Pairs of these chains are bridged by two P_4Se_3 molecules *via* two basal phosphorus atoms to give a 2D layer (Figure 26). The 2D structure may formally be extended into a 3D one if pairs of apical P atoms of parallel layers are connected by planar castellated $(CuX)_n$ chains. This building principle has been realized in the structures of $(CuBr)_3(P_4Se_3)_2$ (**52**) (Figure 27) and the S-homologue $(CuCl)_3(P_4S_3)_2$, respectively.[76]

The structure of $(CuI)_3(P_4Se_3)_2$ (**53**) is built up of 1D stacks of $(CuI)P_4Se_3$ as found in the structure of **49** (Figure 24), but the apical P atoms of these stacks coordinate to castellated $(CuI)_n$ chains running along the *a*-axis, too. By this way an unprecedented 3D structure is formed (Figure 28).

Stimulated by the high-temperature preparation of $(CuI)_3P_4Q_4$ (Q = S, Se),[67,68] the thermal behavior of compounds with already preformed building blocks like in **48-I**, **50-I**, and **51** has been studied. The results and annealing temperatures are summarized in Scheme 12. The new phase transformations **48-I** → **50-I**, **50-I** → **42**, and **51** → **54** have been proved by ^{31}P MAS NMR spectroscopy and x-ray diffraction analyses. The new compound $(CuCl)_3(P_4Se_3)_2$ (**54**) is formed, which is isostructural with **52** (Figure 27).[79]

1.29.3.4 As_4S_3 and PAs_3S_3 Containing Copper Halide Polymers

As_4S_3 occurs in nature as α- and β-dimorphite,[30] which have very low solubility in common solvents. Therefore, the adduct

Copyright © 2013. Elsevier. All rights reserved.

Comprehensive Inorganic Chemistry II : From Elements to Applications, Elsevier, 2013. ProQuest Ebook Central, http://ebookcentral.proquest.com/lib/inflibnet-ebooks/detail.action?docID=1330977.
Created from inflibnet-ebooks on 2021-02-09 22:27:26.

$As_4S_3{\cdot}Cr(CO)_5$ (**9**) was used in the reaction with CuCl/CH_3CN under diffusion conditions. $(CuCl)As_4S_3$ (**55**) was obtained, which could also be prepared from As_4S_3, but in much lower yield. The reaction of **9** with $CuCl_2$/MeOH gave $(CuCl)_2As_4S_3$ (**56**), probably as the result of a redox process. The corresponding CuBr-containing polymers have been prepared analogously.[34] During the reactions the $Cr(CO)_5$ fragment is lost, but its fate is still unknown because of the low concentrations of the employed solutions.

The crystal structure of **55** contains a zigzag $(CuCl)_n$ chain in sawlike conformation running down the *c*-axis. This backbone bears the cage molecules alternately on both sides (Figure 29), coordination being achieved by two of the three sulfur bridges. Opposite strands are packed into parallel sheets by As–Cl interactions between 3.14 and 3.30 Å (sum of Van der Waals radii = 3.81 Å), thus forming a layered structure, which is characterized by a hexagonal rod packing. Crystallographic data also reveal a stretching of As–S bonds by 0.035 Å compared to free As_4S_3, which is indicative of significant Cu–S interactions. Such interactions also follow from a comparison of Raman spectra of As_4S_3 and **55**, which reveal a significant blue shift of the As–S vibrations in the polymer.[34]

The crystal structure of **56** is built up of sheets, in which the As_4S_3 cages are linked with folded four-membered $(CuCl)_2$ rings by coordination of all sulfur atoms (Figure 30). As in the structure of **55**, As···Cl interactions are responsible for a packing of the resulting 2D networks into interconnected parallel layers in the solid state.[34]

DFT calculations on P_4S_3[24] and As_4S_3[81] have been carried out, but cannot explain the different coordination behavior, for energies and shapes of highest occupied and lowest unoccupied molecular orbitals of both cage molecules are comparable. It is striking, however, that in both structures attractive As–Cl interactions in the range between 3.14 and 3.40 Å are observed, while the sum of Van der Waals radii is 3.81 Å. These interactions may be responsible for the organization into 2D (**55**) or 3D (**56**) networks. They may also compensate the energy gain provided by side-on coordination of copper across two basal arsenic atoms. Such As–Cu interactions have been observed in the structure of $[(CuBr)\{(C_5H_5)(CO)_2MoAs_3\}]_2$ (**30**) (Figure 9).[13]

A possibility to combine the coordination properties of As_4S_3 with those of P_4S_3 may be given in PAs_3S_3,[82,83] because this cage molecule combines the PS_3 building block of P_4S_3 with the As_3 basis of As_4S_3.[84] For the introduction of the cage in coordination polymers the synthesis of the soluble adduct $PAs_3S_3{\cdot}W(CO)_5$ (**57**) was achieved, which bears the $W(CO)_5$ fragment at the apical P atom and which is considerably more soluble than the free cage.[85]

The reaction of **57** with CuCl gave the salt-like compound $[Cu(PAs_3S_3)_4]Cl$ (**58**). The structure of **58** contains two different $[(PAs_3S_3)_4Cu]^+$ cations (**58A**, **58B**) and attached Cl^-

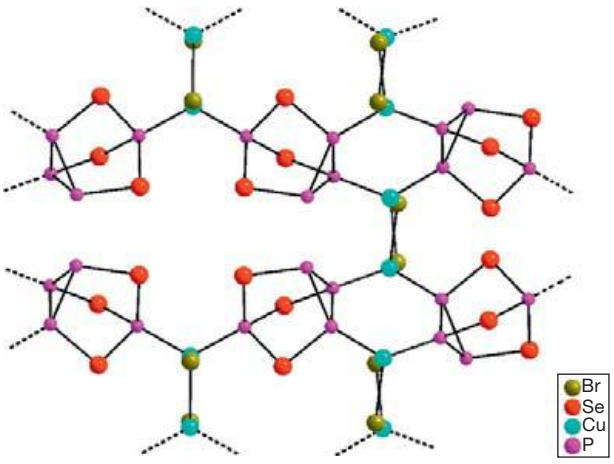

Figure 27 Section of the structure of $(CuBr)_3(P_4Se_3)_2$ (**52**), projection on *ab* plane. Adapted from Biegerl, A.; Gröger, C.; Kalbitzer, H. R.; Pfitzner, A.; Wachter, J.; Weihrich, R.; Zabel, M. *J. Solid State Chem.* **2011**, *184*, 1719.

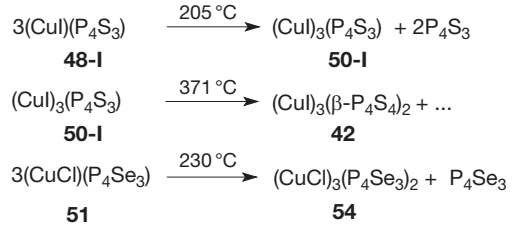

Scheme 12 Thermal conversion reactions of **48-I**, **50-I**, and **51**.

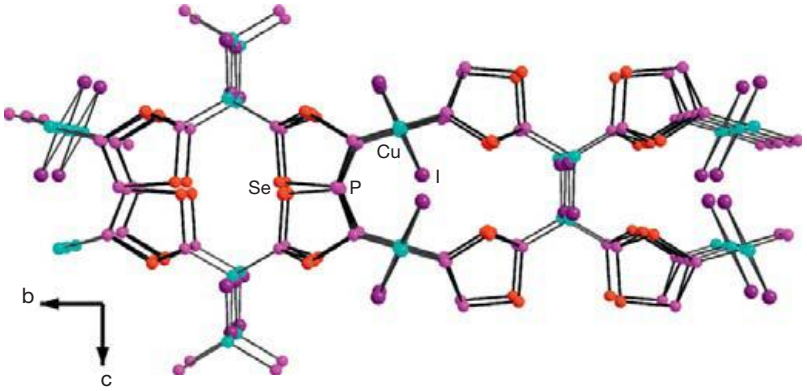

Figure 28 Section of the structure of $(CuI)_3(P_4Se_3)_2$ (**53**). Adapted from Biegerl, A.; Gröger, C.; Kalbitzer, H. R.; Pfitzner, A.; Wachter, J.; Weihrich, R.; Zabel, M. *J. Solid State Chem.* **2011**, *184*, 1719.

Copyright © 2013. Elsevier. All rights reserved.

Comprehensive Inorganic Chemistry II : From Elements to Applications, Elsevier, 2013. ProQuest Ebook Central, http://ebookcentral.proquest.com/lib/inflibnet-ebooks/detail.action?docID=1330977.
Created from inflibnet-ebooks on 2021-02-09 22:27:26.

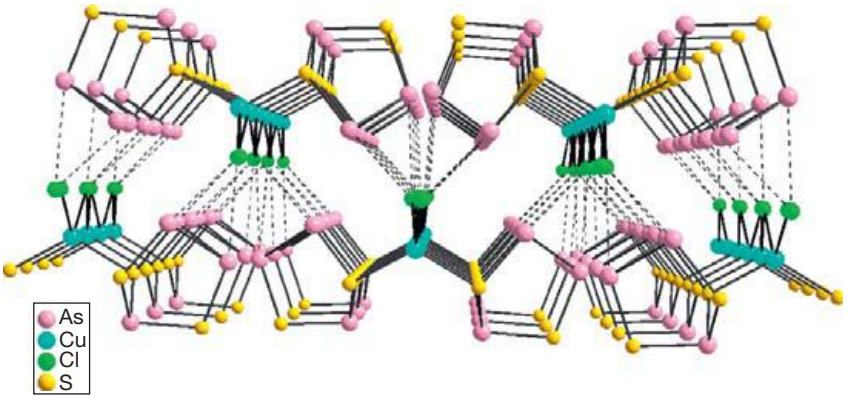

Figure 29 Section of the structure of $(CuCl)As_4S_3$ (**55**). As···Cl interactions are indicated by dotted lines. Adapted from Schwarz, P.; Wachter, J.; Zabel, M. *Eur. J. Inorg. Chem.* **2008**, 5460.

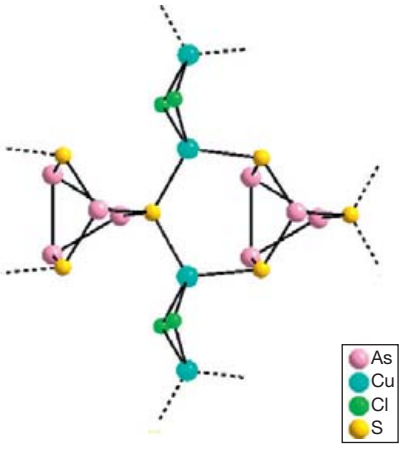

Figure 30 Section of the structure of $(CuCl)_2As_4S_3$ (**56**). Adapted from Schwarz, P.; Wachter, J.; Zabel, M. *Eur. J. Inorg. Chem.* **2008**, 5460.

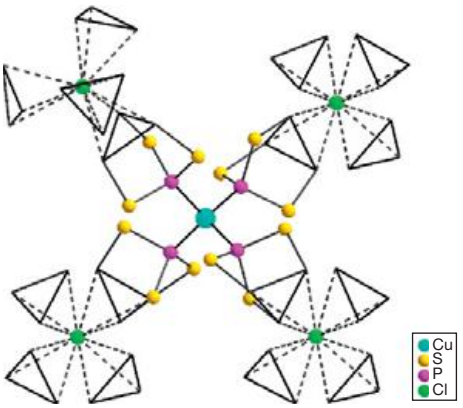

Figure 31 Structure of the cation $[Cu(PAs_3S_3)_4]^+$ (**58A**) with attached Cl^- anions. Each anion is surrounded by four PAs_3S_3 molecules. The triangles represent As_3 basal atoms. Adapted from Schwarz, P.; Wachter, J.; Zabel, M. *Inorg. Chem.* **2011**, *50*, 12692.

anions. The cations contain a central copper atom, which is tetrahedrally surrounded by four apical P atoms of PAs_3S_3 molecules (Figure 31). The coordination of apical phosphorus to copper is reminiscent of that of P_4S_3, but attractive As···Cl interactions of the As_3 basis resemble those of As_4S_3 and seem to provoke the dissociation of CuCl, which is unprecedented in cage coordination chemistry.[85]

The crystal structure of **58** is determined by interactions between As_3 basal atoms and Cl^- anions. The two different types of $[(PAs_3S_3)_4Cu]^+$ cations may be distinguished by the number of Cl^- anions interacting with PAs_3S_3 cages. In cation **58A** four PAs_3S_3 molecules are arranged around one Cl^- anion [d(As···Cl) = 3.14–3.18 Å] (Figure 31), whereas in cation **58B** there are only three PAs_3S_3 molecules around Cl^- [d(As···Cl) = 3.13–3.20 Å] (Figure 32). In the latter case, a 2D network is formed with voids of 10.7 Å diameter, which are penetrated by the 3D network of $[(\mathbf{58A})Cl]_n$ to give a polycatenated structure.[86]

1.29.4 Organic–Inorganic and Organometallic–Inorganic Hybrid Polymers

The coordination abilities of the multifunctional spherical P_4Q_3 building block (Q = S, Se) for the construction of

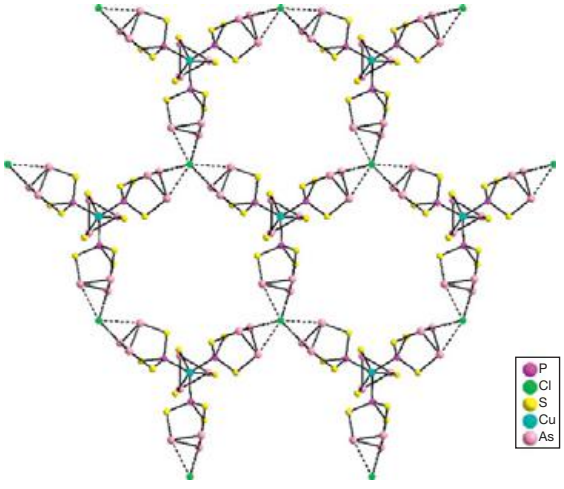

Figure 32 Section of the 2D network of **58** as built up by cation **58B** and As···Cl interactions. Adapted from Schwarz, P.; Wachter, J.; Zabel, M. *Inorg. Chem.* **2011**, *50*, 12692.

Copyright © 2013. Elsevier. All rights reserved.

Comprehensive Inorganic Chemistry II : From Elements to Applications, Elsevier, 2013. ProQuest Ebook Central, http://ebookcentral.proquest.com/lib/inflibnet-ebooks/detail.action?docID=1330977.
Created from inflibnet-ebooks on 2021-02-09 22:27:26.

inorganic polymers have already been described in the preceding section. The combination of organic and inorganic donors as cross-linking ligands with copper halide aggregates is a still poorly explored field. Organic–inorganic hybrid materials with new and interesting properties have been obtained from bifunctional organic P,N[16] or S,N ligands.[87] In the following sections the potential of P_4Q_3/CuX secondary building units (SBUs) in combination with organic P,P′ or N,N′ multidentate cross-linkers for the formation of organic–inorganic hybrid polymers is investigated. The replacement of the organic donors by organometallic E15/E16 ligand complexes gives access to organometallic–inorganic hybrid polymers and opens another attractive field of research.

1.29.4.1 Copper Halide Polymers Assembled by P_4S_3 and Organic P,P′ and N,N′ Donors

The formation of organic–inorganic hybrid polymers from mono- or bidentate phosphanes and P_4S_3 with copper(I) halides seems to formally proceed in a stepwise manner. Thus, reaction of a mixture of CuX (X = Cl, Br, I), triethylphosphane, and P_4S_3 gives mononuclear complexes $[CuX(P_4S_3)(PEt_3)_2]$ (**59**) in high yields (Figure 33). This means that the competing formation of $[(CuX)_4(PEt_3)_4]$[88] or binary polymers **47**, **48**, or **50** is suppressed. On the other hand, the integration of **59** as an SBU into larger networks was not possible.[89]

According to the great structural flexibility of polymers obtained from bidentate bis(diphenylphosphane)alkanes and Ag(I) or Cu(I) compounds,[90] the reaction of equimolar mixtures of P_4S_3 and dppe with copper(I) halides under diffusion conditions was investigated. Depending on the polarity of the employed solvents 1D-$[CuI(P_4S_3)(dppe)]_n$ (**60**) or 2D-$[(CuX)_2(P_4S_3)(dppe)]_n$ (**61**: X = Br, I) were obtained.

The structure of compound **60** is composed of 1D strands, which are formed by alternating four-membered planar $(CuI)_2$ rings and trans-coordinated dppe ligands. The coordination sphere around copper is completed by trans-coordinated P_4S_3. Only apical phosphorus atoms are involved in coordination (Figure 34). The ^{31}P MAS NMR spectrum of **60** is in agreement with the crystal structure determination.[89]

The structures of the isostructural compounds **61-Br** and **61-I** can be easily derived from that of **60**, for they contain an analogous backbone of planar $(CuX)_2$ rings and trans-coordinated dppe ligands. Contrary to the structure of **60**, the

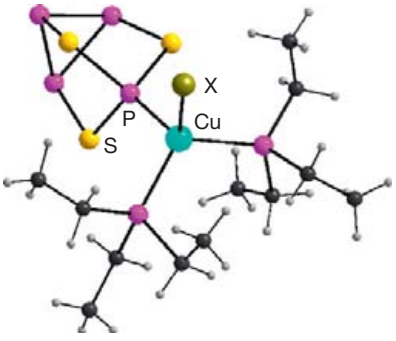

Figure 33 Molecular structure of $[CuX(P_4S_3)(PEt_3)_2]$ (**59**; X = Cl, Br, I). Adapted from Biegerl, A.; Piryazev, D.; Scheer, M.; Wachter, J.; Virovets, A.; Zabel, M. *Eur. J. Inorg. Chem.* **2011**, 4248.

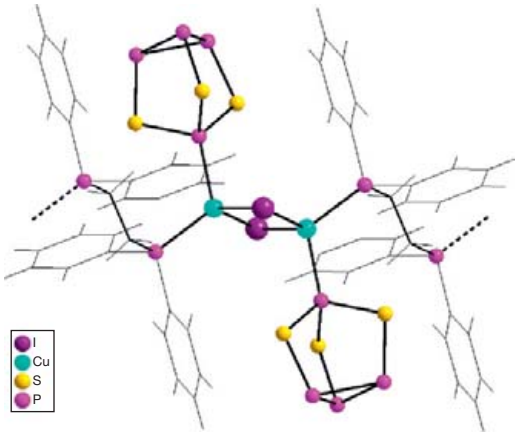

Figure 34 Section of the crystal structure of 1D-$[CuI(P_4S_3)(dppe)]_n$ (**60**). Adapted from Biegerl, A.; Piryazev, D.; Scheer, M.; Wachter, J.; Virovets, A.; Zabel, M. *Eur. J. Inorg. Chem.* **2011**, 4248.

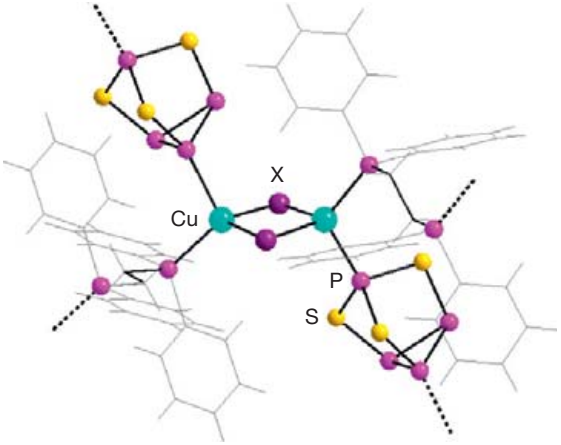

Figure 35 Section of the crystal structure of 2D-$[(CuX)_2(P_4S_3)(dppe)]_n$ (**61**; X = Br, I). Adapted from Biegerl, A.; Piryazev, D.; Scheer, M.; Wachter, J.; Virovets, A.; Zabel, M. *Eur. J. Inorg. Chem.* **2011**, 4248.

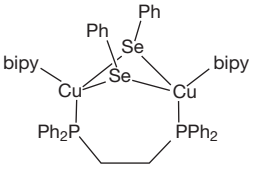

Scheme 13 Schematic representation of the (selenolato)(dppe)copper building block in 1D-$[Cu_2(SePh)_2(dppe)(bipy)]_n$ (**62**). Adapted from Fu, M.-L.; Fenske, D.; Weinert, B.; Fuhr, O. *Eur. J. Inorg. Chem.* **2010**, 1098.

P_4S_3 ligands are inversely coordinated through apical and basal phosphorus. Then, the opposite phosphorus sites of each cage molecule coordinates to copper of neighboring strands thus giving 2D networks (Figure 35).

A different coordination behavior of the dppe ligand has been observed in 1D-$[Cu_2(SePh)_2(dppe)(bipy)]_n$ (**62**) (Scheme 13), where dppe bridges the folded four-membered $Cu_2(SePh)_2$ ring, while the linear bipy ligand functions as the linker between the small cluster units.[91]

Copyright © 2013. Elsevier. All rights reserved.

Comprehensive Inorganic Chemistry II : From Elements to Applications, Elsevier, 2013. ProQuest Ebook Central, http://ebookcentral.proquest.com/lib/inflibnet-ebooks/detail.action?docID=1330977.
Created from inflibnet-ebooks on 2021-02-09 22:27:26.

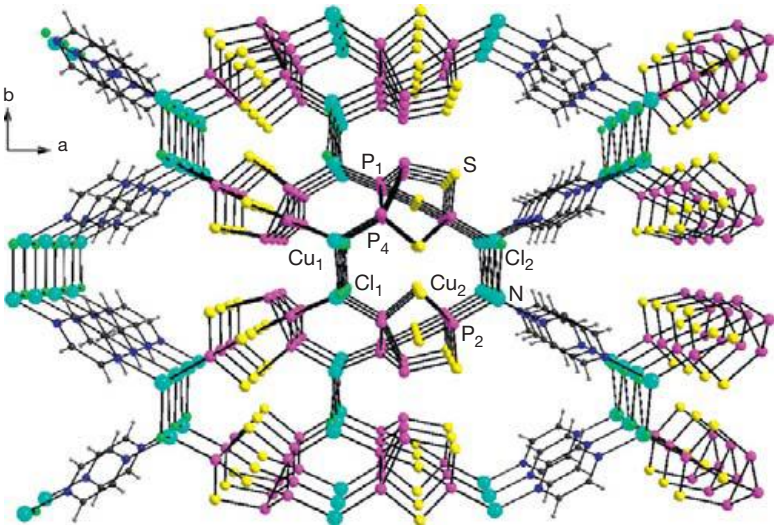

Figure 36 Section of the crystal structure of 3D-$[(CuCl)_4(P_4S_3)_2(pyz)]_n$ (**63**). Adapted from Biegerl, A.; Piryazev, D.; Scheer, M.; Wachter, J.; Virovets, A.; Zabel, M. *Eur. J. Inorg. Chem.* **2011**, 4248.

Substitution of the conformationally flexible dppe ligand by the rigid pyz ligand in the P_4S_3 reactions leads to less selective results. Thus, $[(CuCl)_4(P_4S_3)_2(pyz)]_n$ (**63**) and $[(CuCl)(pyz)]_n$[92] form from solutions of P_4S_3, pyrazine, and CuCl in CH_2Cl_2/CH_3CN. Both compounds can be distinguished by the photoluminescence of $[(CuCl)(pyz)]_n$.[89]

The structure of compound **63** can formally be described as a mixed polymer constructed from sections of $[(CuCl)P_4S_3]$ (c.f. the structure of **51**) and of $[CuCl(pyz)]_n$.[92] This means that two differently twisted castellated $(CuCl)_n$ chains are running along the *c*-axis. Pairs of those $(CuCl)_n$ chains (Cu1, Cl1), which are twisted by 12°, are bridged by P_4S_3 molecules through P1 and P4 forming a planar $(CuCl)_2(P_4S_3)_2$ sheet. This sheet is confined by the apical atoms P2. Neighboring P2 atoms are linked by another twisted (8°) $(CuCl)_n$ chain (Cu2, Cl2). The coordination spheres of Cu2 are completed by nitrogen of the pyz ligands. By this way the resulting 3D network contains alternating planar layers of organic and inorganic building blocks orthogonal to the *ab* and *ac* planes (Figure 36). As all of the hybrid polymers are insoluble, their purity with respect to other phosphorus-containing compounds can be checked by ^{31}P MAS NMR spectroscopy.[89]

The reaction of a P_4S_3/pyz/toluene mixture with CuBr/CH_3CN produces $(CuBr)_2(P_4S_3)_2$, which is a new polymer in the P_4S_3/CuBr system, red prisms of $(CuBr)(pyz)$,[93] and yellow-orange prisms of 3D-$[(CuBr)_3(P_4S_3)(pyz)]_n$ (**64**). Again, the products can be distinguished by their luminescence, for the P_4S_3-containing polymers do not emit in the visible spectrum. The influence of the halide on the nature of the reaction products may be drastically illustrated by the system P_4S_3/pyz/CuI. In this case only orange crystals of $(CuI)_3P_4S_3$ (**50-I**) (Figure 25) were found.[89]

Central structural feature of **64** is a cradle composed of two nearly planar twelve-membered $(CuBr)_6$ rings bridged by two opposed pyz and two P_4S_3 ligands. Neighboring $(CuBr)_6$ rings are connected by four-membered $(CuBr)_2$ rings (Cu3, Br3). Each $(CuBr)_6$ ring is *trans*-annular, spanned by basal atoms P2 and P3 of a P_4S_3 cage, while the apical atom P1 of the same cage is bound to the opposite $(CuBr)_6$ ring. A second cage molecule serves as a linker in the inversed direction. Two pyrazine molecules are bridging opposite and slightly displaced $(CuBr)_6$ rings through N2 (Figure 37). The volume of the thus formed cage-like substructure is ca. 270 Å^3.

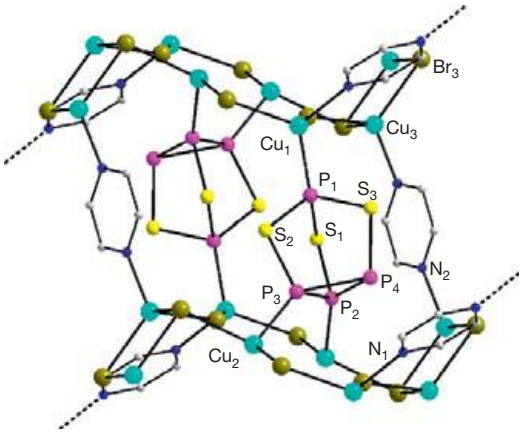

Figure 37 Section of the crystal structure of 3D-$[(CuBr)_3(P_4S_3)(pyz)(0.5C_7H_8)]_n$ (**64**). Hydrogen atoms are omitted for the sake of clarity. Adapted from Biegerl, A.; Piryazev, D.; Scheer, M.; Wachter, J.; Virovets, A.; Zabel, M. *Eur. J. Inorg. Chem.* **2011**, 4248.

A 3D framework is built up by layers formed of condensed $(CuBr)_6$ rings and orthogonal pyrazine spacers (Figure 38). The shortest distance between parallel pyrazine molecules is ca. 9 Å, and that between P_4S_3 molecules of neighboring layers is ca. 5 Å. The resulting cavities are occupied by toluene molecules.

1.29.4.2 Copper Polymers Assembled by P_4Q_3 and E15/E16 Ligand Complexes

The class of organometallic/inorganic hybrid polymers described here includes examples comprising the E15/E16 ligand complexes $[Cp^*_2Mo_2P_4S]$ (**13**), $[Cp^\circ_2Mo_2P_4S]$ (**22**), and

Copyright © 2013. Elsevier. All rights reserved.

Comprehensive Inorganic Chemistry II : From Elements to Applications, Elsevier, 2013. ProQuest Ebook Central, http://ebookcentral.proquest.com/lib/inflibnet-ebooks/detail.action?docID=1330977.
Created from inflibnet-ebooks on 2021-02-09 22:27:26.

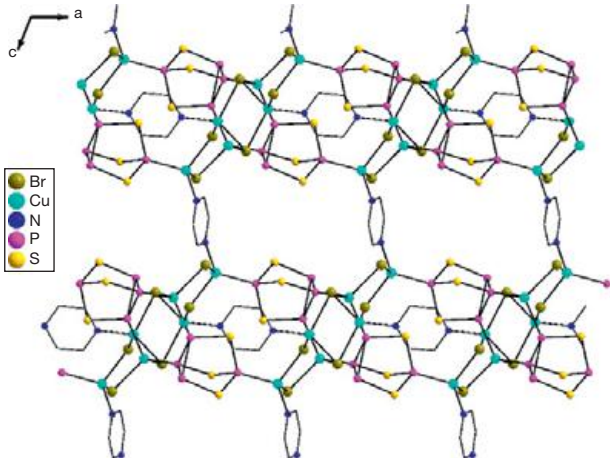

Figure 38 Section of the crystal structure of **64**, projection on the *ac* plane. Hydrogen atoms and solvent molecules are omitted for the sake of clarity. Adapted from Biegerl, A.; Piryazev, D.; Scheer, M.; Wachter, J.; Virovets, A.; Zabel, M. *Eur. J. Inorg. Chem.* **2011**, 4248.

$[Cp^*_2Mo_2P_2Q_3]$ (**14** and **18**), the cage compounds P_4S_3 and P_4Se_3, and Cu_2X_2 building blocks. Only unequivocally resolved structures are described, for often there are crystallographic problems inherent to structures of molybdenum triple-decker complexes with an E15/E16 middle deck and P_4Q_3 cages.

The reaction of a mixture of **22** and P_4S_3 with CuI gives the structurally related $[(Cp^\circ{}_2Mo_2P_4S)(P_4S_3)(CuI)_2]_n$ (**65a**) and $[(Cp^\circ{}_2Mo_2P_4S)(P_4S_3)(CuI)_2{\cdot}2CH_2Cl_2]_n$ (**65b**). Both compounds are distinguished by cell **65b** and the of the in **65a** **65b**. Additionally, a is observed for **65b**, what allows the incorporation of solvent molecules between the layers.

Common feature of the crystal structures of **65a** and **65b** are linear strands of *trans*-$[\mathbf{22}(CuI)_2]_n$ and *trans*-$[(P_4S_3)(CuI)_2]_n$, which are cross-linked by planar four-membered $(CuI)_2$ rings (Figure 39). Thus, the inorganic and organometallic building blocks form a crosswise pattern of strands within the *ac* plane. The coordination of the *cyclo*-P_4S middle deck in **65a** is achieved by P1 of the η^3-P_3 and P4 of the η^2-PS ligands (Figure 39).[49] Whereas the apical P5 atoms in **65a** are equally oriented in one direction, those in **65b** vary in their orientation from one ring to the other.

The structure of 1D-$[(Cp^*_2Mo_2P_4S)(P_4S_3)(CuI)_2]_n$ (**66**) is closely related to that of **65a**. However, the neighboring atoms P1 and P4 of the η^3-P_3 ligand and the η^2-PS dumbbell are used for coordination of two $(CuI)_2$ rings (Figure 40). The *trans*-coordinated P_4S_3 cages serve as bridges between two $(CuI)_2$ rings. As a result two sinoidal strands are connected in an antiparallel manner to give 1D ribbons, which are packed into zigzag stacks in the solid state (Figure 41). Voids between the ribbons may contain solvent molecules. In spite of the high content of inequivalent phosphorus atoms, there is a detailed ^{31}P MAS NMR spectroscopic study, which allows for the assignment of main group atoms.[49]

The combination of **14** or **18** with the respective cage molecules P_4S_3 or P_4Se_3 and CuX gives the hybrid polymers 1D-$[(Cp^*_2Mo_2P_2S_3)(P_4S_3)(CuX)_2]_n$ (**67-Cl**, **67-I**) and 1D-$[(Cp^*_2Mo_2P_2Se_3)(P_4Se_3)(CuI)_2]_n$ (**68-Br**, **68-I**)). Their structures are closely related and as a representative example that

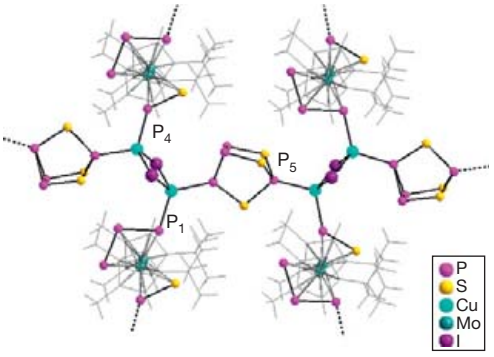

Figure 39 Section of the crystal structure of 2D-$[(Cp^\circ{}_2Mo_2P_4S)(P_4S_3)(CuI)_2]_n$ (**65a**). Adapted from Gröger, C.; Kalbitzer, H. R.; Pronold, M.; Piryazev, D.; Scheer, M.; Wachter, J.; Virovets, A.; Zabel, M. *Eur. J. Inorg. Chem.* **2011**, 785.

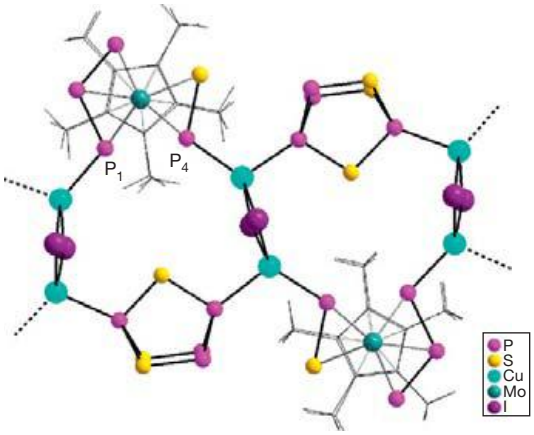

Figure 40 Section of the crystal structure of 1D-$[(Cp^*_2Mo_2P_4S)(P_4S_3)(CuI)_2]_n$ (**66**). Only one set of the disordered main group elements is shown. Adapted from Gröger, C.; Kalbitzer, H. R.; Pronold, M.; Piryazev, D.; Scheer, M.; Wachter, J.; Virovets, A.; Zabel, M. *Eur. J. Inorg. Chem.* **2011**, 785.

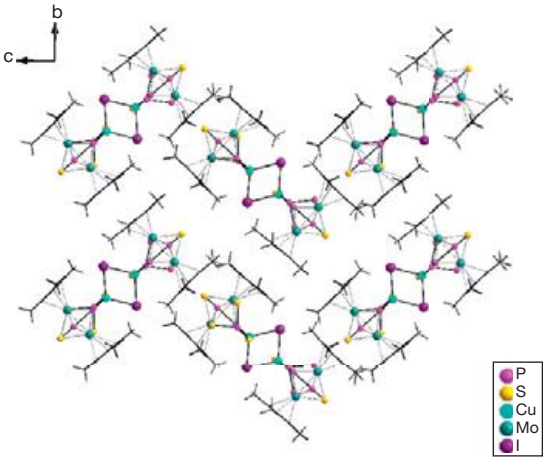

Figure 41 Crystal structure of **66**. Zigzag packing of stacks of $[(Cp^*_2Mo_2P_4S)(P_4S_3)(CuI)_2]_n$ viewed down the *a*-axis. Adapted from Gröger, C.; Kalbitzer, H. R.; Pronold, M.; Piryazev, D.; Scheer, M.; Wachter, J.; Virovets, A.; Zabel, M. *Eur. J. Inorg. Chem.* **2011**, 785.

Copyright © 2013. Elsevier. All rights reserved.

Comprehensive Inorganic Chemistry II : From Elements to Applications, Elsevier, 2013. ProQuest Ebook Central, http://ebookcentral.proquest.com/lib/inflibnet-ebooks/detail.action?docID=1330977.
Created from inflibnet-ebooks on 2021-02-09 22:27:26.

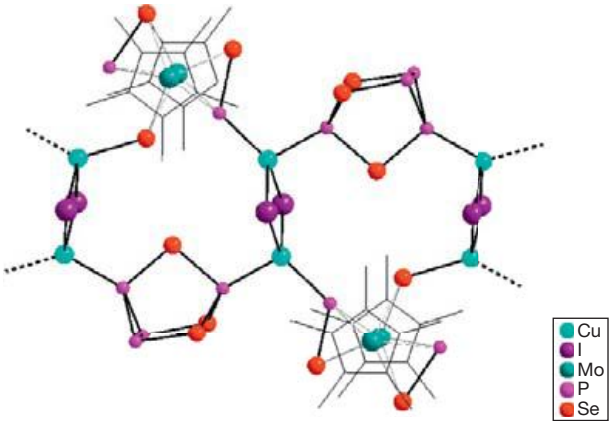

Figure 42 Section of the crystal structure of 1D-$[(Cp^*_2Mo_2P_2Se_3)(P_4Se_3)(CuI)_2]_n$ (**68-I**). Only one set of the disordered main group elements is shown. Hydrogen atoms are omitted. Adapted from Bodensteiner, M.; Dušek, M.; Kubicki, M. M.; Pronold, M.; Scheer, M.; Wachter, J.; Zabel, M. *Eur. J. Inorg. Chem.* **2010**, 5298.

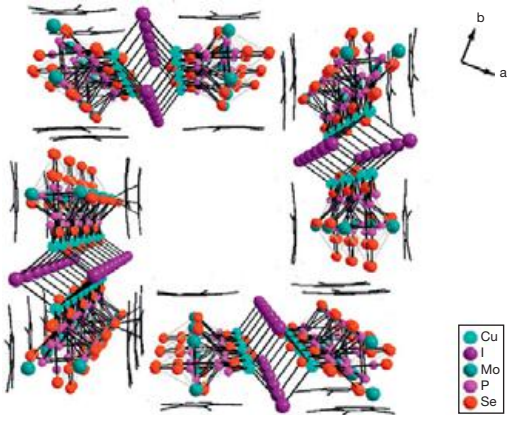

Figure 43 Formation of channels in the crystal structure of **68-I**. Disordered solvent molecules (CH_2Cl_2 and CH_3CN) are not shown. Adapted from Bodensteiner, M.; Dušek, M.; Kubicki, M. M.; Pronold, M.; Scheer, M.; Wachter, J.; Zabel, M. *Eur. J. Inorg. Chem.* **2010**, 5298.

of **68-I** is described in the following. As in the structure of **65** and **66**, a 1D-ribbon is constructed of triple-decker building blocks, P_4Se_3 molecules, and planar four-membered $(CuI)_2$ rings. The organometallic unit employs phosphorus of one of the η^2-PSe dumbbells and one lone pair of the single-bridging Se atom for coordination (Figure 42). The resulting ribbons form channels along the *c*-axis (Figure 43) containing mobile solvent and cage molecules, which cannot be located.[46]

The packing in the solid state is common for the compounds **67-Cl**, **68-Br**, and **68-I**, whereas **67-I** is packed in the zigzag type typical of $[(Cp^*_2Mo_2P_4S)(P_4S_3)(CuI)_2]_n$ (Figure 41).

1.29.5 Conclusion

New developments in the coordination chemistry of intact E_nQ_m cage molecules and ligand complexes containing small mixed E_nQ_m ligands from cage fragmentation reactions are summarized with particular emphasis on their potential as building blocks in polymers. An important subgroup are group 15/16 element triple-decker complexes, the middle decks of which behave as multifunctional donors for the construction of various copper(I) halide aggregates. The structural diversity of coordination polymers assembled by E_nQ_m cage molecules and CuX is based on the donor capacity of the cage molecules, which ranges from all P atoms in P_4S_3 to all S atoms in As_4S_3. First results in the assembly of inorganic–organic hybrid polymers by copper(I) halide units were obtained by combining P_4Q_3/(CuX) (Q = S, Se) SBUs with pyrazine or dppe linkers. This chemistry looks promising for the construction of MOFs, if one considers the extremely rich ligand pool of multidentate nitrogen donors. The assembly of organometallic–inorganic hybrid polymers from group E15/E16 element triple-decker complexes, multifunctional organic donor ligands, and copper(I) halides may become another attractive field of research. For a related chapter in this Comprehensive, we refer to **Chapter 5.04**.

Acknowledgment

This work was supported by the Deutsche Forschungsgemeinschaft. The author gratefully acknowledges Prof. Dr. M. Scheer for generous support and Dr. G. Balázs for helpful discussions.

References

1. Biradha, K.; Ramanan, A.; Vittal, J. J. *Cryst. Growth Des.* **2009**, *9*, 2969.
2. Tranchemontagne, D. J.; Mendoza-Cortés, J. L.; O'Keeffe, M.; Yaghi, O. M. *Chem. Soc. Rev.* **2009**, *38*, 1257.
3. Degtyarenko, A. S.; Solntsev, P. V.; Krautscheid, H.; Russanov, E. B.; Chernega, A. N.; Domasevitch, K. V. *J. New Chem.* **2008**, *32*, 1910.
4. Peng, R.; Li, M.; Li, D. *Coord. Chem. Rev.* **2010**, *254*, 1.
5. Vegas, A.; Saillard, J.-Y. *Inorg. Chem.* **2004**, *43*, 4012 and references therein.
6. (a) Fu, W.-F.; Gan, X.; Che, C.-M.; Cao, Q.-Y.; Zhou, Z.-Y.; Zhu, N. N.-Y. *Chem. Eur. J.* **2004**, *10*, 2228; (b) Scherer, M.; Stein, D.; Breher, F.; Geier, J.; Schönberg, H.; Grützmacher, H. *Z. Anorg. Allg. Chem.* **2005**, *631*, 2770.
7. Cecconi, F.; Ghilardi, C. A.; Midollini, S.; Orlandini, A. *J. Chem. Soc. Chem. Commun.* **1982**, 229.
8. Lobana, T. S.; Kaur, P.; Nishioka, T. *Inorg. Chem.* **2004**, *43*, 3766.
9. (a) Bai, J.; Leiner, E.; Scheer, M. *Angew. Chem. Int. Ed.* **2002**, *41*, 783; (b) Scheer, M.; Gregoriades, L. J.; Zabel, M.; Sierka, M.; Zhang, L.; Eckert, H. *Eur. J. Inorg. Chem.* **2007**, 2775.
10. Bai, J.; Virovets, A. V.; Scheer, M. *Angew. Chem. Int. Ed.* **2002**, *41*, 1737.
11. (a) Bai, J.; Virovets, A. V.; Scheer, M. *Science* **2003**, *300*, 781; (b) Scheer, M.; Bai, J.; Johnson, B. P.; Merkle, R.; Virovets, A. V.; Anson, C. E. *Eur. J. Inorg. Chem.* **2005**, 4023; (c) Scheer, M.; Schindler, A.; Gröger, C.; Virovets, A. V.; Peresypkina, E. *Angew. Chem. Int. Ed.* **2009**, *48*, 4870; (d) Scheer, M.; Schindler, A.; Bai, J.; Johnson, B. P.; Merkle, R.; Winter, R.; Virovets, A. V.; Peresypkina, E. V.; Blatov, V. A.; Sierka, M.; Eckert, H. *Chem. Eur. J.* **2010**, *16*, 2092.
12. Scheer, M. *Dalton Trans.* **2008**, 4372.
13. (a) Gregoriades, L. J.; Krauss, H.; Wachter, J.; Virovets, A. V.; Sierka, M.; Scheer, M. *Angew. Chem. Int. Ed.* **2006**, *45*, 4189; (b) Krauss, H.; Balázs, G.; Bodensteiner, M.; Scheer, M. *Chem. Sci.* **2010**, *1*, 337.
14. (a) Healy, P. C.; Skelton, B. W.; White, A. W. J. *Chem. Soc. Dalton Trans.* **1989**, 971; (b) Chen, L.; Thompson, L. K.; Tandon, S. S.; Bridson, J. N. *Inorg. Chem.* **1993**, *32*, 4063; (c) Lobana, T. S.; Hundal, G. J. *Chem. Soc. Dalton Trans.* **2002**, 2203; (d) Llobana, T. S.; Rimple, ; Castineiras, A.; Turner, P. *Inorg. Chem.* **2003**, *43*, 4731; (e) Cheng, J.-K.; Chen, Y.-B.; Wu, L.; Zhang, J.; Wen, Y.-H.; Li, Z.-J.; Yao, Y.-G. *Inorg. Chem.* **2005**, *44*, 3386; (f) Zhou, J.; Bian, G.-Q.; Dai, J.; Zhang, Y.; Zhu, Q.-Y.; Lu, W. *Inorg. Chem.* **2006**, *45*, 8486.

Copyright © 2013. Elsevier. All rights reserved.

Comprehensive Inorganic Chemistry II : From Elements to Applications, Elsevier, 2013. ProQuest Ebook Central, http://ebookcentral.proquest.com/lib/inflibnet-ebooks/detail.action?docID=1330977.
Created from inflibnet-ebooks on 2021-02-09 22:27:26.

15. Knorr, M.; Guyon, F. *Luminescent Oligomeric and Polymeric Copper Coordination Compounds Assembled by Thioether Ligands*. In Abd-El Aziz, A. S., Carraher, C. E., Pittman, C. U., Zeldin, M., Eds.; Wiley: Hoboken, NJ, 2010; Vol. 10, pp 89–157.
16. (a) Amoore, J. J. M.; Hanton, L. R.; Spicer, M. D. *J. Chem. Soc. Dalton Trans.* **2003**, 1056; (b) Wang, J.; Zheng, S.-L.; Hu, S.; Zhang, Y.-H.; Tong, M.-L. *Inorg. Chem.* **2007**, *46*, 795; (c) Bai, S.-Q.; Koh, L. L.; Hor, T. S. A. *Inorg. Chem.* **2009**, *48*, 1207; (d) Lobana, T. S.; Khanna, S.; Castineiras, A.; Hundai, G. Z. *Anorg. Allg. Chem.* **2010**, *636*, 454.
17. (a) Riess, J. G. *ACS Symp. Ser.* **1983**, *232*, 17; (b) Di Vaira, M.; Stoppioni, P.; Peruzzini, M. *Comments Inorg. Chem.* **1990**, *11*, 1; (c) Di Vaira, M.; Stoppioni, P. *Coord. Chem. Rev.* **1992**, *120*, 259.
18. Wachter, J. *Angew. Chem. Int. Ed.* **1998**, *37*, 750.
19. Blachnik, R.; Hoppe, A. *Z. Anorg. Allg. Chem.* **1979**, *457*, 91.
20. (a) Bues, W.; Somer, M.; Brockner, W. Z. *Naturforsch.* **1981**, *36a*, 842; (b) Griffin, A. M.; Minshall, P. C.; Sheldrick, G. M. J. *Chem. Soc. Chem. Commun.* **1976**, 809.
21. Cordes, A. W.; Joyner, R. D.; Shores, R. D.; Dill, E. D. *Inorg. Chem.* **1974**, *13*, 132.
22. Balázs, G.; Biegerl, A.; Gröger, C.; Wachter, J.; Weihrich, R.; Zabel, M. *Eur. J. Inorg. Chem.* **2010**, 1231.
23. Aubauer, C.; Irran, E.; Klapötke, T. M.; Schnick, W.; Schulz, A.; Senker, J. *Inorg. Chem.* **2001**, *40*, 4956.
24. Guidoboni, E.; de los Rios, I.; Ienco, A.; Marvelli, L.; Mealli, C.; Romerosa, A.; Rossi, R.; Peruzzini, M. *Inorg. Chem.* **2002**, *41*, 659.
25. (a) Di Vaira, M.; de los Rios, I.; Mani, F.; Peruzzini, M.; Stoppioni, P. *Eur. J. Inorg. Chem.* **2004**, 293; (b) de los Rios, I.; Mani, F.; Peruzzini, M.; Stoppioni, P. J. *Organomet. Chem.* **2004**, *689*, 164; (c) Di Vaira, M.; Peruzzini, M.; Seniori Costantini, S.; Stoppioni, P. J. *Organomet. Chem.* **2010**, *695*, 816.
26. Barbaro, P.; Di Vaira, M.; Peruzzini, M.; Seniori Costantini, S.; Stoppioni, P. *Chem. Eur. J.* **2007**, *13*, 6682.
27. (a) Adolf, A.; Gonsior, M.; Krossing, I. J. *Am. Chem. Soc.* **2002**, *124*, 7111; (b) Raabe, I.; Antonijevic, S.; Krossing, I. *Chem. Eur. J.* **2007**, *13*, 7510.
28. (a) Nowottnick, H.; Stumpf, K.; Blachnik, R.; Reuter, H. Z. *Anorg. Allg. Chem.* **1999**, *625*, 693; (b) Hoppe, D.; Pfitzner, A. *Z. Naturforsch.* **2009**, *64b*, 58.
29. Hoppe, D.; Schemmel, D.; Schütz, M.; Pfitzner, A. *Chem. Eur. J.* **2009**, *15*, 7129.
30. (a) Whitfield, H. J. *J. Chem. Soc. A* **1970**, 1800; (b) Frankel, L. S.; Zoltai, T. Z. *Kristallogr.* **1973**, *138*, 161; (c) Whitfield, H. J. J. *Chem. Soc. Dalton Trans.* **1973**, 1737.
31. Bonazzi, P.; Bindi, L.; Pratesi, G.; Menchetti, S. *Am. Mineral.* **2006**, *91*, 1323 and references therein.
32. (a) Brunner, H.; Kauermann, H.; Poll, L.; Nuber, B.; Wachter, J. *Chem. Ber.* **1996**, *129*, 657; (b) Brunner, H.; Leis, F.; Wachter, J.; Nuber, B. *Organometallics* **1997**, *16*, 4954.
33. Brunner, H.; Leis, F.; Nuber, B.; Wachter, J. *Polyhedron* **1999**, *18*, 347.
34. Schwarz, P.; Wachter, J.; Zabel, M. *Eur. J. Inorg. Chem.* **2008**, 5460.
35. Schwarz, P. Ph.D. Thesis, Universität Regensburg, Germany, 2010.
36. (a) Douglass, D. L.; Shing, C.; Wang, G. *Am. Mineral.* **1992**, *77*, 1266; (b) Kyono, A.; Kimata, M.; Hatta, T. *Am. Mineral.* **2005**, *90*, 1563; (c) Naumov, P.; Makreski, P.; Jovanovski, G. *Inorg. Chem.* **2007**, *46*, 10624; (d) Naumov, P.; Makreski, P.; Petruševski, G.; Runčevski, T.; Jovanovski, G. *J. Am. Chem. Soc.* **2010**, *132*, 11398.
37. Goh, L. Y. *Coord. Chem. Rev.* **1999**, *185*, 257.
38. Drake, G. W.; Kolis, J. W. *Coord. Chem. Rev.* **1994**, *137*, 131.
39. (a) Scherer, O. J.; Schwalb, J.; Swarowsky, H.; Wolmershäuser, G.; Kaim, W.; Gross, R. *Chem. Ber.* **1988**, *121*, 443; (b) Jemmis, E. D.; Reddy, A. C. *Organometallics* **1988**, *7*, 1561.
40. Scherer, O. J.; Schwalb, J.; Wolmershäuser, G.; Kaim, W.; Gross, R. *Angew. Chem. Int. Ed. Engl.* **1986**, *25*, 363.
41. (a) Rheingold, A. L.; Foley, M. J.; Sullivan, P. J. *J. Am. Chem. Soc.* **1982**, *104*, 4727; (b) Tremel, W.; Hoffmann, R.; Kertesz, M. J. *Am. Chem. Soc.* **1989**, *111*, 2030; (c) DiMaio, A.-J.; Rheingold, A. L. *Chem. Rev.* **1990**, *90*, 169.
42. Scherer, O. J.; Sitzmann, H.; Wolmershäuser, G. *Angew. Chem. Int. Ed. Engl.* **1985**, *24*, 351.
43. Scherer, O. J. *Angew. Chem. Int. Ed. Engl.* **1990**, *29*, 1104.
44. Wachter, J. *Angew. Chem. Int. Ed. Engl.* **1989**, *28*, 1613.
45. Brunner, H.; Klement, U.; Meier, W.; Wachter, J.; Serhadle, O.; Ziegler, M. L. *J. Organomet. Chem.* **1987**, *335*, 339.
46. Bodensteiner, M.; Dušek, M.; Kubicki, M. M.; Pronold, M.; Scheer, M.; Wachter, J.; Zabel, M. *Eur. J. Inorg. Chem.* **2010**, 5298.
47. Bernal, I.; Brunner, H.; Meier, W.; Pfisterer, H.; Wachter, J.; Ziegler, M. L. *Angew. Chem. Int. Ed. Engl.* **1984**, *23*, 438.
48. DiMaio, A.-J.; Rheingold, A. L. *Inorg. Chem.* **1990**, *29*, 798.
49. Gröger, C.; Kalbitzer, H. R.; Pronold, M.; Piryazev, D.; Scheer, M.; Wachter, J.; Virovets, A.; Zabel, M. *Eur. J. Inorg. Chem.* **2011**, 785.
50. Gröger, C.; Kubicki, M. M.; Meier, W.; Pronold, M.; Wachter, J.; Zabel, M. *Organometallics* **2009**, *28*, 5633.
51. (a) Brunner, H.; Poll, L.; Wachter, J.; Nuber, B. J. *Organomet. Chem.* **1994**, *471*, 117; (b) Brunner, H.; Poll, L.; Wachter, J. *Polyhedron* **1996**, *15*, 573.
52. Blacque, O.; Brunner, H.; Kubicki, M. M.; Leis, F.; Lucas, D.; Mugnier, Y.; Nuber, B.; Wachter, J. *Chem. Eur. J.* **2001**, *7*, 1342.
53. (a) Scherer, O. J.; Schwarz, G.; Z. Wolmershäuser, G. *Allg. Anorg. Chem.* **1996**, *622*, 951; (b) Scherer, O. J.; Hilt, T.; Wolmershäuser, G. *Organometallics* **1998**, *17*, 4110.
54. Barr, M. E.; Dahl, L. F. *Organometallics* **1991**, *10*, 3991.
55. Pronold, M.; Wachter, J.; Zabel, M. Unpublished results **2007**.
56. Ly, H. V.; Parvez, M.; Rösler, R. *Inorg. Chem.* **2006**, *45*, 345.
57. Gregoriades, L. J.; Balázs, G.; Brunner, E.; Gröger, C.; Wachter, J.; Zabel, M.; Scheer, M. *Angew. Chem. Int. Ed.* **2007**, *46*, 5966.
58. Gröger, C.; Kalbitzer, H. R.; Meier, W.; Pronold, M.; Scheer, M.; Wachter, J.; Zabel, M. *Inorg. Chim. Acta* **2011**, *370*, 191.
59. Pronold, M.; Scheer, M.; Wachter, J.; Zabel, M. *Inorg. Chem.* **2007**, *46*, 1396.
60. (a) Brunner, H.; Guggolz, E.; Meier, W.; Wachter, J.; Zahn, T.; Ziegler, M. L. *Organometallics* **1982**, *1*, 1107; (b) Tremel, W.; Hoffmann, R.; Jemmis, E. D. *Inorg. Chem.* **1989**, *28*, 1213; (c) Bursten, B. E.; Cayton, R. H. *Inorg. Chem.* **1989**, *28*, 2846.
61. Brunner, H.; Graßl, R.; Wachter, J.; Nuber, B.; Ziegler, M. L. *J. Organomet. Chem.* **1990**, *393*, 119.
62. Ren, Z.-G.; Yang, J.-Y.; Li, N.-Y.; Li, H.-X.; Chen, Y.; Zhang, Y.; Lang, J.-P. *Dalton Trans.* **2009**, 2578.
63. Lang, J.; Kawaguchi, H.; Tatsumi, K. *Inorg. Chem.* **1997**, *36*, 6447.
64. Zhang, W.-H.; Song, Y.-L.; Ren, Z.-G.; Li, H.-X.; Li, L.-L.; Zhang, Y.; Lang, J.-P. *Inorg. Chem.* **2007**, *46*, 6647.
65. Pfitzner, A. *Chem. Eur. J.* **2000**, *6*, 1891.
66. Pfitzner, A.; Bräu, M. F.; Zweck, J.; Brunklaus, G.; Eckert, H. *Angew. Chem. Int. Ed.* **2004**, *43*, 4228.
67. Reiser, S.; Brunklaus, G.; Hong, J. H.; Chan, J. C. C.; Eckert, H.; Pfitzner, A. *Chem. Eur. J.* **2002**, *8*, 4228.
68. Pfitzner, A.; Reiser, S. *Inorg. Chem.* **1999**, *38*, 2451.
69. Brunklaus, G.; Chan, J. C. C.; Eckert, H.; Reiser, S.; Nilges, T.; Pfitzner, A. *Phys. Chem. Chem. Phys.* **2003**, *5*, 3768.
70. Rödl, T.; Pfitzner, A. *Z. Anorg. Allg. Chem.* **2010**, *636*, 2033.
71. Bräu, M.; Pfitzner, A. *Angew. Chem. Int. Ed.* **2006**, *45*, 4464.
72. Bräu, M.; Pfitzner, A. *Z. Anorg. Allg. Chem.* **2007**, *633*, 935.
73. Bonazzi, P.; Bindi, L.; Muniz-Miranda, M.; Chelazzi, L.; Rödl, T.; Pfitzner, A. *Am. Mineral.* **2011**, *96*, 646.
74. Ibáñez, W. F.; González, M. G.; Clavijo, C. E. *Z. Anorg. Allg. Chem.* **1977**, *432*, 253.
75. Wachter, J. *Coord. Chem. Rev.* **2010**, *254*, 2078.
76. Biegerl, A.; Brunner, E.; Gröger, C.; Scheer, M.; Wachter, J.; Zabel, M. *Chem. Eur. J.* **2007**, *17*, 9270.
77. Biegerl, A.; Gröger, C.; Kalbitzer, H. R.; Wachter, J.; Zabel, M. *Z. Anorg. Allg. Chem.* **2010**, *636*, 770.
78. (a) Blake, A. J.; Brooks, N. R.; Champness, N. R.; Hanton, L. R.; Hubberstey, P.; Schröder, M. *Pure Appl. Chem.* **1998**, *70*, 2351; (b) Blake, A. J.; Brooks, N. R.; Champness, N. R.; Cooke, P. A.; Daveson, A. M.; Fenske, D.; Hubberstay, P.; Li, W.-S.; Schröder, M. *J. Chem. Soc., Dalton Trans.* **1999**, 2103.
79. Biegerl, A.; Gröger, C.; Kalbitzer, H. R.; Pfitzner, A.; Wachter, J.; Weihrich, R.; Zabel, M. *J. Solid State Chem.* **2011**, *184*, 1719.
80. Li, G.; Shi, Z.; Liu, X.; Dai, Z.; Feng, S. *Inorg. Chem.* **2004**, *43*, 6884.
81. Kubicki, M. M. Personal communication **2008**.
82. (a) Blachnik, R.; Wickel, U. *Angew. Chem. Int. Ed. Engl.* **1983**, *22*, 317; (b) Leiva, A. M.; Fluck, E.; Müller, H.; Wallenstein, G. *Z. Anorg. Allg. Chem.* **1974**, *409*, 215.
83. Di Vaira, M.; Stoppioni, P.; Peruzzini, M. *J. Organomet. Chem.* **1989**, *364*, 399.
84. (a) Bues, W.; Somer, M.; Brockner, W. *Z. Naturforsch.* **1980**, *35b*, 1063; (b) Brockner, W.; Somer, M.; Cyvin, B. N.; Cyvin, S. J. *Z. Naturforsch.* **1980**, *36a*, 846.
85. Schwarz, P.; Wachter, J.; Zabel, M., *Inorg. Chem.* **2011**, *50*, 12692.
86. (a) Qin, C.; Wang, X.; Wang, E.; Su, Z. *Inorg. Chem.* **2008**, *47*, 5555; (b) Carlucci, L.; Ciani, G.; Proserpio, D. M. *Coord. Chem. Rev.* **2003**, *246*, 247.
87. (a) Araki, H.; Tsuge, K.; Sasaki, Y.; Ishizaka, S.; Kitamura, N. *Inorg. Chem.* **2007**, *46*, 10032; (b) Kirillov, A. M.; Smoleński, P.; Haukka, M.; Guedes da Silva, M. F. C.; Pombeiro, A. J. L. *Organometallics* **2009**, *28*, 1683; (c) Kirillov, A. M.; Smoleński, P.; Mha, Z.; Guedes da Silva, M. F. C.; Haukka, M.; Pombeiro, A. J. L. *Organometallics* **2009**, *28*, 6425.

Copyright © 2013. Elsevier. All rights reserved.

Comprehensive Inorganic Chemistry II : From Elements to Applications, Elsevier, 2013. ProQuest Ebook Central, http://ebookcentral.proquest.com/lib/inflibnet-ebooks/detail.action?docID=1330977.
Created from inflibnet-ebooks on 2021-02-09 22:27:26.

88. Churchill, M. R.; Kalra, K. L. *Inorg. Chem.* **1974**, *13*, 1899.
89. Biegerl, A.; Piryazev, D.; Scheer, M.; Wachter, J.; Virovets, A.; Zabel, M., *Eur. J. Inorg. Chem.* **2011**, 4248.
90. (a) Di Nicola, C.; Effendy, ; Fazaroh, F.; Pettinary, C.; Skelton, B. W.; Somers, N.; White, A. H. *Inorg. Chim. Acta* **2005**, *358*, 720; (b) Cingolani, A.; Di Nicola, C.; Effendy, ; Pettinary, C.; Skelton, B. W.; Somers, N.; White, A. H. *Inorg. Chim. Acta* **2005**, *358*, 748; (c) Effendy, ; Di Nicola, C.; Fianchini, M.; Pettinary, C.; Skelton, B. W.; Somers, N.; White, A. H. *Inorg. Chim. Acta* **2005**, *358*, 763; (d) Effendy, ; Di Nicola, C.; Pettinary, C.; Pizzabiocca, A.; Skelton, B. W.; Somers, N.; White, A. H. *Inorg. Chim. Acta* **2006**, *359*, 64.
91. Fu, M.-L.; Fenske, D.; Weinert, B.; Fuhr, O. *Eur. J. Inorg. Chem.* **2010**, 1098.
92. (a) Näther, C.; Jeß, I.; Greve, J. *Polyhedron* **2001**, *20*, 1017; (b) Näther, C.; Jeß, I. *J. Solid State Chem.* **2002**, *169*, 103.
93. Graham, P. M.; Pike, R. D.; Sabat, M.; Bailey, R. D.; Pennington, W. T. *Inorg. Chem.* **2000**, *39*, 5121.

Copyright © 2013. Elsevier. All rights reserved.

Comprehensive Inorganic Chemistry II : From Elements to Applications, Elsevier, 2013. ProQuest Ebook Central, http://ebookcentral.proquest.com/lib/inflibnet-ebooks/detail.action?docID=1330977.
Created from inflibnet-ebooks on 2021-02-09 22:27:26.